APPLICATIONS OF MID-IR SPECTROSCOPY FOR IDENTIFICATION OF WINE AND OLIVE YEASTS AND CHARACTERIZATION OF ANTIMICROBIAL ACTIVITIES OF PHENOLICS ON YEASTS

A Thesis Submitted to
the Graduate School of Engineering and Sciences of
İzmir Institute of Technology
in Partial Fulfillment of the Requirements for the Degree of

DOCTOR OF PHILOSOPHY

in Food Engineering

by
Canan CANAL

December 2015
İZMİR

We approve the thesis of **Canan CANAL**

Examining Committee Members:

Prof. Dr. Banu ÖZEN
Department of Food Engineering, Izmir Institute of Technology

---

Prof.Dr. Figen TOKATLI
Department of Food Engineering, Izmir Institute of Technology

---

Prof. Dr. Duygu KIŞLA
Department of Food Engineering, Ege University

Assoc. Prof. Dr. Efe SEZGİN
Department of Food Engineering, Izmir Institute of Technology

---

Assist. Prof. Dr. Erdal EROĞLU
Department of Bioengineering, Celal Bayar University

25 December 2015

Prof. Dr. Banu ÖZEN
Supervisor, Department of
Food Engineering
Izmir Institute of Technology

Assoc. Prof. Dr. A. Handan BAYSAL
Co-Supervisor, Department of
Food Engineering
Izmir Institute of Technology

Prof. Dr. Ahmet YEMENİCİOĞLU
Head of the Department of
Food Engineering

Prof. Dr. Bilge Karaçalı
Dean of the Graduate School of
Engineering and Sciences

ACKNOWLEDGMENTS

ABSTRACT

APPLICATIONS OF MID-IR SPECTROSCOPY FOR IDENTIFICATION OF WINE AND OLIVE YEASTS AND CHARACTERIZATION OF ANTIMICROBIAL ACTIVITIES OF PHENOLICS ON YEASTS

The aim of this study was application of mid-IR spectroscopy in combination with multivariate statistical analysis for characterization of yeasts from two fermented products, wine and olive, in comparison with cultural and molecular tests and characterization of antimicrobial effects induced by olive phenolics on yeasts. Totally 19 wine yeasts were molecularly identified as *M. pulcherrima* (11%), *P. membranifaciens* (16%), *H. uvarum* (5%) and *S. cerevisiae* (68%). According to FTIR spectroscopic data of wine samples, *S. cerevisiae* isolates formed a cluster which were generally separated from all other yeasts. Totally 182 olive yeasts were identified from naturally debittered Hurma and a common olive variety and their leaves. The most common yeasts were *Metschnikowia* sp. (39%) and *Aureobasidium* sp (78%) in the first and the second harvest years, respectively. Since only *Aureobasidium* sp. was the common yeast isolated from Hurma during both years, any link between natural debittering of Hurma and the yeast population of this olive type might be related to *Aureobasidium* sp. Molecularly identified yeast types generally formed different clusters and showed spectral differences. For antimicrobial activity tests, all phenolic compounds were found effective on both *S. cerevisiae* and *A. pullulans*; however, *A. pullulans* was observed to be more sensitive. Antimicrobial activity was differentiated with respect to treatment time and phenol concentration with statistical treatment of FTIR data. As a complementary technique, FTIR could be successfully used for identification of yeasts and characterization of antimicrobial activity of phenolics against yeasts.

ÖZET

ŞARAP VE ZEYTİN MAYALARININ TANIMLANMASI VE FENOLİKLERİN MAYALAR ÜZERİNE ANTİMİKROBİYEL AKTİVİTELERİNİN KARAKTERİZASYONU İÇİN MİD-IR SPEKTROSKOPİ UYGULAMALARI

Bu çalışmada, fermente gıdalar olan şarap ve zeytinden izole edilen mayaların kültürel ve moleküler yöntemlerle karşılaştırmalı olarak karakterizasyonu ve zeytin fenollerinin mayalar üzerindeki antimikrobiyel etkilerinin incelenmesi için çok değişkenli istatistiksel analizler ile birlikte mid-IR spektroskopi uygulamaları amaçlanmıştır. Şarap örneklerinden toplam 19 maya izole edilerek moleküler tekniklerle *M. pulcherrima* (%11), *P. membranifaciens* (%16), *H. uvarum* (%5) ve *S. cerevisiae* (%68) olarak tanımlanmışlardır. FTIR spektroskopi sonuçlarına göre, *S. cerevisiae* izolatları genel olarak bir küme oluşturarak izole edilen diğer mayalardan ayrılmışlardır. Zeytin örneklerinden toplam 182 maya izole edilerek 1. yıl hasat edilenlerden en çok *Metschnikowia* sp. (%39); 2. yıl hasat edilenlerden en çok *Aureobasidium* sp. (%78) moleküler olarak tanımlanmıştır. Sadece *Aureobasidium* sp. her iki yılın hurma zeytinlerinden ortak olarak izole edildiğinden, hurma zeytin oluşumu ve zeytin-maya populasyonu arasındaki ilişki bu mayaya bağlanmıştır. FTIR spektroskopi verilerine göre, moleküler olarak tanımlanan maya tipleri genel olarak farklı kümeler oluşturmuş ve spektral olarak da farklılıklar göstermişlerdir. Antimikrobiyel aktivite çalışmalarında ise, kullanılan tüm fenoller hem *S. cerevisiae* hem de *A. pullulans* üzerinde etkili bulunmuş, ancak *A. pullulans*'ın daha duyarlı olduğu gözlenmiştir. FTIR verilerinin istatistiksel işlenmesi sonuçlarına göre antimikrobiyel aktivite hem örnekleme zamanı hem de fenol konsantrasyonları açısından farklılık göstermiştir. Antimikrobiyel etkilerin spektral bölgelerde yol açtığı farklılıklar da rahatça görülmüştür. Sonuç olarak, FTIR spektroskopi yöntemi hem mayaların tanımlanmasında hem de fenolik bileşenlerin mayalar üzerindeki etkilerinin karakterizasyonu için tamamlayıcı bir teknik olarak başarıyla kullanılabilir.

TABLE OF CONTENTS

APPENDICES

LIST OF FIGURES

LIST OF TABLES

CHAPTER 1

INTRODUCTION

Turkey is one of the most suitable countries of the world for wine grape vineyards having convenient climatic conditions for viticulture and many vine grape varieties; therefore, it is one of the significant grape growing countries in the world with its large vineyards (Gümüş and Gümüş, 2009). Wine production requires strict monitoring of a series of parameters for a long period of time. Since the living microorganism content of the must beginning from harvest until the end of fermentation of wine varies during the whole process, microbiological analysis play an important role to control wine production.

Turkey is also one of the main producer of another fermented product, naturally black olive types, with over 100 000 tones/year (about 25% of world production) (Garrido-Fernandez et al., 1997). Among these olive varieties, Erkence olive, grown in nearby area around Karaburun Peninsula of Izmir, goes through a natural debittering phase on the tree during its ripening. After this phase, this naturally debittered olive type is called by the name of "Hurma" and since it loses its bitter taste while still on the tree, it does not need to go through further table olive processing operations. According to an old study performed in Greece with a similar type of olive, the debittering process was attributed to the action of a fungus, *Phoma olea*, which hydrolyses oleuropein, a bitter phenolic compound of olives (Kalogereas, 1932). Therefore, it is important to determine the microorganisms which play a role in maturation stage of Hurma olives growing near Karaburun. Results of microbial characterization studies could help better understanding of debittering process.

Until recent years, the characterization of yeasts has been performed through biochemical and morphological methods, using the taxonomic keys of Looder (1970), Barnett et al. (1990) and Kurztman and Fell (1998) which are complex, laborious and time consuming analyses and their capacities are often limited, although the methodology permits the isolation and characterization of a great variety of genera and species around the world. Various rapid and automated identification systems for routine analyses of yeasts are commercially available and easy to use, however, identification results are

questionable to a certain degree because these systems were developed originally for clinical applications and databases, therefore, do not include an adequate number of common yeast species (Arias et al., 2002). More recently, novel molecular methods have been used for the identification of yeasts from food products due to being rapid, easy and more precise techniques for yeast identification by eliminating part of the subjectivity that originates from the results of the biochemical tests. On the other hand, these techniques have some technical limitations due to protocol complexities, reagent costs, choice of specific primers for each species, sensitivity to mutations and they are not applied as routine analysis up to now (Maquelin et al., 2003). Recent developments in analytical instrumentation showed that Fourier Transform Infrared (FTIR) Spectroscopy is an emerging technique when used with multivariate statistical analysis tools, which provides unique "fingerprint" of any compound with its spectrum (Santos et al., 2010). Besides its use in characterization of microorganisms, FTIR spectroscopy has also been applied to the assessment of stress response of environmental conditions on microorganisms.

In this thesis study, first, the application of FTIR spectroscopy was performed for characterization of wine yeasts in comparison with both cultural and molecular identification techniques, as described in the 3rd chapter. After enumeration, isolation and purification of yeasts from seven different wine types (2 white wines: Muscat and Chardonnay; 1 rose wine: Sangiovese; 4 red wines: Syrah, Merlot, Cabernet Sauvignon and Bogazkere), characterization analysis were performed with morphological analysis, sugar and nitrogen assimilation tests for cultural techniques; DNA isolation of yeasts, Polymerase Chain Reaction (PCR) and sequence analysis with molecular techniques; and finally with mid-IR spectroscopy using both dried yeast cells and yeast cells directly without a dehydration step in combination with multivariate statistical techniques.

As expressed in details in the 4th chapter, the application of FTIR spectroscopy was carried on also for characterization of yeast flora of naturally debittered Hurma olives and a common table olive variety, Gemlik olives and their leaves of two harvest years, in comparison with both cultural and molecular identification techniques with the same analysis methods mentioned in Chapter 3.

In the 5th Chapter, two yeasts including *S. cerevisiae,* as a model and a "wine yeast" and *A. pullulans,* as the most common yeast identified from both harvest years of olive samples were selected to investigate the antimicrobial effects induced by several olive phenolic compounds, including tyrosol, hydroxytyrosol, oleuropein, luteolin and

apigenin using FTIR spectroscopy, besides absorbance measurements with microplate reader, yeast colony count and microscope images.

The overall objective of this thesis study was application of mid-IR spectroscopy with multivariate statistical analysis methods for both identification of yeasts from two fermented products: wine and olive in comparison with cultural and molecular tests and characterization of antimicrobial effects of some olive phenolics on yeasts besides absorbance measurements, yeast colony count and microscope images.

CHAPTER 2

LITERATURE REVIEW

2.1. Wine and Wine Yeasts

Turkey is one of the most convenient countries in the world for the cultivation of wine grape vineyards due to its favorable climatic conditions and various suitable soil structures. The vineyards are spread all over the country but especially Aegean, Mediterranean, Central Anatolian and Thrace regions are the main wine production areas (Gümüş and Gümüş, 2009).

Turkish Food Codex (2008a) defines the wine as the fully or partially fermented product of crushed or uncrushed grapes or grape must with or without the protected designation of origin or protected geographical origin indication labels. The classification of wines is basically made with respect to the place of origin or appellation, vinification techniques, sugar content, vintage, and variety of the grapes used to produce wine. Wines may be classified by vinification methods including red, rose or white wine, sparkling, fortified and dessert wines. Among these classifications, red wines differ from white wines due to the stage of processing after crushing where the skins and seeds are not removed and fermentation is carried out in the presence of the grape juice, skins and seeds together at higher temperatures in the range of 25-30°C. The fermentation temperature of white wines ranges between 18-24°C. The only difference between red and rose wine production is the temperature and length of the fermentation period of grape juice with seeds and skins.

Several factors such as variety of the grape used in wine production, ripeness of the grape, geographical origin, vintage, viticultural and vinification techniques have considerable influences on the compositional variations of the wine (Serban et al., 2004). Wine production requires strict monitoring of a series of parameters for a long period of time. The diversity of parameters and the complexity of this living liquid lead to search for fast, selective, precise, and sensitive methods of analysis. The most important parameters for the wine process are various chemical properties of wines. Additionally, since the living microorganism content of the must beginning from the harvest until the

end of fermentation of wine varies during the whole process, microbiological analysis also play an important role to control wine production.

Wine fermentation is the result of a complex evolution of microorganisms involving both yeasts and bacteria (Cocolin et al., 2000). Yeasts have been considered as nature's one of the most important group of microorganisms since they have been used industrially for making bread, wine, beer, cider and other alcoholic beverages. In general, yeasts predominate during the alcoholic fermentation, and the low pH values and nutritional content of the grape juice are the factors that support the yeast growth. In the initial stages of most wine fermentations, a diverse population of yeasts such as species of *Kloeckera, Metschnikowia, Candida, Hanseniaspora* and *Saccharomyces* exists. The non-*Saccharomyces* yeasts typically grow for several days before the fermentation. However, one or more *Saccharomyces cerevisiae* strains dominate with an increase in ethanol concentration. In general, classical microbiological methods was used in most of the previous studies to determine the microbial constituents of fermenting wines (Cocolin et al., 2000).

2.2. Hurma Olive and Olive Yeasts

Table olives are one of the most important and well-known fermented products of the food industry, with an estimated worldwide production of over 2 500 000 tons in 2014/2015. They are traditional foods of mainly Mediterranean countries including Turkey where table olive production has been increasing constantly over the years. EU countries rank first in table olive production while Turkey and Egypt follow them (IOC, 2015).

The olive fruit has a low sugar concentration (2.6 –6.0%) and high oil content (12–30%), and its bitter taste comes from a bitter phenolic compound, oleuropein. However, composition of olive could vary depending on maturity stage and olive variety (Garrido-Fernandez et al., 1997). This bitter characteristic of olives prevent them from being consumed directly from the tree and a series of processes have been developed to make olives eatable and these table olive processing practices differ considerably from region to region (Arroyo-Lopez et al., 2008).

The most common classification of table olives are; the green Spanish style, ripe olives by alkaline oxidation (Californian-style) and naturally black olives which is also

called as Greek style. According to the Unified Qualitative Standard Applying to Table Olives in International Trade and Spanish Standard, naturally black olive type are those obtained from fruits harvested when they are fully or slightly ripe before the full maturity is reached. The main producing country of these olive types is Turkey with over 100 000 tones/year (about 25% of world production) (Garrido-Fernandez et al., 1997). Among these olive varieties in Turkey, Erkence olives, grown in nearby area around Karaburun Peninsula of Izmir, go through a natural debittering phase on the tree during its ripening. As a result of this phase, the olives lose their bitter taste while still on the tree and have a dark brownish color in the inside and a wrinkled outer layer which are their differentiating appearance characteristics from olives that do not undergo this process. This naturally debittered olive type is known by the name of "Hurma". Since Hurma olive is already debittered on the tree it does not need to go through further table olive processing operations that other table olives are required to. Therefore, consumers having health problems such as hypertension might prefer this olive type over table olives that have a higher salt content (Aktas et al., 2014a; Aktas et al., 2014b). Similar types of olives were also reported in the previous studies from Greece, known as 'thrubolea' or 'Throuba Thassos' and from Tunisia, known as 'Dhokar' (Jemai et al., 2009; Zoidou et al., 2009).

According to an old study performed in Greece with a similar type of olive, the debittering process was attributed to the action of a fungus, *Phoma olea*, which hydrolyses oleuropein, a bitter phenolic compound of olives (Kalogereas, 1932). This enzymatic hydrolyzation reaction occurs by β-glucosidase enzyme produced by both bacteria and fungi (Ciafardini and Zullo, 2000). This group of fungi has also been isolated from many green-leaf vegetables, namely "herbaceous" vegetables such as leaf and root of thyme, stem, root and leaf of lemon balm and St. John's wort trunk and stem of mint from young olive trees. Therefore, it is important to determine the microorganisms which play a role in debittering process of Hurma olive growing near Karaburun and to identify whether there is a fungus namely *Phoma oleae* specific to that region.

For the debittering process on the tree, the effect of climate and/or soil was also mentioned by the local people since this phenomenon is confined only to certain geographical locations. The natural microbiological flora of olive consists of great variety of microorganisms including bacteria, yeasts and molds. The type and ratio of microorganisms present on the olive surface is affected by climatic conditions, olive type and maturity stage of olive. These naturally occurring microorganisms on olive start the spontaneous fermentation (Kailis and Harris, 2007). Both lactic acid bacteria (LAB) and

yeast play a critical role in all olive fermentations, especially in natural black olives (Arroyo-Lopez et al., 2006). Since LAB are partially inhibited in natural black olives due to the presence of phenolic compounds, yeasts become especially important (Arroyo-López et al., 2012). Fermentative yeasts can contribute to the organoleptic characteristics of table olives (Aponte et al., 2010).

Concerning natural black olives, yeasts are responsible for the fermentation process, contrary to green olives in which the fermentation is performed by LAB (Garrido-Fernandez et al., 1997). Black olive fermentations have been studied in different countries, mainly Spain, Portugal, Greece and Morocco and showed biodiversity of yeast species, yet a few species were dominant: *Pichia membranifaciens, Saccharomyces oleaginosus, P. anomala, Candida boidinii* and *Torulaspora delbrueckii* (Kotzekidou, 1997; Coton et al., 2006). There are also different yeast species isolated and identified from naturally black olive brines, such as *Hansenula anomala, H. subpelliculosa, Torulopsis candida, T. norvegica, Debaryomyces hansenii, C. diddensii, C. krusei, C. valida, P. farinosa, P. fermentans, Kluyveromyces veronae* and *Cryptococcus ater*. The debittering effect of yeasts was studied by Materassi et al. (1975) and it was found that 8 of 36 yeast species had the capacity of hydrolysing oleuropein. The two most active species were found as *Rhodotorula* and *Candida* (Garrido Fernandez et al., 1997). It was observed that the species found depended on the maturation degree of the olive. However, yeast counts on the surface of fresh olive fruits were generally low ($< 1 \log_{10}$ CFU g^{-1}), as was reported by Arroyo Lopez et al. (2008) with Manzanilla–Alorena olives during three consecutive seasons. Several species of the genera *Candida, Debaryomyces, Kluyveromyces, Pichia, Rhodotorula* and *Saccharomyces* were isolated directly from brined green and turning color olives (Marquina et al., 1992). In addition, presence of yeasts belonging to the genera of *Trichosporon, Candida, Pichia, Kloeckera, Torulopsis* and *Debaryomyces* during the fermentation of directly brined natural black olives from Greek cultivars was also reported. Researchers also identified *S. cerevisiae* and *P. anomala* as the main species in Spanish natural black olive fermentations (Arroyo-Lopez et al., 2006) while *Debaryomyces* species were isolated from Turkish cultivars (Borcakli et al., 1993). *Torulaspora delbrueckii, D. hansenii* and *Cryptococcus laurentii* were isolated from Greek-style black olives as the predominant species (Kotzekidou, 1997). Green table olives from Portugal was reported to have *P. anomala, K. marxianus, D. hansenii* and *S. cerevisiae* as the main species (Hernandez et al., 2007). *P. anomala, C. boidinii* and *D. etchelsii* were isolated as the predominant species in black olive natural

fermentations from France (Coton et al., 2006). Yeast population dynamics during the processing of Arbequina table olives were also investigated and it was reported that, *C. diddensiae* was the most abundant species in brine at the beginning of the fermentation, and it was reported to be a strong fermentative yeast and well adapted to the first stage of the fermentation (Hurtado et al., 2008). Another yeast species identified in the first samples was *R. glutinis*, probably proceeding from the olives' surface. It has been described as a pink yeast related to the softening of olives and could play a beneficial role in the diffusion of nutrients. *C. boidinii* is one of the most abundantly identified yeast species of table olives (Coton et al., 2006) while *P. kluyveri* is well known as a killer toxin producing yeast and has also been isolated from naturally fermented olives by Oliveira et al. (2004). Later, when the LAB counts dominated the yeast population, *P. membranifaciens* and *K. lactis* appeared until the end of the process. Campaniello et al. (2005) reported the frequency of the identified yeast species in table olives of Spanish style and natural processing which showed that *Candida* was the mainly isolated genus in addition to *R. mucilaginosa* and *Cryptococcus laurentii*. The most frequently isolated genera are *Candida, Pichia, Saccharomyces* and to a lesser extent, *Debaryomyces, Issatchenkia, Zygotorulaspora* and *Wickerhamomyces* from different olive varieties (Alves et al., 2012; Arroyo-Lopez et al., 2006; Bautista-Gallego et al., 2011; Coton et al., 2006; Nisiotou et al., 2010).

It has been reported that the effect of yeasts on the flavor and texture of olives is an important factor. Hernández et al. (2007) investigated the presence of yeasts with esterase and polysaccharolytic activities in green olive fermentations and showed that the activities of these yeasts may have an important role on the organoleptic characteristics of the fermentations at the end. Strains of *Rhodotorula* species produce polygalacturonases causing a softening (Vaughn et al., 1972). Olives are fruits with high fat content. The presence of lipolytic yeasts and their activities in table olives could cause changes in the nutritional composition of the fruits and also in their organoleptic characteristics. Biodegradation of polyphenols by yeast is another interesting aspect. Some strains of *C. tropicalis* and *Yarrowia lipolytica* have potential to reduce the chemical oxygen demand, monophenols and polyphenols in olive mill wastewater (Lanciotti et al., 2005). Yeasts biodiversity reported in distinct olive types may explain the different characteristics in terms of chemical, microbiological and sensorial quality of table olives. It was indicated that it would be interesting to study the relation between the microbiota present during the processing and the development of the final product's

organoleptic profile (Alves et al., 2012). However, there is no study in the literature related to the identification of yeasts on this unique type of olive, Hurma. The number of scientific studies about the composition and also the changes during the maturation of Hurma olive is also very limited. Actually, the studies on characterization of olives are much less than the studies on olive oil in the literature. In the recent years, the favorable health effects of olive oil due to its fatty acid and phenolic composition have gained attention. As the source of olive oil, it has been thought that olive fruit also would have the same favorable effect on human health.

2.3. Characterization of Yeasts

2.3.1. Cultural Methods

The first biotechnologically produced foods such as wine, bread, and fermented milk products are produced as a result of the action of yeasts; however, yeasts are also responsible for food spoilage. In addition, some yeast species are reported to have medical importance. Therefore, a reliable and accurate method for identification is significant and essential (Bautista-Gallego et al., 2011). Until recent years, the characterization of yeasts, especially associated with table olives, has been performed through biochemical and morphological methods, using the taxonomic keys of Looder (1970), Barnett et al. (1990), and Kurztman and Fell (1998). Conventional differentiation systems which are based on morphological characters as well as assimilation patterns and fermentation of carbon sources require evaluation of many tests for a correct species identification, which is a complex, laborious and time consuming process and their capacity is often limited, although the methodology permits the isolation and characterization of a great variety of genera and species around the world.

Various rapid and automated identification systems for routine analyses of yeasts are commercially available and easy to use. One of these methods, the API 20C AUX system (bioMèrieux, Lyon, France), has been widely used for the evaluation of assimilation of 19 carbon sources (D-GLUcose, GLYcerol, calcium 2-Keto-Gluconate, L-ARAbinose, D-XYLose, ADOnitol, XyLiTol, D-GALactose, INOsitol, D-SORbitol, Methyl-αD-Glucopyronoside, N-Acetyl-Glucosamine, D-CELlobiose, D-LACtose (bovine origin), D-MALtose, D-SACcharose (sucrose), D-TREhalose, D-MeLeZitose,

D-RAFfinose). However, identification results are questionable to a certain degree because these systems originally were developed for clinical applications and databases, therefore, do not include an adequate number of common yeast species (Arias et al., 2002). More recently, molecular methods have been used for the identification of yeasts from food products due to being rapid, easy and more precise techniques since they eliminate part of the subjectivity that originates from the results of the biochemical tests. These techniques offer a higher degree of accuracy for the final identification compared to classical cultural methods.

2.3.2. Molecular Methods

The molecular methods used in the identification of yeast species are generally based on the variability of the ribosomal genes 5.8S, 18S and 26S (Cai et al., 1996; Kurtzman et al., 2011). The ribosomal genes are preferred for species identification since they show a low intra-specific polymorphism and a high inter-specific variability. Previous results have demonstrated that the complex internal transcribed spacer (ITS) regions (non-coding and variable) and the 5.8S rRNA gene (coding and conserved) are useful in measuring close fungus phylogenetic relationships since they exhibit far greater inter-specific differences than the 18S and 26S rRNA genes (Cai et al., 1996; Kurtzman et al., 2011). NL1 and NL4 primers which amplify the domain D1/D2 of 26S rRNA were first described by Kurtzman and Robnett (1998). However, there is more phylogenetic information (variation) contained within the ITS locus, which is probably why it became the standard. It was indicated that ITS1 and ITS2 regions are not only phylogenetically informative, as shown in previous studies, but they are also useful in distinguishing both closely and distantly related taxa (Chen et al., 2001). Granchi et al. (1999) reported in their study that the large differences found in ITS region sizes and restriction patterns among yeast species could mean that species-specific primers could be designed so that single yeast species would be detectable by simple PCR within a short time by eliminating the restriction step. The approximate locations of ITS region (a) and D1/D2 domains (b) are shown in Figure 2.2.

The polymerase chain reaction (PCR) is a molecular technique developed by Karry Mullis in 1983 which is used to amplify a single or a few copies of a piece of DNA, generating thousands to millions of copies of a particular DNA sequence. The method

relies on thermal cycling, consisting of cycles of repeated heating and cooling of the reaction for DNA melting and enzymatic replication of the DNA (Saiki et al., 1988). There are three major steps (denaturation, annealing and extension) in a PCR, which are repeated for 30-40 cycles by an automated thermal cycler (Figure 2.1). During the denaturation step at 94°C, the double strand of DNA melts open to single stranded DNA. In annealing step at 54°C, ionic bonds are constantly formed and broken between the single stranded primer and the single stranded DNA template. The more stable bonds last longer where the primers fit exactly and on that little piece of double stranded DNA (template and primer), the polymerase enzyme can attach and starts copying template. In the extension step at 72°C, the DNA polymerase enzyme starts to work and add dNTP's from 5' to 3' to extend the strand with the bases (complementary to the template) coupled to the primer.
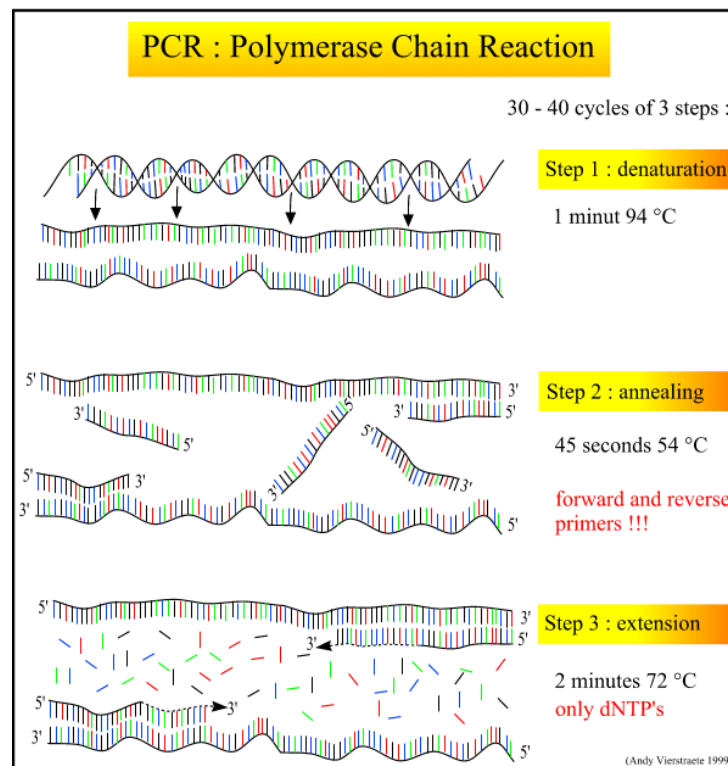
Figure 2.1. The different steps in PCR
(Source: Vierstraete, 1999)

(a)

(b)

(c)
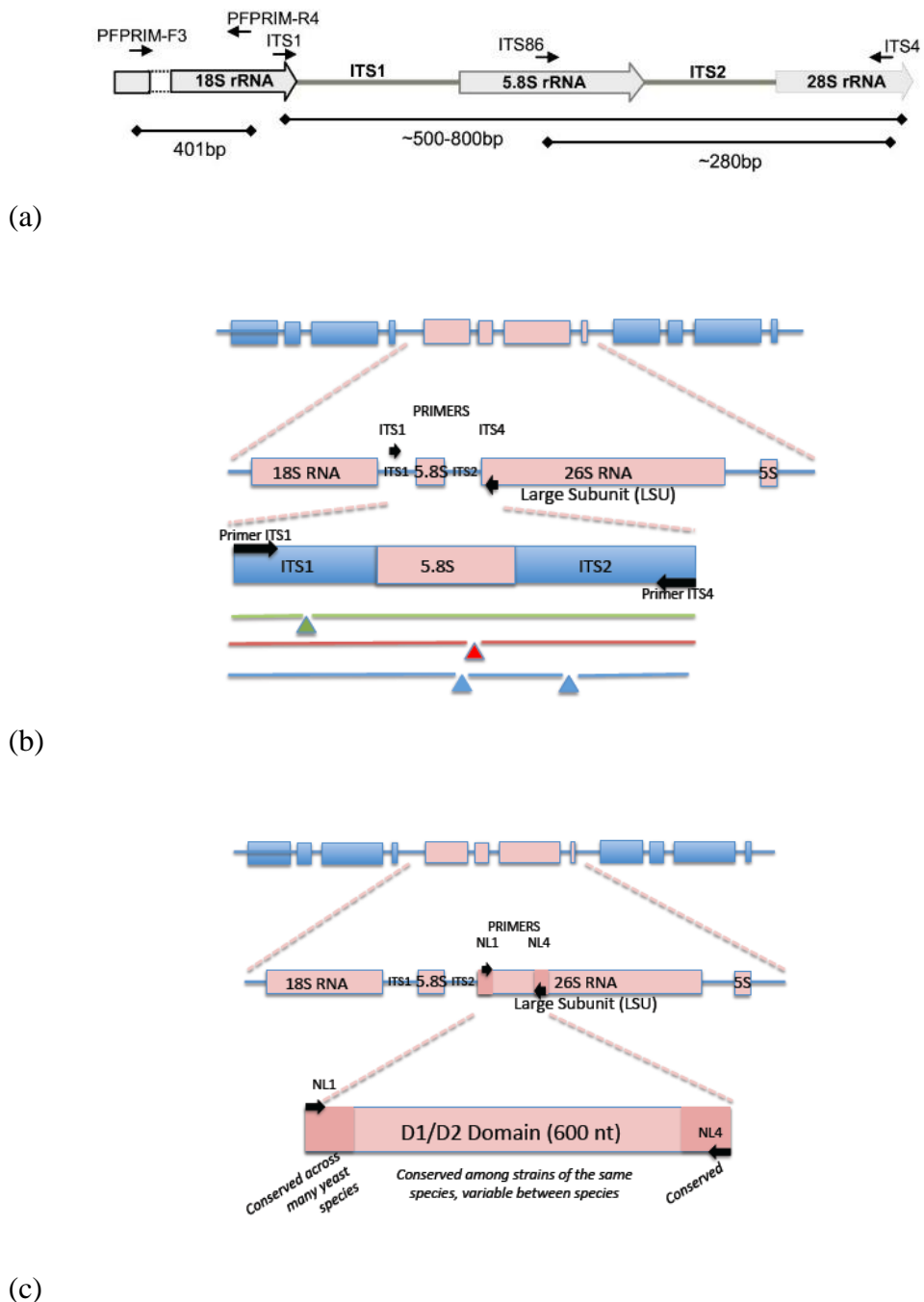
Figure 2.2. Location of the (a, b) ribosomal genes and ITS regions and (c) D1/D2 domains with primer binding locations (Source, (a): Embong et al., 2008 and (b, c): https://www.studyblue.com)

Only recently, molecular methods have been used to explore the yeast biodiversity associated with the different types of olive processes as directly brined green olives (Aponte et al., 2010; Arroyo-Lopez et al., 2006; Hurtado et al., 2008), natural black olives (Coton et al., 2006; Nisiotou et al., 2010) and ripe olive processing (Arroyo-Lopez et al., 2006) which confer a higher degree of accuracy in the final identification.

2.3.3. Mid-IR Spectrophotometric Methods

Novel molecular methods for rapid identification of microorganisms are widely used for various species; however, these techniques have some technical limitations due to protocol complexities, reagent costs, choice of specific primers for each species, sensitivity to mutations and they are not applied as routine analysis until now (Maquelin et al., 2003). The ideal method for replacing these labor-intensive processes would involve minimum sample preparation, direct analyses of samples (no requirement of reagents), requirement of small quantitiy of biomass, rapidity, automation and low cost. A radically different approach to the development of identification methods is based on optical spectroscopic techniques. Furthermore, with recent developments in analytical instrumentation, some spectroscopic or spectrometry techniques could provide not only qualitative but also quantitative information about a given sample. Spectrum of any compound obtained from spectroscopic analysis is known to give a unique "fingerprint" (Santos et al., 2010).

2.3.3.1. Principles of Mid-Infrared Spectroscopy

Fourier transform infrared spectroscopy (FTIR) is an old and powerful technique for identifying types of chemical bonds in a molecule. One of the strengths of FTIR spectroscopy is its ability, as an analytical technique, to obtain spectra from a very wide range of compounds. The infrared region of the electromagnetic spectrum extends from the visible to the microwave (Figure 2.3). Infrared radiation originates from a thermal emission of a hot source. It is conventionally specified by the ''wave number'', i.e. the number of waves per centimeter (expressed by the unit cm^{-1}), extending from 10,000 to 10 cm^{-1}. Moreover, infrared radiation is divided into near (NIR, 10000-4000 cm^{-1}), middle (Mid-IR, 4000-200 cm^{-1}) and far (FIR, 200-10 cm^{-1}) infrared regions (Santos et al., 2010).
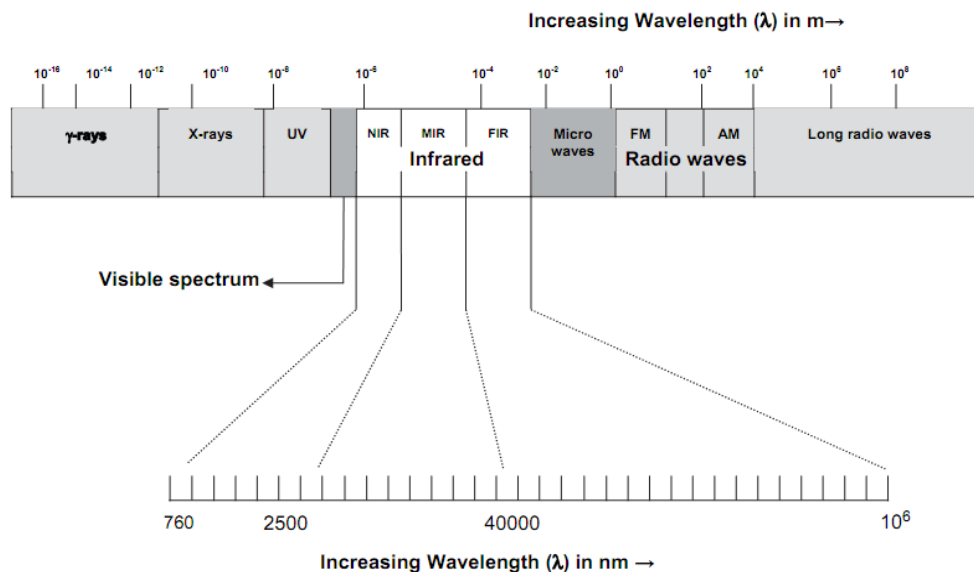
Figure 2.3. Schematic representation of the electromagnetic spectrum
(Source: Santos et al., 2010)

The basis of FTIR spectroscopy is the absorption of the infrared light by several molecules in a sample. Thus, the FTIR technique involves subjecting an infrared beam energy that is emitted from a glowing ember source and crossing of beam through a chamber for controlling the amount of radiated energy on the sample. The IR beam enters the interferometer where ''spectral encoding'' takes place; then, the resulting interferogram signal exits the interferometer. In addition, infrared beam energy enters the sample compartment where it is transmitted through or reflected away from the sample surface depending on the type of analysis being accomplished. Finally, the beam passes to the detector for the final measurement and the measured signal is digitalized and sent back to the computer where Fourier transformation takes place, as shown in Figure 2.4. The final infrared spectrum is then presented to the user.
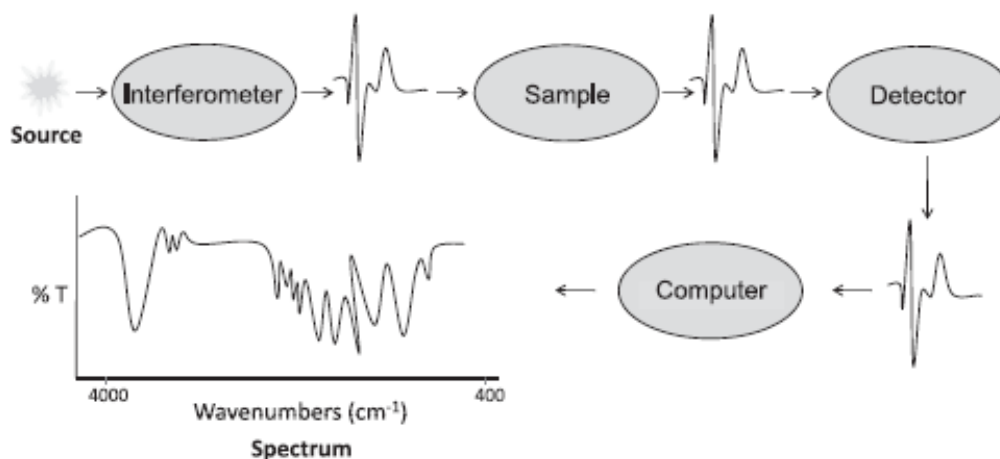
Figure 2.4. Step by step IR spectrum acquisition
(Source: Santos et al., 2010)

FTIR spectra of pure compounds are generally so unique that they look like molecular ''fingerprints''. For most common materials, the spectrum of an unknown compound can be identified by comparison with a library of known compounds. The chemical structure and three-dimensional orientation of the molecules are responsible for generating different IR absorptions (Ngo-Thi et al., 2003).

FTIR spectroscopy was introduced in 1991 as a technique to identify and classify microbes and applications of FTIR spectroscopy in the biomedical field, particularly in the identification of microorganisms, have become increasingly interesting (Wenning and Scherer, 2013). This approach shows a high potential not only for identification at the genus and species levels but also for strain discrimination within the same species. FTIR spectroscopy is an analytical, fast, simple, non-destructive and dynamic method to investigate a population of whole cells with only little biomass (Timmins et al., 1998). It has been also reported by several authors (Sockalingum et al., 1997; Sandt et al., 2003) that FTIR spectroscopy has been increasingly used for the identification of microorganisms at the species level, but it has been proven to have the potential to discriminate between strains of the same species. It permits not only the identification and characterization of microbial cells (phenotype, species, sub-species, pathogenicity, virulence, etc.) but also a detailed structural analysis to identify certain macromolecules (nature, quantity, and conformation of molecular links) present in the cells (Essendoubi et al., 2005). Absorption of infrared light by cellular compounds results in a fingerprint-like spectrum that can be identified by comparison to reference spectra. Once an extensive and well-designed database of reference spectra is established, reliable identification

15

results are obtained within 25 h of starting the identification from a single colony (Oberreuter et al., 2002).

The five spectral windows W1 to W5 shown in Figure 2.5 provide information regarding the identification of microorganisms by FTIR spectroscopy (Kümmerle et al., 1998). Ranges of wave numbers can be related to special chemical bonds. As IR radiation is passed through a sample, absorption at specific wavelengths takes place and this causes the chemical bonds in the material to undergo vibrations such as stretching, contracting, and bending (Table 2.1). Functional groups of a molecule absorb IR radiation and spectral peaks are from the result of the absorption of bond vibrational energy changes in the IR region. Thus, a correlation exists between the chemical structures of the molecules and IR band positions. In terms of wave numbers; W1 is the fatty acid region (3050-2800 cm^{-1}), where peaks correspond to the vibrations of the $-CH_2$ and $-CH_3$ groups of fatty acids. W2 region is the amide part (1750-1500 cm^{-1}), where protein and peptide bands exist. W3, which ranges from 1500-1200 cm^{-1}, is a mixed region including vibrations of fatty acids, proteins, and polysaccharide. W4 (1200-900 cm^{-1}) is dominated by the peaks that belong to polysaccharides. 900-700 cm^{-1} region (W5) is called as the fingerprint region . This part contains bands which are the most characteristic at the species level. The studies also revealed that the best results were obtained with the second derivatives of the spectrum corresponding to 3030-2830 cm^{-1}, 1350-1200 cm^{-1} and 900-700 cm^{-1} ranges and these regions yield reliable identification results for unknown yeast isolates (Figure 2.6).
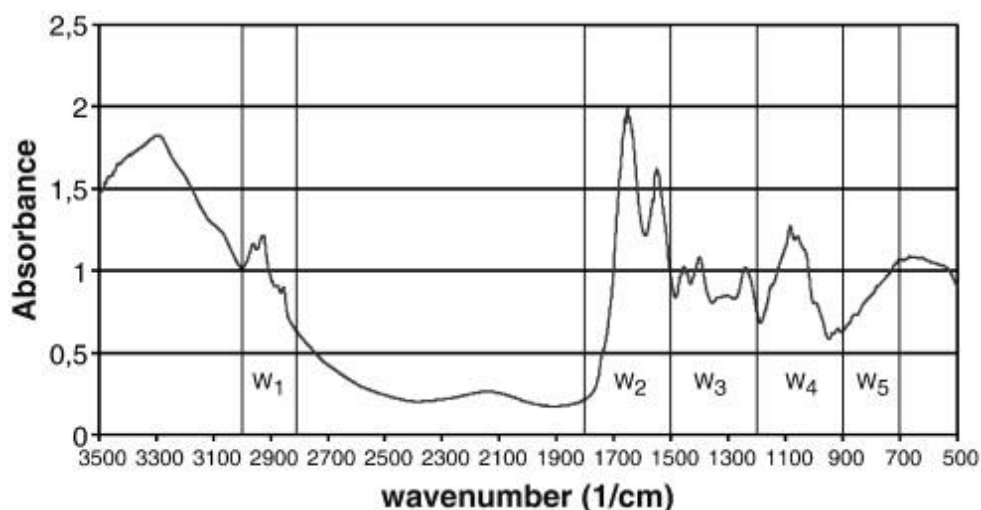
Figure 2.5. Representative FTIR spectrum (3500 to 500 cm^{-1}) from a bacterial cell sample (Source: Alvarez-Ordonez et al., 2011)

Table 2.1. Assignment of some bands frequently found in FTIR spectra respective of biological specimens (Source: Maquelin et al., 2003)

Frequency (cm^{-1})	Assignment[a]
3500	O−H str of hydroxyl groups
3200	N−H str (amide A) of proteins
2955	C−H str (asym) of −CH$_3$ in fatty acids
2930	C−H str (asym) of >CH$_2$
2918	C−H str (asym) of >CH$_2$ in fatty acids
2898	C−H str of C−H in methine groups
2870	C−H str (sym) of −CH$_3$
2850	C−H str (sym) of >CH$_2$ in fatty acids
1740	>C=O str of esters
1715	>C=O str of carbonic acid
1680−1715	>C=O in nucleic acids
1695, 1685, 1675	amide I band components resulting from antiparallel pleated sheets and β-turns of proteins
1655	amide I of α-helical structures
1637	amide I of β-pleated sheet structures
1550−1520	amide II
1515	"tyrosine" band
1468	C−H def of >CH$_2$
1400	C=O str (sym) of COO$^-$
1310−1240	amide III band components of proteins
1250−1220	P=O str (asym) of >PO$_2^-$ phosphodiesters
1200−900	C−O, C−C str, C−O−H, C−O−C def of carbohydrates
1090−1085	P=O str (sym) of >PO$_2^-$
720	C−H rocking of >CH$_2$
900−600	"fingerprint region"

[a] str=stretching; def=deformation; sym=symmetric; asym=antisymmetric.

IR spectra are highly specific for each strain and species, representing the total cell chemical composition such as lipids, proteins, nucleic acids and polysaccharides. By interpreting the infrared absorption spectrum, information about the chemical bonds in a molecule could be obtained. The sum of vibrational spectra for macromolecule content of cells (nucleic acids, proteins, lipids, polysaccharides, etc.) can produce an infrared absorption spectrum that is like a molecular ''fingerprint'' for that biological material. By itself, this spectrum can be diagnostically used in typing or identification application through clustering. Furthermore, FTIR can be utilized to identify some components of an unknown mixture (Essendoubi et al. 2007). This spectroscopic technique presents reliable and rapid results in which identification is cosely related with the quality of the reference

spectral library, and spectral library could be improved by adding more yeast isolates to the database (Kümmerle et al., 1998; Sandt et al., 2003; Timmins et al., 1998).
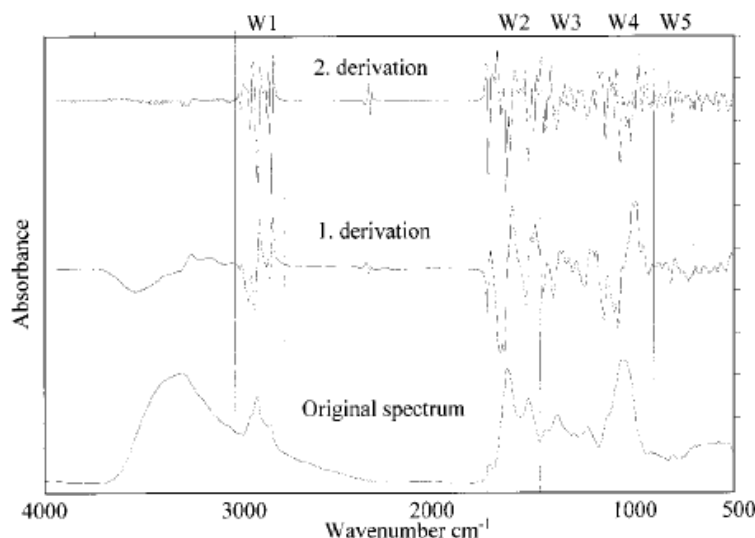
Figure 2.6. Original, 1st and 2nd derivatives spectra of an FTIR measurement of an *S.cerevisiae* strain. Spectral windows (W1-W5) are shown (Source: Santos et al., 2010)

2.3.3.2. Applications of FTIR Spectroscopy

There are some applications of IR spectroscopy to wine analysis for the monitoring of large scale wine fermentations (Di Egidio et al., 2010; Urtubia et al., 2004; Buratti et al., 2011; Moreira and Santos, 2004). In additon to the applications of FTIR on monitoring of wine process to predict the chemical properties, FTIR techniques in combination with different chemometric analyses also could be used in food microbiology applications such as detection, differentiation, quantification, and taxonomic level classification of microorganisms. Therefore, it could provide an idea about the microorganism diversity in the must before fermentation and in the wine during the fermentation process. Although there are many studies on the application of FTIR spectroscopy in wine analysis for monitoring of the chemical properties of the process, there is limited information regarding the monitoring of microbiological content or characterization of yeast flora of wine during whole fermentation process. The only study was by Puxeu et al. (2015) who evaluated the potential of using ATR-FTIR combined with soft independent modeling of class analogy (SIMCA) to discriminate and classify *S. cerevisiae* strains and analyze their chemical changes produced by their different

18

physiological states during a fermentation process. In terms of olive studies, FTIR spectroscopy has been generally applied for evaluation of olive oils rather than table olives (Lerma-Garcia et al., 2010).

An infrared spectrum represents a fingerprint which is the characteristic of any chemical compound. The composition of biological material and its FTIR spectrum is complex and represents a characteristic fingerprint (Kümmerle et al., 1998). Almost 25 years ago, Naumann and coworkers suggested identifying microorganisms by FTIR spectroscopy (Naumann et al., 1991). They assembled a reference spectrum library based on well-characterized strains and species. The FTIR spectra of unidentified isolates are then obtained under the same conditions of the reference spectra and are compared with spectra from the reference spectrum library. If the library has an identical or a very similar spectrum, identification is successful. Therefore, the success of the identification method depends largely on the complexity of the reference spectrum library. Although there are reports with preliminary data indicating that eukaryotic microorganisms such as yeasts may also be identified by FTIR (Henderson et al., 1996); they are based on a very limited number of species and isolates. In order to investigate whether FTIR spectroscopy was an alternative identification method, a standardized sample preparation procedure for yeasts was developed, and the most significant spectral windows were selected for efficient identification, and a spectral reference library of sufficient complexity constructed (Kümmerle et al., 1998).

After 20 years of research, the potential of FTIR spectroscopy for the identification of microorganisms is well documented, and the technique has been applied in many different fields like food microbiology, medical diagnostics and microbial ecology (Wenning and Scherer, 2013). The spectrum of applications ranges from the identification of clinical and food pathogens (Maquelin et al., 2003) or food contaminants to starter and probiotic cultures in food as well as series of bacterial species (Helm et al., 1991), yeasts (Timmins et al., 1998; Ngo et al., 2003; Kümmerle et al., 1998; Oelofse et al., 2010; Büchl et al., 2008; Wenning et al., 2002; Essendoubi et al., 2005; Sandt et al., 2003) and fungi (Santos et al., 2010).

2.4. Phenolic Compounds of Olives

Besides the monounsaturated fat content, the nutritional benefits of table olives are associated with minor constituents such as phenolic compounds (Simopoulos, 2001). Table olives are very good sources of phenolic compounds which have features on demand. It has been claimed that consuming 5–10 table olives a day might cover the daily intake of polyphenols (Boskou et al., 2006). Phenolic compounds have both antimicrobial and antioxidant properties and contribute to prevention of *Dacus olea* infestation of olives. In addition, they play a role in the formation of the black color of olives through a browning reaction. Also, their amounts in olives affect textural and sensorial qualities of this produce. Especially oleuropein and hydroxytyrosol have been reported with their positive health effects such as the prevention of cardiovascular disease, degenerative disease protection, anti-inflammatory and anti-carcinogenic activities due to their antioxidant characteristics (Aktas et al., 2014a).

Although the phenolic content of olive oil has been under investigation for many years, table olives have not been studied to equal extent. The phenolic fraction of table olives is very complex and can vary both in the quality and quantity of phenolic compounds, as it is depended upon processing method, the cultivar, irrigation regimes, and the degree of drupe maturation. The most important changes in the phenolic fraction are the decrease of oleuropein concentration during the olive fruit development and the increase of tyrosol and hydroxytysol concentration. The major phenolic compounds present in table olives are tyrosol, and hydroxytyrosol and the concentration of these compounds is depended upon the degree of maturation and the method of treatment of olive drupe till they become edible (Boskou et al., 2006).

Secoiridoides (oleuropein and derivatives), one of the major classes of polyphenols contained in olives and olive oil, have recently been shown to inhibit or delay the rate of growth of a range of bacteria and microfungi; therefore, they might be efficiently used as alternative food additives or in integrated pest-management programs. Among the bioactive compounds in olives and olive oils, oleuropein and hydroxytyrosol have several biological properties, particularly antioxidant and anti-inflammatory activities (Bisignano et al., 1999).

Comparable to olive oil and fruits, recent studies suggest that olive leaves are also significant sources of bioactive phenolic compounds, especially oleuropein (Lee et al.,

2009). Leaves have been widely used in folk medicine for several thousands of years within Mediterranean islands and countries. Several reports have shown that olive leaf extract could lower blood pressure in animals and increase blood flow in the coronary arteries, relieve arrhythmia and prevent intestinal muscle spasms. In addition, leaves may be used in infusions, allowing a considerable intake/uptake of bioactive compounds (Pereira et. al., 2007). The major physiological substances of olive leaf are hydroxytyrosol, tyrosol, caffeic acid, *p*-coumaric acid, vanillic acid, vanillin, oleuropein, luteolin, diosmetin, rutin, verbascoside, luteolin-7-glucoside, apigenin-7-glucoside, and diosmetin-7-glucoside (Lee and Lee, 2010).

Changes in phenol content during olive fruit development are important. In unripened olives, one of the main phenolic compounds responsible for producing bitterness in fruits is oleuropein, a 3,4-dihydroxy-phenylethanol (hydroxytyrosol) ester with a β-glucosylated elenolic acid. It belongs to a specific group of coumarin-like compounds, the secoiridoids, which are abundant in Oleaceae. Secoiridoids are compounds that are usually glycosidically bound and produced from the secondary metabolism of terpenes (Bendini et al., 2007). This compound is known to be the most prominent and significant individual phenolic of olive pulp. The concentration of oleuropein varied with olive variety and declined with the fruit physiological development. Hydroxytyrosol (3,4-dihydroxyphenyl-ethanol) is one of the principal degradation products of oleuropein. In previous studies, it was found in much smaller quantities relative to oleuropein and showed an inverse evolution any trend during ripening. The enhancement of hydroxytyrosol concentrations could be attributed to the increased activity of the hydrolytic enzymes, in particular, glycosidases and esterases which catalyze the hydrolysis of the oleuropein, with the production of oleuropein aglycon, elenolic acid and 3,4-dihydroxyphenylethanol. Tyrosol (p-hydroxyphenyl-ethanol) is another phenolic monomeric compound like hydroxytyrosol. Both hydroxytyrosol and tyrosol are the most abundant phenolic alcohols in olives (Jemai et al., 2009). Flavonoids are also widespread secondary plant metabolites. During the past decade, an increasing number of publications on the beneficial health effects of flavonoids have been reported, and these effects are related to cancer and coronary heart diseases. Flavonoid aglycones are subdivided into flavones, flavonols, flavanones, and flavanols depending upon the presence of a carbonyl carbon at C-4, an OH group at C-3, a saturated single bond between C-2 and C-3, and a combination of no carbonyl at C-4 with an OH group at C-3, respectively. Several authors have reported that flavonoids such

as luteolin and apigenin are also phenolic components of olive oils. Luteolin may originate from rutin or luteolin-7-glucoside, and apigenin from apigenin glucosides. There are also several interesting studies in which several flavonoids have been found in olive leaves and fruits (Bendini et al., 2007).

There are some studies about phenolic profiles of natural black olives, similar with Hurma olives. In the study by Zoidou et al. (2009), it was determined that Throuba Thassos olive had a higher oleuropein content compared to other nine Greek olive varieties. In another study (Jemai et al., 2009), the phenolic profile of the Dhokar variety grown in Tunisia was followed up during its maturation period and compared with a common variety, Chemlali. It was concluded that oleuropein was the main phenolic compound for both varieties at the early stages of ripening; however, the amount of this phenolic compound decreased with maturation, even to very low levels in Dhokar while it was still in measurable amounts in Chemlali, and the hydroxytyrosol concentration increased.

2.5. Characterization of Antimicrobial Activity using FTIR Spectroscopy

Some of the applications of FTIR spectroscopy technique include the assessment of the mechanisms of bacterial inactivation by food processing technologies and antimicrobial compounds (Zoumpopoulou et al., 2010; Schleicher et al., 2005), monitoring of membrane properties in changing environments (Ami et al., 2009), detection of stress-injured microorganisms in food-related environments (Al-Qadiri et al., 2008a; Al-Qadiri et al., 2008b), assessment of dynamic changes in bacterial populations (Ngo-Thi and Naumann, 2007), study of bacterial tolerance responses (Alvarez-Ordonez et al., 2010) and study of spore ecology in foodborne pathogenic bacteria (Subramanian et al., 2007). In addition to the research about the cellular characterization and discrimination by FTIR spectroscopy of diverse foodborne pathogenic bacteria at the species and subspecies level, an increasing number of researches have been emerging in the last years using this spectroscopic technique for the assessment of the structural modifications occurring in food-associated microorganisms in response to stress conditions. Some of these researches have shown the efficacy of FTIR spectroscopy for the study of the mechanisms of death induction resulting from vegetative cell exposure

to different food processing technologies, antimicrobial compounds and adverse environmental conditions. These studies have been particularly focused on effects of stress conditions on the cytoplasmic membrane composition and structure. This technique has recently been used to determine the presence and quantity of injured vegetative cells in food products and the efficacy of food processing treatments. IR spectroscopy was also reported to be a suitable method to evaluate stress-induced changes in spore components, suggesting the use of this technology to monitor the efficacy of sterilization techniques in the inactivation of spore-forming microorganisms (Alvarez-Ordonez et al., 2011). Besides bacteria, FTIR spectroscopy has also been used for assessment of stress response in yeasts, e.g. *Saccharomyces cerevisiae.* This yeast can be considered a valid model as it has the combined advantages of manipulating microbial cells and its eukaryotic nature, and these advantages allow extending the bioassay results to other eukaryotes, including human (Corte et al., 2010). However, although there are many studies monitoring the stress response of bacterial cells by FTIR spectroscopy, only a few researches have been published about yeasts (Corte et al., 2010; Corte et al., 2014; Saharan and Sharma, 2011).

2.6. Multivariate Statistical Analysis

Introduction of modern instrumental analysis and the availability of computers have allowed in collection of large data sets which leads the necessity of using multivariate statistical analysis techniques. Multivariate statistical analyses (chemometrics) provide information about the relationship among variables in the whole sample matrix (Sen and Tokatli, 2014). Multivariate statistical analysis of FTIR spectra (chemometrics) can be classified as supervised and unsupervised methods. The objective of unsupervised methods is to extrapolate the spectral data without a prior knowledge about the sample studied whereas supervised methods require prior knowledge of the sample to build a model for the prediction of the identity of unknown samples (Cozzolino et al., 2009).

The unsupervised statistical techniques investigate the similarity and/or relationship within the data set without the prior information of any class membership. For unsupervised techniques, no information or grouping is necessary for the model development. The two techniques which are commonly used in microbiological applications are principal component analysis (PCA) and hierarchical cluster analysis

(HCA). PCA is the most widely used multivariate statistical technique. It is used for screening, extracting and compressing multivariate data. This technique builds a mathematical model by transforming a matrix of correlated response variables into a set of non-correlated variables and these new variables are called as principal components (PC). With this operation, the numbers of variables are reduced to a smaller number of scores and scores explains the particular structure of original data matrix (Cozzolino et al., 2009). HCA is another unsupervised pattern recognition technique and classifies samples according to their similarities and the results are shown as the groups in the form of a 2-dimensional plot called dendrogram. The first step is to calculate the similarities between objects and then use linkage methods to link the objects. The dendrogram or tree diagram has the vertical axis that indicates the similarity of or distance between samples while horizontal axis organizes objects according to their similarities in a row (Figure 2.7).
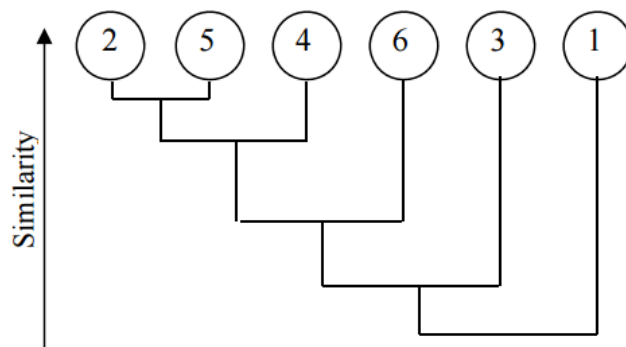
Figure 2.7. Dendrogram of a cluster analysis
(Source: Brereton, 2003)

Supervised statistical techniques are used to group samples using variables with predefined groups. Among them, the partial least squares-discriminant analysis (PLS-DA) is a supervised pattern recognition technique and it has the advantage of applying partial least squares (PLS) algorithm for the discrimination of samples. The purpose of this technique is to discriminate two or more groups with respect to a set of variables. SIMCA is a soft modeling technique and this technique is based on the idea that the observations may belong to either one of the two classes. However, the observations may belong to both classes at the same time or they may not be in either class.

CHAPTER 3

CHARACTERIZATION OF WINE YEASTS

3.1. Materials and Methods

3.1.1. Wine Samples

Seven wine samples (2 white wines: Muscat and Chardonnay; 1 rose wine: Sangiovese; 4 red wines: Syrah, Merlot, Cabernet Sauvignon and Bogazkere) were obtained from a local winery (Urla Winery, Urla-Izmir, Turkey). Grapes used for the wine processes were from vineyards in Urla, Izmir. Some critical stages during the wine production was chosen as the sampling sites (Figure 3.1). A total of 35 wine samples were obtained at the end of the process as shown in the diagram. Transfer of the samples to the laboratory were done on the sampling day. Process of Bogazkere wine was halted after the third stage of production due to a problem; therefore, data was only collected before this stage for this wine sample. Samples were kept in the Schott bottles at 4°C. The samples which were not analyzed at the same day were stored at -20°C till usage. The general schematic diagram of wine analysis are shown in Figure 3.2.
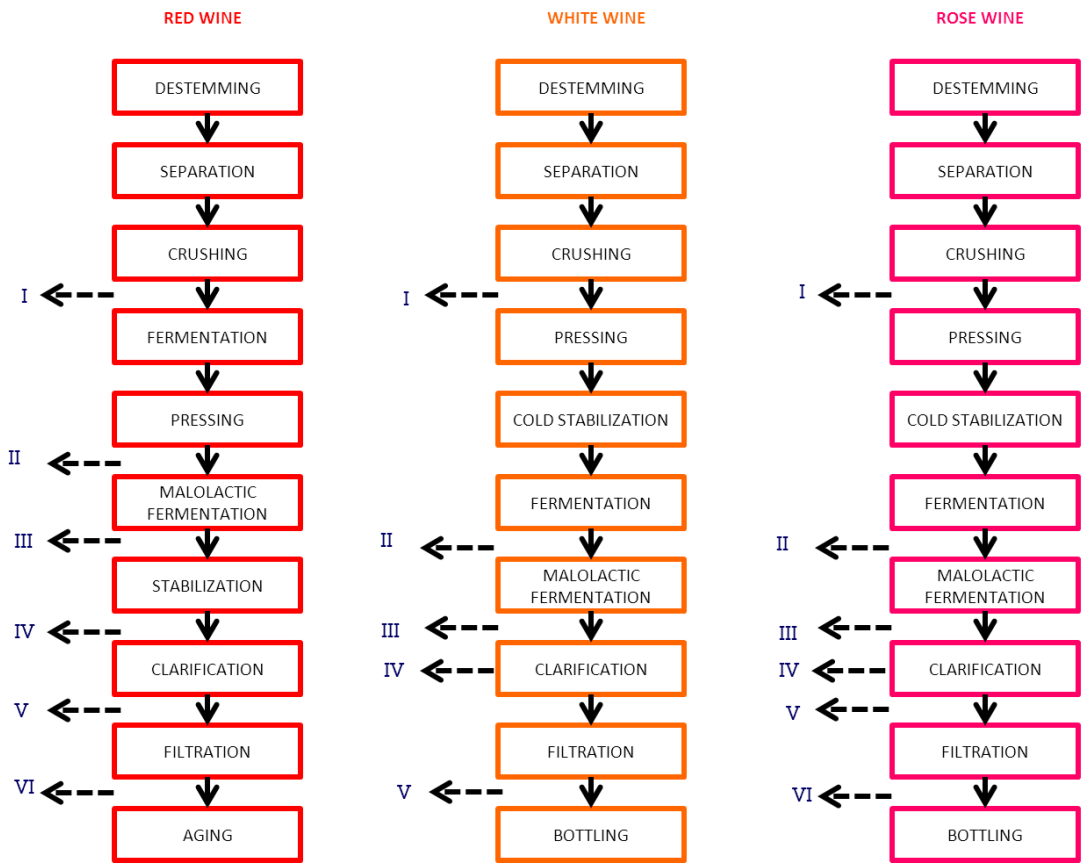
Figure 3.1. Red, white and rose wine processes and the sites of sampling
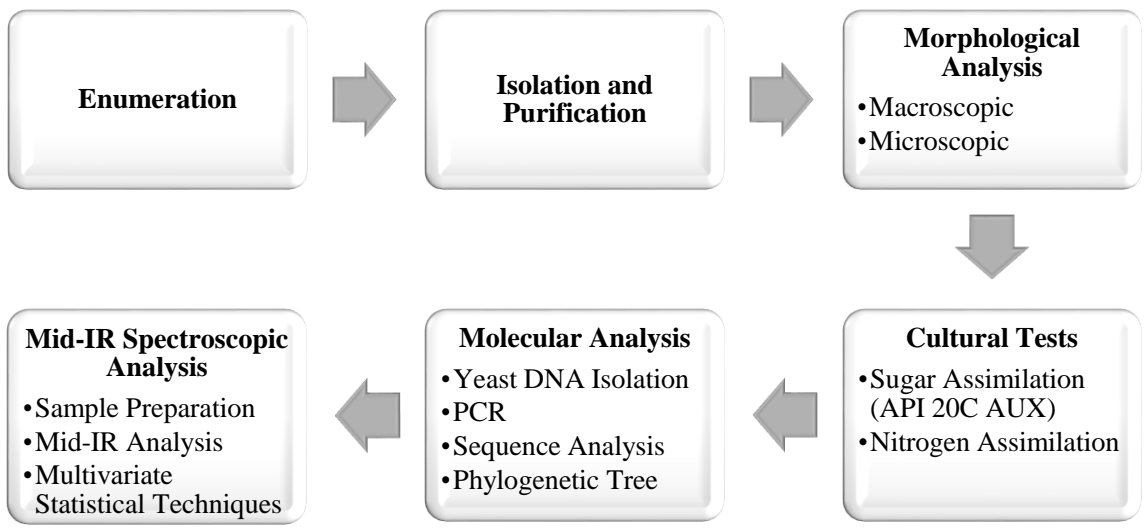
Figure 3.2. Schematic diagram of wine analysis

3.1.2. Enumeration, Isolation and Purification of Yeasts

Method provided by International Organization of Vine and Wine (OIV, 2009) was used in the microbiological analysis of the must and wine samples. Since it has been used for inoculation of all wines for fermentation process, *Saccharomyces cerevisiae* (NRRL Y-139, ATCC 2366) was chosen as a positive control. This reference yeast was prepared from its glycerol stock solution (25%) at -80°C and subcultured on yeast extract peptone dextrose (YEPD) agar medium (10 g/L yeast extract, 20 g/L peptone, 20 g/L dextrose and 20 g/L agar) at 28-30°C for 48 h.

The enumeration of the wine samples was done with serial 10 fold dilutions in 0.1% peptone water, with three replicates. Inoculation was done into YEPD agar medium, followed by incubation at 28-30°C for 48 h. All of the suspected yeast colonies were counted (CFU/mL) and evaluated directly under phase contrast microscope (Olympus-CX31, USA).

Besides typic *S. cerevisiae* colonies, each atypic yeast colony was also isolated and purified in order to observe the microbial diversity of must and wine samples during fermentation. All of the suspected yeast colonies were isolated from the agar plates according to the morphological differences in colony shapes, colors, size and the specific yeast odour for direct examination under phase contrast microscope. The purified yeast cultures were stored in both 4°C and -80°C for further experiments.

3.1.3. Morphological Analysis

For characterization of purified yeast colonies, primarily morphological analysis were performed on Malt Extract Broth (MEB, Difco) and Malt Extract Agar (MEA, Difco) media using the protocol described by Kurtzman et al (2011).

For examination of *macroscopic morphology*, yeasts were grown in both liquid (MEB) and solid (MEA) media at 28-30°C for 48-72 h. Yeast cultures in MEB were evaluated in terms of film formation at the surface, haze formation, gas formation in Durham tubes, presence and type of sediment (fine/coarse), presence of suspended particle; whereas yeast colonies in MEA were evaluated by their texture (dull/shiny), shape (convex/concave), border (smooth/rough), color and size.

For *microscopic morphology*, yeast smear was prepared using colonies on MEA to examine cell shape, cell size, mycelium formation and form of asexal reproduction and using colonies on Gorodkowa agar (glucose 0.1%, peptone 1%, NaCl 0.5%, agar 2.5%) and McClary acetate agar (glucose 0.1%, KCl 0.18%, yeast extract 0.25%, sodium acetate 0.82%, agar 1.5%) to examine sporulation. Prepared slides were viewed under phase contrast microscope.

3.1.4. Cultural Tests

In order to evaluate the cultural characterization results, the identification key introduced firstly by Kurtzman and Fell (1998) was used.

3.1.4.1. Sugar Assimilation Test (API 20C AUX)

The API 20C AUX system (bioMe´rieux, Marcy l'Etoile,France), a commercial kit for the evaluation of the assimilation of 19 carbon sources, including D-GLUcose, GLYcerol, calcium 2-Keto-Gluconate, L-ARAbinose, D-XYLose, ADOnitol, XyLiTol, D-GALactose, INOsitol, D-SORbitol, Methyl-αD-Glucopyronoside, N-Acetyl-Glucosamine, D-CELlobiose, D-LACtose (bovine origin), D-MALtose, D-SACcharose (sucrose), D-TREhalose, D-MeLeZitose and D-RAFfinose, was used according to the manufacturer's instructions. These commercial test strips consist of 20 cupules which contain dehydrated carbon substrates for assimilation reaction. Briefly, cupules on plastic strips were inoculated with yeast suspensions having a turbidity equal to 2 McFarland standard according to the manufacturer's instructions, followed by incubation of strips at 28-30°C for 48-72 h. At the end of incubation period, cupules which show turbidity greater than that of the negative control were accepted as positive result and a profile number was generated based upon the reactions observed for each strip. Identifications were made by the software program (bioMe´rieux, apiweb, v4.0) using this generated microcode. If the profile was listed as excellent, very good or acceptable or the results were in agreement with the reference identification, then the results were considered correct (Arias et al., 2002). The flow diagram of application of API 20C AUX commercial kit is shown in Figure 3.3.

PREPARATION
- Preparation of a suspension equal to 2 McFarland using fresh yeast cultures (48 h) in 0.85 % NaCl solution
- Transfer of 100 µL solution into API C Medium in the ampoules supplied by the manufacturer and homogenization of the mixture

INOCULATION
- Filling of cupules in the strips with this suspension according to instructions, avoiding bubble formation
- Closing the cap and incubation of the strips at 29 °C for 48-72 h.

READING
- Comparison of the 19 cupules with "0" (as negative control) cupule after 48 and 72 h
- Turbidity significantly greater than that of the negative control → positive result

EVALUATION
- Observation of a profile number based upon the each positive reactions for each strip
- Identifications were made using this microcode with 7 digits for each strip by identification software program

Figure 3.3. The flow diagram of application of API 20C AUX commercial kit

3.1.4.2. Nitrogen Assimilation Test

Assimilation of nitrogen compounds by yeast colonies was evaluated using yeast carbon base agar (YCBA, Sigma-Aldrich) medium as it was reported by Pincus et al. (1988) with some modifications. Briefly, a single colony of each yeast isolate was suspended in tubes containing 15 mL of sterile YCBA medium at 50°C. Suspension was then poured into a petri plate and allowed to solidify at 25°C. Sterile 3 mm-diameter paper disks were impregnated with KNO_3 by soaking in a sterile 3% aqueous solution of KNO_3 and were air-dried for 1 h. Positive growth control disks were prepared similarly by soaking paper disks in a 3% solution of peptone. These two disks were placed aseptically 4 cm apart on the surface of each seeded plate. The plates were incubated at 25-30°C and examined daily for growth (turbidity) around the KNO_3 and peptone disks. The growth around KNO_3 disks shows positive result.

3.1.5. Molecular Tests

3.1.5.1. DNA Isolation of Yeasts

DNA of yeast cells were isolated according to the yeast DNA preparation protocol by Hoffman and Winston (1987) with some modifications (Figure 3.4). Briefly purified fresh yeast cells grown in YEPD agar medium were transferred into 1 mL sterile deionized H_2O and centrifuged at 14,800 rpm for 10 min. The supernatant was removed and 400 µL of lysis buffer (2% Triton X-100, 1% SDS, 100 mM NaCl, 10 mM TrisCl-pH 8.0, 1 mM EDTA-pH 8.0), 0.3 g glass beads (0.25-0.5 mm, Carl Roth, Germany) and 250 µL of phenol/chloroform/isoamylalcohol (25:24:1) were added to supernatant. The suspension was mixed by a vortex for 5 min, kept in waiting for 30 sec and mixed for additional 1 min. After centrifugation of the mixture at 14,000 rpm for 10 min, upper aqueous phase was transferred to a new eppendorf tube and 100 µL of chloroform was added. The mixture was mixed again with vortex for 1 min, followed by centrifugation at the same speed for 10 min. The upper aqueous phase was transferred to a new tube and 650 µL of ice-cold ethanol was added. By inverting the tube it was generally possible to see DNA. After the last centrifugation at the same speed for 10 min, the supernatant was removed and the pellets were vacuum-dried for 30 min using vacuum concentrator with centrifuge (Thermo, Savant ISS110, USA). The dried pellet was resuspended in 40 µL of TE (10 mM Tris-pH 8.0 and 1 mM EDTA-pH 8.0) buffer and DNA concentration was measured using nanodrop (Thermoscientific, USA).

DISRUPTION of the CELL WALL
- Transfer of many yeast cells to 1 mL sterile dH$_2$O in an eppendorf tube and obtaining pellet by centrifugation at 14,800 rpm for 10 min
- Addition of lysis buffer+0.3 g glassbeads+250 µL of phenol/chloroform/isoamylalcohol (25:24:1) to the pellet and mixing by vortex for 5 min, waiting for 30 sec and mixing for 1 min again

PURIFICATION of DNA
- Obtaining pellet by centrifugation at 14,000 rpm for 10 min and transfer of upper aqueous phase to a new tube
- Addition of 100 µL chloroform and mixing by vortex for 1 min

PRECIPITATION of DNA
- Obtaining pellet by centrifugation at 14,000 rpm for 10 min and transfer of upper aqueous phase to a new tube
- Addition of 650 µL ice-cold ethanol and mixing by inverting the tube
- Obtaining pellet by centrifugation at 14,000 rpm for 10 min and vacuum-drying of pellets for 30 min
- Resuspension of the pellet in 40 µL TE buffer and measurement of DNA concentration using nanodrop

Figure 3.4. The flow diagram of rapid yeast DNA isolation

3.1.5.2. Polymerase Chain Reaction (PCR)

The amplification reaction of 5.8S rRNA gene and the intergenic spacers ITS1 and ITS2 was performed using ITS1 and ITS4 primers having the sequences 5'-TCCGTAGGTGAACCTGCGG-3' and 5'-TCCTCCGCTTATTGATATGC-3', respectively (Esteve-Zarzoso et al., 1999). Since some of the yeast species could not be identified by amplification of 5.8S rRNA gene and intergenic spacers, the amplification reaction of unidentified species was performed using D1 and D2 domains of the 26S rRNA gene using NL1 and NL4 primers, having the sequences 5'-GCATATCAATAAGCGGAGGAAAAG-3' and 5'-GGTCCGTGTTTCAAGACGG-3', respectively (Kurtzman and Robnett, 1998).

PCR analyses were optimized and performed in a 50-µL volume PCR reaction mix containing 5 µL of 10x reaction buffer (Fermentas, USA), 5 µL of 25 mM MgCl$_2$ (Fermentas, USA), 5 µL of 2 mM dNTP mix (Fermentas, USA), 0.5 µL of 0.2 pmol each forward and reverse primer (Fermentas, USA), 5 µl (~100 ng/µL) of DNA as template,

31

0.1 µL of 0.5 U/rxn Taq DNA polymerase (Fermentas, USA) and 28.9 µL of deionized H_2O. Amplification was carried out in a thermal cycler (Bio-Rad, C-1000, France) using the following thermal cycling conditions: initialization at 94°C for 5 min, denaturation at 94°C for 1 min, annealing at 55°C for 1 min and elongation at 72°C for 1 min. This was repeated for 40 cycles plus a final incubation step at 72°C for 10 min (Arroyo-Lopez et al., 2006). Resulting PCR products were analysed by electrophoresis through 1% (w/v) agarose gel (Bio-Rad, Versadoc 4000MP) including 10 mg/mL ethidium bromide solution, in 1xTAE buffer. For loading samples, 2 µL of 6x loading dye (Fermentas) was mixed with 10 µL of PCR product. DNA molecular weight marker GeneRuler 100 bp Plus DNA Ladder (Fermentas, USA) was used as standard. The electrophoresis was run through 80 mV followed by screening of PCR products using UV illuminator and gel documentation system (Vilber Lourmat, France).

3.1.5.3. Purification of PCR Products

All amplicons were purified using the Sephadex G-50 spin column (Sigma) with a receiver column (MN 740522). For this aim, 1 g of Sephadex G-50 was dissolved in deionized H_2O, mixed vigorously for 5 min and 650 µL of the solution was added to spin columns. After 30 min, the column stopper was discarded and the solution was centrifuged at 5,400 rpm for 2 min. Then, the supernatant was removed and Sephadex spin columns were placed into eppendorf tubes to collect samples. 10-15 µL of PCR product was poured into the middle of the spin column containing Sephadex G-50 and centrifuged again at the same conditions. Purity of the purified PCR products was then measured by nanodrop (Thermoscientific, USA) and samples having 260/280 absorbance between 1.8 and 2.0 were used for DNA sequence analysis.

3.1.5.4. Sequence Analysis

The cycle sequence was performed before sequence analysis to label nucleotides by fluorescence in a thermal cycler. The differences between this cycle sequence from previous PCR analysis are; (1) using just one primer in each cycle sequencing reaction and (2) use of dideoxynucleotides which interrupt the extension of the DNA strand.

For this aim, DNA fragments were sequenced in forward direction using either ITS1 or NL1 primers and a BigDye Terminator Cycle Sequencing system (version 3.1; Applied Biosystems, USA) according to the manufacturer's instructions. The PCR mixture included 2 µL of DNA template (3-10 ng/µL), 1 µL of primer (3.2 pmol/µl), 1 µL of BigDye terminator v1.1, v3.1 5x sequencing buffer, 2µL of BigDye (3.2 pmol/µl) and 4 µL of deionized H_2O. The cycle sequencing conditions were the same with that of PCR analysis. At the end of cycle sequencing, the products were placed into ABI 3130XL genetic analyzer (Applied Biosystems, Taipei, Taiwan) sequence device which is based on capillary electrophoresis. The capillaries were loaded with 7 mL of flowable polymer (3130 POP-7 polymer) and 25 mL of buffer for anode and cathode poles (Genetic Analyzer 10x running buffer with EDTA) prior to run. Finally, the nucleotide sequence results were evaluated by a software (Finch TV v.1.4.0, Geospiza.Inc, USA) and species were identified by searching databases using the BLAST sequence analysis tool (http://www.ncbi.nlm.nih.gov/BLAST/). The sequence was compared using nucleotide-nucleotide BLAST (blastn) with default settings. Species identification was determined from the lowest expect value of the BLAST output.

3.1.5.5. Construction of Phylogenetic Trees

A phylogenetic tree is a diagram showing the evolutionary relationships among a group of organisms (taxa or genes) from a common ancestor. The tips of the tree represent groups of descendant taxa (often species) and the nodes on the tree represent the common ancestors of those descendants. Two descendants that split from the same node are called sister groups which are each other's closest relatives (Baum, 2008).

Phylogenetic analysis of the DNA sequences of wine yeasts were performed by Mega6 software using the Neighbor-Joining method, after alignment by Clustal Omega program (with default settings; http://www.ebi.ac.uk/Tools/msa/clustalo/).

3.1.6. Mid-Infrared Spectroscopic Measurements

3.1.6.1. Sample Preparation

The yeast colonies of wine samples were used in FTIR spectroscopy analysis by either *directly*, which is a faster method; or after a *drying step,* since sample desiccation is necessary to avoid strong water absorption bands especially in the protein region of the spectra. In both methods, culturing was carried out with the same medium (YGC agar) at 28-30°C for 48 h. For direct measurement of yeast samples, yeast colonies were carefully scraped from the agar plate with a 10 µL plastic loop and were spread on ZnSe crystal as a thin film.

In order to obtain dried yeast colonies, yeast cells were harvested by carefully scraping the agar plate with a 10 µL plastic loop and were resuspended in 1 mL of distilled water. The concentration of each suspension was spectrophotometrically measured (Thermo, Vario Skan Flash) at 500 nm and adjusted to an optical density of 3±0.1 to control film thickness (Sandt et al., 2003). 35 µL of each suspension was transferred to a ZnSe optical sample carrier and dried at 42±2°C for 1 h to yield transparent films, which were used directly for FTIR spectroscopy (Kümmerle et al., 1998).

3.1.6.2. Mid-Infrared Spectroscopy Analysis

All yeast samples were scanned through an FTIR spectrometer (Perkin Elmer Spectrum 100, Wellesley, MA) within the range of 4000-650 cm^{-1} wavenumber. This equipment has a horizontal attenuated total reflectance (HATR) accessory with ZnSe crystal (45 deg. Trough Plate) and deuterated tri-glycine sulphate (DTGS) detector. The scanning was carried out at 4 cm^{-1} resolution with 64 scans for each spectrum and 1 cm/s scan speed. The sampling crystal was cleaned with ethanol, and distilled water after each measurement and dried under nitrogen flow.

3.1.6.3. Multivariate Statistical Analysis

The data from the FTIR spectrometer was evaluated statistically by using multivariate statistical techniques including PCA (Principal Component Analysis) and HCA (Hierarchical Cluster Analysis) with SIMCA software (SIMCA 13.0.3, Umetrics Inc., Sweden).

3.2.   Results and Discussion

3.2.1. Enumeration and Isolation of Yeasts

The total yeast counts of each wine process at different sampling stages and yeast growth during the process are shown in the Table 3.1 and Figure 3.5, respectively. It is observed from Table 3.1 that the yeast count is variable during the process for all wine samples. The microbial population including yeasts and bacteria at the beginning of the process comes from the grape itself and passes to the must through pressing step. As the fermentation proceeded, yeasts similarly used the sugars, increased their population and produced ethanol which is the reason for the decrease in the total population by suppressing the bacterial growth. Figure 3.5 also showed that yeast population decreased during fermentation process of Cabernet and Boğazkere; whereas a decrease and rise trend of the count was observed for the other wines. The reasons for this can be explained by two problems encountered in fermentation process of these two wines. Because of the softness of Boğazkere grape, stems could not be successfully separated from the grape and fermentation was performed with grapes and stem, which resulted in bitter and astringent flavor in this wine due to the components in the stems (Oral communication with Urla Winery). These components might have influenced and decreased the yeast growth from the beginning of wine process. On the other hand, since too much SO_2 was applied to Cabernet grapes in vineyards and this chemical reversely influenced the growth of yeast, the sugar content of this wine could not be taken under control according to information obtained from Urla Winery. Our results did not show any unusual values for sugar analysis (Canal and Ozen, 2015) but this information may explain the decrease of yeast count.

Table 3.1. Total yeast counts of wine samples during the processes of various wines

Wine Variety	Process Steps*	Yeast (CFU/mL)
Muscat	*I*	3.3×10^4
	II	1×10^2
	III	6.7×10^4
	IV	<10
	V	4.7×10^1
Chardonnay	*I*	1.1×10^2
	II	1.4×10^7
	III	5.2×10^6
	IV	1.2×10^4
Sangiovese	*I*	1.4×10^4
	II	2.5×10^5
	III	5.5×10^5
	IV	1.3×10^4
	V	5×10^1
	VI	3.4×10^2
Syrah	*I*	3.1×10^5
	II	4.1×10^5
	III	7×10^4
	IV	6.3×10^4
	V	9.6×10^2
	VI	1.8×10^5
Merlot	*I*	1.8×10^5
	II	1.1×10^5
	III	8.2×10^4
	IV	1.6×10^3
	V	8.3×10^1
	VI	1×10^3
Cabernet	*I*	7.3×10^6
	II	5.1×10^5
	III	1.3×10^4
	IV	4.3×10^2
	V	2.3×10^2
Boğazkere	*I*	1.8×10^7
	II	2×10^3
	III	2×10^1

* Numbers I-VI corresponding to sampling stages of wines; (I) beginning of fermentation for red, before pressing of white and rose wines, (II) end of fermentation, (III) beginning of stabilization for red wines and clarification of rose/white wines, (IV) before clarification of red wines and during clarification of white/rose wines, (V) end of clarification of red/rose wines and before bottling of white wines and finally (VI) beginning of aging and bottling.
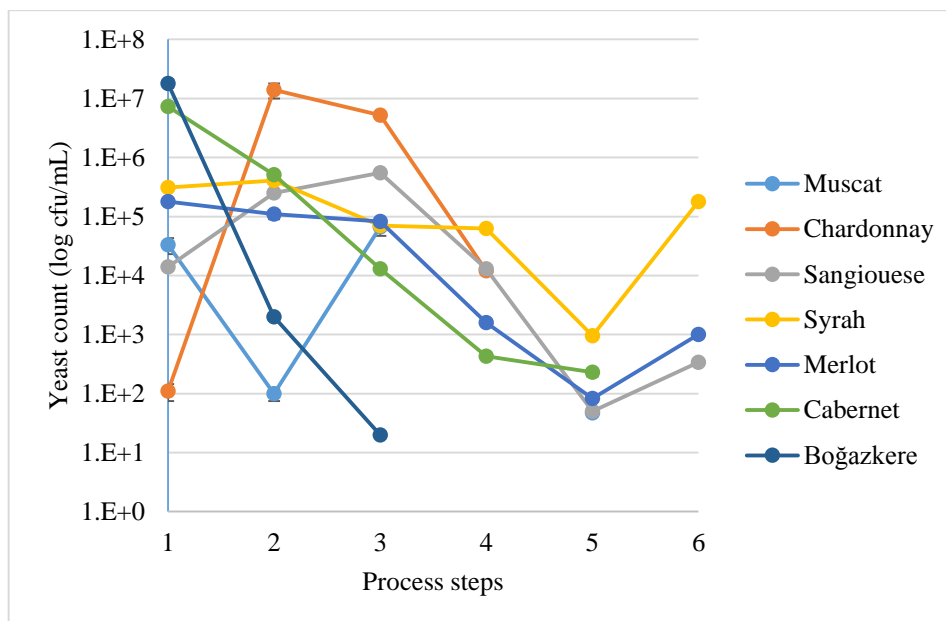
Figure 3.5. The yeast growth during wine process. Process steps (1-6) correspond to 1st, 13rd, 32nd, 46th, 59th, 65th days for wine samples, respectively. Sampling was done at six points for Sangiovese, Merlot and Syrah, at five points for Muscat and Cabernet, at four points for Chardonnay and at three points for Boğazkere

Wine fermentation is typically performed by a complex and gradual change of microorganisms including both yeasts and bacteria. In general, alcoholic fermentation stage is dominated by yeasts since chemical composition and the low pH values of the grape juice favor the yeast growth. Most wine fermentations have a diverse population of yeasts including *Saccharomyces* in the beginning. The non-*Saccharomyces* yeasts typically grow for several days before the fermentation is dominated by *Saccharomyces cerevisiae* strains and a simultaneous increase in ethanol concentration is also observed at this stage. The predominance of *S. cerevisiae* is probably related to its high ethanol tolerance as compared with other yeasts present in the wine environment (Cocolin et al., 2000). Since the quality of wines is directly related to the gradual change of the microbial flora of the must during fermentation, it is important to determine and identify the yeast isolates that play a role on fermentation of different wine samples during a whole wine process.

Following enumeration, a total of 19 typic yeast colonies were isolated from different samples in order to observe the yeast diversity of must and wine during fermentation. The purified yeast colonies were examined under phase contrast microscope, as shown in the Figure 3.6.

37

3.2.2. Morphological and Cultural Analysis

The evaluation of *macroscopic* and *microscopic* morphology of the wine yeasts are shown in the Appendix Tables A.1 and A.2, respectively. The cultural test results including API 20C AUX carbohydrate assimilation reaction, nitrogen assimilation and durham tests are presented in Appendix Table A.3. Appendix B shows the identification key of yeasts described by Kurtzman and Fell (1998) according to cultural test results. As a result, it was possible to characterize these 19 wine yeasts according to cultural test results with the help of this identification key. The characterization results of wine yeasts by all of the cultural methods in comparison with API 20C AUX commercial kit, in addition to molecular test results are given in Table 3.2. According to this table, it can be concluded that API 20C AUX test results showed 7/19 (37%) similarity at the genus level and 5/19 (26%) similarity at the species level with the results of identification key and all yeast samples could be identified by API test kit. The most isolated yeasts with both commercial kit and cultural methods belong to the genus of *Candida* and *Saccharomyces*.
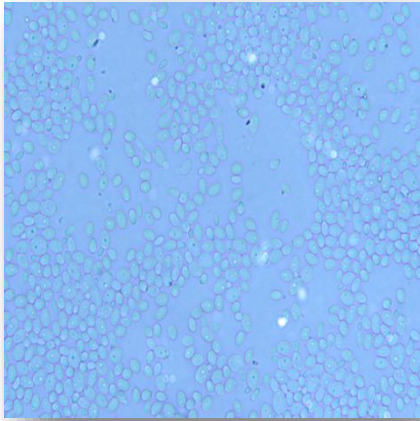
(a)
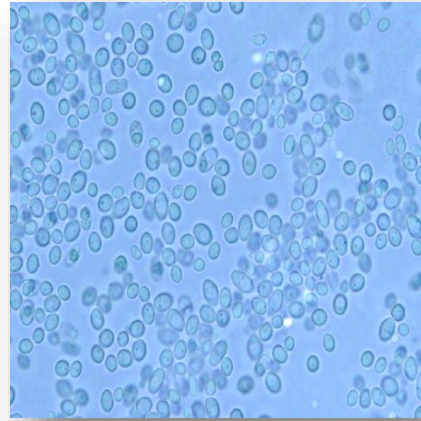
(b)
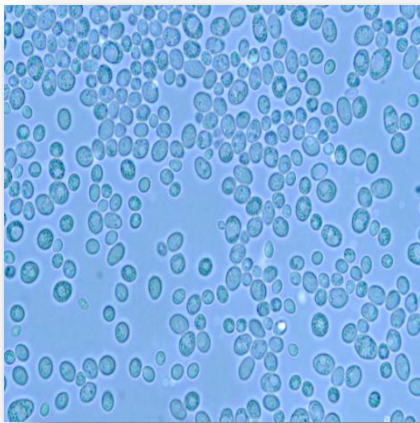
(c)
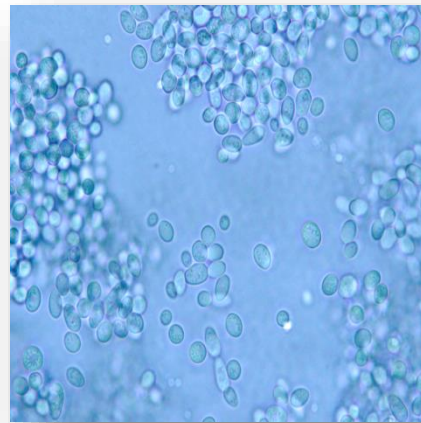
(d)
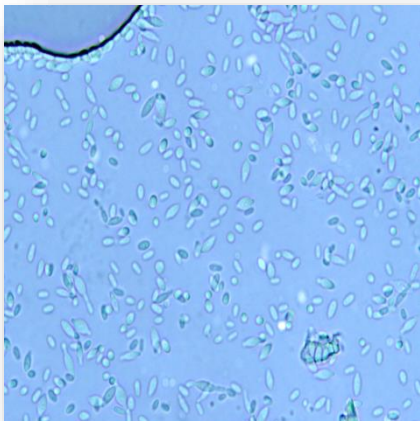
(e)
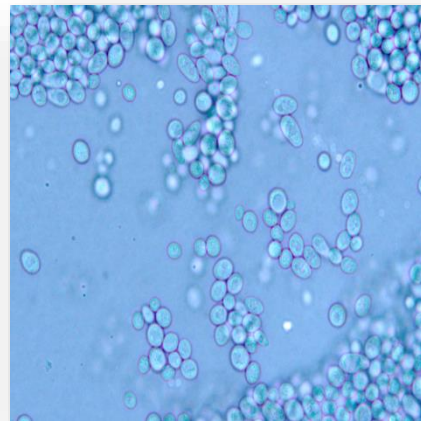
(f)

Figure 3.6. Images (a-f) of wine yeasts under phase contrast microscope using 100X magnification, corresponding to Mp2 (Sangiovese-I), Pm1 (Muscat-I), Sc1 (Chardonnay-II), Sc3 (Muscat-III), Hu1 (Merlot-I), Pm3 (Syrah-I), respectively

3.2.3. Molecular Analysis

In order to perform molecular identification, firstly DNA of isolated wine yeast species were extracted and DNA concentrations were obtained from nanodrop measurements. DNA of yeasts having purity ratio (260/280) ~1.8 were used for further amplification reaction (data not shown). Following DNA extraction, PCR was applied to amplify the selected region of yeast DNA using ITS primers and for ITS-unidentified-yeasts using NL primers. The agarose gel electrophoresis results of PCR products of all wine yeasts are shown in Figure 3.7 and the results of sequence analysis in comparison with other cultural test results are provided in Table 3.2.

According to Table 3.2, 11 of 19 (58%) and only 4 of 19 (21%) yeast isolates showed similarity at the genus level with API 20C AUX test results and with the results of identification key, respectively. Since *Kloeckera appiculata* is the anamorphic state of *Hanseniaspora uvarum*, they were counted in subgroup of *Hanseniaspora* sp. when comparing cultural and molecular test results (Garcia-Martos et al., 1999). All of the isolated wine yeasts were successfully identified molecularly, including the species *Metschnikowia pulcherrima* (2/19, 11%), *Pichia membranifaciens* (3/19, 16%), *Hanseniaspora uvarum* (1/19, 5%) and *Saccharomyces cerevisiae* (13/19, 68%). *S. cerevisiae* is the most isolated yeast species particularly toward the end of wine process since the starter culture (*S. cerevisiae*) was added before fermentation step (Figure 3.1); whereas must samples belonging to different wines contain various types of yeast species isolated at the beginning of the process. As the process proceeded *S. cerevisiae* became dominant species due to high ethanol concentration. The only exception of this situation was observed for the sample "Sc13" which was isolated from Cabarnet at the beginning of fermentation and identified as *S. cerevisiae*.

Table 3.2. Characterization of wine yeasts by cultural and molecular methods

| Yeast code* | Wine source-Sampling time | CULTURAL | | | | MOLECULAR | | |
| | | *API 20C AUX* | | | *with identification key* (Kurtzman and Fell, 1998) | *Sequence analysis* | | |
		Significant Taxa	% ID	Identification Note		*Species*	*Max ID %-*	*GenBank Accession Number*
1 (Mp1)	Syrah-I	*Candida famata*	68.8	very good	*C.guilliermondii, see also C.famata and C.norvegensis*	*M.pulcherrima*	90	HM067867.1
2 (Mp2)	Sangiovese-I	*Candida famata*	90.0	good	*C.guilliermondii, see also C.famata and C.norvegensis*	Similar** to Mp		
3 (Pm1)	Muscat-I	*Candida famata*	47.9	low	*C.glabrata*	*P.membranifaciens*	88	FJ770511.1
4 (Sc1)	Chardonnay-II	*Rhodotorula glutinis*	66.1	low	*C.haemulonii*	Similar to Sc		
5 (Sc2)	Sangiovese-II	*Saccharomyces cerevisiae*	99.0	very good	*C.haemulonii*	Similar to Sc		
6 (Sc3)	Muscat-III	*Saccharomyces cerevisiae*	94.3	good	*C.haemulonii*	*S.cerevisiae*	86	JQ824869.1
7 (Sc4)	Merlot-III	*Saccharomyces cerevisiae*	98.7	good	*C.haemulonii*	*S.cerevisiae*	85	JX129896.1
8 (Sc5)	Cabernet-II	*Saccharomyces cerevisiae*	90.2	good	*if methanol assimilated: P.angusta, if not: P.jadinii*	*S.cerevisiae*	85	JX423564.1
9 (Sc6)	Sangiovese-IV	*Saccharomyces cerevisiae*	69.9	low	*S.cerevisiae*	*S.cerevisiae*	85	HM191645.1
10 (Hu1)	Merlot-I	*Kloeckera spp*	99.9	excellent	*C.guilliermondii, see also C.famata and C.norvegensis*	*H.uvarum*	83	KC510077.1
11 (Sc12)	Boğazkere-II	*Candida utilis*	88.0	acceptable	*S.cerevisiae*	*S.cerevisiae*	99	GU080048.1
12 (Sc8)	Chardonnay-III	*Candida pelliculosa*	71.6	low	*C.haemulonii*	*S.cerevisiae*	99	HN191649.1
13 (Sc9)	Syrah-III	*Saccharomyces cerevisiae*	99.6	very good	*if methanol assimilated: P.angusta, if not: P.jadinii*	*S.cerevisiae*	83	JQ824876.1
14 (Pm2)	Merlot-I	*Candida glabrata*	47.9	low	*if methanol assimilated: P.angusta, if not: P.jadinii*	*P.membranifaciens*	99	DQ466534.1
15 (Sc10)	Merlot-IV	*Saccharomyces cerevisiae*	97.9	good	*C.haemulonii*	*S.cerevisiae*	84	JQ824876.1
16 (Sc11)	Cabernet-III	*Saccharomyces cerevisiae*	97.9	good	*C.haemulonii*	*S.cerevisiae*	99	JX867131.1
17 (Sc7)	Boğazkere-II	*Saccharomyces cerevisiae*	98.7	good	*C.haemulonii*	*S.cerevisiae*	83	JX021603.1
18 (Pm3)	Syrah-I	*Candida glabrata*	47.9	low	*C.glabrata*	*P.membranifaciens*	84	DQ104717.1
19 (Sc13)	Cabernet-I	*Saccharomyces cerevisiae*	90.2	good	*S.cerevisiae*	*S.cerevisiae*	84	JX021603.1

*Yeast codes that were reformed after sequence analysis.

**Yeasts that were not sequenced but found similar according to gel electrophoresis images of PCR products.
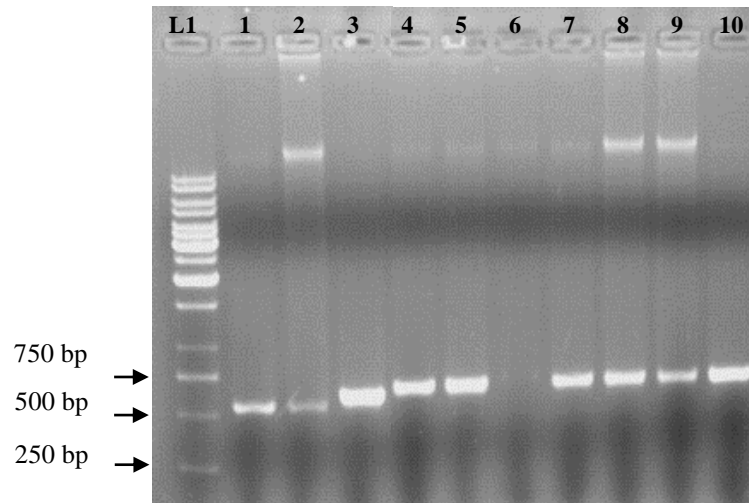
(a)
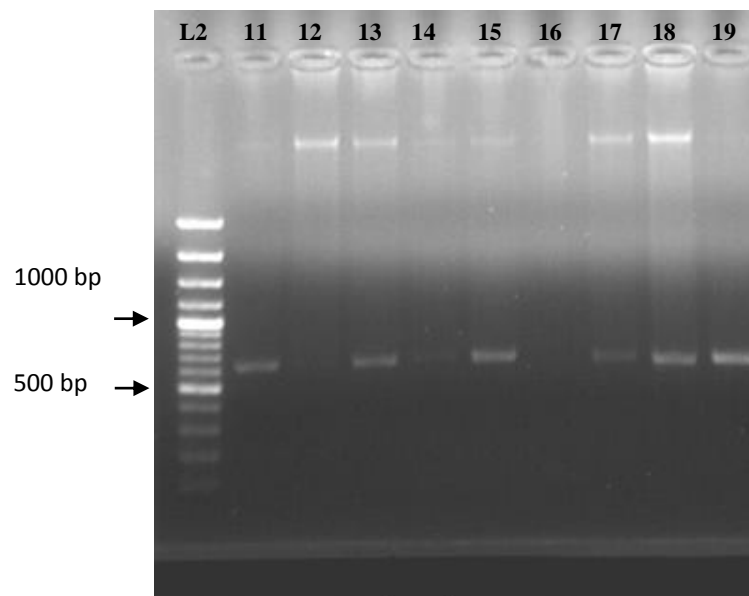
(b)

Figure 3.7. The agarose gel electrophoresis images of PCR products of the wine yeasts, amplified with NL primers. L1: GeneRuler 1kb DNA Ladder, L2: GeneRuler 100 bp plus DNA Ladder

Wine fermentation is a complex ecological and biochemical process involving the sequential development of different yeast species. The origin of these yeasts are the grape skin and the winery equipment and it was shown that the yeast microbiota on grapes are influenced by climatic conditions, including temperature and rainfall, the geographical location of the vineyard, the use of antifungals, the type of soil, the age of the vineyard, the grape variety and the harvest technique. The results in this study also showed similarity with the previous researches about yeast microflora during wine process.

Recent studies agreed with that yeasts, *H. uvarum* and its anamorphic form *K. apiculata* and *Hansenula, Candida, Pichia, Rhodotorula, Kluyveromyces*, dark mucoid and carotenoid pigmented yeasts as *Sporobolomyces, Cryptococcus and Rhodotorula,* the yeast-like organism *Aureobasidium pullulans* are the predominant species on the grape (Barata et al., 2012). *H. uvarum* has been generally isolated from industrial food production process and used as a biocontrol agent. *P. membranifaciens* has been isolated from rots of spoiled fruit and other plant materials as well as a contaminant of fermented beverages. In high sugar grape musts, osmotolerant non-*Saccharomyces* yeasts are commonly found (Mills et al., 2002). *C. zemplinina* has been recently identified as a new osmotolerant and psychrotolerant yeast, fermenting sweet and botrytized musts (Sipiczki, 2003). However, contrary to popular belief, *S. cerevisiae* does not occur in high populations on healthy grapes and is uncommonly isolated from intact berries and vineyard soils. These fermentative species could be originated from the wine cellar and included into the must during mechanical treatment of the grape and fermentation. The non-*Saccharomyces* yeasts could grow well at the beginning of fermentation, when the ethanol concentration is low, and then replaced by *Saccharomyces*, which are more tolerant to ethanol and more competitive for growth in media with high sugar concentrations (Sabate et al., 2002).

In contrast to cultural methods, molecular techniques provide rapid and reliable identification, hence allowing a large number of samples to be analyzed. In the study of Sabate et al. (2002), identification of yeast species associated with vineyard and winery was carried out using molecular methods including RFLP and PCR analysis. It was found that *H. uvarum* was the predominant species in the must (60%) while *A. pullulans* (15%), *P. kluyveri* (10%), *C. stellata* (5%), *M. pulcherrima* (5%) and *R. mucilaginosa* (5%) were also isolated less frequently. It was reported that oxidative basidiomycetous yeasts without enological potential were predominant in the vineyard environment, whereas fermentative yeasts, which grow efficiently in sugary media, are not competitive on this substrate. However, the last stages of grape maturation could allow the growth of fermentative yeasts on grape surface due to loss in the integrity of the grape skin and leakage of the must from the fruit. These species on grape surface is the predominant microbiota in must and could easily grow during the beginning of the process. Later, *S. cerevisiae* becomes dominant due to its higher tolerance to ethanol and SO_2 (added as antioxidant and antimicrobial preservative). This organism also has the most efficient fermentative catabolism in a high sugary media to let it finish the wine process. This yeast

was also suggested as a starter for winemaking of partially dried grapes due to its ability to overcome osmotic stress and produce ethanol by fermenting high sugar grape musts (Malacrino et al., 2005).

Tofalo et al. (2009) studied the molecular identification of yeast species during a wine process and used 5.8-ITS rRNA amplification and subsequent restriction analysis. The isolates were reported as *C. apicola*, *S. cerevisiae*, *C. zemplinina* and *Z. bailii*. As the isolates were collected at different stages of fermentation like our study, the RAPD-PCR analysis allowed the observation of microbiota evolution during winemaking. In Vino cotto must, before the start of fermentation, only the osmotolerant species *C. apicola*, and *Z. bailii* were isolated, whereas yeasts belonging to the species of *S. cerevisiae* and genera of *Hanseniaspora, Kloeckera* and *Metschnikowia* were not found. During fermentation, *S. cerevisiae* became the prevalent yeast, whereas only few strains, belonging to this species, were isolated at the end. *C. apicola* was the dominant species both at the start and at the end of fermentation. It was reported that vino cotto was appeared to be a stressful environment for the survival of the majority of the yeasts, so few species could grow. At the end, *C. apicola* was the prevalent species, followed by *Z. bailii, C. zemplinina* and *S. cerevisiae*. Various authors have reported that indigenous yeast species, such as *K. apiculata*, *C. stellata* and *T. delbrueckii*, may have better ability than *S. cerevisiae* to grow during fermentations conducted at high sugar concentrations.

Querol et al. (1992) performed the first study of population dynamics and the roles of active dried yeast strains and the native *Saccharomyces* flora during inoculated industrial fermentations using mtDNA restriction patterns. The inoculated strains competed with the native strains but did not completely suppress their growth until several days after inoculation. Therefore, the predominance of the inoculated strain was evident at the end of the fermentations. Schütz and Gafner (1993) used physiological tests and chromosomal patterns to analyze the succession of three different dried yeasts at three different time points during fermentation. *H. uvarum* was present at the beginning of fermentation, but only the inoculated strains of *S. cerevisiae* were observed in the middle and at the end of the fermentation.

3.2.3.1. Phylogenetic Tree of Wine Yeasts

Phylogenetic analysis of the DNA sequences of wine yeasts were performed using Mega6 software after alignment by Clustal Omega program (with default settings). The phylogenetic tree was constructed using the Neighbor-Joining method. The optimal tree with the sum of branch length = 3.50849836 is shown in Figure 3.8. The percentage of replicate trees in which the associated taxa clustered together in the bootstrap test (500 replicates) is shown next to the branches. The tree is drawn to scale, with branch lengths in the same units as those of the evolutionary distances used to infer the phylogenetic tree. The evolutionary distances were computed using the p-distance method and are in the units of the number of base differences per site. The analysis involved 17 nucleotide sequences. As it could be observed in the Figure 3.8, one species of *P. membranifaciens* (Pm1) is clustered with the type strain of *S. cerevisiae. H. uvarum* (Hu1) is also placed close to *S. cerevisiae* isolates. Pm2 and Pm3 are closely related to each other and closer to isolated *S. cerevisiae* than Pm1. This result confirms a previous report in which one of the synonyms of *Pichia* was indicated as *Saccharomyces membranifaciens*; and of *H. uvarum* was indicated as *Saccharomyces apiculatus*. *Hanseniaspora* was accepted as a sister genus to Saccharomycodes (Kurtzman and Fell, 2006).
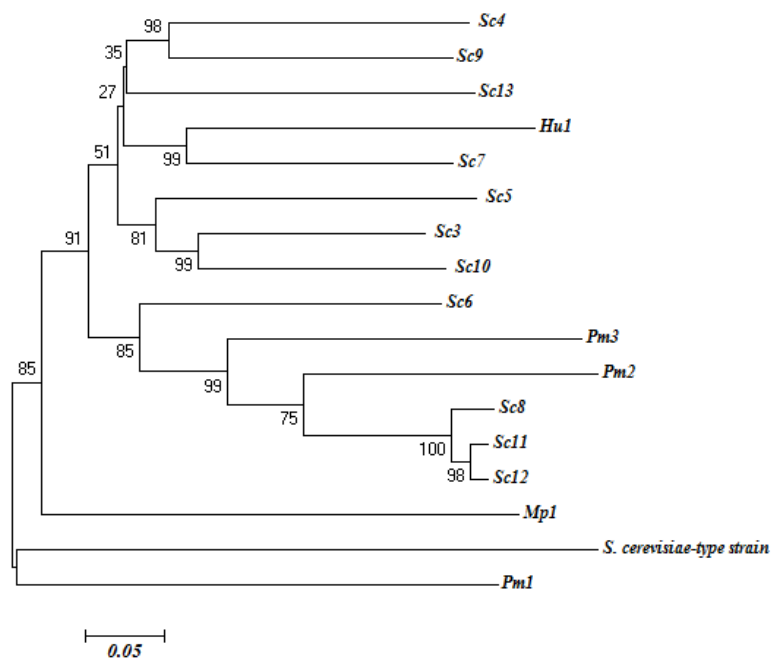
Figure 3.8. Phylogenetic tree of wine yeasts constructed using DNA sequences

3.2.4. Mid Infrared Spectroscopy Analysis

In the previous studies related with FTIR analysis to identify microorganisms, mostly used technique for sample preparation has been drying of yeast cells on ZnSe crystal to form a thin film. Methods in literature involves preparing a yeast suspension with a constant OD: 3±1 (corresponding to 6.8 x 10^9 cfu/mL) at 500 nm and drying of the cells for 50 min at the constant temperature (42°C±2) for all isolates before FTIR spectroscopic measurement (Kümmerle et al., 1998). However, these preparation stages are time consuming. Therefore, a new simple procedure for yeast sample preparation was developed in this study. Besides the use of dried yeast cell suspension on ZnSe plate, the yeast colonies were also directly used after collecting from agar plate and spreading on to ZnSe crystal plate like a thin film as shown in the Figure 3.9. Spectra of both directly prepared and dried yeast samples are shown in Figure 3.10.

(a)

(b)

Figure 3.9. The preparation of the yeasts (a) after a drying step of culture suspension and (b) without drying step for FTIR spectroscopy analysis
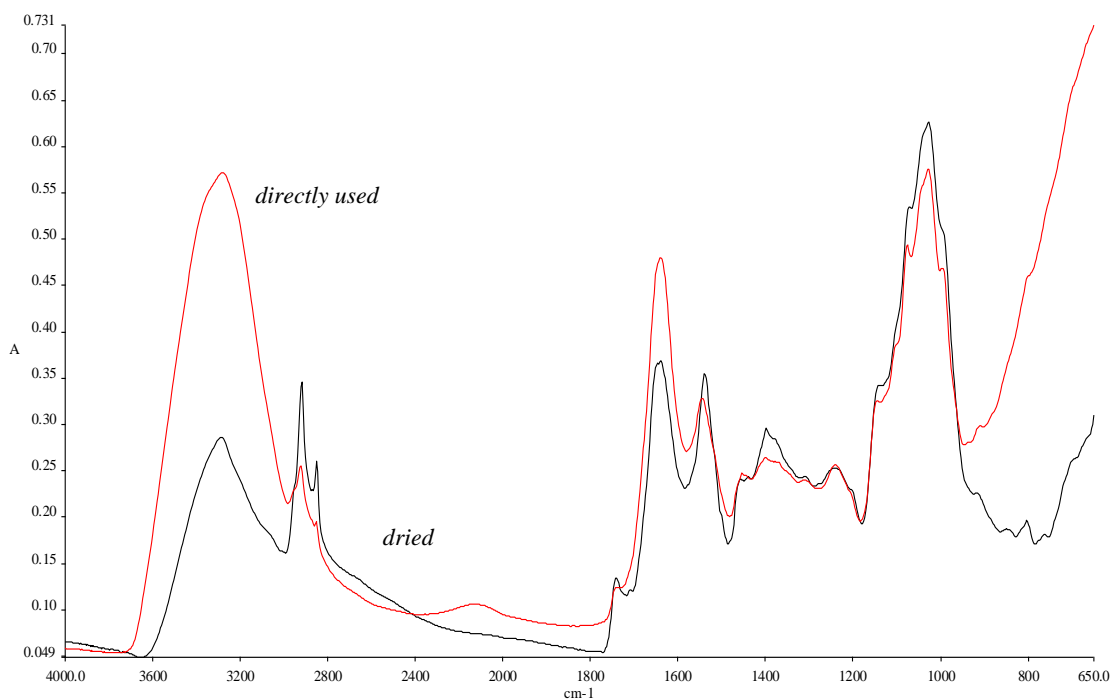
Figure 3.10. FTIR spectra of dried and directly used *S. cerevisiae* colonies

3.2.4.1. Evaluation of the Results with Multivariate Statistical Analysis

Previous studies revealed that comparison of three spectral windows (3030-2830 cm^{-1}, 1350-1200 cm^{-1} and 900-700 cm^{-1}) of the second derivatives corresponding to discriminative parts of the mid-infrared spectrum yield reliable identification results for unknown yeast isolates (Büch et al., 2008; Kümmerle et al., 1998; Wenning et al., 2002). Lasch and Naumann (2000) and Udelhoven et al. (2000) reported that these spectral windows are characterized by the absorption of fatty acid compounds, carboxylic groups of proteins, RNA/DNA and phospholipid content. Therefore, both full (4000-650 cm^{-1}) and partial (3030-2830 cm^{-1}, 1350-1200 cm^{-1} and 900-700 cm^{-1}) spectral regions were used for chemometric analysis of FTIR data for dried and directly used yeast cells. First, PCA was applied to mid-infrared spectra of yeasts to investigate if the separation of different yeasts is possible. Statistical results of the constructed PCA models are shown in Table 3.3. Figure 3.11 shows the PCA score plots of the dried yeast cells including full (a) and partial (b) spectral regions; whereas the plots of directly used yeast cells including full (a) and partial (b) spectral regions are provided in Figure 3.12. The full spectral regions of *dried* yeast cells were evaluated without any spectral filters; whereas the best plots were obtained with 2nd derivatives of partial spectral data of dried yeast

47

cells and both full and partial spectral regions of *directly used* yeast cells. 2nd derivative was applied to the original FTIR spectra in order to reduce the problems coming from baseline shifts and to enhance the resolution of complex bands (Kümmerle et al., 1998).

Table 3.3. Statistical information about the PCA models for wine yeasts

Model		2nd Derivative	Number of PC	R^2	Q^2
Dried yeast	Total region	-	3	0.994	0.986
	Partial region	+	3	0.821	0.57
Directly used yeast	Total region	+	4	0.541	0.154
	Partial region	+	3	0.603	0.281

*PC: Principle component

As it could be seen from Figure 3.11 (a) and (b), *S. cerevisiae* isolates formed a cluster in score plot and were probably starter culture. This cluster was generally separated from all other yeasts which were isolated at the beginning of wine process including *H. uvarum, P. membranafaciens* and *M. pulcherrima*. The only exception was the yeast coded by "Sc13" which was located with the other types of yeasts as it was also isolated in the step-I of the process and it was originated from grape/must sample (Figure 3.11, a). The differentiation of this yeast, "Sc13", was achieved only when using of dried yeast cell method. The difference of two sample preparation methods might be probably originated from the differences in DNA fingerprint regions since the most significant difference between infrared spectra of directly used and dried samples is in this region. In addition, molecular methods also group Sc13 with other *Sacchromyces* samples on contrary to infrared analysis of directly used yeasts. While infrared spectroscopy provides information on cellular composition of microorganisms, molecular methods identify microorganisms depending on their DNA. Sample, Sc13, which is differentiatiated from the other *Sacchromyces* samples originated from the must. As it is well-known microorganisms may produce different metabolites depending on their environment. Therefore, Sc13 may differ from other *Sacchromyces* samples in this respect and this difference might have been reflected in infrared spectra of Sc13. As a result, this particular sample is separated from the other *Sacchromyces* samples in PCA score plot of directly prepared yeasts. Since it is hard to reach a decisive conclusion with only one sample; further studies should be conducted on this matter. FTIR data showed a differentiation between different yeast species in which three clusters could be seen

clearly. Therefore, it could be concluded that use of FTIR with both sample preparation method as dried or directly used cells for differentiation of wine yeast species is possible.

Aim of the cluster analysis is to to find a natural grouping of a data set which defines less variation (greater similarity) within the clusters and more variation between the clusters. The similarity or distance between the clusters is indicated as "ward". The heights of the clusters are proportional to the distance between the clusters; therefore, the clusters are far apart when the vertical lines are tall and are close together when they are short (Eriksson et al., 2013). In Figure 3.13, HCA dendrogram of the full spectrum data of *dried* (a) and *directly used* (b) yeast cells are presented. For dried cells, it could be seen that yeasts were mainly clustered in two groups as *S. cerevisiae* and the others; except for the yeast coded by *Sc13* which was not grouped under *Saccharomyces* species. However, all *Saccharomyces* species were clustered under the same group for directly used cells as shown in Figure 3.13 (b). Here, the closeness of Pm2 and Pm3 to each other and also to *S. cerevisiae* rather than *M. pulcherrima* or Pm1 could also be observed which was similar to the results of phylogenetic tree.
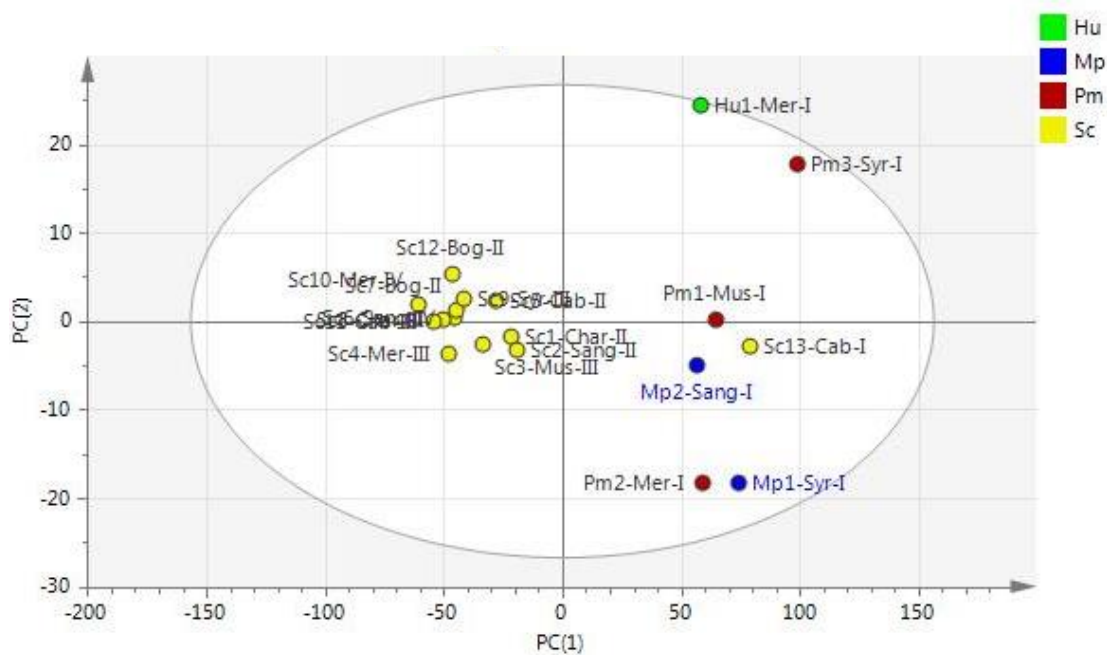
(a)
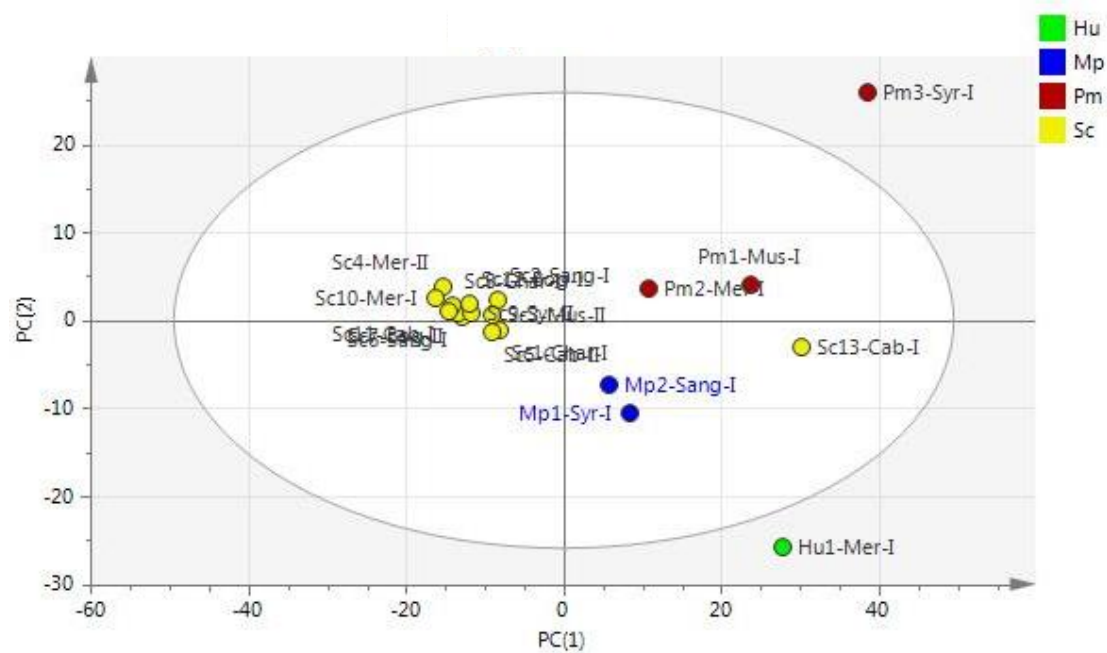
(b)

Figure 3.11. PCA score plots of the *dried* yeasts created with data in (a) full, 4000-650 cm^{-1} and (b) partial, 3030-2830 cm^{-1}, 1350-1200 cm^{-1} and 900-700 cm^{-1} spectral regions

50
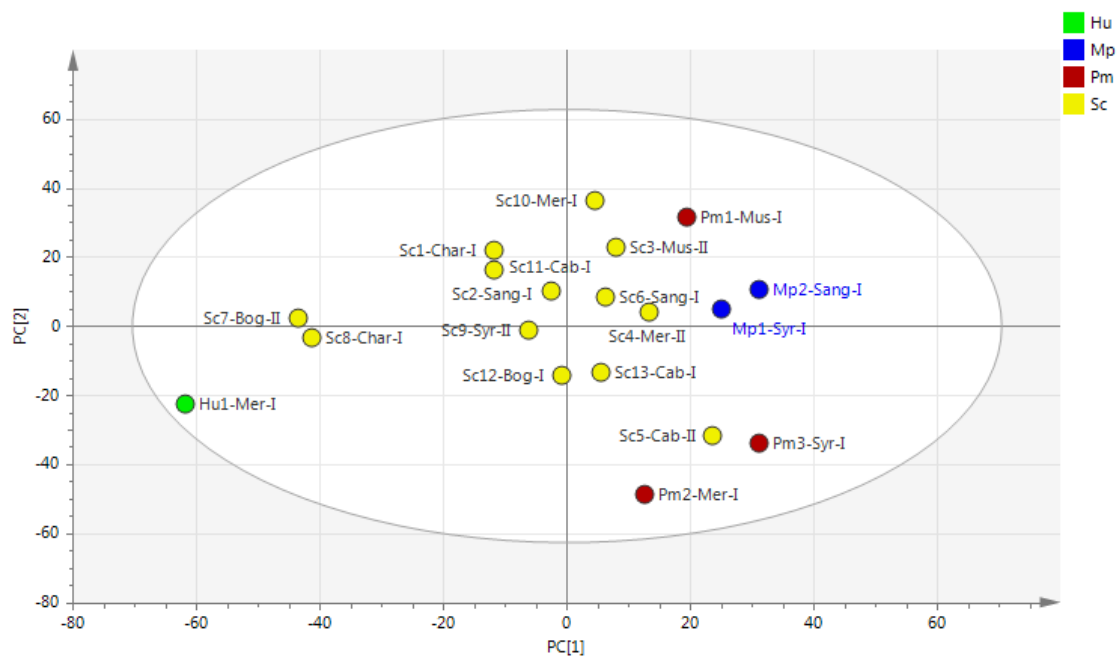
(a)
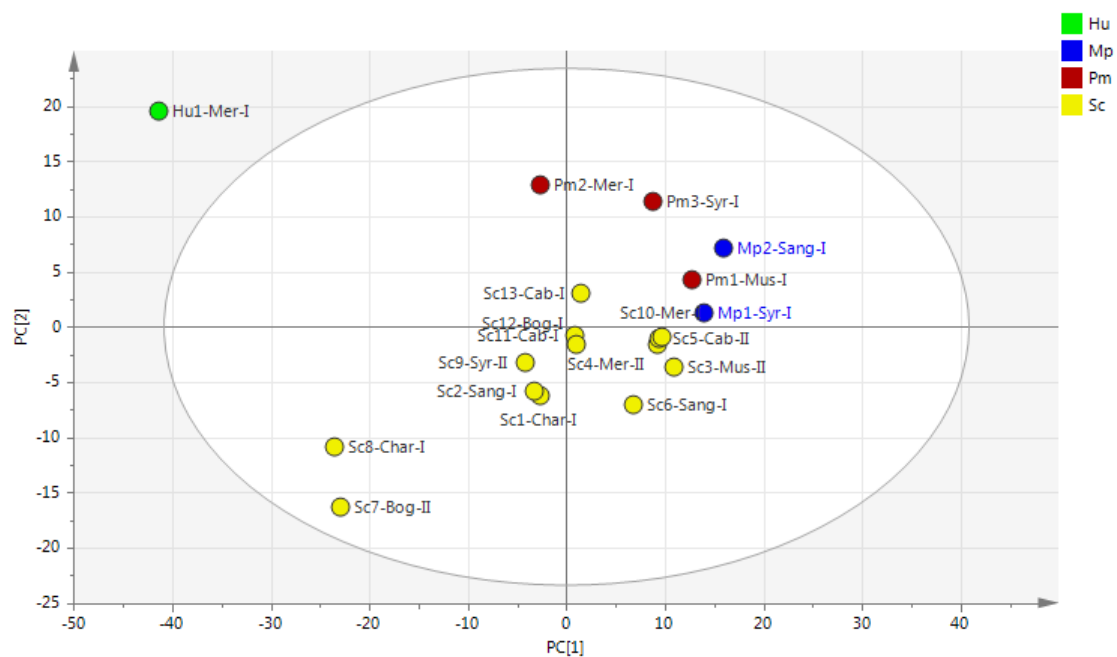
(b)

Figure 3.12. PCA score plots of the *directly used* yeasts created with data in (a) full, 4000-650 cm^{-1} and (b) partial, 3030-2830 cm^{-1}, 1350-1200 cm^{-1} and 900-700 cm^{-1} spectral regions
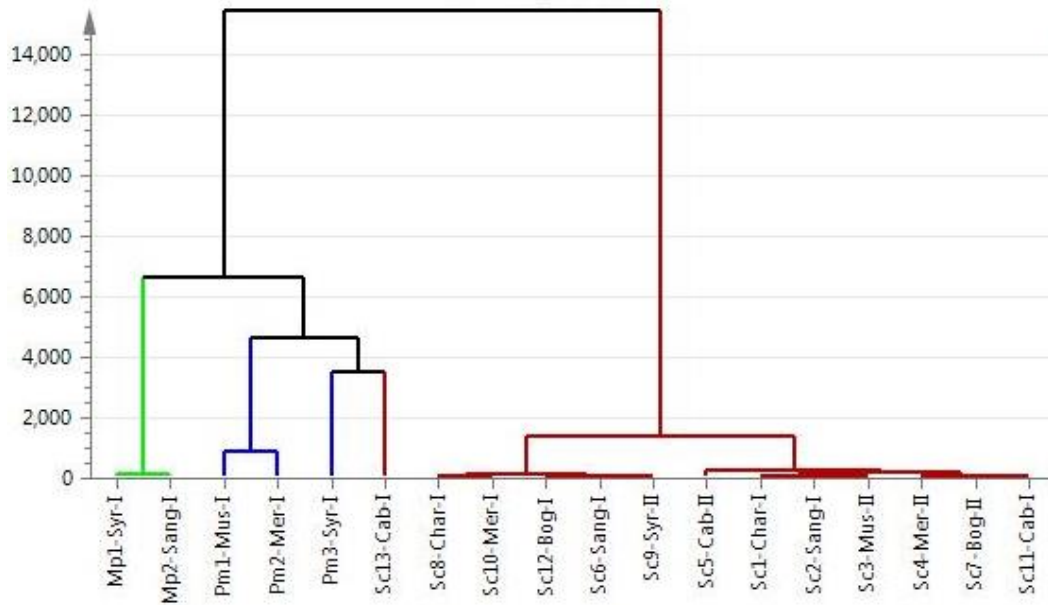
(a)
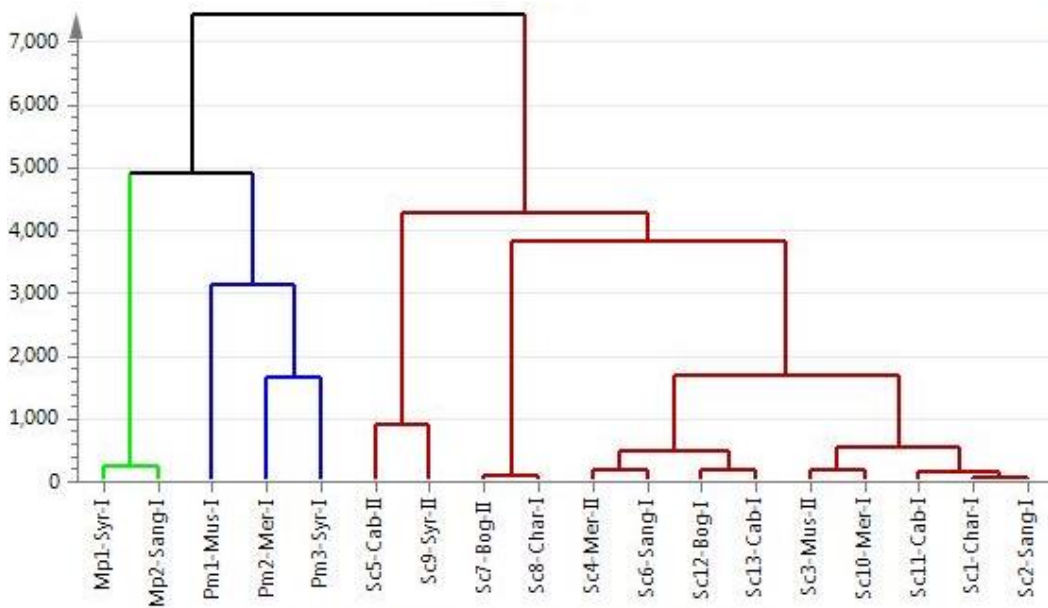
(b)

Figure 3.13. HCA created with the full spectrum mid-IR data of (a) *dried* and (b) *directly used* yeasts

3.3. Conclusions

In this chapter of the thesis study, it was aimed the application of FTIR spectroscopy for characterization of wine yeasts in comparison with both cultural and molecular identification techniques.

A total of 19 typical yeast colonies were isolated from different sampling steps of various wine processes. Among the identification techniques, API 20C AUX test results had 7/19 (37%) similarity at the genus level with the results of identification key Molecular analysis showed that 11 of 19 (58%) and 4 of 19 (21%) yeast isolates showed similarity at the genus level with API 20C AUX test results and with the results of identification key, respectively. All of the isolated wine yeasts were successfully identified molecularly, including the species *M. pulcherrima* (2/19, 11%), *P. membranifaciens* (3/19, 16%), *H. uvarum* (1/19, 5%) and *S. cerevisiae* (13/19, 68%) which are similar yeasts with previous wine studies.

With regard to chemometric analysis of FTIR spectroscopy data, it was possible to cluster different yeasts with both sample preparation method, as *directly used cells* (newly-developed method) and *dried cells* (well-known procedure), using both total and partial spectral regions. *S. cerevisae* from the beginning of process could succesfully be differentiated from that of at the end, using *dried yeast cells* which might be due to the spectral differences between two methods presence in DNA fingerprint regions. HCA showed parallel findings with both PCA and phylogenetic tree of wine yeasts. Therefore, it could be concluded that FTIR could be used with both sample preparation method for differentiation of wine yeasts during whole wine process, complementary with molecular and cultural methods.

CHAPTER 4

CHARACTERIZATION OF OLIVE YEASTS

4.1. Materials and Methods

4.1.1. Olive Samples

Two different types of olives as well as their leaves in addition to air samples from the orchards where the olives were grown were used in the analyses: Gemlik (GO) and Hurma (HO) (naturally debittered) olives, leaves of Gemlik (GL) and Hurma (HL) olive trees and air (A) samples. Hurma olives were hand-picked from an olive orchard (latitude 38°54'07"N, longitude 26°57'24"E) which is located in Karaburun Peninsula of Izmir. Gemlik type, on the other hand, was obtained from an orchard in Izmir Institute of Technology campus area (latitude 38°19'30.84"N, longitude 26°37' 48.87"E) which is 30 km south of the first orchard. Olives of about half a kilogram and olive leaf samples were hand-picked from the all sides of three trees weekly during 8 weeks of maturation period from the end of October until the beginning of December for two consecutive harvest years (2011 and 2012). Kernels of olives were immediately removed following the harvest. The general schematic diagram of olive analysis is shown in Figure 4.1.

4.1.2. Enumeration, Isolation and Purification of Yeasts

Olives were destoned aseptically before microbiological analysis. 10 g of each olive samples (either olive fruit or leaf) were mixed in a stomacher bag with 90 mL Ringer's solution and homogenized for 1 min. Serial dilutions of this stock solutions were prepared and 0.1 mL aliquots of each dilution were spread onto Potato Dextrose agar (PDA, pH: 3.5, acidified with tartaric acid), Sabouraud dextrose agar (SDA, Merck, Germany), Czapek Dox agar (CDA, Merck, Germany) and Oatmeal agar (OA, Merck, Germany) in duplicates, followed by incubation at 28-30°C for 48–72 h for enumeration of total yeasts count and isolation of yeasts. The isolates were purified by conventional

streaking method onto YEPD (yeast extract 1%, peptone 2%, dextrose 2% and agar 2%) agar media. According to the morphological differences in colony shapes, colors, size (typical diameter of 0.5-1 mm) and specific yeast odour, the purified isolates were directly examined under phase contrast microscope (Olympus-CX31, Japan) and stored in 25% glycerol stock solution at -80°C for further analysis.
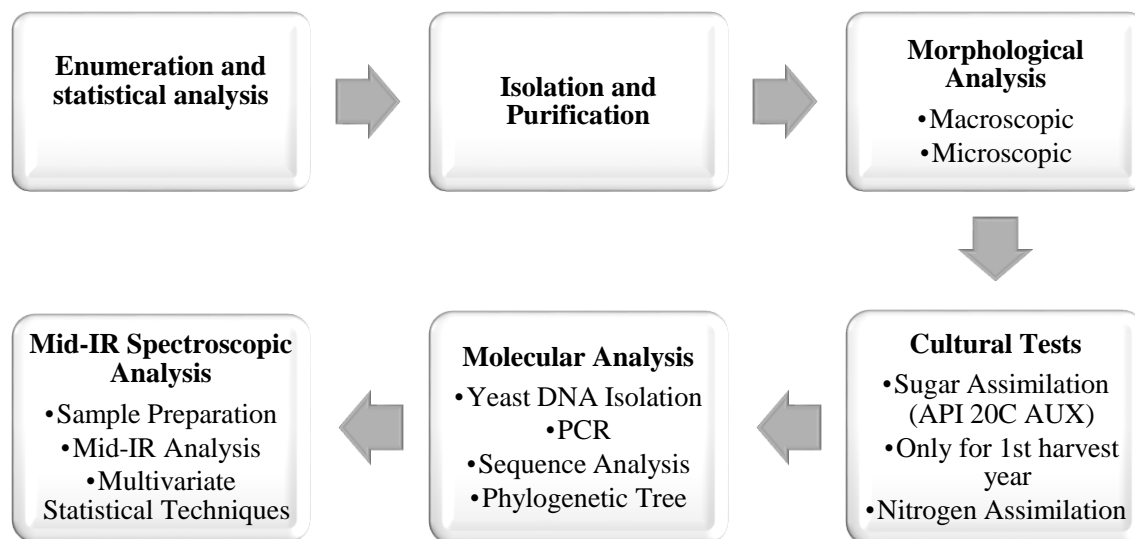
Figure 4.1 Schematic diagram of olive analysis

4.1.3. Cultural Tests

For characterization of yeast isolates, all cultural tests including morphology analyses, sugar assimilation test with the commercial kit API 20C AUX and assimilation of nitrogen compounds were performed as they were described in details in Chapter 3 in this thesis. Cultural identification of olive yeasts was also based on established schemes of Kurtzman and Fell (1998). As a result of the comparison of the results of the API 20C AUX test kit with the molecular identification results of both wine and first year-olive yeasts, it was decided not to use this commercial test kit for the yeast samples isolated in the second harvest year.

4.1.4. Molecular Tests

DNA isolation of yeasts, amplification reaction of yeast DNA with ITS and ITS-unidentified yeasts with NL primers, purification of PCR products, sequence analysis of yeast species and construction of phylogenetic trees for the olive yeasts were performed as defined in Chapter 3.

4.1.5. Mid-IR Spectroscopic Measurements

The sample preparation of olive yeasts for FTIR spectroscopy analysis, conditions of mid-IR spectroscopy and the multivariate statisctical analysis performed for evaluation of FTIR data of olive samples were also carried on as they desribed in Chapter 3 for wine yeast samples.

4.1.6. Statistical Analysis

For evaluation of the enumeration results statistically, general full factorial design was performed using MINITAB (V.14, USA) to investigate the effects of olive variety, harvest year and sampling time on yeast count. On the other hand, the data from the FTIR spectrometer was evaluated statistically by using multivariate statistical techniques including PCA, PLS-DA and HCA with SIMCA software (SIMCA 13.0.3, Umetrics Inc., Sweden).

4.2. Results and Discussion

4.2.1. Enumeration of Yeasts

All samples including two types of olive fruits and the leaves from the first and the second harvest years, in addition to air samples were investigated for their yeast population during the maturation period for 8 weeks of two harvest years. The yeast counts (Table 4.1 and 4.2) for each sampling time of two harvest years were determined

using PDA and the yeast growth for all olive samples during maturation period was observed almost every week (Figure 4.2 and 4.3). The yeast count data of air samples is not shown since only a few yeast colonies were counted.

As shown in Table 4.1 and Figure 4.2, the highest yeast population was observed on HO samples. Yeast count of HO had a fluctuating trend during maturation in the first harvest year; however it reached to its highest level at the last week. Fluctuations might be due to the changes of air conditions including temperature and the amount of rain during maturation (Figure 4.4). Number of yeasts for HL and GL were similar on weekly basis (Table 4.1). The total number of yeasts in HO is 1 log higher than that of HL, whereas almost 1 log more yeasts were enumerated in GL than that of GO.

The yeast enumeration results of the second harvest year of olive samples showed that HO samples had the highest yeast population again after 4th week of maturation (Figure 4.3). In general, changes in yeast population isolated from HL were small during sampling period. In addition, yeast counts of GO and of GL were higher at the end of maturation period. There were also some fluctuations in yeast counts, but this might be again due to the changes of air conditions at the time of sampling (Figure 4.5). According to the enumeration results, yeast counts of HO were very close to the counts of GO and the yeast counts of GL were 1 log higher than that of HL. The amount of yeasts from HO was 2 log higher than that of HL, whereas almost 1 log more yeasts were counted on GO than that of GL.

Comparison of two harvest years in terms of yeast population reveals that more yeasts were counted in the second year totally. Although the yeast population of HO and leaves of both olives from the first year were higher than that of the second year, almost 3 log more yeasts were counted from GO in the second year which was reflected to the total results. The reason of high yeast content of samples in the second year might be the climactic conditions. When HO and GO were compared, it could be seen that more yeast species were counted on HO for both harvest years. This difference in yeast counts could be attributed to the lower phenolic compound concentration of Hurma olives compared to regular olives (Aktas et al., 2014a). It has been well established in the literature that phenolic compounds have antimicrobial effects. In addition, GO having lower phenolic content in the second harvest year (Aktas et al., 2014a) also have much higher yeast count compared to the first harvest year yeast count.

Table 4.1. Yeast counts (CFU/g) of olive samples during maturation period of the first year (2011)

Sample type	Sampling time (week)*	Media			
		PDA	SDA	CDA	OA
HO	1	<10	<10	<10	<10
	2	5.3×10^4	<10	<10	<10
	3	2×10^2	8.1×10^3	2.2×10^5	1.9×10^4
	4	1.8×10^5	7×10^5	1.4×10^6	2×10^4
	5	2.6×10^4	5.3×10^4	9.8×10^4	3×10^4
	6	1.6×10^3	6×10^5	6×10^5	3×10^5
	7	<10	<10	<10	<10
	8	8.9×10^5	1.2×10^7	5.1×10^7	3×10^7
HL	1	<10	<10	<10	<10
	2	<10	<10	<10	<10
	3	4.7×10^3	2.6×10^5	6.1×10^4	5×10^2
	4	1.1×10^4	2.9×10^6	5.5×10^5	1.4×10^5
	5	7.3×10^3	1.8×10^5	1×10^5	7.2×10^4
	6	3.4×10^4	3.1×10^5	2.4×10^5	1.3×10^5
	7	<10	<10	<10	1.2×10^4
	8	<10	2.6×10^5	4×10^4	<10
GO	1	<10	<10	<10	<10
	2	<10	<10	<10	<10
	3	3×10^3	<10	<10	<10
	4	<10	<10	<10	<10
	5	<10	<10	4.8×10^3	<10
	6	<10	<10	<10	<10
	7	<10	<10	<10	<10
	8	<10	<10	<10	<10
GL	1	<10	<10	<10	<10
	2	<10	<10	<10	<10
	3	<10	<10	<10	<10
	4	1.1×10^2	1.3×10^2	1.4×10^2	10
	5	1.8×10^3	<10	<10	<10
	6	4.7×10^4	2.6×10^3	4.4×10^4	<10
	7	<10	<10	2.1×10^5	<10
	8	<10	<10	<10	<10

*The sampling time (1-8) corresponds to 14th, 19th, 26th of October, 2nd, 11th, 18th, 25th of November and 2nd of December, respectively. HO: Hurma olives, HL: Hurma leaves, GO: Gemlik olives, GL: Gemlik leaves.

Table 4.2. Yeast counts (CFU/g) of olive samples during maturation period of the second year (2012)

Sample type	Sampling time (week)*	Media			
		PDA	SDA	CDA	OA
HO	1	<10	1×10^2	1.1×10^4	1.3×10^4
	2	<10	<10	<10	<10
	3	<10	<10	2×10^2	<10
	4	<10	<10	<10	3.6×10^4
	5	1.27×10^5	4.72×10^5	1.02×10^5	<10
	6	3×10^4	2×10^5	1.14×10^5	<10
	7	1.27×10^5	1.62×10^6	8×10^5	1.27×10^5
	8	1.08×10^4	2.72×10^5	2.04×10^6	1.82×10^6
HL	1	2×10^2	1.05×10^4	<10	2.5×10^3
	2	2.7×10^3	4.4×10^4	2.3×10^4	4.8×10^4
	3	4×10^2	4.6×10^3	1.43×10^4	7×10^3
	4	5.2×10^3	3×10^3	5.9×10^3	3.1×10^4
	5	1×10^3	7.5×10^3	1.97×10^4	<10
	6	2.2×10^3	9.4×10^3	1.7×10^3	<10
	7	6.7×10^3	5.18×10^4	4.25×10^4	1.4×10^4
	8	1.5×10^3	1.98×10^4	1.05×10^4	9×10^3
GO	1	1×10^3	1×10^4	1×10^3	<10
	2	<10	<10	3×10^2	<10
	3	<10	<10	<10	<10
	4	<10	<10	<10	<10
	5	2.05×10^5	2.29×10^5	2.6×10^5	2.35×10^5
	6	<10	8×10^2	<10	<10
	7	4×10^2	9×10^2	1.1×10^3	<10
	8	5×10^3	1.9×10^3	8.4×10^3	7×10^4
GL	1	<10	2×10^2	4×10^2	3×10^2
	2	<10	7×10^3	<10	1×10^3
	3	<10	1×10^3	<10	<10
	4	1×10^2	2×10^2	3×10^2	<10
	5	1.1×10^4	4×10^4	1.4×10^3	6×10^3
	6	4×10^2	4.3×10^3	3×10^3	<10
	7	3×10^4	4.3×10^4	<10	4.6×10^4
	8	7×10^3	1.34×10^4	2.3×10^4	2.3×10^3

*The sampling time (1-8) corresponds to 16th, 22nd, 31st of October, 6th, 13th, 20th, 27th of November and 4th of December, respectively. HO: Hurma olives, HL: Hurma leaves, GO: Gemlik olives, GL: Gemlik leaves.
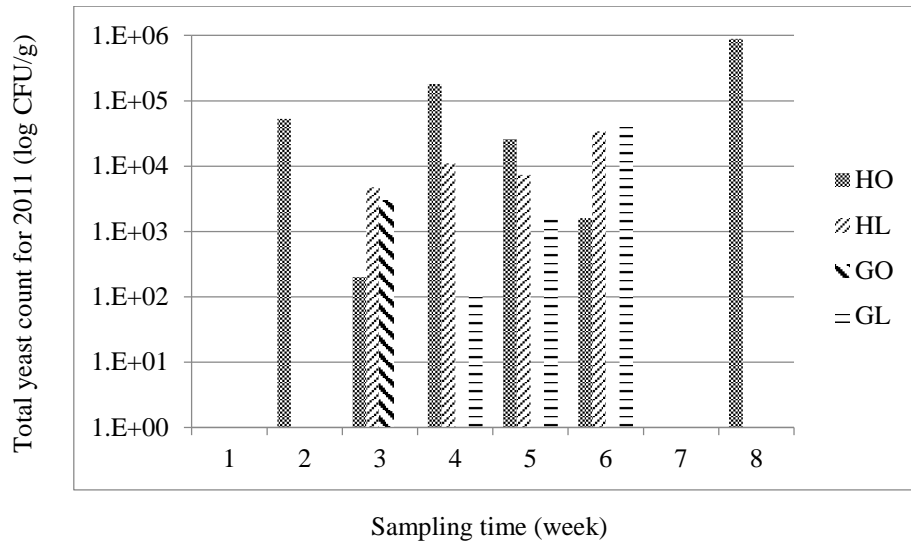
Figure 4.2. Yeast growth on selected (PDA) medium during maturation of olive samples in 2011
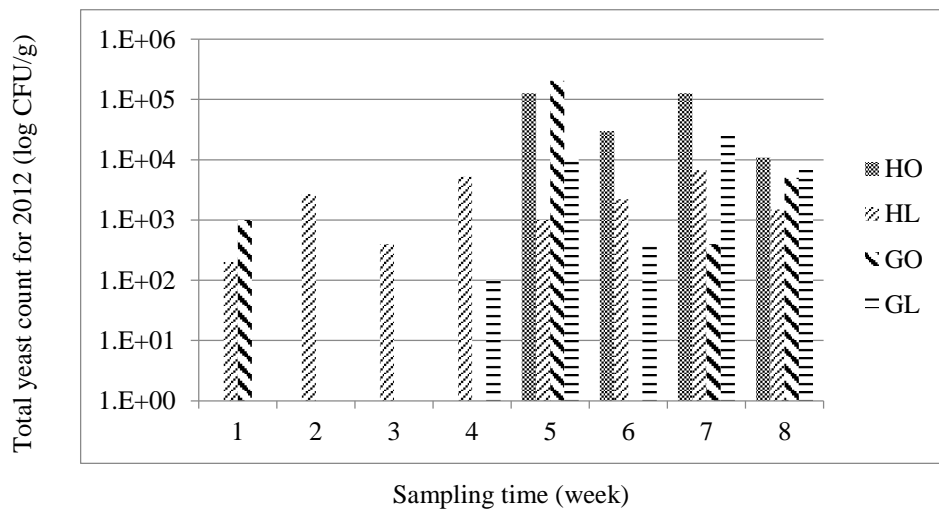
Figure 4.3. Yeast growth on selected (PDA) medium during maturation of olive samples in 2012
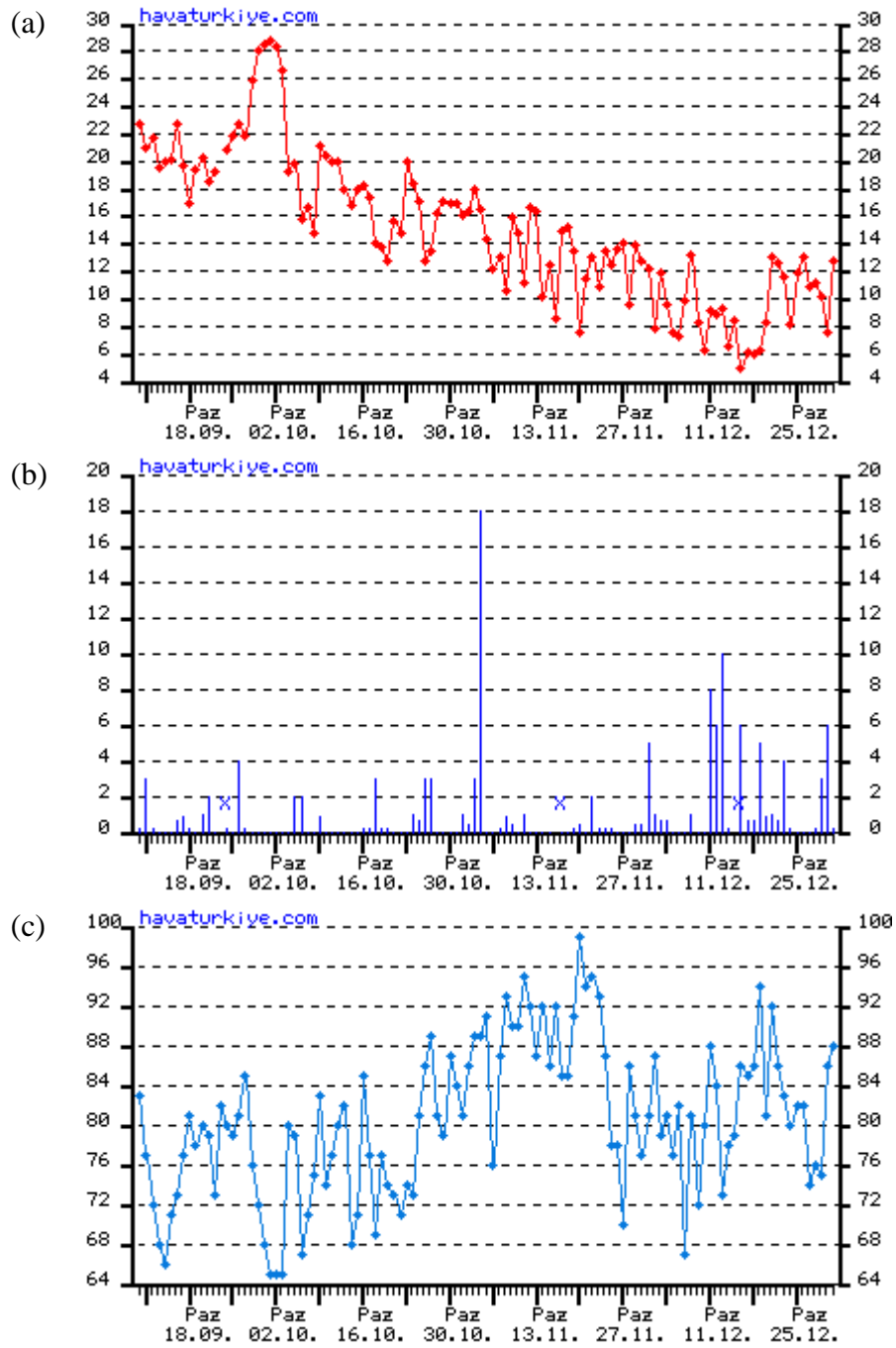
Figure 4.4. The weather conditions of İzmir-Turkey during maturation period of olives in 2011. (a) The temperature changes (°C), (b) rainfall amounts (mm) and (c) relative humidity (%) between September-December of 2011 (havaturkiye.com)
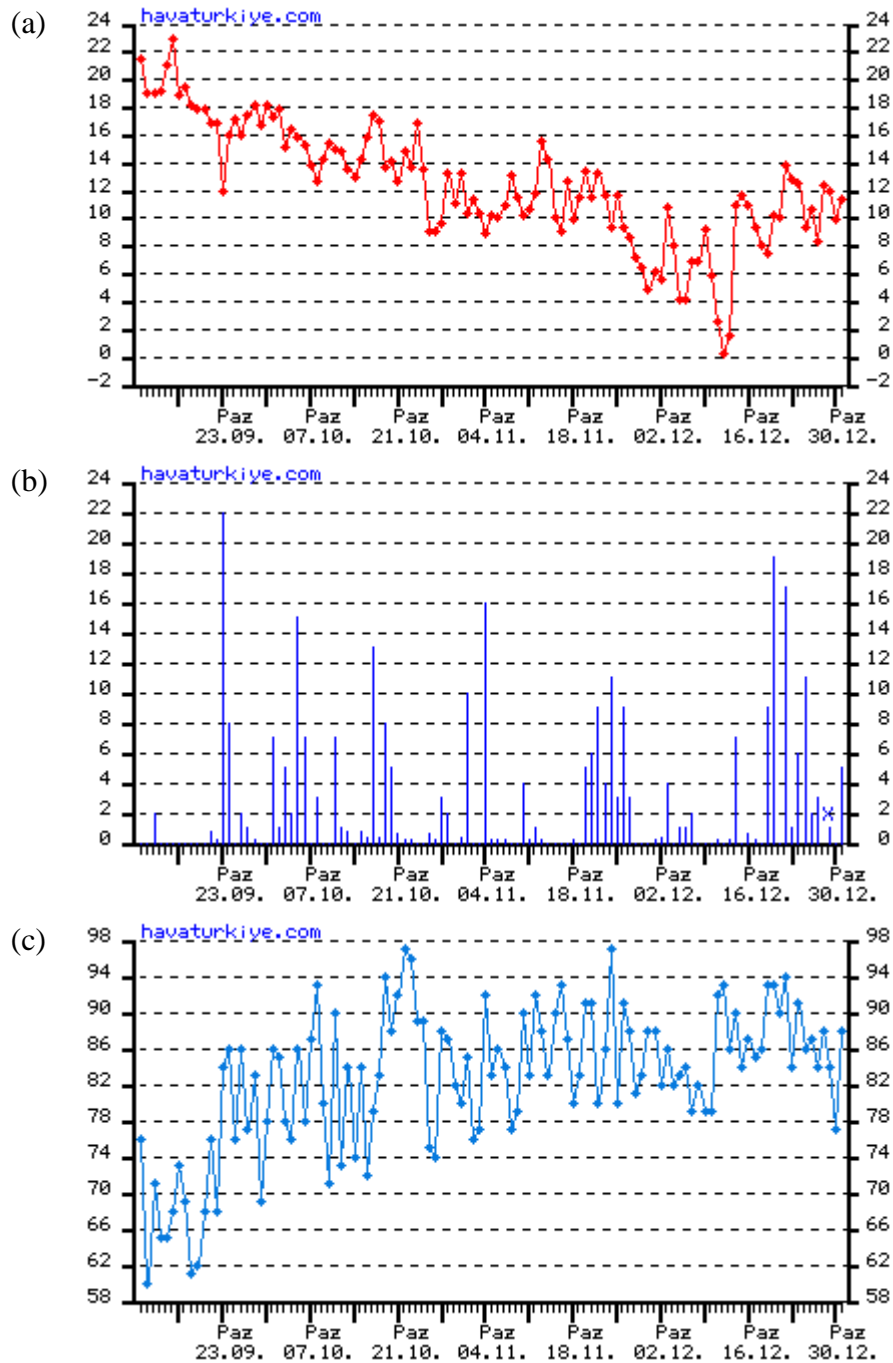
Figure 4.5. The weather conditions of İzmir-Turkey during maturation period of olives in 2012. (a) The temperature changes (°C), (b) rainfall amounts (mm) and (c) relative humidity (%) between September-December of 2012 (havaturkiye.com)

Several studies have focused on the detection of yeasts adhered to the surface of olive fruits. It has been observed that the species found on olive surface depended on the maturation degree of the olive. However, yeast counts on the surface of fresh olive fruits have been found generally low (<1 $\log_{10}$ CFU/g), as was reported by Arroyo-Lopez et.

al. (2008) with Manzanilla–Alorena olives during three consecutive seasons. Some studies reported the microbial changes on olive samples during fermentation. Aponte et al. (2010) studied the production of five different green table olive cultivars through microbiological, chemical and sensory analyses during 84 days of fermentation. It was observed that, within the first 42 days, counts on the media remained at undetectable levels (<2 log CFU/mL); however, after day 42, the microbial population of each cultivar mainly consisted of yeasts (2 log CFU/mL) and bacteria. Finally, at the 63rd day, yeast microflora increased to 6 log CFU/mL. Results showed that the activity of the high counts of yeast population throughout the fermentation stage could play a significant role in the final sensory characteristics of green table olives. Alves et al. (2012) presented a study for the microbiological characteristics and yeast population evolution during the fermentation of cracked green olives. It was concluded that the yeasts were the predominant microorganisms while lactic acid bacteria were not detected and the mold population decreased dramatically during fermentation. It was also remarked that yeasts were present all along the fermentation process studied in fermenters and seem to be responsible for the main changes occurring in the table olive fermentation in their study. Hernandez et al. (2007) investigated the yeast population during the processing of green table olives and isolated 83 yeast strains during 80 days of fermentation. Approximately 3 log CFU/g yeast was counted from fresh fruit, while higher counts were obtained in the olive brine during fermentation (4.93-5.75 log CFU/mL). The highest yeast count was obtained after 50 days of fermentation. Therefore, it was concluded that yeast counts in olive brines during the fermentation stage might have a significant effect on the sensory characteristics of olives.

4.2.1.1. Statistical Analysis for Enumeration

Yeast enumeration results of olive samples were analyzed statistically by using 3-factorial design. When olive variety (HO, HL, GO, GL), harvest year (1 and 2) and sampling time as weeks of harvesting (1-8) were investigated for their importance on the yeast count, all terms other than harvest year were found statistically significant on the yeast population at $p<0.05$ while harvest year was significant at $p<0.1$ (Table 4.3).

Table 4.3. Effects of different parameters on yeast count

Source	F-value	P-value
Variety	4.95	**0.002**
Harvest year	3.39	**0.067**
Time (week)	3.82	**0.001**
Variety*Harvest year	2.76	**0.043**
Variety*Time (week)	3.9	**0.000**
Harvest year*Time (week)	2.86	**0.007**
Variety*Harvest year*Time (week)	2.89	**0.000**

4.2.2. Isolation of Yeasts

A total of 46 yeast colonies were isolated during the first harvest year, of which 29 (63%) isolates from HO, 8 (17%) isolates from HL, 3 (7%) isolates from GO and 6 isolates (13%) from GL; whereas 136 yeast colonies were isolated during the second harvest year including 25 (18%) isolates from HO, 53 (39%) isolates from HL, 18 (13%) isolates from GO, 35 (26%) isolates from GL and 5 (4%) isolates from A.

The purified yeast colonies of the years 2011 and 2012 were examined under phase contrast microscope, as shown in Figure 4.5 and Figure 4.7.
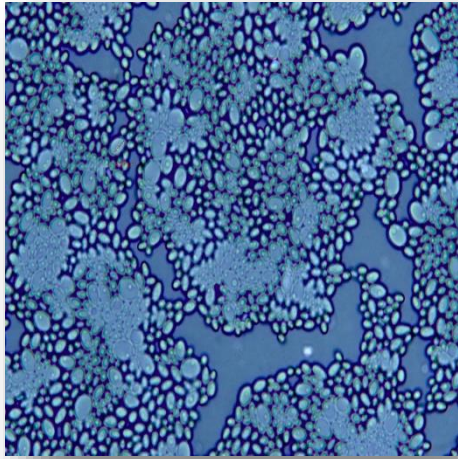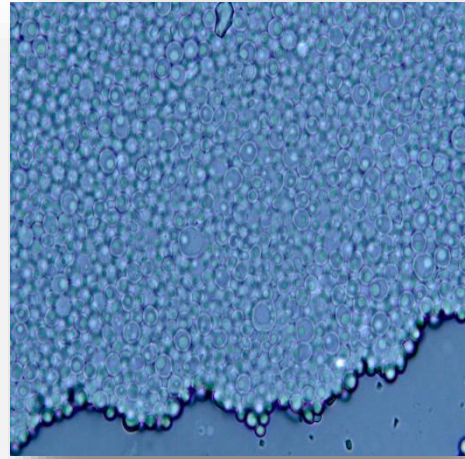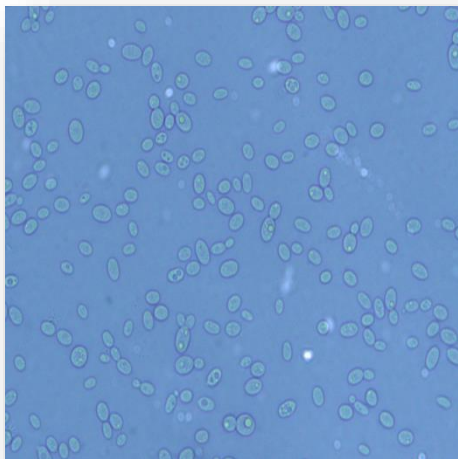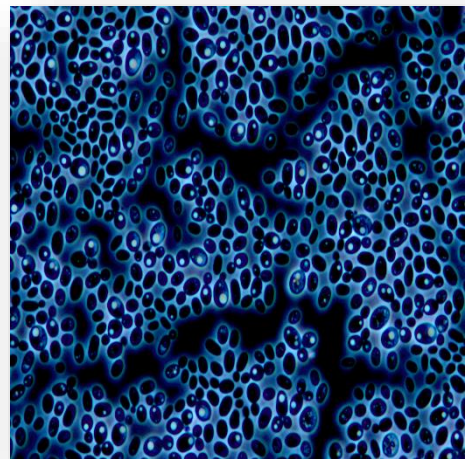
Figure 4.6. Images of olive yeasts (2011) under phase contrast microscope using 100X magnification. (a): Mv4, HO; (b): Cz2, HL; (c): Rm2, GO and (d): Rm1, GL. Yeasts were recoded after sequence analysis
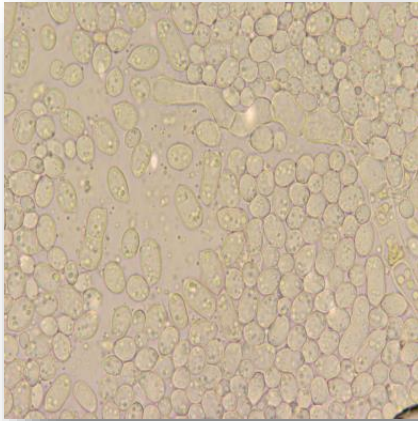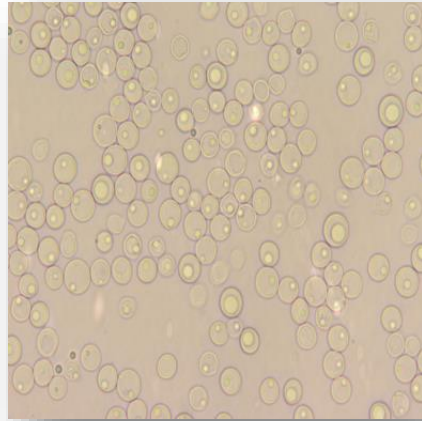
(a)　　　　　　　　　　　　　　　　(b)
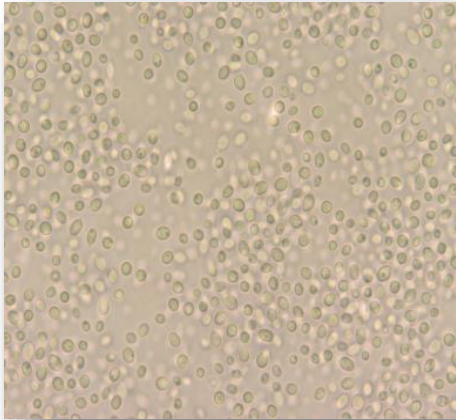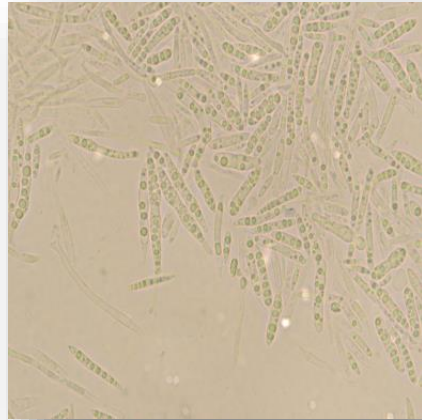
(c)　　　　　　　　　　　　　　　　(d)
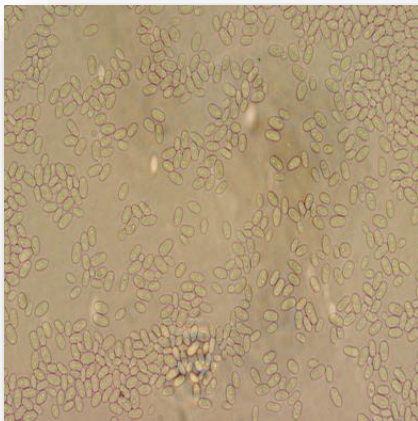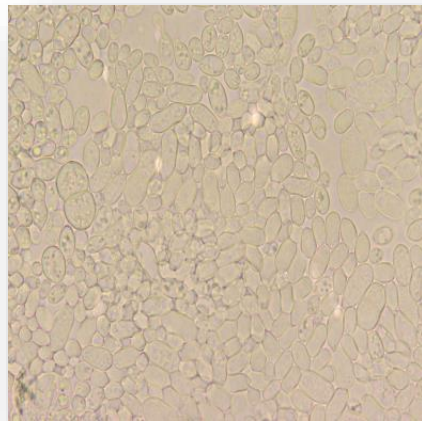
(e)　　　　　　　　　　　　　　　　(f)

Figure 4.7. Images of olive yeasts (2012) under phase contrast microscope using 100X magnification. (a): Ap12, HO; (b): Cp2, HL; (c): Rm16, HL; (d): Ph2, A; (e): Cg1, GO; (f): Ap54, GL. Yeasts were recoded after sequence analysis

4.2.3. Morphological and Cultural Analysis

In this study, totally 182 yeast strains were isolated, purified and evaluated using both cultural and molecular methods in parallel. The evaluation of *macroscopic* and *microscopic* morphology of the olive yeasts from the harvest year 2011 are shown in Appendix Tables C.1 and C.2, respectively, whereas the same evaluation results belonging to the year of 2012 are presented in Appendix Tables C.3 and C.4, respectively. API 20C AUX commercial test kit was first applied for the identification of the isolates of the first year. The cultural test results including API 20C AUX carbohydrate assimilation reaction, nitrogen assimilation and durham tests of olive yeasts from 2011 are presented in Appendix Table C.5. When the results of the commercial kit were compared with the other cultural methods with identification key for the yeasts from 2011 (Table 4.4), it was observed that API 20C AUX test had 65% (30/46) similarity at the genus level and 57% similarity (26/46) at the species level. 5 of 46 (11%) yeast strains could not be identified with API test and the most frequently isolated yeast species were found as *Candida* sp. Since its results showed less similarity with molecular methods and yeasts isolated in this study are not in API database, the test kit was not used for the identification of the second harvest year's isolates. Therefore, only the results of nitrogen assimilation and durham tests of olive yeasts from 2012 are shown in Appendix Table C.6. The yeast identification key (Kurztman and Fell, 1998) given in details in Appendix B was used to identify the yeast samples according to cultural test results. The characterization results of olive yeasts from the harvest year 2011 by all of cultural methods in comparison with API 20C AUX commercial kit are given in Table 4.4.

Table 4.4. Characterization of olive yeasts from harvest year 2011 by cultural methods

Yeast code*	Oive source**- Sampling week	CULTURAL			
		API 20C AUX			*with identification key* (**Kurtzman and Fell, 1998**)
		Significant Taxa	**% ID**	**Identification Note**	
Cd1	HO-2	*Candida guilliermondii*	90.2	acceptable	*Candida guilliermondii (see also C. famata and C. norvegensis)*
Cd2	HO-2	*Candida guilliermondii*	90.2	acceptable	*Candida guilliermondii (see also C. famata and C. norvegensis)*
Dh1	HO-2	*Candida guilliermondii*	90.2	acceptable	*Candida guilliermondii (see also C. famata and C. norvegensis)*
Dh2	HO-2	-	-	-	if Galacticol +, *Candida haemulonii*; if -, *Candida glabrata/C.norvegensis (Pichia norvegensis)*
Dh3	HO-2	*Candida guilliermondii*	88.7	good	*Candida guilliermondii (see also C. famata and C. norvegensis)*
Dh4	HO-2	-	-	-	if Galacticol +, *Candida haemulonii*; if -, *Candida glabrata/C.norvegensis (Pichia norvegensis)*
Cz1	HO-2	*Candida famata*	99.8	very good	*Candida famata*
Dh5	HO-2	-	-	-	if Galacticol +, *Candida haemulonii*; if -, *Candida glabrata/C.norvegensis (Pichia norvegensis)*
Mv1	HO-3	*Candida lusitaniae*	81.5	good	*Candida tropicalis*
Mv2	HL-4	*Trichosporan asahii*	-	unacceptable profile	if DBB +, *Trichosporon avoides* complex. İf -, *Geotrichum fermentans*
Cz2	HL-4	*Cryptococcus humicola*	76.4	low discrimination	*Cryptococcus laurentii*
Dh6	HO-4	*Candida lusitaniae*	52.1	very good	if Rhamnose +, *Candida lusitaniae*; if -, *Candida tropicalis/C. viswanathii*
Mv3	HO-4	*Candida lusitaniae*	52.1	very good	if Rhamnose +, *Candida lusitaniae*; if -, *Candida tropicalis/C. viswanathii*
Mv4	HO-4	*Candida lusitaniae*	52.1	very good	if Rhamnose +, *Candida lusitaniae*; if -, *Candida tropicalis/C. viswanathii*
Mv5	HO-4	*Candida lusitaniae*	52.1	very good	if Rhamnose +, *Candida lusitaniae*; if -, *Candida tropicalis/C. viswanathii*
Mv6	HO-4	*Candida lusitaniae*	52.1	very good	if Rhamnose +, *Candida lusitaniae*; if -, *Candida tropicalis/C. viswanathii*
Mv7	HO-4	*Candida lusitaniae*	52.1	very good	if Rhamnose +, *Candida lusitaniae*; if -, *Candida tropicalis/C. viswanathii*
Mv8	HO-4	*Candida lusitaniae*	52.1	very good	if Rhamnose +, *Candida lusitaniae*; if -, *Candida tropicalis/C. viswanathii*
Mv9	HO-4	*Candida lusitaniae*	52.1	very good	if Rhamnose +, *Candida lusitaniae*; if -, *Candida tropicalis/C. viswanathii*

Table 4.4 (Cont.)

Yeast code*	Oive source**-Sampling week	CULTURAL			
		API 20C AUX			*with identification key* *(Kurtzman and Fell, 1998)*
		Significant Taxa	% ID	Identification Note	
Mv10	HO-4	*Candida lusitaniae*	52.1	very good	if Rhamnose +, *Candida lusitaniae*; if -, *Candida tropicalis/C. viswanathii*
Mv11	HO-4	*Candida famata*	78.4	very good	*Candida guilliermondii (see also C. famata and C. norvegensis)*
Ap1	HO-4	*Cryptococcus laurentii*	68.1	doubtful profile	if Galacticol +, *Candida haemulonii*; if -, *Saccharomyces cerevisiae*
Ap2	HO-4	*Cryptococcus laurentii*	99.8	good	if Galacticol +, *Candida haemulonii*; if -, *Saccharomyces cerevisiae*
Mp1	HO-4	*Candida lusitaniae*	52.1	very good	if Rhamnose +, *Candida lusitaniae*; if -, *Candida tropicalis/C. viswanathii*
Mv12	HO-4	*Candida lusitaniae*	52.1	very good	if Rhamnose +, *Candida lusitaniae*; if -, *Candida tropicalis/C. viswanathii*
Me1	HO-4	-	-	-	if Galacticol +, *Candida haemulonii*; if -, *Candida glabrata/C.norvegensis (Pichia norvegensis)*
Mv13	HO-4	*Candida lusitaniae*	52.1	very good	if Rhamnose +, *Candida lusitaniae*; if -, *Candida tropicalis/C. viswanathii*
Mv14	HO-4	*Candida lusitaniae*	52.1	very good	if Rhamnose +, *Candida lusitaniae*; if -, *Candida tropicalis/C. viswanathii*
Mv15	HO-4	*Candida lusitaniae*	52.1	very good	if Rhamnose +, *Candida lusitaniae*; if -, *Candida tropicalis/C. viswanathii*
Mv16	HO-4	*Candida lusitaniae*	52.1	very good	if Rhamnose +, *Candida lusitaniae*; if -, *Candida tropicalis/C. viswanathii*
Ap3	GL-4	*Cryptococcus uniguttulatus*	99.9	very good	if Galacticol +, *Candida haemulonii*; if -, *Saccharomyces cerevisiae*
Rm1	GL-4	*Cryptococcus uniguttulatus*	99.9	very good	*Rhodotorula mucilaginosa*
Ap4	GL-4	*Cryptococcus laurentii*	98.8	good	*Cryptococcus laurentii*
Rm2	GO-4	*Geotrichum capitatum*	66.6	identification not valid	if DBB +, *Trichosporon avoides* complex. İf -, *Geotrichum capitatum*. But pink: *R.mucilaginosa*
Rm3	GO-4	-	-	-	if Galacticol +, *Candida haemulonii*; if -, *Candida glabrata/C.norvegensis (Pichia norvegensis)*
Rm4	HL-5	*Stephanoascus ciferri*	99.9	good	if Methanol +, *Pichia angusta*; if-, *P.jadinii*
Rm5	GO-5	*Stephanoascus ciferri*	99.8	doubtful profile	*Candida famata*
Rm6	HL-5	*Trichosporan asahii*	99.9	very good	if DBB +, *Trichosporon avoides* complex. İf -, *Geotrichum fermentans*

(Cont. on next page)

Table 4.4 (Cont.)

Yeast code*	Oive source**- Sampling week	CULTURAL			
		API 20C AUX			*with identification key* (Kurtzman and Fell, 1998)
		Significant Taxa	**% ID**	**Identification Note**	
Rm7	HO-5	*Stephanoascus ciferri*	99.8	doubtful profile	*Candida famata*
Ap5	GL-7	*Cryptococcus laurentii*	99.4	good	*Candida guilliermondii (see also C. famata and C. norvegensis)*
Rm8	GL-7	*Cryptococcus laurentii*	99.4	good	*Rhodotorula mucilaginosa*
Rm9	GL-7	*Cryptococcus laurentii*	98.2	good	*Candida famata*
Rm10	HL-7	*Rhodotorula mucilaginosa*	99.5	very good	*Rhodotorula mucilaginosa*
Rm11	HL-7	*Rhodotorula mucilaginosa*	99.9	excellent	*Rhodotorula mucilaginosa*
Rm12	HL-7	*Trichosporan asahii*	99.9	very good	*Rhodotorula mucilaginosa*
Rm13	HL-6	*Rhodotorula mucilaginosa*	99.9	excellent	*Rhodotorula mucilaginosa*

* Yeasts were recoded after sequence analysis.

**HO: Hurma olive, GO: Gemlik olive, HL: Hurma leaves, GL: Gemlik leaves, A: air samples

4.2.4. Molecular Analysis

Following the evaluation of the yeast strains by cultural methods and taxonomic key, amplification reaction was performed for all yeast isolates of both harvest years using ITS primers. The agarose gel electrophoresis results of PCR products of olive yeasts from 2011 are shown in Figure 4.8; whereas the results for 2012 are shown in Figure 4.9. Since some of the yeast species could not be identified with ITS primers, one more PCR was employed with NL primers for ITS-unidentified yeast species and all previously unidentified yeasts could successfully be identified as shown in Figure 4.10. For sequencing, morphologically and biochemically the same strains isolated from the same plates of the same sampling week were selected as representative strains and accession numbers were obtained after submission of sequences to Genbank (Table 4.5).

Table 4.5 shows the results of sequence analysis including GenBank Accession Numbers belonging to the each yeast isolated from different olive sources during varied harvest years and sampling weeks. According to Table 4.5, all yeasts were successfully identified using molecular identification tests. With regard to comparison of the results of molecular tests and API 20C AUX kit, it could be seen that only 6 of 46 (13%) yeast isolates showed similarity at the genus level with API test results.

According to this table, a total of 46 yeasts were identified in the first harvest year using molecular methods and the most identified yeast species in the first year were *Metschnikowia* sp. (18/46, 39%), followed by *R. mucilaginosa* (13/46, 28%) and *D. hansenii* (6/46, 13%) (Figure 4.11 a). The distribution of HO yeasts (29/46) in this year were as mostly *Metschnikowia* sp. (17/29, 59%), followed by *D. hansenii* (6/29, 21%) (Figure 4.11 b); whereas HL yeasts were mostly identified as *R. mucilaginosa* (6/8, 75%) (Figure 4.11 c). All yeasts from GO samples (3/46) were identified as *R. mucilaginosa* (3/46, 7%) (Figure 4.11 d) while both *A. pullulans* and *R. mucilaginosa* were identified in the same ratios among GL yeasts (3/6, 50%) (Figure 4.11 e). In the second harvest year, a total of 136 yeasts were identified by molecular methods. Figure 4.12 (a) shows that *Aureobasidium* sp. was the most commonly found yeast in the second year among all olive types (106/136, 78%) and on HO (19/25, 76%) (Figure 4.12 b) and also HL (42/53, 79%) (Figure 4.12 c). Similarly, GO and GL yeasts in this year included mostly *Aureobasidium sp.* (13/18, 72% and 30/35, 85%), respectively (Figure 4.12 d, e). Besides, yeasts different from the first year were also identified in the second year, including

Cryptococcus sp. (6/136, 4.4%), *Sporidiobolus* sp. (6/136, 4.4%), *Wickerhamiella* sp. (4/136, 3%) and *Pseudozyma* sp. (3/136, 2.2%). The only yeast identified in the first year but not existed in the second year was *D. hansenii* which of all isolated from HO type (Figure 4.11, b). In the second harvest year, it could be seen that HO type was the source for almost all of these yeasts listed here, except for *R. mucilaginosa* and *Metschnikowia* sp. (Figure 4.12, b). When HO of two harvest years were compared in terms of yeast types it could be observed that only *Aureobasidium* sp. was the common yeast isolated during both years. Therefore, if there would be any link between natural debittering of Hurma olives and the yeast population of this olive type this could involve *Aureobasidium* sp.

GO samples of the first year included only *R. mucilaginosa* which was also isolated from HO samples in the same harvest year. However, *Candida* sp., *Metschnikowia* sp. and *Aureobasidium* sp. were isolated from GO samples during the second harvest year, of which only *Aureobasidium* sp. was the common species isolated also from HO samples in the same year. According to the yeast genera and species isolated from olive leaves, HL samples in the first year included the same yeast species as HO samples of the same year: *Candida* sp., *Metschnikowia* sp. and *R. mucilaginosa*. In the second year, both of HO and HL samples had the same yeast types in addition to *Candida* sp. of HL samples. GL samples in the first year contained both *R. mucilaginosa* and *Aureobasidium* sp., whereas only *Aureobasidium* sp. was isolated from GO samples in this year. In the second year, GL samples included *Candida* sp. and *Aureobasidium* sp. which were common with GO samples in the same harvest year.

In Figure 4.13 (a) and (b), the distribution of yeasts during the sampling weeks for the first and second harvest years is shown, respectively. According to the results of the first year, there were fluctuations in yeast types during maturation period. *D. hansenii* and *Candida* sp. were identified only during the first half of the harvest season when there was quite variable yeast species in comparison with the end of maturation period. As the maturation proceeded, especially beginning from the fifth week, the dominant yeast flora has become as *R. mucilaginosa* (weeks 4-8) and *Aureobasidium* sp. (weeks 4 and 8). *Metschinikowia* which was the most isolated genus in this year were dominant only in the third and fourth week of the maturation period. Figure 4.13 shows that *Aureobasidium* sp. were the only and the most isolated yeasts identified from every week of the second year. Although the yeast variety was more at the beginning of sampling weeks than at the end of maturation period also in the second year, especially after the fourth week the yeasts *Aureobasidium* sp., *Metschnikowia* sp., *Candida* sp., *Cryptococcus* sp.,

Sporidiobolus sp., *Pseudozyma* sp. and *Wickerhamiella* sp. were isolated and *Aureobasidium* sp. were dominant among others.
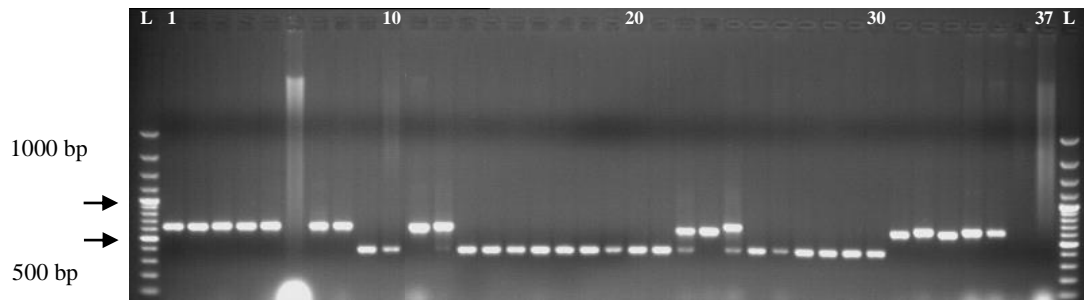
(a)
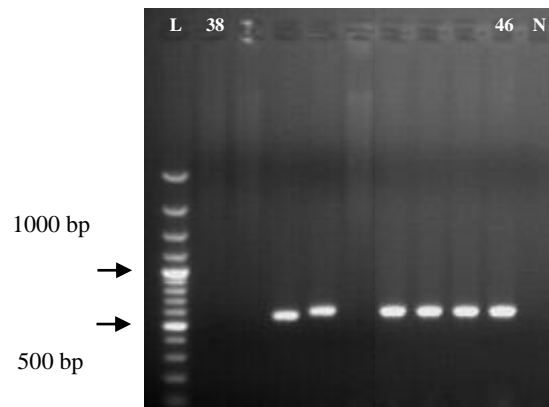
(b)

Figure 4.8. The agarose gel electrophoresis images of PCR products of the yeast isolates from 2011. L: GeneRuler 100 bp Plus DNA Ladder. N: negative control. Lanes 1-46 correspond to yeast codes defined in Table 4.4, in the order of up to down. The numbers: 6, 36, 37,38, 39 and 42 were re-amplified with NL primers
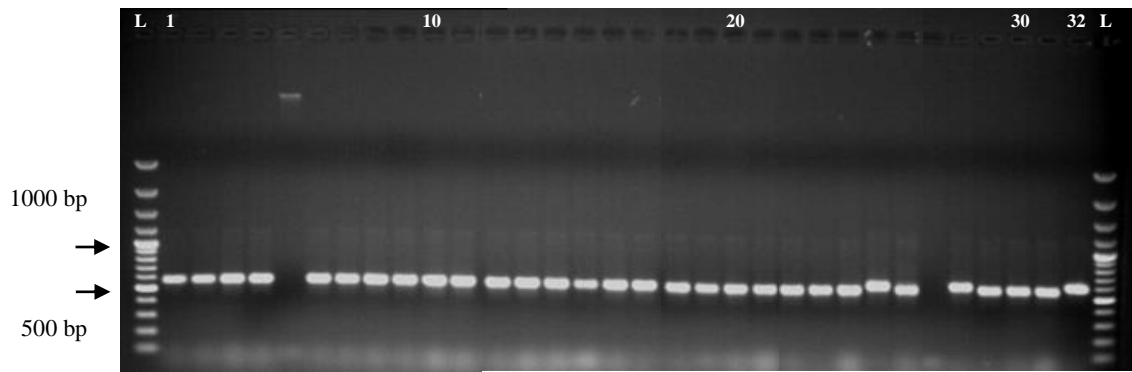
(a)
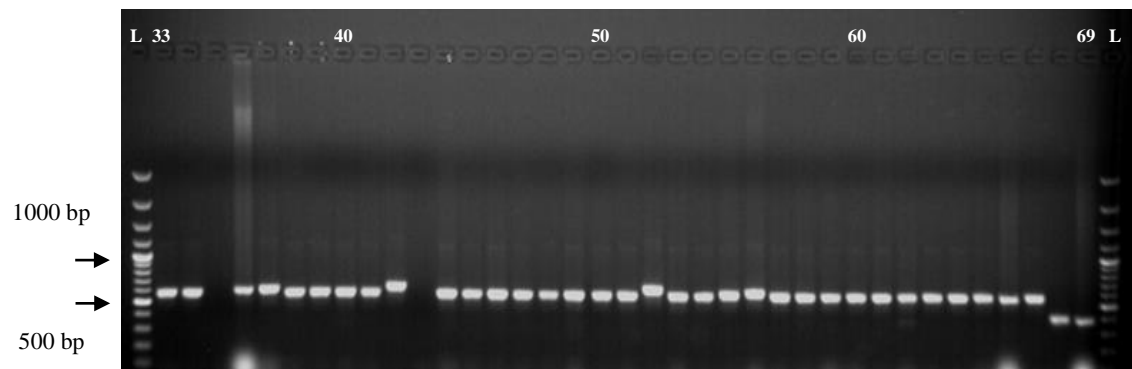
(b)
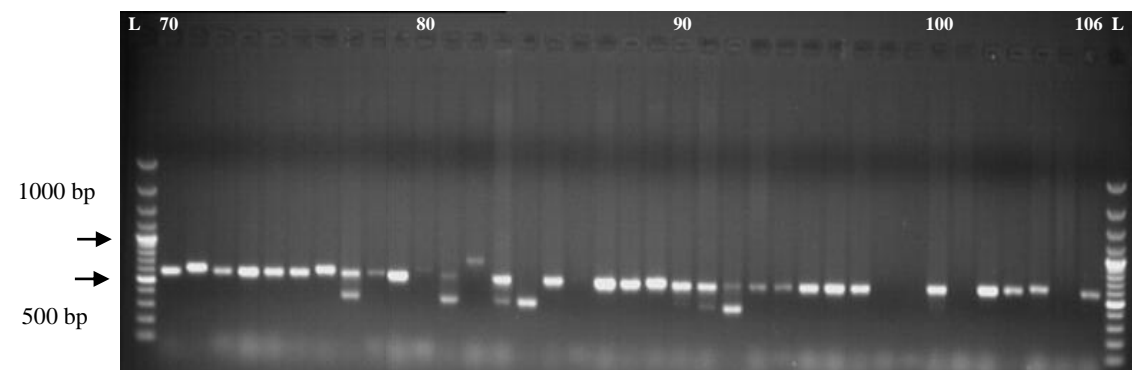
(c)

Figure 4.9. The agarose gel electrophoresis images of PCR products of the yeast isolates from 2012. L: GeneRuler 100 bp Plus DNA Ladder. N: negative control. Lanes 1-136 correspond to yeast codes defined in Table C.3, in the order of up to down. The numbers: 27, 35, 43, 69, 86, 98, 99, 101, 105, 107, 108, 109, 112, 117, 118, 121, 123, 125, 126, 127 and 131 were re-amplified with NL primers
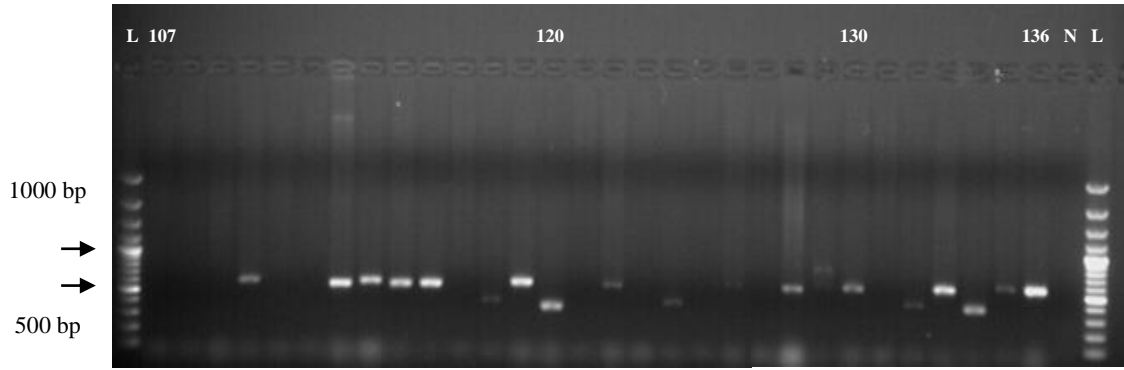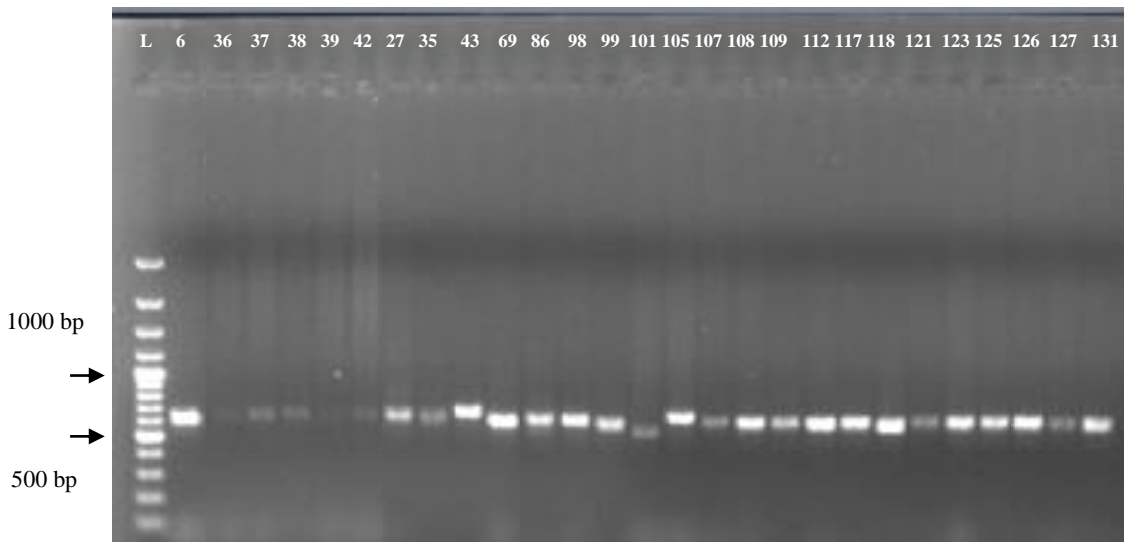
Figure 4.10. The agarose gel electrophoresis images of PCR products of the ITS-
unidentified (identified with NL primers) yeast isolates from 2011 and
2012. L: GeneRuler 100 bp Plus DNA Ladder. Lanes 6, 36, 37, 38, 39, 42:
NL-identified yeasts from 2011; Lanes: 27, 35, 43, 69, 86, 98, 99, 101, 105,
107, 108, 109, 112, 117, 118, 121, 123, 125, 126, 127 and 131: NL-
identified yeasts from 2012

Table 4.5. Molecularly identified olive yeasts from the first and the second harvest years

Yeast code-harvest year	Olive source-sampling week	Sequence analysis (Genus/Species-Max ID %-GenBank Accession Number)		
Cd1-I	HO-2	*Candida diddensiae*	99	KU240594
Cd2-I	HO-2	Similar to *Cd*		
Cz1-I	HO-2	*Candida zeylanoides*	86	KU240595
Cz2-I	HL-4	*Candida zeylanoides*	92	KU240596
Cp1-II	GO-5	Similar to *Cp*		
Cp2-II	HL-7	*Candida pimensis*	96	KU240597
Cp3-II	GL-7	Similar to *Cp*		
Cg1-II	GO-5	Candida geochares	74	KU240598
Dh1-I	HO-2	*Debaryomyces hansenii*	100	KU240599
Dh2-I	HO-2	Similar to *Dh*		
Dh3-I	HO-2	*Debaryomyces hansenii*	94	KU240600
Dh4-I	HO-2	*Debaryomyces hansenii*	93	KU240601
Dh5-I	HO-2	*Debaryomyces hansenii*	99	KU240602
Dh6-I	HO-4	*Debaryomyces hansenii*	91	KU240603
Mv1-I	HO-3	*Metschnikowia viticola*	98	KU240604
Mv2-I	HL-4	*Metschnikowia viticola*	99	KU240605
Mv(3-16)-I	HO-4	Similar to *Mv*		
Mp1-I	HO-4	*Metschnikowia pulcherrima*	97	KU240606
Mp2-II	GO-5	*Metschnikowia pulcherrima*	97	KU240607
Me1-I	HO-4	*Metschnikowia* sp.	96	KU240608
Me2-II	GO-6	*Metschnikowia* sp.	97	KU240609
Me3-II	GO-5	Similar to *Me*		
Mf1-II	HL-8	*Metschnikowia fructicola*	89	KU240610
Ap1-I	HO-4	*Aureobasidium pullulans*	98	KU240611
Ap2-I	HO-4	*Aureobasidium pullulans*	99	KU240612
Ap(3,4)-I	GL-4	Similar to *Ap*		
Ap5-I	GL-7	*Aureobasidium pullulans*	99	KU240613
Rm1-I	GL-4	Similar to *Rm*		
Rm2-I	GO-4	*Rhodotorula mucilaginosa*	99	KU240614
Rm3-I	GO-4	Similar to *Rm*		
Rm4-I	HL-5	*Rhodotorula mucilaginosa*	83	KU240615
Rm5-I	GO-5	*Rhodotorula mucilaginosa*	89	KU240616
Rm6-I	HL-5	Similar to *Rm*		
Rm7-I	HO-5	Similar to *Rm*		
Rm(8,9)-I	GL-7	Similar to *Rm*		
Rm10-I	HL-7	*Rhodotorula mucilaginosa*	94	KU240617
Rm11-I	HL-7	Similar to *Rm*		
Rm12-I	HL-7	*Rhodotorula mucilaginosa*	98	KU240618
Rm13-I	HL-6	Similar to *Rm*		
Ap6-II	A-5	Similar to *Ap*		
Ap(7,17,49,52,56,73,82)-II	HL-5	Similar to *Ap*		
Ap8-II	HO-5	*Aureobasidium pullulans*	99	KU240619
Ap(9,15,66)-II	HO-5	Similar to *Ap*		
Ap(10,16,25,28,35)-II	HL-6	Similar to *Ap*		
Ap(11,12,14,21,75,80)-II	HO-6	Similar to *Ap*		
Ap(13,20)-II	GO-6	Similar to *Ap*		
Ap(18,42,46,55,70)-II	GL-5	Similar to *Ap*		
Ap(19,29,32)-II	HL-2	Similar to *Ap*		
Ap(22,69,71,85)-II	HO-7	Similar to *Ap*		
Ap(23,59,60,76,77,84)-II	HL-7	Similar to *Ap*		
Ap24-II	GL-7	*Aureobasidium pullulans*	94	KU240620
Ap(26,33)-II	HL-4	Similar to *Ap*		
Ap(27,34,37,38,79)-II	GL-6	Similar to *Ap*		
Ap40-II	GL-6	*Aureobasidium pullulans*	88	KU240621
Ap(30,31)-II	GL-2	Similar to *Ap*		
Ap36-II	GL-3	Similar to *Ap*		
Ap39-II	GL-3	*Aureobasidium pullulans*	90	KU240622
Ap41-II	HO-5	*Aureobasidium pullulans*	89	KU240623
Ap43-II	GO-5	*Aureobasidium pullulans*	99	KU240624

(Cont. on next page)

Table 4.5 (Cont.)

Yeast code-harvest year	Olive source-sampling week	Sequence analysis (Genus/Species-Max ID %-GenBank Accession Number)		
Ap(44,47,48,51,83)-II	GO-5	Similar to *Ap*		
Ap45-II	GO-5	*Aureobasidium pullulans*	81	KU240625
Ap50-II	HL-5	*Aureobasidium pullulans*	99	KU240626
Ap53-II	HL-8	Similar to *Ap*		
Ap54-II	GL-8	*Aureobasidium pullulans*	99	KU240627
Ap57-II	GO-8	Similar to *Ap*		
Ap(58,64,67,68,74)-II	GL-7	Similar to *Ap*		
Ap61-II	HL-7	*Aureobasidium pullulans*	92	KU240628
Ap62-II	GL-7	*Aureobasidium pullulans*	87	KU240629
Ap63-II	HL-7	*Aureobasidium pullulans*	90	KU240630
Ap65-II	HO-6	*Aureobasidium pullulans*	89	KU240631
Ap(72,78)-II	GO-7	Similar to *Ap*		
Ap81-II	A-7	Similar to *Ap*		
Au(1,19)-II	HO-6	Similar to *Au*		
Au2-II	HL-7	Similar to *Au*		
Au(3,6,9,20,23)-II	GL-6	Similar to *Au*		
Au(4,8,10)-II	HL-4	*Aureobasidium* sp.	95	KU240632
Au(5,7,24,25)-II	HL-6	Similar to *Au*		
Au(11,17)-II	GL-4	Similar to *Au*		
Au(12,14,18)-II	HL-1	Similar to *Au*		
Au(13,15)-II	HL-4	Similar to *Au*		
Au16-II	HL-2	Similar to *Au*		
Au21-II	GO-8	Similar to *Au*		
Au22-II	HL-8	Similar to *Au*		
Au26-II	HO-7	*Aureobasidium* sp.	91	KU240633
Cu1-II	HL-5	*Cryptococcus uzbekistanensis*	99	KU240634
Ca1-II	HL-4	*Cryptococcus aerius*	93	KU240635
Ca2-II	HL-2	*Cryptococcus aerius*	92	KU240636
Ca3-II	HL-2	*Cryptococcus aerius*	98	KU240637
Cu2-II	HO-5	*Cryptococcus uzbekistanensis*	99	KU240638
Cm1-II	GL-4	*Cryptococcus magnus*	100	KU240639
Ss1-II	HL-2	*Sporidiobolus salmonicolor*	84	KU240640
Ss2-II	GL-6	*Sporidiobolus salmonicolor*	96	KU240641
Ss3-II	HL-2	Similar to *Ss*		
Ss4-II	HO-8	*Sporidiobolus salmonicolor*	99	KU240642
Ss5-II	GL-7	*Sporidiobolus salmonicolor*	99	KU240643
Sp1-II	HL-2	*Sporidiobolus pararoseus*	97	KU240644
Rm14-II	A-2	Similar to *Rm*		
Rm15-II	A-1	*Rhodotorula mucilaginosa*	90	KU240645
Rm16-II	HL-2	*Rhodotorula mucilaginosa*	99	KU240646
Ph1-II	HO-6	*Pseudozyma hubeiensis*	92	KU240647
Ph2-II	A-6	Similar to *Ph*		
Pp1-II	HO-6	*Pseudozyma prolifica*	94	KU240648
Wi1-II	HL-5	*Wickerhamiella* sp.	89	KU240649
Wi2-II	GL-5	*Wickerhamiella* sp.	88	KU240650
Wi3-II	HO-3	Similar to *Wi*		
Wi4-II	HO-1	Similar to *Wi*		
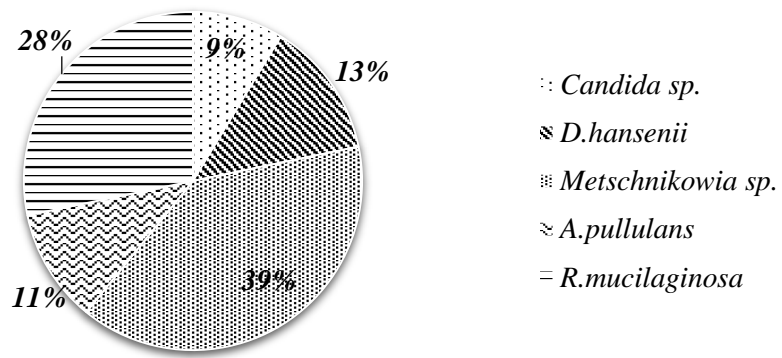
(a)
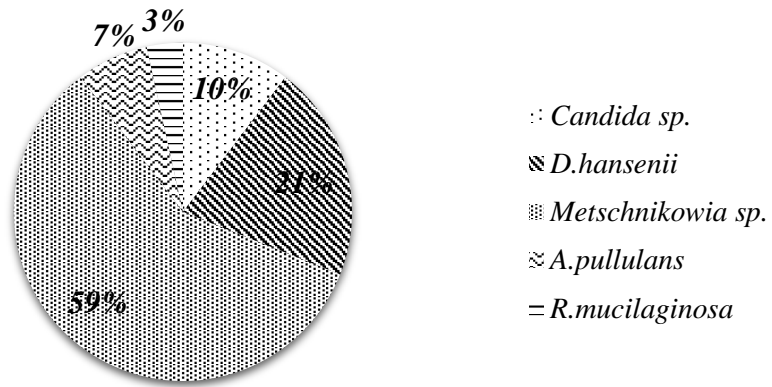
(b)
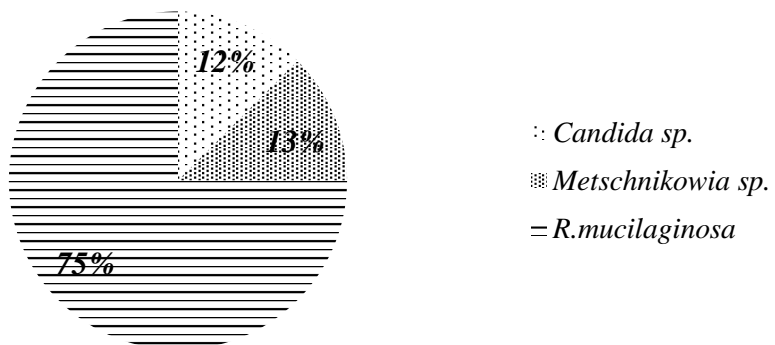
(c)

Figure 4.11. The distribution of (a) total olive, (b) HO, (c) HL, (d) GO and (e) GL yeasts identified in the first harvest year

(Cont. on next page)

Figure 4.11 (Cont.)
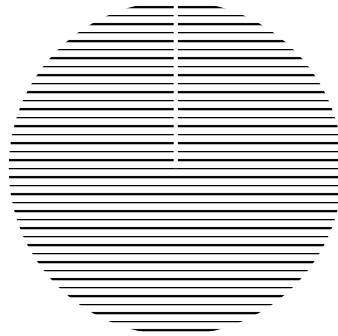
R.mucilaginosa;
100%

(d)

50%   50%
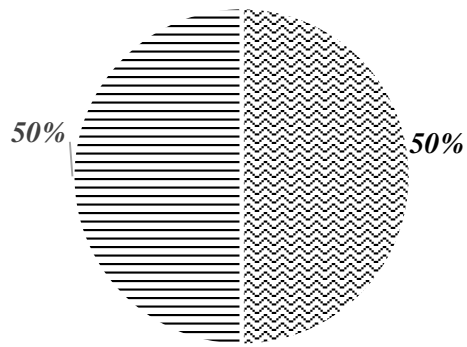
≋ A.pullulans

‒ R.mucilaginosa

(e)
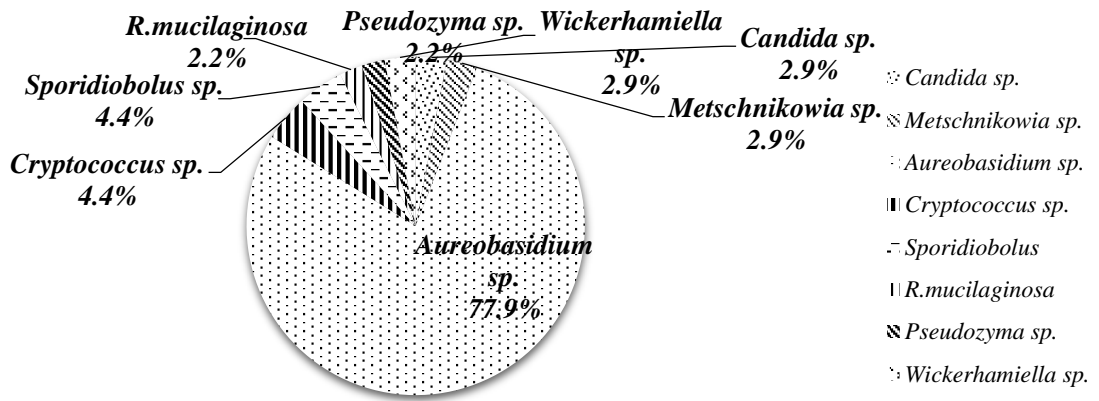
(a)
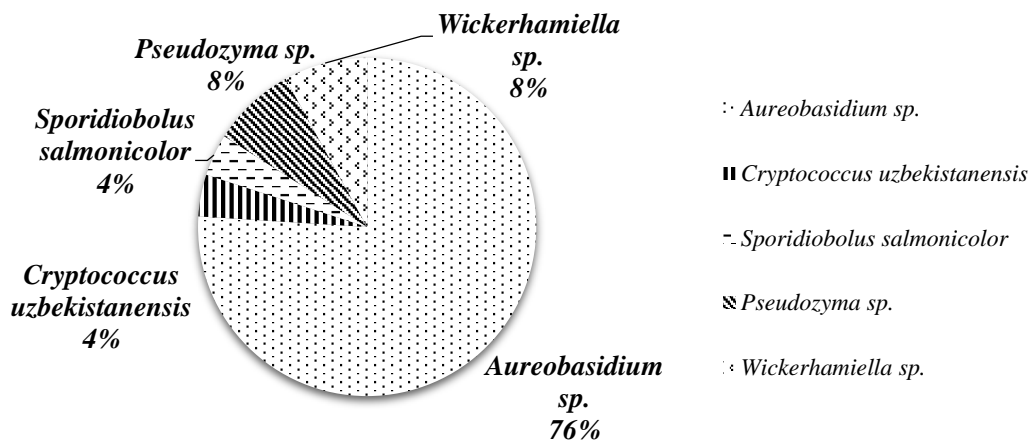
(b)
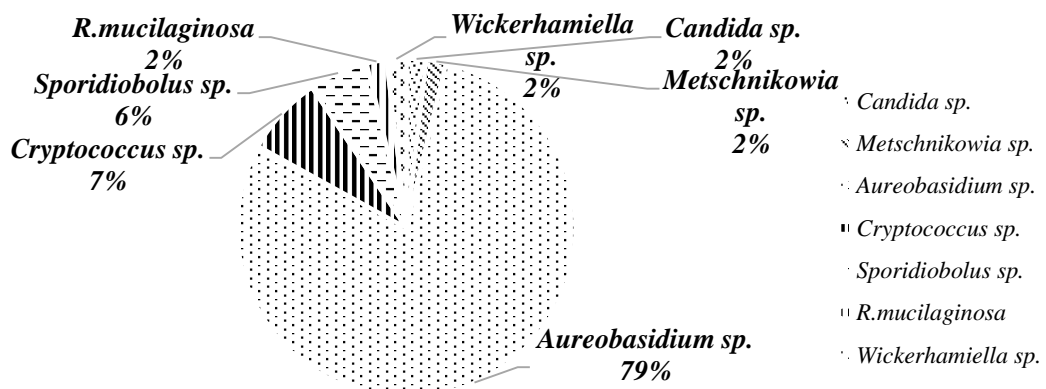
(c)

Figure 4.12. The distribution of (a) total olive, (b) HO, (c) HL, (d) GO and (e) GL yeasts identified in the second harvest year

Figure 4.12 (Cont.)

Candida sp.

Metschnikowia sp.

Aureobasidium sp.

(d)

Candida sp.

Aureobasidium sp.

Cryptococcus sp.

Sporidiobolus sp.

Wickerhamiella sp.
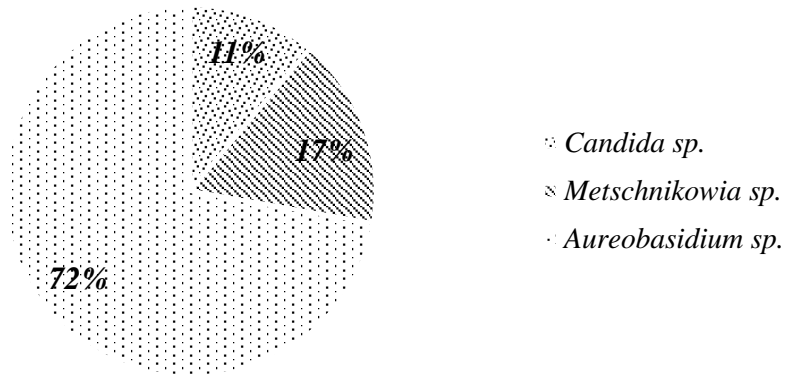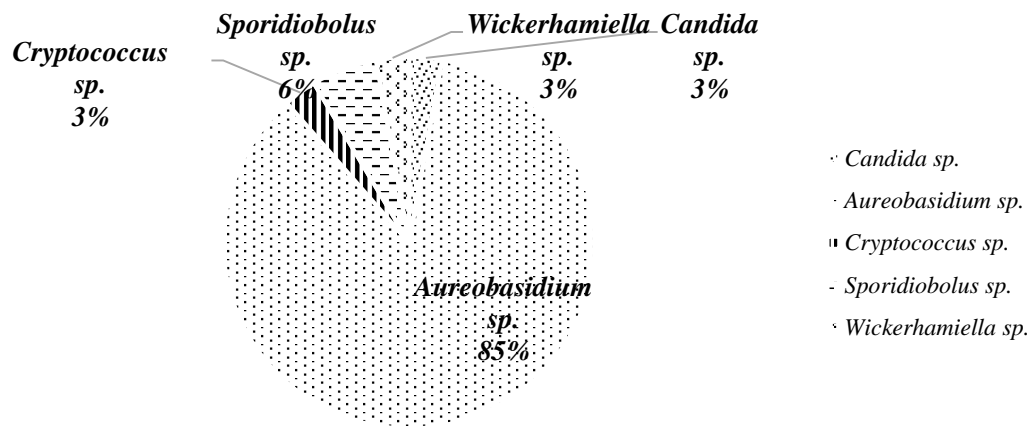
(e)
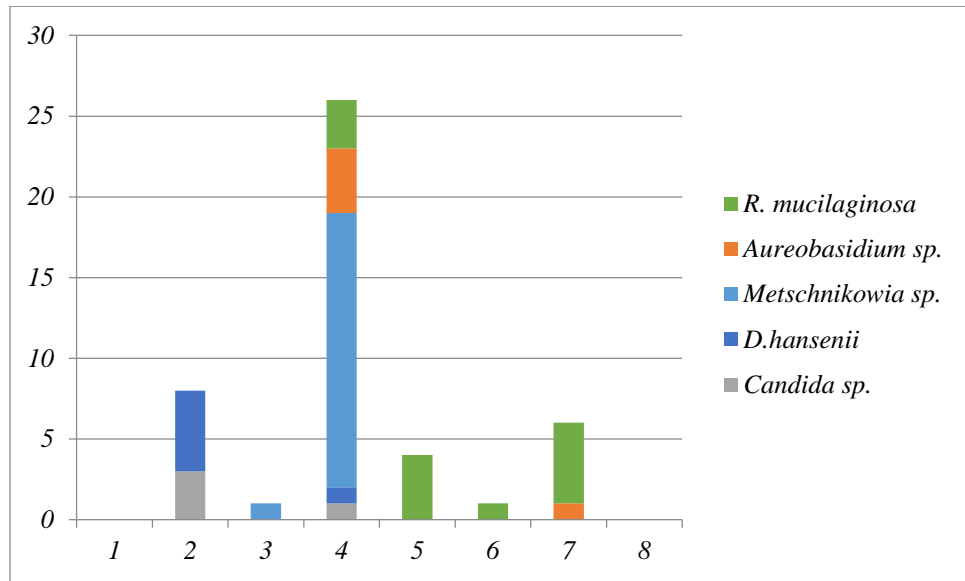
(a)
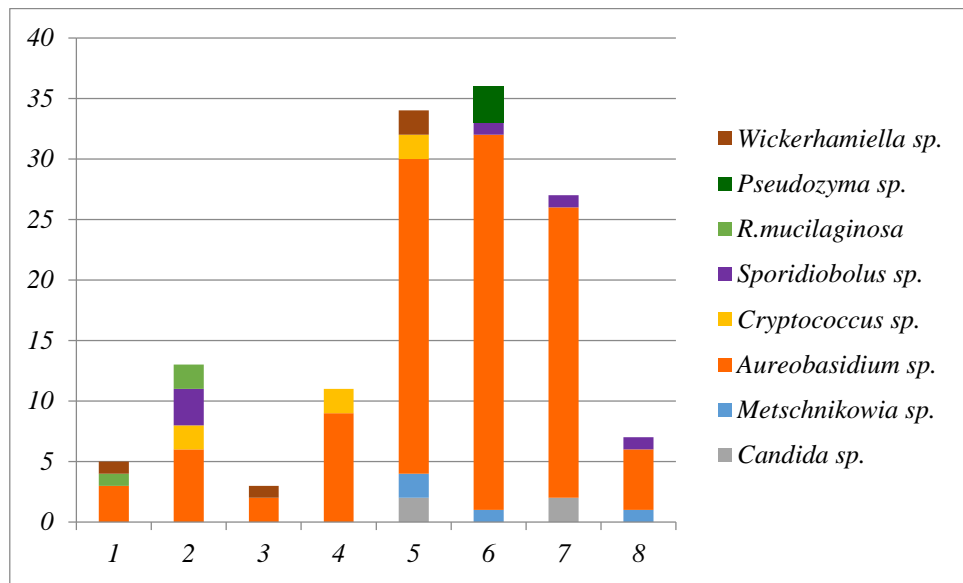
(b)

Figure 4.13 The distribution of yeasts during eight sampling weeks for the (a) first and (b) second harvest years

Our results show similarity with the previous researches about the other natural black olives. Some of the yeasts isolated from naturally black olive brines were identified as *S. oleaginosus, H. anemola, H. subpelliculosa, D. hansenii, P. membranaefaciens, P. farinosa, P. fermentans, K. veronae*, *T. candida, T. norvegica, C. diddensii, C. boidinii, C. krusei, C. valida* and *Cryptococcus ater* (Garrido Fernandez et al., 1997). Materassi et al. (1975) studied debittering effect of 36 yeast species and found 8 of them had the capacity of hydrolysing oleuropein including the most active species *Rhodotorula* and *Candida*. Sibbett and Ferguson (2005) reported in their research that the pink yeasts (*Rhodotorula* sp.) are associated with softening of olives due to their product of polygalacturonase. Marquina et al. (1992) reported *C. hellenica, C. oleophila, D. hansenii, P. anomala* and *R. mucilaginosa* as the yeast species which are able to use oleuropein as carbohydrate substrate and these findings are similar with our results. Other researchers studied with traditional Greek-style product of natural black olives and identified *Saccharomyces, Hansenula, Candida, Torulopsis, Debaryomyces, Pichia*, *M. pulcherrima, Kluyveromyces, A. pullulans* and *Cryptococcus* (Hui and Evranuz, 2012). There have been also some studies with Throuba-style olives grown mainly in Greece which were thought to sustain natural debittering and transformation by a fungal enzyme (Kailis and Harris, 2007). These authors also reported that *C. veronae* was found as having oleuropein hydrolysing properties. Kotzekidou (1997) identified yeast population including *T. delbrueckii, D. hansenii* and *C. laurentii* associated with Greek olive cultivars and *S. cerevisiae* and *P. anomala* associated with Spanish cultivars. Coton et al. (2006) identified *P. anomala, C. boidinii* and *D. etchellsii* in French natural black olives. When the results of this study are compared with previous researches, it was observed that the yeast flora of Hurma and Gemlik olive samples is more like Greek olive cultivars. Different yeast species from the literature were also identified from Hurma olives in this study, including *Pseudozyma hubeiensis, Pseudozyma prolifica, Cryptococcus uzbekistanensis, Sporidiobolus salmonicolor* and *Wickerhamiella* sp.

4.2.4.1. Phylogenetic Tree of Olive Yeasts

Phylogenetic trees of polymorphic sequences belonging to all yeasts isolated from both two harvest years are shown in Figure 4.14 (a). In order to check the relationships of the most commonly isolated yeasts with respect to harvest years, phylogenetic trees of

polymorphic sequences belonging to *Metschnikowia* sp. (Figure 4.14, b) and *A. pullulans* (Figure 4.14, c) from the first and the second harvest year, respectively, were also constructed. Therefore, it was possible to see the homogeneity and heterogeneity between olives. Evolutionary analyses were conducted with MEGA6 software. The phylogenetic trees were constructed using the Neighbor-Joining method. The percentages of replicate trees in which the associated taxa clustered together in the bootstrap test (500 replicates) are shown next to the branches. The tree is drawn to scale, with branch lengths in the same units as those of the evolutionary distances used to infer the phylogenetic tree. The evolutionary distances were computed using the p-distance method and are in the units of the number of base differences per site. The optimal tree for all yeasts with the sum of branch length = 8.45201505 is shown (Figure 4.14, a) and this analysis involved 57 nucleotide sequences. On the other hand, the optimal trees for *Metschnikowia* sp. and *A. pullulans* with the sum of branch lengths = 1.34974522 (Figure 4.14, b) and 2.53185009 (Figure 4.14, c) are shown and these analysis involved 8 and 19 nucleotide sequences, respectively.

As it can be seen in Figure 4.14 (a), *Aureobasidium* species were clustered in two different groups. *Metschnikowia* species were generally close to each other except for the species Mf1-II and Me2-II which showed very high specifity (100%) with Ap. *Candida* species were differentiated also in two groups as from the first year (Cz and Cd) and from the second year (Cp and Cg). Two species of *Pseudozyma* (Pp and Ph) fell apart from each other. *Cryptococcus* species were generally clustered close to each other except for Ca2-II. *Sporidibolus* species were also clustered close to each other with one exception with Ss1-II. *Wickerhamiella sp.* were observed together. As it can be seen in Figure 4.14 (b), *Metschnikowia* sp. isolated from different harvest years (as I and II) did not separate clearly from each other. Therefore, it is likely that there is a homogeneity between olives from two years in terms of *Metschnikowia* sp. Figure 4.14 (b) shows *A. pullulans* isolated from the first year clustered almost with each other and close to type strain.
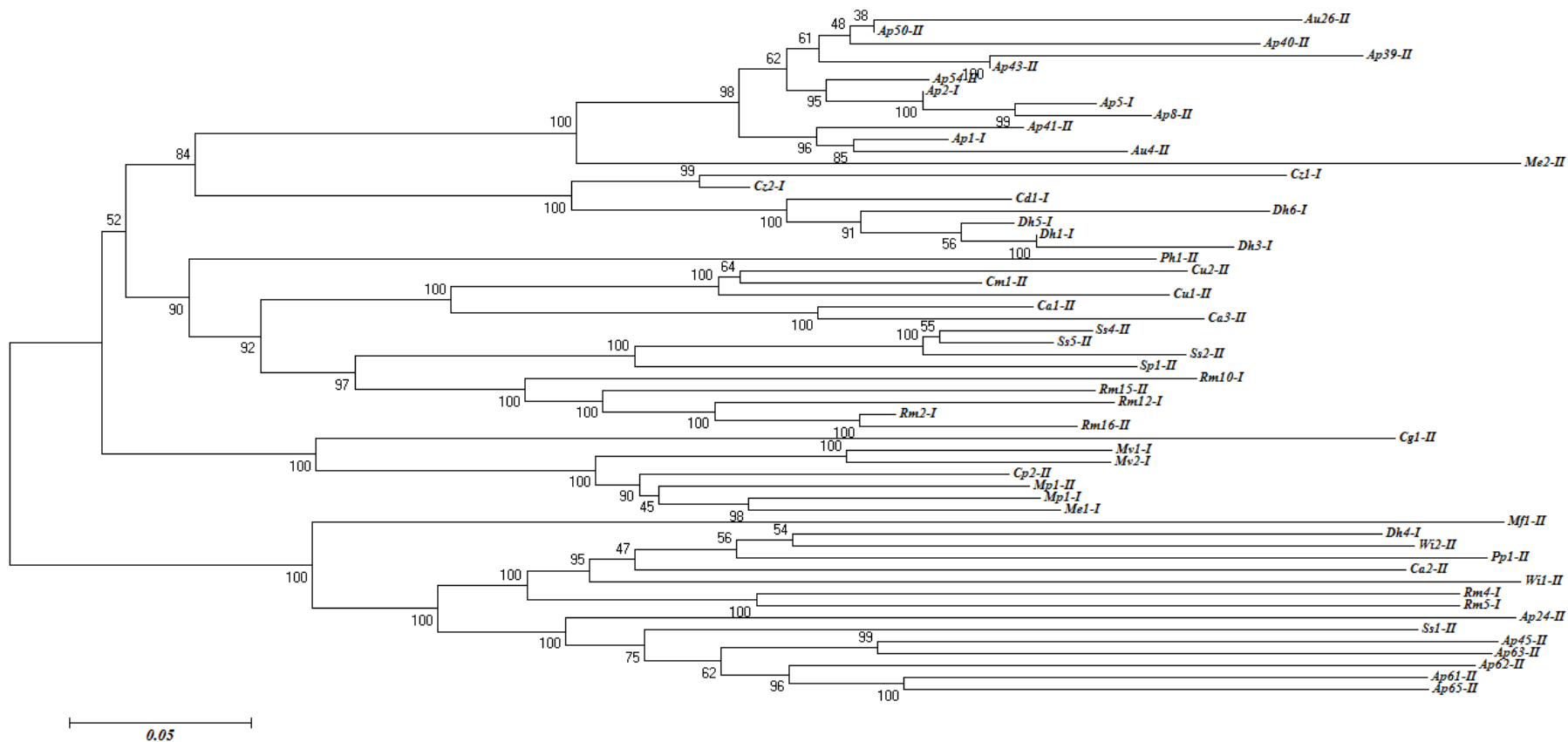
(a)

Figure 4.14. Neighbour-joining phylogenetic tree of the polymorphic sequences of the D1/D2 domains of the 26S rDNA of (a) all olive yeasts harvested from both harvest years (b) *Metschnikowia* sp. and (c) *A. pullulans*. I and II: First and second harvest years. All the yeast codes are listed in Table 4.5

(Cont. on next page)

Figure 4.13 (Cont.)
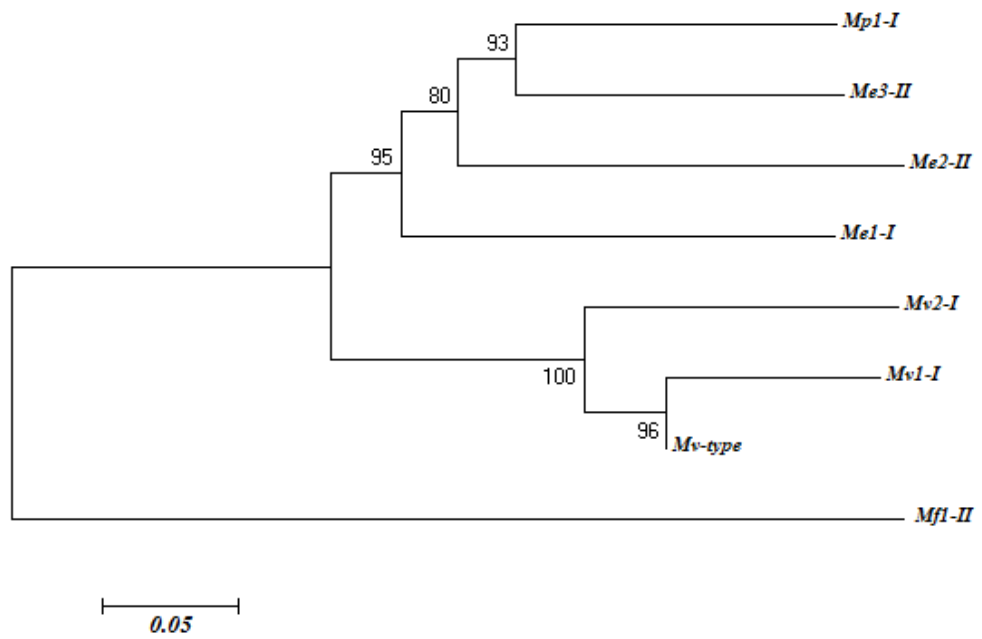
(b)
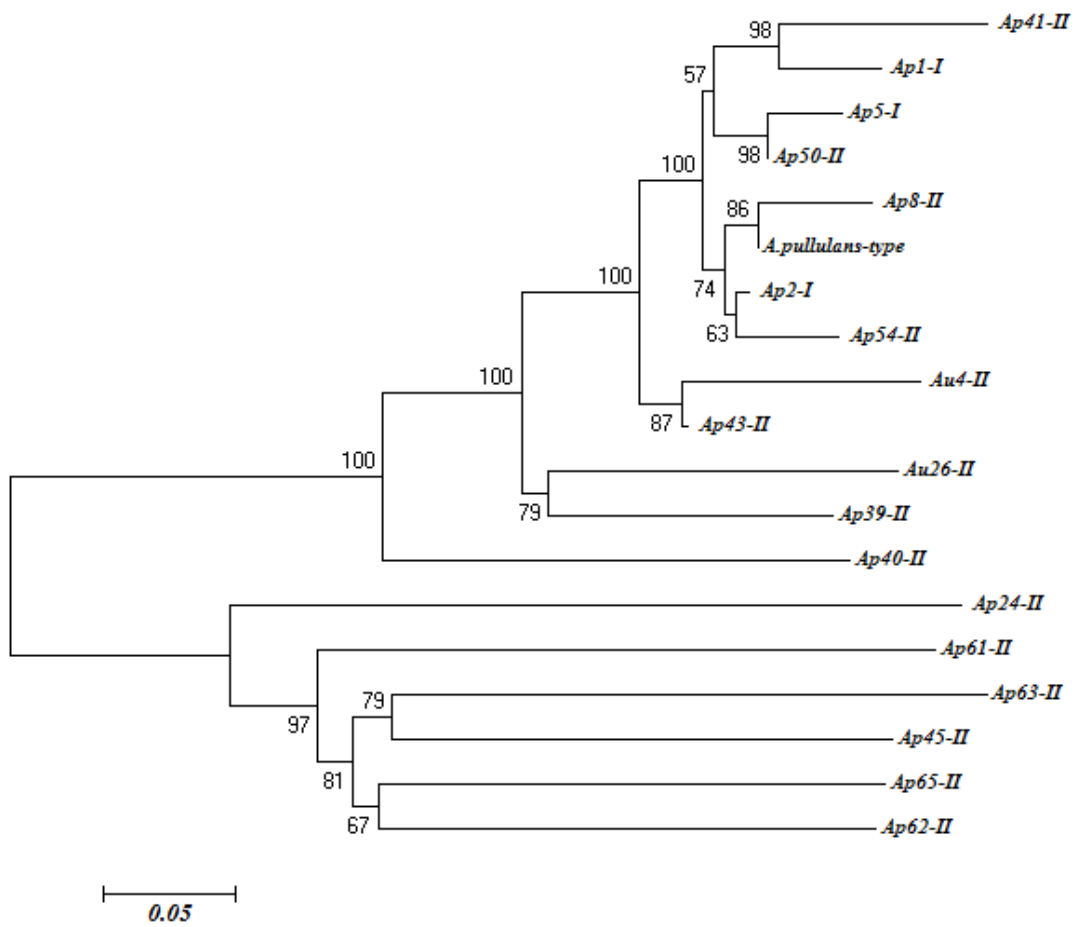
(c)

4.2.5. Mid-Infrared Spectroscopy Analysis

As it was described in details in Chapter 3, besides the use of dried yeast cell suspension on ZnSe plate, the yeast colonies from olive samples were also directly used after collecting from agar plate and spreading on to ZnSe crystal plate like a thin film. In the Figure 4.15 (a) and (b), the overlay and split displays of FTIR spectra (4000-650 cm^{-1}) of the *dried* yeast colonies are shown, respectively. The same graphics of *directly* used yeast colonies are presented in Figure 4.16 (a) and (b). The spectral differences between various yeasts could be easily observed. As can be seen from these figures, some peaks for dried samples, especially the ones in 900-600 cm^{-1} DNA fingerprint region, were resolved better compared to directly prepared yeasts. In addition, a dominant high water peak (-OH band, ~3200 cm^{-1}) could be seen in directly used yeast colonies.
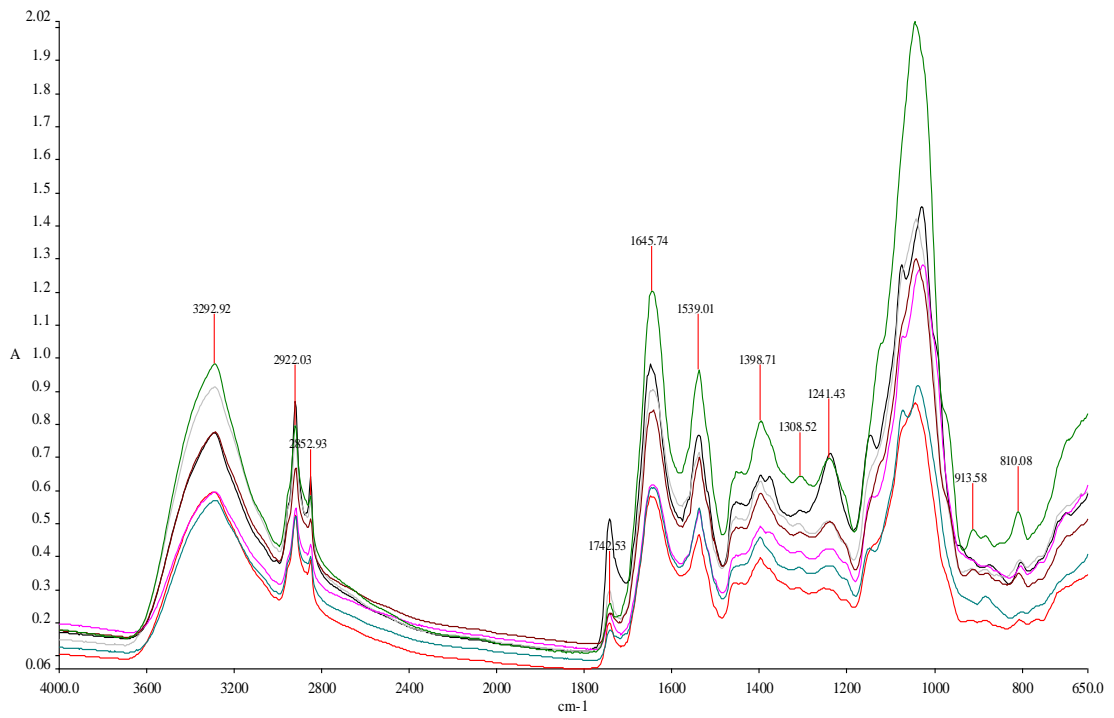
(a)
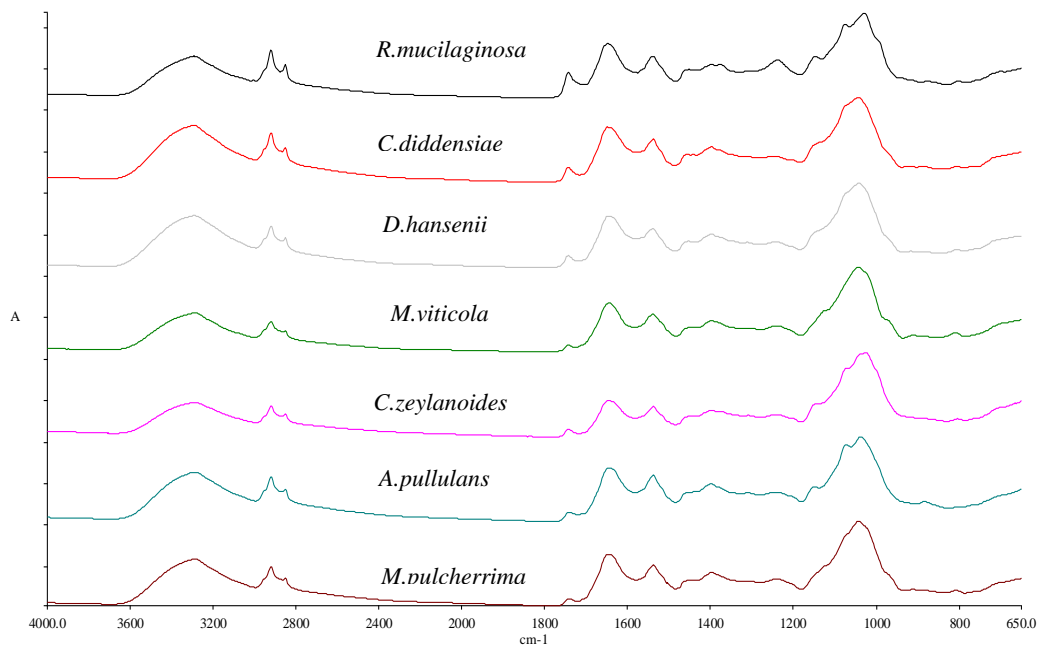
(b)

Figure 4.15. The (a) overlay and (b) split displays of FTIR spectra of some of *dried* yeast colonies which were molecularly identified
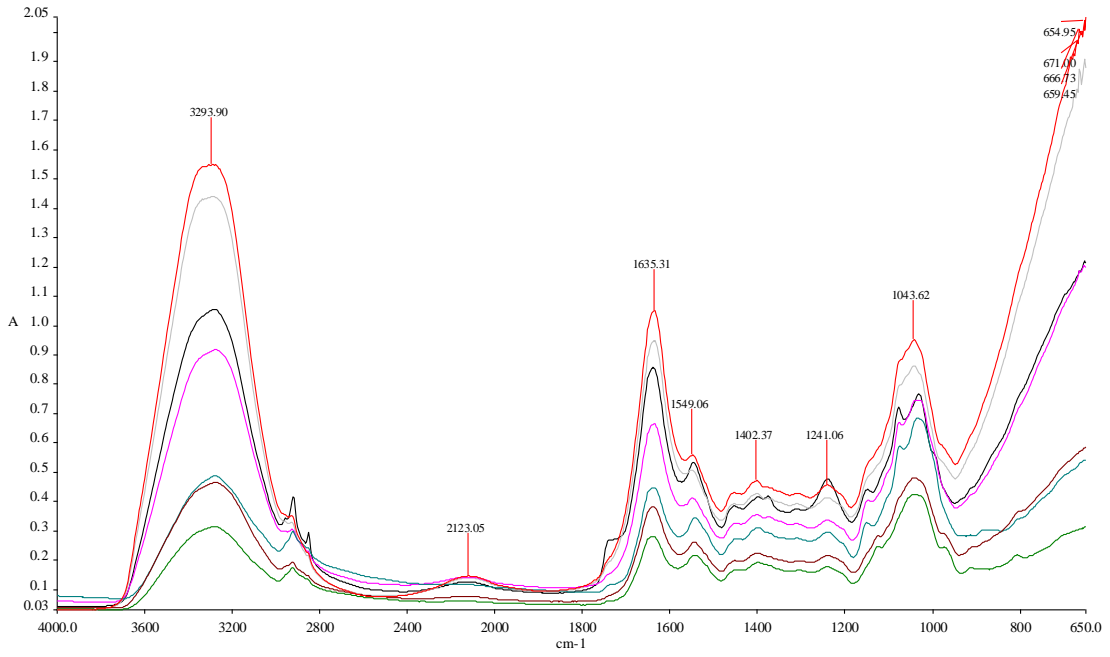
(a)
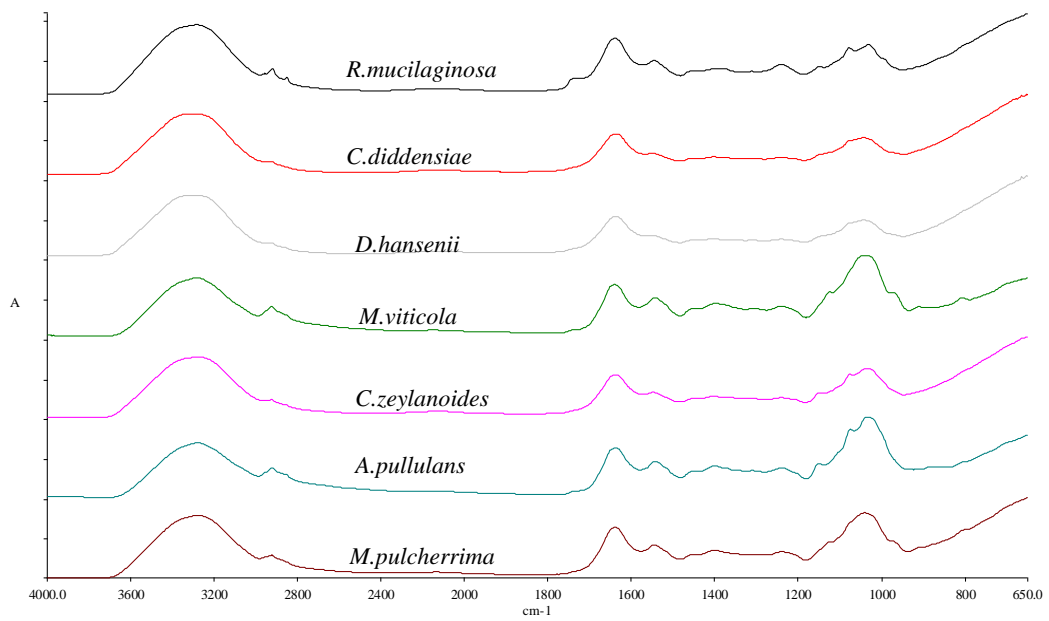
(b)

Figure 4.16. The (a) overlay and (b) split displays of FTIR spectra of some of *directly used* yeast colonies which were molecularly identified

4.2.5.1. Evaluation of the Results with Multivariate Statistical Analysis

As wine yeast samples, both full (4000-650 cm^{-1}) and partial (3030-2830 cm^{-1}, 1350-1200 cm^{-1} and 900-700 cm^{-1}) spectral regions were used for chemometric analysis of FTIR data for dried and directly used olive yeast cells.

First, PCA was applied to mid-infrared spectra of yeasts from both harvest years to investigate if the separation of different yeasts is possible. Since some differentiation in yeast species was observed with PCA, data was also analyzed with another multivariate statistical technique; PLS-DA and statistical information about the models are indicated in Table 4.6. Figure 4.17 shows the PLS-DA score plots of the *dried* yeast cells including full (a) and partial (b) spectral regions; whereas the plots of *directly* used yeast cells including full (a) and partial (b) spectral regions are provided in Figure 4.18. Both the full and partial spectral regions of dried and directly used yeast cells provided the best results after application of 2nd derivative and PLS-DA to data.

Table 4.6. Statistical information about the PLS-DA models for the olive yeasts

Model		2nd Derivative	Number of PC	R^2	Q^2
Dried yeast	Total region	+	10	0.886	0.434
	Partial region	+	10	0.665	0.363
Directly used yeast	Total region	+	8	0.781	0.338
	Partial region	+	6	0.518	0.323

Figure 4.17 (a) and (b) indicate similar results for differentiation of dried yeast species using either total or partial spectral regions. It could be observed that the best results for clustering were obtained for the species of *Wickerhamiella* and *Cryptococcus*. *Candida* species were seen to be divided into two groups as 1st (Cd, Cz) and 2nd (Cg, Cp) year yeasts which were clustered close to *Wickerhamiella*. Previous phylogenetic analysis of RNA gene sequences demonstrated that many *Candida* species were related to *Wickerhamiella*, e.g. gene sequences placed *C. versatilis* as a sister species to *W. domercqiae*; *C. galacta* into the *Wickerhamiella clade*, *C. lipophila* is the anamorph of *W. lipophila* (Kurtzman and Robnett, 1997). *Aureobasidium* species generally grouped under the same cluster with a few exceptions (e.g. Ap-2-41, Ap-2-42). This yeast which has been also isolated during the 1st year, has been known as a primary invader of all

kinds of leaves. During the summer season its spores are deposited on the leaf surface without attacking the cells; however, in autumn, when the leaves reach over-ripening, they begin to spread (Zalar, 2008). This yeast is one of the few yeasts isolated from both harvest seasons of olives and in the score plot it could be observed that there is a difference between the 1st and 2nd year *Aureobasidium* sp. which might be due to the production of different metobolites in different harvest years having varied conditions.

Metschnikowia species generally differentiated from other yeasts but also close to some of *Candida* isolates. It was reported that this yeast is sister genus to *Clavispora*; e.g. *M. agaves* was found 100% similar with *C. lusitaniae*, which is the telemorph of *Candida lusitaniae*. The anamorph of *M. pulcherrima* has been remarked as *Candida pulcherrima* and it showed also 100% similarity with *M. fructicola* and 99% with *Candida pimensis*. In addition, *M. viticola* was reported to be a telemorph of *C. kofuensis* (Kurtzman and Fell, 2006). The main and may be the only difference between Figure 4.17 (a) and (b) is the differentiation of *Cryptococcus* species, which were divided into two groups when whole infrared spectrum was used, whereas they were clustered almost together in the right side of the plot when partial spectral region was used. In both graphics, each group was close to *Candida* species, which confirms a previously published report indicating that an isolate belonging to *Cryptococcus neoformans* was classified by NMR as *Candida glabrata* (Himmelreich, 2003). *Sporidiobolus salmonicolor* cells were clustered together and differentiated from *S. pararoseus*. Figure 4.18 (a) and (b) showing the differentiation of directly used cells using total and partial spectral regions, respectively, indicated more scattered results compared to Figure 4.17. Although clustering of *Aureobasidium* and *Wickerhamiella* species showed similar results, species of *Sporidiobolus* and *Candida* could not be put together closely within themselves; however, *Metschnikowia* sp. except for a few species and *Cryptococcus* sp. were gathered together better for directly used cells.

(a)

(b)

Figure 4.17. PLS-DA score plots of the *dried* yeasts including data in (a) full, 4000-650 cm^{-1} and (b) partial, 3030-2830 cm^{-1}, 1350-1200 cm^{-1} and 900-700 cm^{-1} spectral regions

(a)

(b)

Figure 4.18. PLS-DA score plots of of the *directly used* yeasts including data in (a) full, 4000-650 cm^{-1} and (b) partial, 3030-2830 cm^{-1}, 1350-1200 cm^{-1} and 900-700 cm^{-1} spectral regions

Some of the yeast species, which were a few in number (*Pseudozyma* sp.) and showed very scattered scheme (*Debaryomyces* sp.*, Rhodotorula* sp.) were excluded from PLS-DA models. *Pseudozyma* is an "oleaginous" yeast which means "lipid accumulating" and some of these yeasts can accumulate 20-70% of their biomass as lipids. Besides *Pseudozyma*, this group includes *D. hansenii, Candida, Cryptococcus, Metschnikowia, Pichia* and *Rhodotorula* (Cohen and Ratledge, 2005). This ability of these yeasts provides the commercial production of lipids, single cells, biodiesel generation etc. *P. hubeiensis* and *P. prolifica* were clustered in the group of the *Sporisorium* clade. In another study by Wenning et al. (2002), it was reported that especially for *Clavispora lusitaniae*, which is the telemorph of *Candida lusitaniae* and *Debaryomyces hansenii*, identification by FTIR microspectroscopy was difficult, since *D. hansenii* is highly heterogenous species according to a taxonomy based on physiological markers and spectroscopically similar with the species e.g. *Candida parapsilosis*, *C. intermedia* and *Clavispora lusitaniae*, as also have been reported by Breuer et al. (2006) and Kümmerle et al. (1998). Desnos-Ollivier et al. (2008) also indicated that *D. hansenii* and *P. guilliermondiii* are extremely difficult to differentiate phenotypically. It was shown that this yeast belongs to the large clade of yeast species involving most of the *Candida* and *Pichia*. *R. mucilaginosa* have 100% similarity with *Sporobalomyces alborubescens* which are telemorphs with *Sporidiobolus*. It was previously shown that *S. salmonicolor* was 100% similar with *R. mucilaginosa* and *R. glutinis* (Libkind et al., 2005). It was also reported that one of the reason of unsuccessful clustering of the same species' strains by FTIR could be detection of novel species, subspecies or mutants. Habitat variants may result in separate clusters for one species and have different FTIR spectra. Some examples for this situation are *D. hansenii* and *S. cerevisiae*. Strains of *S. cerevisiae* cluster in different groups but it is still unknown whether these groups represent isolates from definite habitats. Another sign for the existence of different species has been reported to be different degrees of homogeneity in the spectral distances between strains. Kurtzman et al. (2011) indicated that *D. hansenii* is a heterogeneous species according to a taxonomy based on physiological markers.

In order to evaluate identification ability of FTIR spectroscopy, the method has been used with 717 yeast isolates, which were obtained from different habitats, mostly from the food industry (Kümmerle et al., 1998). Among them, 699 yeast strains were identified correctly by FTIR spectroscopy with an identification rate of 97.5%. It was concluded that FTIR spectroscopy provides a comparable, rapid alternative to

conventional identification systems for food-borne yeasts. However, identification by FTIR spectroscopy is limited only by the the reference spectrum library, which can be improved by adding further yeast isolates to the database. Wenning et al. (2002) used both FTIR micro- and macrospectroscopy for identification of yeast species. It was found that FTIR microspectroscopy identified 67% of the strains correctly at the species level and FTIR macrospectroscopy identified 65%. Especially identification of *Clavispora lusitaniae* and *D. hansenii* was difficult by FTIR microspectroscopy. Researchers proposed of including more strains of the same species in the library, however, identification of *D. hansenii* was still difficult, since it is a heterogenous species and there are some morphologically, physiologically and spectroscopically similar species, e.g., *C. lusitaniae*, *Candida parapsilosis*, and *Candida intermedia*. Results of this study showed that FTIR microspectroscopy was a useful tool for the identification of yeasts.

FTIR results for differentiation of yeasts using both dried or directly used cells in this study showed that there is a relation between molecular and mid-IR spectroscopy results. There are a few publications about characterization of yeasts using mid-IR spectroscopy and only a few aimed to compare the FTIR results with molecular characterization studies. Kümmerle et al. (1998) reported that since FTIR spectra were influenced by plating methods, type of agar medium, growth temperature, incubation time, and the drying method of the microorganism suspension, the standardized preparation procedure should be developed. It was constructed a dendrogram of 332 reference yeasts from FTIR spectra which showed that different species of the same genus generally formed different clusters, especially the genera *Pichia* and *Candida*. The taxonomy of yeasts generally relies on phenotypic characters; therefore, molecular data was expected to give parallel results with FTIR spectroscopy. However, some of the yeast sequences do not confirm this argument. For instance, although *Candida tropicalis, Candida parapsilosis*, and *Candida maltosa* are very closely related according to 18S rRNA, *C. tropicalis* did not cluster with the rest. It was concluded that the relation between FTIR and molecular analyses could not be explained definitely, but FTIR could be used as a taxonomic tool above the species level. It was also reported that strains of the same species like *Issatchenkia orientalis* and *Issatchenkia occidentalis* fell into different clusters and appear together with *P. membranaefaciens* and *P. norvegensis*. This is also true for some *Kluyveromyces* and *Hanseniaspora* species. The interesting thing is that these species are also hardly separated with physiological markers. Sandt et al. (2003) used FTIR spectroscopy as a new phenotypic tool to evaluate the potential of this physico-

chemical technique for typing yeast strains of the same species. Total of 79 strains of *Candida albicans* isolated from nine patients were analyzed using FTIR. The results showed that only 1/79 spectrum could not be classified correctly by FTIR spectroscopy. All data were compared to randomly amplified polymorphic DNA (RAPD) results. Molecular analyses demonstrated that amplification patterns of strains isolated from a patient were the same and different patients had different patterns. Thus, authors pointed FTIR spectroscopy as an excellent technique for clinical yeast identification. Essendoubi et al. (2005) used FTIR microscopy for rapid and early identification of the most frequently encountered microcolonies of *Candida* species *(C. albicans, Candida glabrata, Candida parapsilosis, Candida tropicalis, Candida krusei* and *Candida kefyr*) and revealed the excellent identification and discriminating potential of this technique. The same authors (2007) investigated the typing of *C. glabrata* by FTIR spectroscopy and they had also succesful results with this yeast like the typing of *C. albicans*, using only the polysaccharide region located between 900 and 1200 cm^{-1} (Sandt et al., 2003). It was reported that polysaccharide region allows significant reduction of the heterogeneity threshold for typing of *C. glabrata*. Büchl et al. (2008) established a reliable identification system for closely related species of the genera *Issatchenkia* and *Pichia* using ANN-based FTIR spectroscopy. It was found that the main differences were between 1330-1380 cm^{-1} and the second derivative of the data was used succesfully to distinguish *P. membranifaciens* and *P. galeiformis*. Oelofse et al. (2010) evaluated FTIR and REA-PFGE for the differentiation of *Brettanomyces bruxellensis* strains isolated from red wines. Their results indicated that ATR-IR spectra could be useful for rapid strain typing in comparison and complementary to molecular techniques. Maquelin et al. (2003) studied identification of bacterial (*S. aureus, E. faecalis, E. coli* and *P. aeruginosa*) and fungal pathogens (*Candida* sp.) using Raman and FTIR spectroscopy and concluded with higher identification accuracy with IR spectroscopy (98.3%) compared with Raman spectroscopy (92.2%).

The plots of HCA of dried and directly used yeast cells are shown in Figure 4.19 (a) and (b), respectively. Since the best clusters were obtained using the second derivatives of total spectral regions in PLS-DA, the results of partial spectra are not shown. As it could be seen in Figure 4.19 (a), yeasts could be clustered under 2 main groups as *Aureobasidium* sp. (except for a few *Metschnikowia* sp. and *Candida* sp.) and the others. In Figure 4.19 (b), there are many subgroups of the main groups and the clusters are not so far apart since their vertical lines are short.
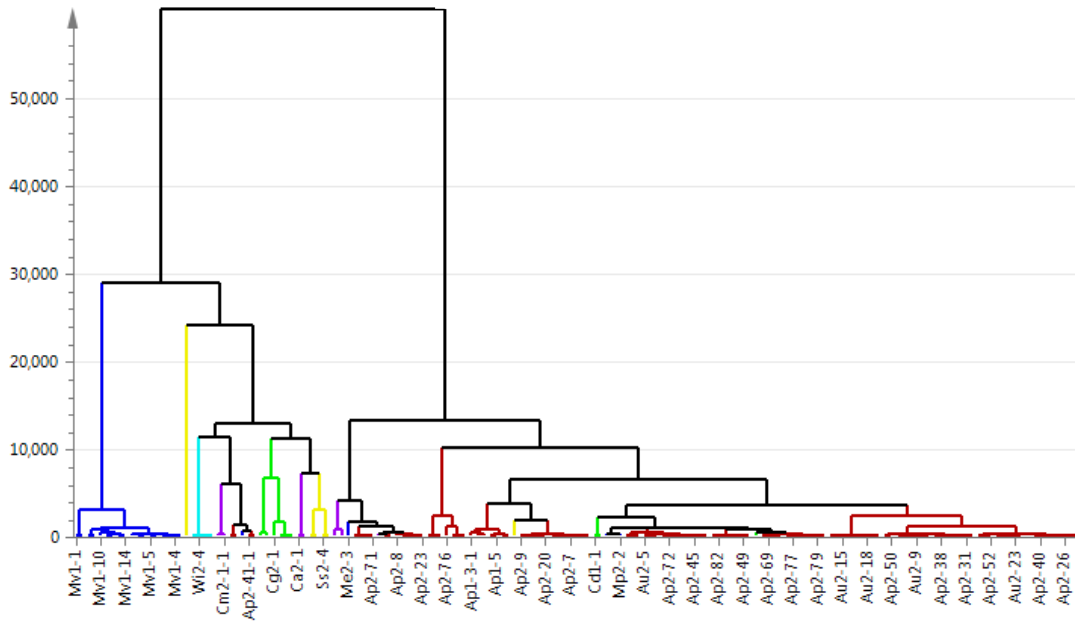
(a)
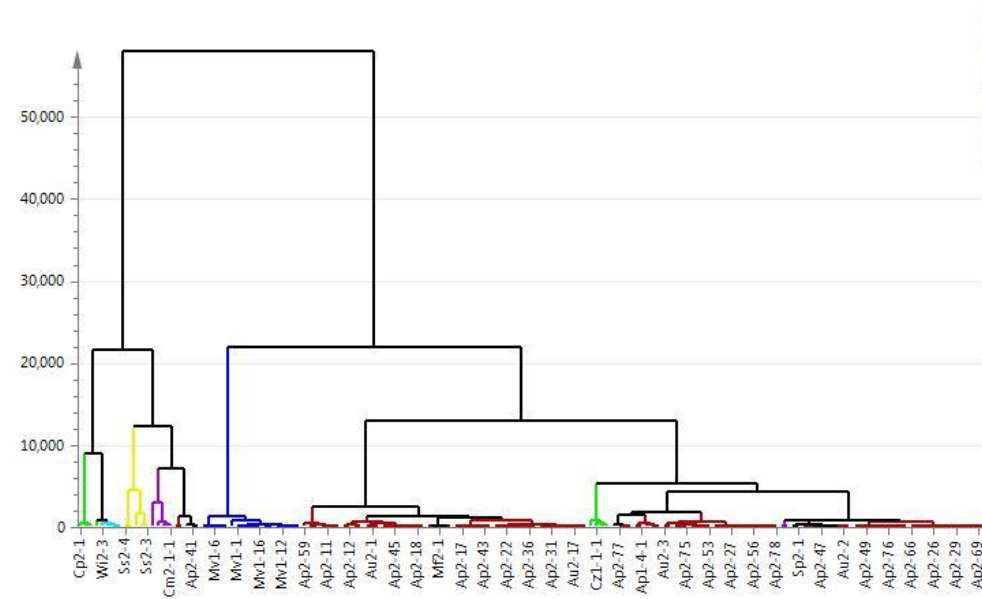
(b)

Figure 4.19. HCA plots of tha data of (a) *dried* and (b) *directly used* yeast cells using total
spectral region

4.3. Conclusions

Yeast flora of naturally debittered HO and common table olive variety GO and their leaves during two harvest years were investigated in this part of the study.

Totally 182 yeasts were evaluated using both cultural and molecular methods in parallel, followed by characterization using mid-IR spectroscopy. Comparison of identification methods reveals that commercial kit showed only 13% similarity with molecular methods and all yeasts could be succesfully identified molecularly. The most identified yeasts in the 1st and 2nd year were *Metschnikowia* sp. and *Aureobasidium* sp., respectively. When HO of two harvest years were compared, it was observed that only *Aureobasidium* sp. was the common yeast. Therefore, if there would be any link between natural debittering of Hurma olives and the yeast population of this olive type this could involve *Aureobasidium* sp.

FTIR spectroscopy results showed that there are spectral differences between different yeast species. Both sample preparation method could be used for differentiation of yeast isolates, however «*directly used cells*» showed more scattered results in comparison with «*dried cells*». The results of multivariate statistical analysis indicated that it is possible to cluster yeast isolates, even isolated from different harvest years; however, it is difficult to differentiate some yeasts due to their heterogeneity, as reported previously. Both PLS-DA and HCA results were in parallel with DNA-based methods including phylogenetic tree. Therefore it could be concluded that FTIR can be used as a complementary method for molecular analysis and need to be improved by adding more yeasts to its reference library.

CHAPTER 5

CHARACTERIZATION OF ANTIMICROBIAL ACTIVITY OF PHENOLICS ON YEASTS WITH FTIR SPECTROSCOPY IN COMPARISON WITH TRADITIONAL METHODS

5.1. Materials and Methods

5.1.1. Construction of Growth Curves

Saccharomyces cerevisiae (NRRL Y-139, ATCC 2366, GenBank accession no: FJ238322.1) as a reference strain and wine yeast, and *Aureobasidium pullulans* as the most commonly isolated strain during two harvest seasons of olive samples were used for characterization of antimicrobial activity of phenolics. Both microorganisms were subcultured at 28-30°C for 48 h before construction of growth curves. Fresh yeast colony suspensions were prepared corresponding to McFarland 0.5, 1 and 2 using a densitometer (HVD, Den1); and growth curve of each cell suspension was constructed using a microplate reader (Varioskan Flash Multimode Reader, Thermo, USA). Besides absorbance measurement in every hour at 600 nm during incubation at 30°C for 48h without shaking, cultural cell counts were also obtained during the growth of yeasts to monitor the growth pattern and phases.

5.1.2. Preparation of Phenolic Compounds

All of the phenolic compounds used for antimicrobial activity tests are provided in Table 5.1 which includes properties, classes and concentration ranges of phenolics found in Hurma olives during both seasons according to the results of chemical analyses (Aktas, 2014a; Aktas et al., 2014b). Since there is not any study in the literature related with the effect of olive phenolics on yeasts; the phenol types and concentrations used in

this study were determined according to the results of a previous chemical characterization study reported by Aktas et al. (2014a). In that study, phenolic profiles of naturally debittering olives were determined and the phenolic compounds with their concentration ranges during 8 weeks of two harvest seasons were reported. In general, the most common phenols found in olives with the highest concentrations were used in the current research and it was aimed to investigate the antimicrobial effects of various types and classes of phenols including *tyrosol, luteolin, hydroxytyrosol, oleuropein* and *apigenin* on the yeasts.
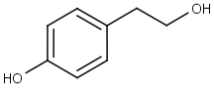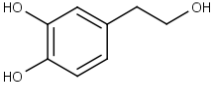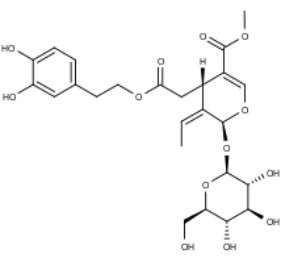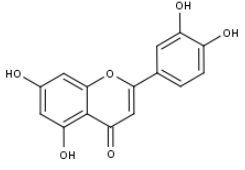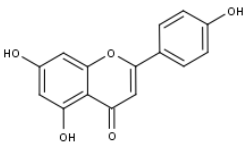
The solutions of each phenolic compound were prepared in various concentrations (800 ppm, 400 ppm, 200 ppm, 100 ppm, 50 ppm and 25 ppm), while one more concentration (2000 ppm) was tested for hyroxytyrosol due to its high amount in Hurma olives (Aktas, 2014a). Each compound was firstly dissolved in ethanol (96%) and then diluted with YEPD broth to the target concentration. Ethanol content of all solutions was decreased below 1% (v/v) during dilutions (Karaosmanoglu et al., 2009).

5.1.3. Determination of Antimicrobial Activity by OD Measurement

Antimicrobial activities of phenolic compounds were first determined by microtiter plate method spectrophotometrically (Dufour et al., 2003). According to this method, 100 µL from each concentration of each phenolic compound was dispensed into a well of flat bottom 96 well microtiter plate (TPP, Sigma). A 100 µL of 1×10^4 cfu/mL yeast culture in early exponential growth phase was added to each well. In order to obtain this concentration, yeast culture suspensions were first set to McFarland=1 and grown at 30°C to make the yeasts, *S. cerevisiae* and *A. pullulans,* to reach to approximately 1×10^6 cfu/mL and 1×10^5 cfu/mL, respectively, as derived from growth curve at the end of 6 h. Then, yeast suspensions were diluted by 1/10 to have 1×10^4 cfu/mL concentrations. When the phenolics and yeast cultures were mixed in the well, concentrations of both yeast suspension and phenolic compounds decreased by half. All phenolics were obtained as 400, 200, 100, 50, 25 and 12.5 ppm in addition to 1000 ppm concentration for hydroxtyrosol; whereas final yeast concentration in the wells was 0.5×10^4 cfu/mL. The absorbance measurements of each plate were taken with 1 hour intervals at 600 nm during incubation at 30°C for 48 h, likewise viable cell count was obtained during this period

using the same conditions. 100 µL of this suspensions for both yeasts and yeast+phenols were used to determine viable yeast cell count on YEPD agar.

Table 5.1. Phenolic compounds used in the FTIR studies with the concentration ranges found in Hurma olives (Source: Aktas, 2014a)

Phenolic compounds	Classes	Properties	Concentration ranges [mg/kg] in Hurma olives during 2011 and 2012	Chemical structure
Tyrosol [2-(4-Hydroxyphenyl)ethanol]	Phenyl ethyl alcohols	Sigma (98%)	0.94-73.10	
Hydroxytyrosol (3-Hydroxytyrosol)	Phenyl ethyl alcohols	Extrasynthese (≥98%, HPLC)	7.17-8183.35	
Oleuropein	Secoiridoids	Sigma (≥98.0%)	17.9-4786.76	
Luteolin	Flavones	Sigma (≥98%, TLC)	0.64-351.19	
Apigenin	Flavones	Sigma (≥97%, TLC)	297.04-31838.78	

5.1.4. Determination of Antimicrobial Activity using FTIR Spectrometer

According to the growth curves of yeasts with various concentrations of tyrosol, hydroxytyrosol, oleuropein, luteolin and apigenin obtained by UV-vis spectrophotometric measurements, different concentrations as the most (400 and 200 ppm for all phenolics and additionally 1000 ppm for HT), moderately (50 ppm) and the least effective (12.5 ppm) were chosen for further investigation of their antimicrobial effects on the same yeasts using FTIR spectroscopy. Cell growth for FTIR biological assay was performed as previously reported (Corte et al., 2014) with some modifications. Briefly, 2 mL of yeast suspensions obtained with dilutions after 6 h of growth with approximately 1×10^4 cfu/mL were added to polypropylene tubes. Then, 2 mL of prepared phenolic standard solutions (800, 400, 100, 25 and additionally 2000 ppm for hydroxytyrosol) were added to test tubes in order to obtain the test concentrations of 400, 200, 50 and 12.5 ppm of all phenolics and additionally 1000 ppm of hydroxytyrosol. The final yeast concentration was 0.5×10^4 cfu/mL as in spectrophotometric analysis. Each tube containing phenolic compounds and control tube with only yeast suspension was centrifuged at 5,300 g (7,000 rpm) for 3 min (2-16 KC, Sigma, Germany), washed twice with distilled sterile water and resuspended in the same amount of distilled water. The procedure of preparation of a ZnSe plate for FTIR analysis was followed similar to mid-IR spectrometric identification of yeasts given in details in Chapter 3. Briefly, 70 µL of each suspension was transferred to a ZnSe optical sample carrier and dried at 42±2°C for 20 min to yield transparent films (Kümmerle et al., 1998). All spectra were recorded through a HATR accessory of a FTIR spectrometer (Perkin Elmer Spectrum 100, Wellesley, MA) with DGS detector within the range of 4000-650 cm^{-1}. The scanning was carried out at 4 cm^{-1} resolution with 64 scans for each spectrum and 1 cm/s scan speed. The sampling crystal was cleaned with ethanol and distilled water after each measurement and dried under nitrogen flow.

5.1.5. Monitoring of Antimicrobial Activity of Some Phenolic Compounds Using Phase Contrast and Scanning Electron Microscopes (SEM)

Selected phenolic compounds according to their antimicrobial effects including tyrosol, hydroxytyrosol and luteolin were assessed at low (200 ppm) and high (800 ppm) concentrations on the yeasts *S. cerevisiae* and *A. pullulans* in order to investigate the changes or damages occurred on yeast cells using phase contrast microscope and SEM.

For phase contrast microscope (Olympus-CX31), the yeasts were prepared as following: 1 mL of yeast+phenol suspension at 0-48h was centrifuged at 10,000 rpm for 5 min, washed with 200 µL of peptone water and centrifuged for 3 min. Pellet was resuspended in 20 µL of peptone water and examined under phase contrast microscope with 100x magnification. For SEM (Quanta-250FEG), the suspension was washed with 100 µL dH_2O followed by centrifugation at 10,000 rpm for 5 min after 18-20 h treatment of the yeasts by these phenolic compounds. The pellet was mixed with 20 µL of dH_2O and air-dried at 30°C, followed by examination under scanning electron microscope with 10,000x magnification.

5.1.6. Multivariate Statistical Analysis

The data obtained from FTIR analysis were evaluated statistically by using multivariate statistical techniques including principal component analysis (PCA) and partial least square discriminant analysis (PLS-DA) with SIMCA software (13.0.3, Umetrics) after application of 2nd derivative to FTIR spectra.

5.2. Results and Discussion

5.2.1. Growth Curves of Yeasts

Before the investigation of the effects of phenolic compounds on yeasts, growth curves of the selected yeasts, *S. cerevisiae* and *A. pullulans* were constructed to determine the exponential phase of the growth. Although both yeast suspensions were prepared in

three different concentrations corresponding to McFarland 0.5, 1 and 2; only the growth graphics of the suspensions with McFarland 1 (corresponding to 2.7×10^6 and 2.9×10^6 cfu/mL for *S. cerevisiae* and *A. pullulans*, respectively) are shown in Figure 5.1. According to this plot, a specific incubation time was determined for further analysis representing early exponential growth phase of these two yeasts, as 6th hour, at which *S. cerevisiae* and *A. pullulans* could reach to 3.8×10^6 and 2.7×10^5 cfu/mL at 30°C, respectively.

Maresova and Syrhova (2007) demonstrated a wide variety of applications of monitoring yeast growth with a microplate reader. Their work was aimed at the applications of a simple absorbance microplate reader in yeast physiology research. Researchers studied both measuring growth curves and monitoring the pH changes of medium using two different pH indicators. Using this technique, it was concluded that as many as 96 samples could be simultaneously analyzed with a microplate reader. In addition, medium consumption could be minimized to 100 µL per sample, and the results could be observed within 24–48 h, providing temperature control and solution agitation.

5.2.2. Antimicrobial Activity of Phenolic Compounds

To evaluate the effectiveness of all phenolics on both yeasts, growth curves of phenolics added yeasts were monitored with UV-vis spectrophotometer and microbial counts were determined at selected intervals. In addition, mid-IR spectroscopic measurements were performed. Then, as a multivariate statistical analysis tool, PCA was applied to mid-infrared spectra to generate score plots. In order to see the differentiation of yeast samples effected by different concentration of phenolics at various treatment times, mid-IR spectroscopic data was also analyzed with another multivariate statistical technique; PLS-DA using 2nd derivative. Statistical information about the PLS-DA models for antimicrobial activity test of *S. cerevisiae* and *A. pullulans* is shown in Table 5.2.

Table 5.2. Statistical information about the PLS-DA models for the antimicrobial activity

Model*		2nd Derivative	Number of PC	R^2Y	Q^2
"T" on	Concentration	+	3	0.69	0.112
S. cerevisiae	Time	+	2	0.583	0.0567
"T" on	Concentration	+	2	0.392	-0.174
A. pullulans	Time	+	6	0.992	0.733
"HT" on	Concentration	+	3	0.517	0.164
S. cerevisiae	Time	+	3	0.877	-0.123
"HT" on	Concentration	+	2	0.351	0.056
A. pullulans	Time	+	2	0.56	-0.0182
"O" on	Concentration	+	3	0.673	0.171
S. cerevisiae	Time	+	2	0.514	-0.0689
"O" on	Concentration	+	2	0.434	0.211
A. pullulans	Time	+	2	0.409	-0.127
"A" on	Concentration	+	2	0.408	0.153
S. cerevisiae	Time	+	2	0.552	0.0744
"A" on	Concentration	+	3	0.625	0.128
A. pullulans	Time	+	2	0.536	-0.0171
"L" on	Concentration	+	2	0.445	0.136
S. cerevisiae	Time	+	2	0.571	-0.176
"L" on	Concentration	+	2	0.399	-0.0867
A. pullulans	Time	+	2	0.535	0.00801

*T: tyrosol, HT: hydroxytyrosol, O: oleuropein, A: apigenin, L: luteolin
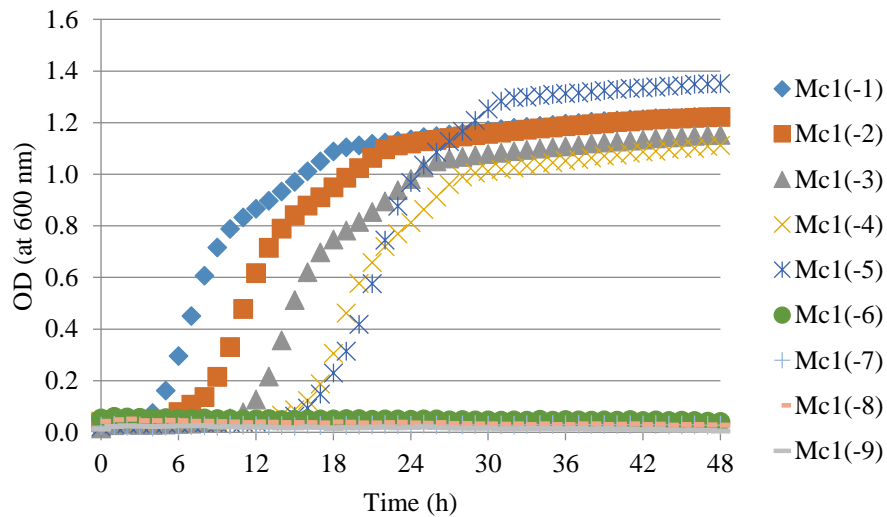
(a)
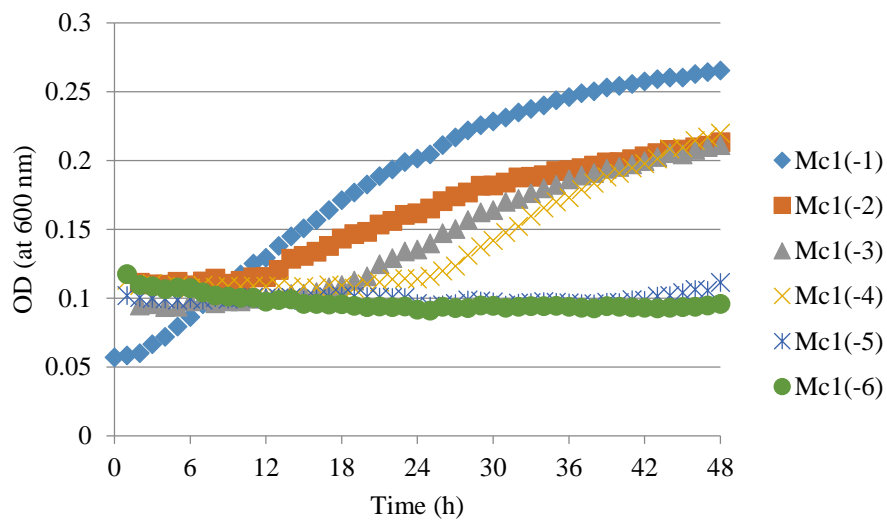
 (b)

Figure 5.1. Growth curves of (a) *S. cerevisiae* and (b) *A. pullulans* suspensions corresponding to McFarland 1 and its dilutions (2.7 x 10^6 and 2.9 x 10^6 cfu/mL for *S. cerevisiae* and *A. pullulans*, respectively)

5.2.2.1. Antimicrobial Activity of *Tyrosol*

The effects of various tyrosol concentrations (12.5, 25, 50, 100, 200 and 400 ppm) on determined level of *S. cerevisiae* (~1.8x 10^4 cfu/mL) as spectroscopic measurements, yeast colony count (CFU/mL) and mid-IR spectroscopic measurements are shown in

Figure 5.2; whereas the results of the same measurements performed for *A. pullulans* (1.2 x 10^4 cfu/mL) are provided in Figure 5.3.

As it could be observed from Figure 5.2 (a), 12.5 and 25 ppm tyrosol concentrations were the least effective concentrations on *S. cerevisiae*, whereas 400, 200 and 100 ppm were the most effective and 50 ppm had moderate effect. At 18 h, which corresponds to exponential phase for *S. cerevisiae*, 400 and 200 ppm tyrosol caused almost 2 log reduction of yeast count (Figure 5.2, b). At 24 h this reduction in number was reduced to 1 log and at 48 h the numbers were almost the same for each tyrosol concentration. Except for 12.5 ppm, effect of tyrosol on *S. cerevisiae* until 18 h was similar, and the other concentrations showed almost 1 log reduction of the yeast count at 18 h. FTIR spectra of the yeasts exposed to phenolics were evaluated visually by statistical analysis. In PLS-DA score plot (Figure 5.2 (c)), it was observed that *S. cerevisae* which was not exposed to tyrosol was differentiated from all of the tyrosol added samples. The highest concentrations (400 and 200 ppm) were clustered close to each other and the lowest concentration was the furthest apart from the others. At 0 h, all tyrosol concentrations were clustered together in the middle of the plot, except for T12.5 ppm and they approach to each other at 18 h and 24 h. Figure 5.2 (d) which was constructed according to treatment time shows clearly four different clusters representing of four treatment times (0, 18, 24 and 48 h). The closeness of 18 and 24 h to each other for each concentration, the distance of 48 h to all of them and the group of 0 h in the right side of the plot could be seen clearly. These results are parallel with OD measurements and yeast count results. Figure 5.2 (e) shows the spectral differences between the yeast itself (Sc) and the yeast treated with various tyrosol concentrations. According to visual examination of the FTIR spectral data, the biggest changes of yeast spectra was in DNA fingerprint region [900-600 cm^{-1}], amide region [1750-1500 cm^{-1}] and –OH groups [3600 cm^{-1}] due to exposure to tyrosol. Variable importance in projection (VIP) values of the PLS-DA model of FTIR data of this yeast for tyrosol indicate that the important spectral regions are [900-1200 cm^{-1}], [1360-1800 cm^{-1}] and [2800-2900 cm^{-1}].
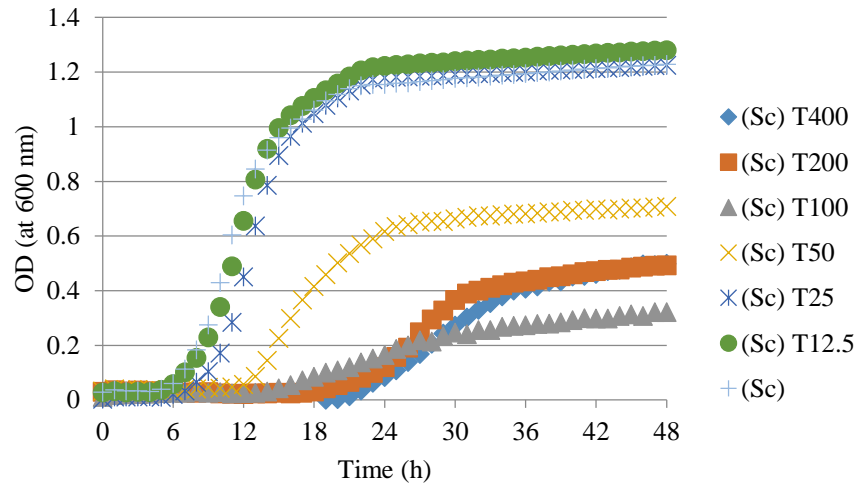
(a)
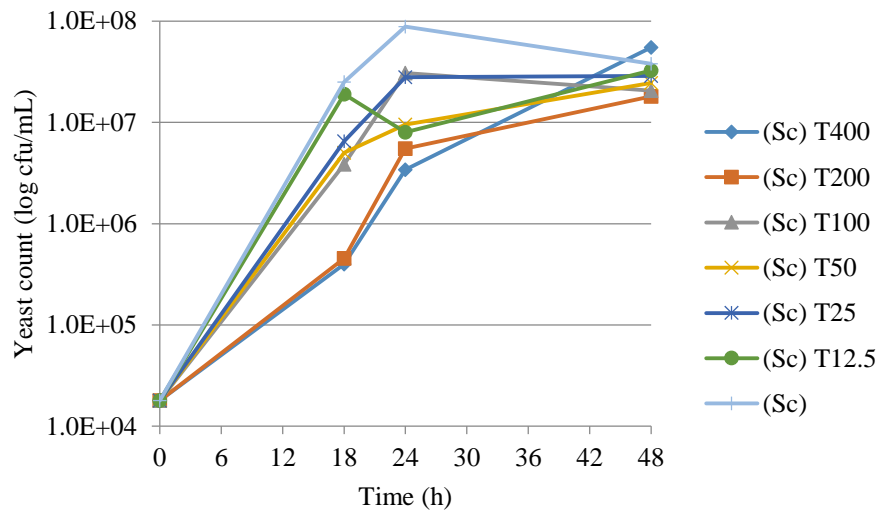
(b)

Figure 5.2. Antimicrobial effects of tyrosol (T) as (a) spectroscopic measurements, (b) yeast colony count (cfu/mL), (c, d) mid-IR measurements shown by score plots of PLS-DA with 2nd derivative and (e) FTIR spectral data at different concentrations (400, 200, 100, 50, 25, 12.5 ppm) on the growth of *S. cerevisiae* (Sc). (a): Readings were carried on with 1 h intervals, at 30°C for 48 h without shaking. (b): Sampling was done at critical points (0, 18, 24, 48 h). (c): Classification according to concentration (d): Classification according to sampling time. (e): Data at 18 h and the colors pink, black, green, grey and red indicates Sc, 400 ppm T, 200 ppm T, 50 ppm T and 12.5 ppm T, respectively

(Cont. on next page)

Figure 5.2 (Cont.)

(c)

(d)

Figure 5.2 (Cont.)
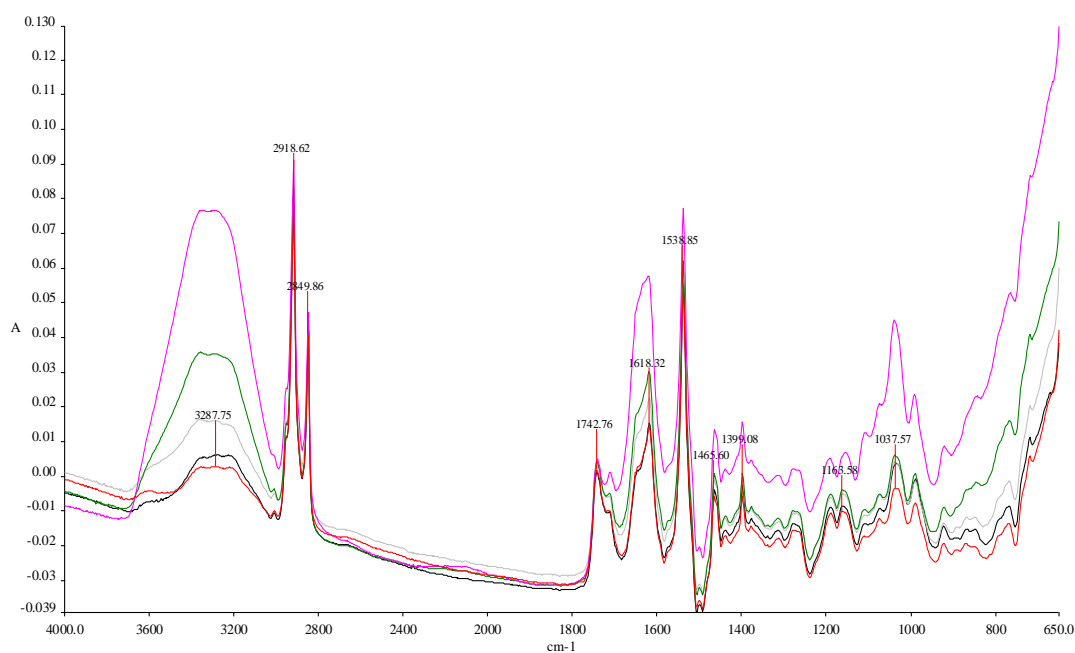
(e)

Figure 5.3 (a) shows that only the highest tyrosol concentration (400 ppm) had an antimicrobial activity on *A. pullulans*; whereas the other concentrations showed similar growth curves as the yeast itself. This result could also be observed in Figure 5.3 (b) in terms of yeast count which indicates that 400 ppm tyrosol caused 4 log decrease of the number of *A. pullulans* in terms of cfu/mL. This showed that the same concentration of tyrosol was more effective on this yeast than *S. cerevisiae*. Score plots of PLS-DA of FTIR data belonging to *A. pullulans* are shown in Figure 5.3 (c) and (d), corresponding to classification by phenol concentrations and time. Interestingly 200 ppm tyrosol concentration was differentiated from the other concentrations (c). Although 400 ppm and 50 ppm tyrosol were different from *A. pullulans* itself, the lowest concentration of tyrosol showed the difference only at 18 h. The main difference between concentrations was at 18 h which is similar with yeast count results. In addition, 48 h results were differentiated from the other time results, as with *S. cerevisiae* (d). According to the visual examination of FTIR spectral data (e), it could also be observed that the biggest changes of yeast spectra was in DNA fingerprint region [900-600 cm^{-1}], amide region [1750-1500 cm^{-1}] and –OH groups [3600 cm^{-1}] due to tyrosol. VIP of the FTIR data of this yeast for tyrosol indicates that the important spectral regions are [1300-1800 cm^{-1}] and [2800-2900 cm^{-1}].

110
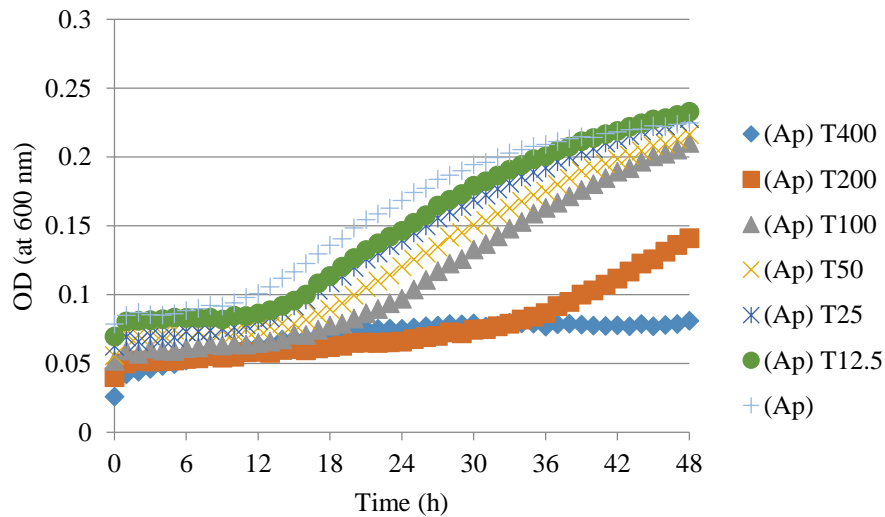
(a)
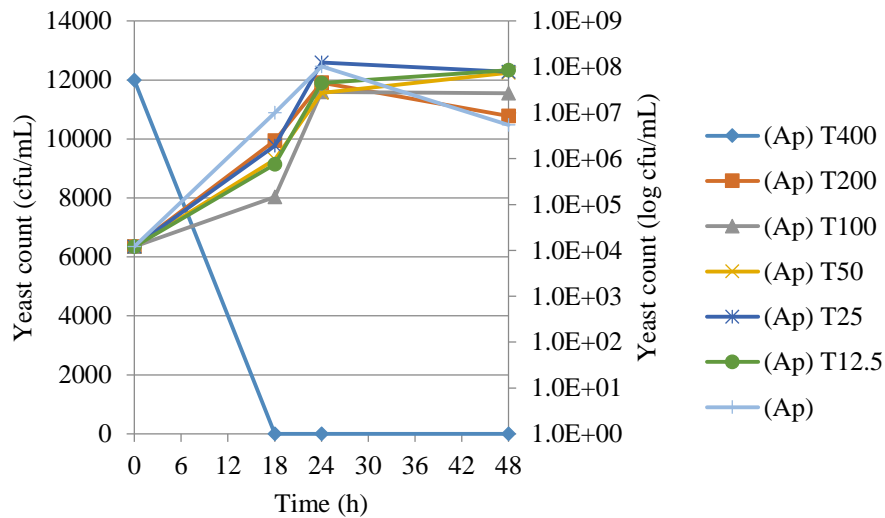
(b)

Figure 5.3. Antimicrobial effects of tyrosol (T) as (a) spectroscopic measurements, (b) yeast colony count (cfu/mL), (c, d) mid-IR measurements shown by score plots of PLS-DA with 2nd derivative and (e) FTIR spectral data at different concentrations (400, 200, 100, 50, 25, 12.5 ppm) on the growth of *A. pullulans* (Ap). (a): Readings were carried on with 1 h intervals, at 30°C for 48 h without shaking. (b): Sampling was done at critical points (0, 18, 24, 48 h). (c): Classification according to concentration. (d): Classification according to sampling time. (e): Data at 18 h and the colors black, red, pink, green and grey indicates Ap, 400 ppm T, 200 ppm T, 50 ppm T and 12.5 ppm T, respectively

Figure 5.3 (Cont.)

(c)

(d)

(Cont. on next page)

Figure 5.3 (Cont.)
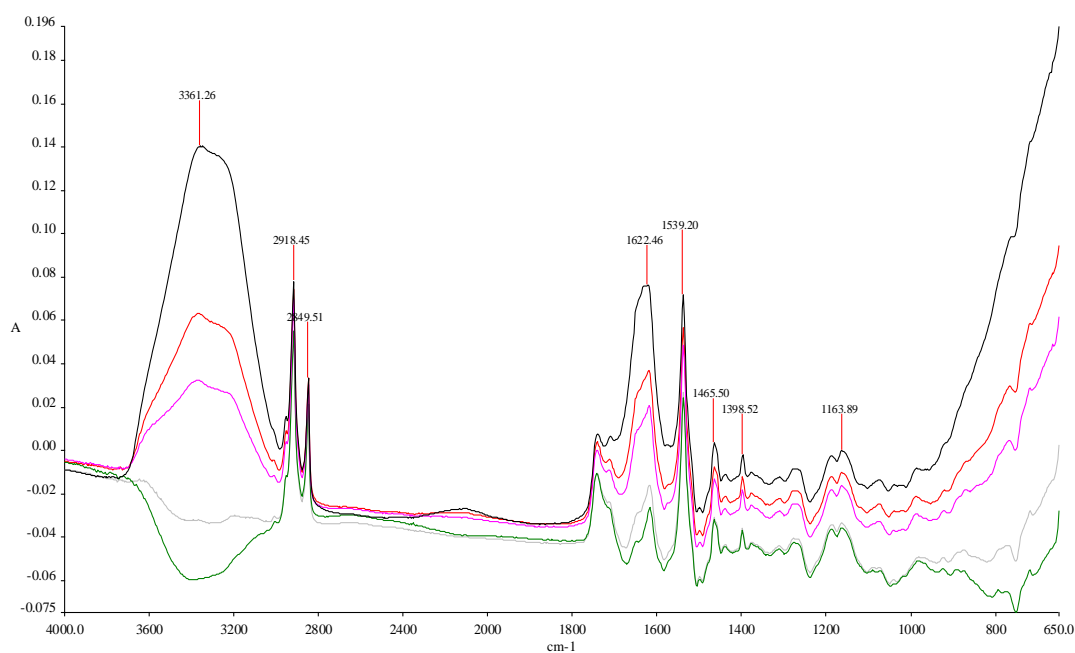
(e)

5.2.2.2 Antimicrobial Activity of *Hydroxytyrosol*

The effects of various hydroxytyrosol concentrations (12.5, 25, 50, 100, 200, 400 and 1000 ppm) on determined level of *S. cerevisiae* (~1.8x 10^4 cfu/mL) as spectroscopic measurements, yeast colony count (CFU/mL) and mid-IR spectroscopic measurements are shown in the Figure 5.4; whereas the results of the same measurements performed for *A. pullulans* (1.2 x 10^4 cfu/mL) are shown in the Figure 5.5.

According to the Figure 5.4 (a), the strongest effect of hydroxytyrosol was observed with 1000 and 400 ppm concentration and 50 ppm of HT still appeared to be effective on the yeast *S. cerevisiae*. According to Figure 5.4 (b) at 18 h which corresponds to exponential phase for *S. cerevisiae*, 200 ppm hydroxytyrosol caused almost 3 log reduction of yeast count. FTIR data shows that (Figure 5.4 (c)), *S. cerevisae* which was not exposed to hydroxytyrosol was differentiated from all of the HT added samples. The highest concentrations (1000 and 400 ppm) were clustered very close to each other and there were no big differences between the lowest concentrations (50 and 12.5 ppm) (Figure 5.4 (c)). From PLS-DA score plot (Figure 5.4 (d)), it was observed that the results of 18 h and 24 h were very close to each other for each concentration; 48 h were far away from them and 0 h in the right side of the plot. These results were parallel with OD

113

measurements and yeast count results. Figure 5.4 (e) indicates that the biggest changes of spectra were in both DNA fingerprint region [900-600 cm^{-1}] and carbohydrate region [1200-900 cm^{-1}] due to hydroxytyrosol. VIP values of the PLS-DA model for FTIR data of this yeast for hydroxytyrosol indicate that the important spectral regions are [900-1200 cm^{-1}], [1300-1700 cm^{-1}] and [2800-2900 cm^{-1}].
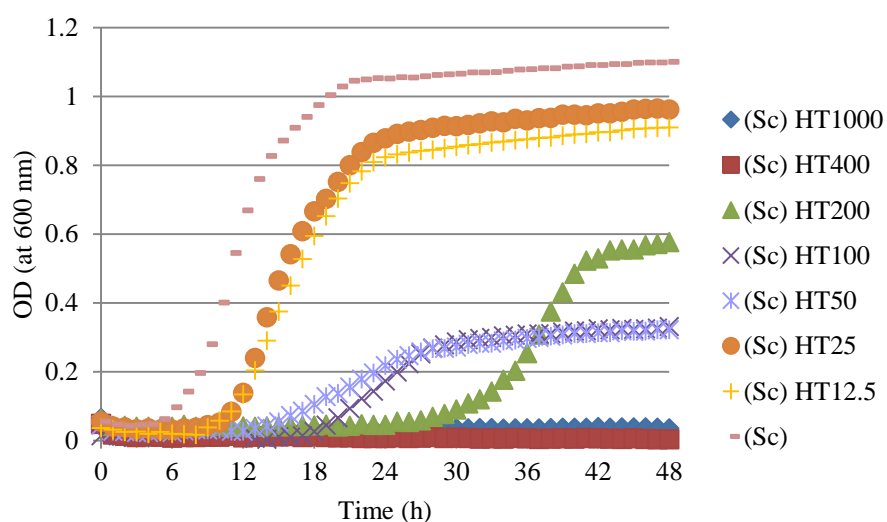
(a)

Figure 5.4. Antimicrobial effects of hydroxytyrosol (HT) as (a) spectroscopic measurements, (b) yeast colony count (cfu/mL), (c, d) mid-IR measurements shown by score plots of PLS-DA with 2nd derivative and (e) FTIR spectral data at different concentrations (1000, 400, 200, 100, 50, 25, 12.5 ppm) on the growth of *S. cerevisiae* (Sc). (a): Readings were carried on with 1 h intervals, at 30°C for 48 h without shaking. (b): Sampling was done at critical points (0, 18, 24, 48 h). (c): Classification according to concentration. (d): Classification according to sampling time. (e): Data at 18 h and the colors black, red, blue, pink, green and grey indicates Sc, 1000 ppm HT, 400 ppm HT, 200 ppm HT, 50 ppm HT and 12.5 ppm HT, respectively

Figure 5.4 (Cont.)

(b)

(c)
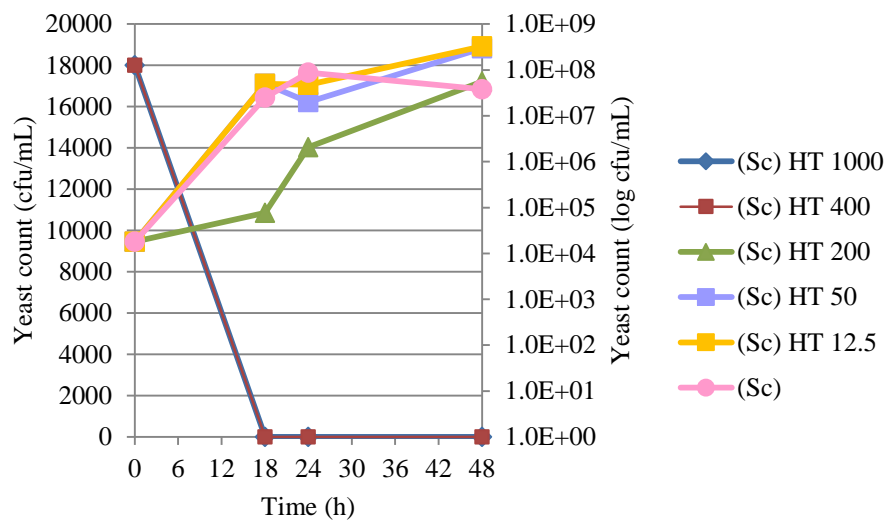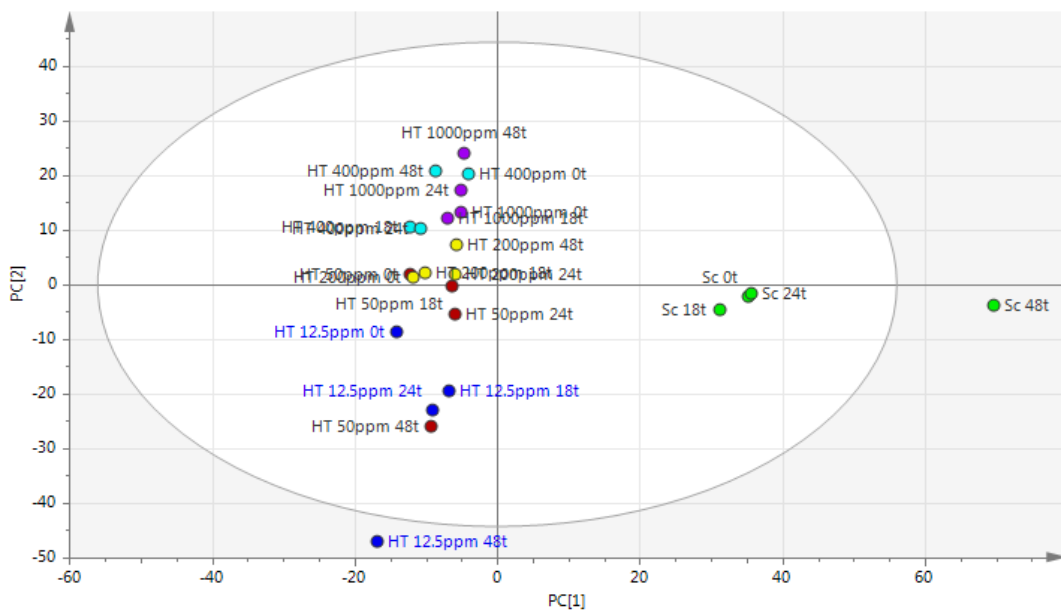
Figure 5.4 (Cont.)
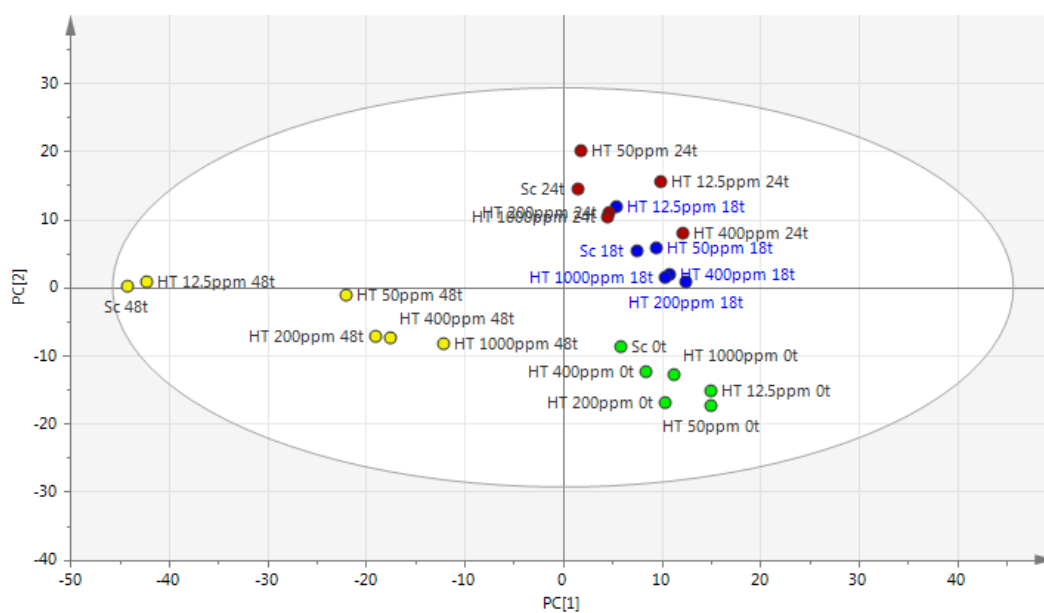
(d)

(e)
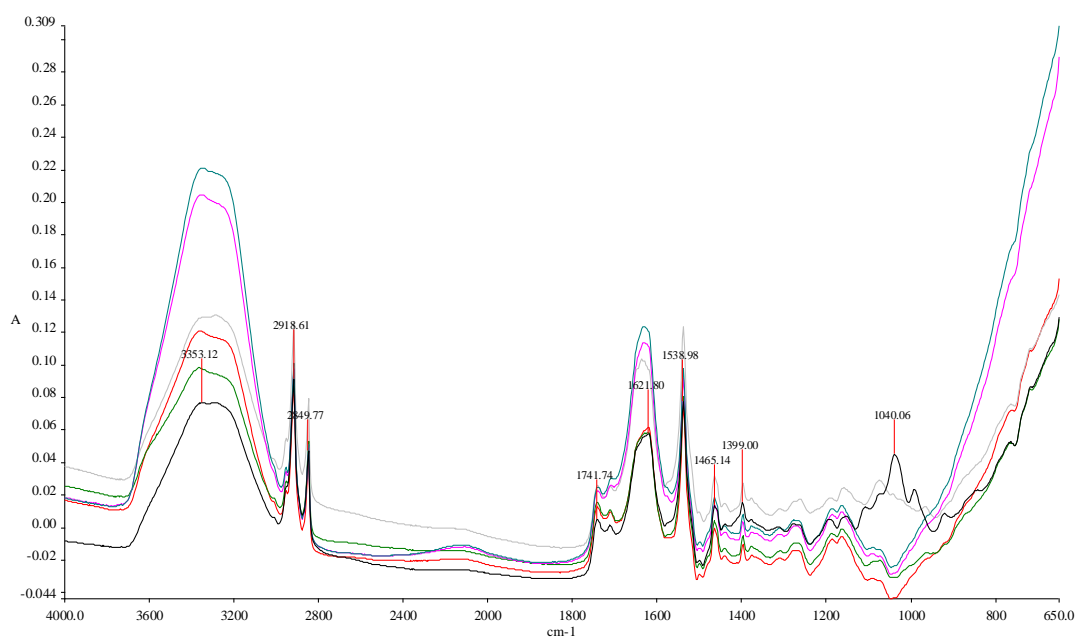
The growth of *A. pullulans* exposed to various concentrations of hydroxytyrosol showed an inhibition pattern with increased concentration (Figure 5.5, a). Figure 5.5 (b) shows that both 1000 ppm and 400 ppm of hydroxytyrosol have antimicrobial activity against *A. pullulans* at 18 h; whereas 200 ppm hydroxytyrosol was effective on this yeast after 24 h. Even 12.5 ppm of hydroxytyrosol caused 2 log reduction at 18 h and 50 ppm

of hydroxytyrosol resulted in 3 log reduction on yeast count. Score plots of PLS-DA of FTIR data for the effect of hydroxytyrosol on *A. pullulans* are shown in the Figure 5.5 (c, d). It was observed that 1000, 400 and 200 ppm hydroxytyrosol had similar effects on *A. pullulans* since they formed close clusters to each other (Figure 5.5, c). This result also confirmed the results of yeast counts. Additionally, 50 and 12.5 ppm hydroxytyrosol formed another group which were close to each other. The biggest difference between time periods of contact was observed between 0 h and 18 h (d). The results of FTIR spectral data (Figure 5.5 (c)), showed that the biggest changes of spectra were in both DNA fingerprint region [900-600 cm^{-1}] and carbohydrate region [1200-900 cm^{-1}] by hydroxytyrosol, which is similar as the results of *S. cerevisiae*. VIP of the PLS-DA model of this yeast for hydroxytyrosol indicates that the important spectral regions are [1200-900 cm^{-1}], [1700-1300 cm^{-1}] and [2900-2800 cm^{-1}].
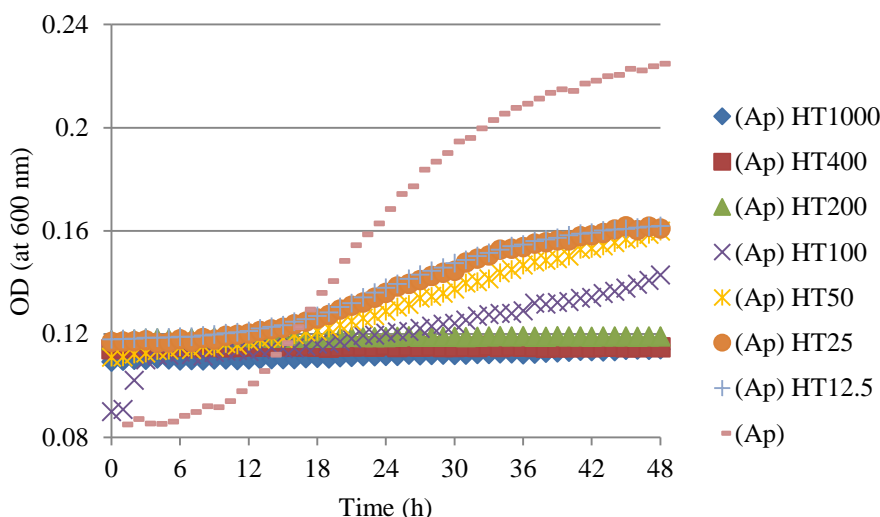
(a)

Figure 5.5. Antimicrobial effects of hydroxytyrosol (HT) as (a) spectroscopic measurements, (b) yeast colony count (cfu/mL), (c, d) mid-IR measurements shown by score plots of PLS-DA with 2nd derivative and (e) FTIR spectral data at different concentrations (1000, 400, 200, 100, 50, 25, 12.5 ppm) on the growth of *A. pullulans* (Ap). (a): Readings were carried on with 1 h intervals, at 30°C for 48 h without shaking. (b): Sampling was done at critical points (0, 18, 24, 48 h). (c): Classification according to concentration. (d): Classification according to sampling time. (e): Data at 18 h and the colors black, red, blue, pink, green and grey indicates Ap, 1000 ppm HT, 400 ppm HT, 200 ppm HT, 50 ppm HT and 12.5 ppm HT, respectively

(Cont. on next page)

Figure 5.5 (Cont.)

(b)

(c)

Figure 5.5 (Cont.)
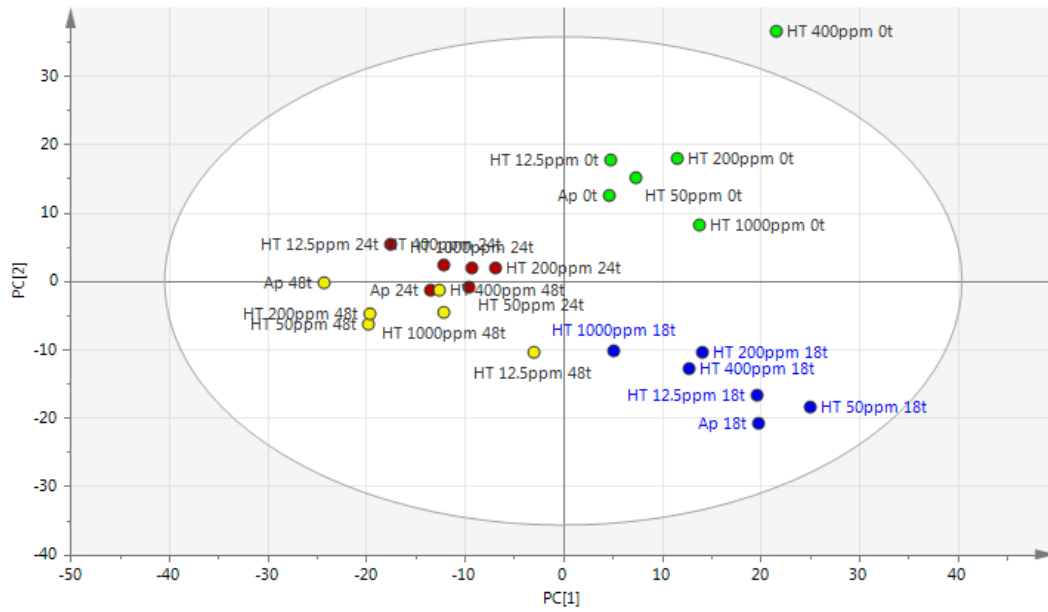
(d)
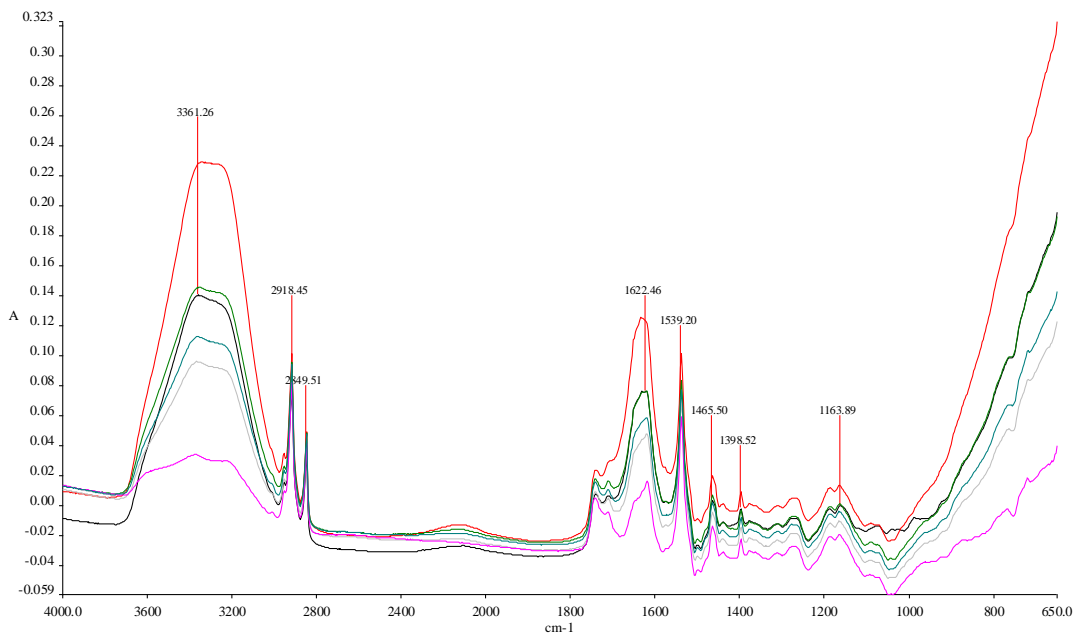

(e)

5.2.2.3 Antimicrobial Activity of *Oleuropein*

The effects of various oleuropein concentrations (12.5, 25, 50, 100, 200 and 400 ppm) on determined level of *S. cerevisiae* ($\sim$1.8x 10^4 cfu/mL) as spectroscopic measurements, yeast colony count (CFU/mL) and mid-IR spectroscopic measurements

are shown in Figure 5.6; whereas the results of the same measurements performed for *A. pullulans* (1.2 x 10^4 cfu/mL) are provided in Figure 5.7.

As it could be observed from Figure 5.6 (a), the most effective concentrations of oleuropein on *S. cerevisiae* are 400, 200 and 100 ppm. In addition, 50 ppm of oleuropein extends the lag phase of this yeast from 6 h to approximately 40 h. At 18 h which corresponds to exponential phase for *S. cerevisiae*, 400 and 200 ppm oleuropein caused totally fatal effect and 50 ppm oleuropein resulted in 2 log reduction in number (Figure 5.6, b). However, this reduction in number was observed as almost 1 log for the same concentration at 24 h. In the Figure 5.6 (c), it was easily observed that the highest oleuropein concentration (400 ppm) clustered very far away from the other concentrations and the yeast itself; however, OD measurements and yeast count results showed that 400 and 200 ppm had similar effects on *S. cerevisiae*. The results of 18 h and 24 h also clustered together and 48 h was distinct from all sample periods (Figure 5.6, d). Figure 5.6 (e) shows that the biggest changes of FTIR spectra were in DNA fingerprint region [900-600 cm^{-1}], carbohydrate region [1200-900 cm^{-1}] and amide region [1750-1500 cm^{-1}]. VIP of the PLS-DA model for FTIR data of this yeast for oleuropein indicates that the important spectral regions are [900-1200 cm^{-1}], [1300-1900 cm^{-1}] and [2800-2900 cm^{-1}].
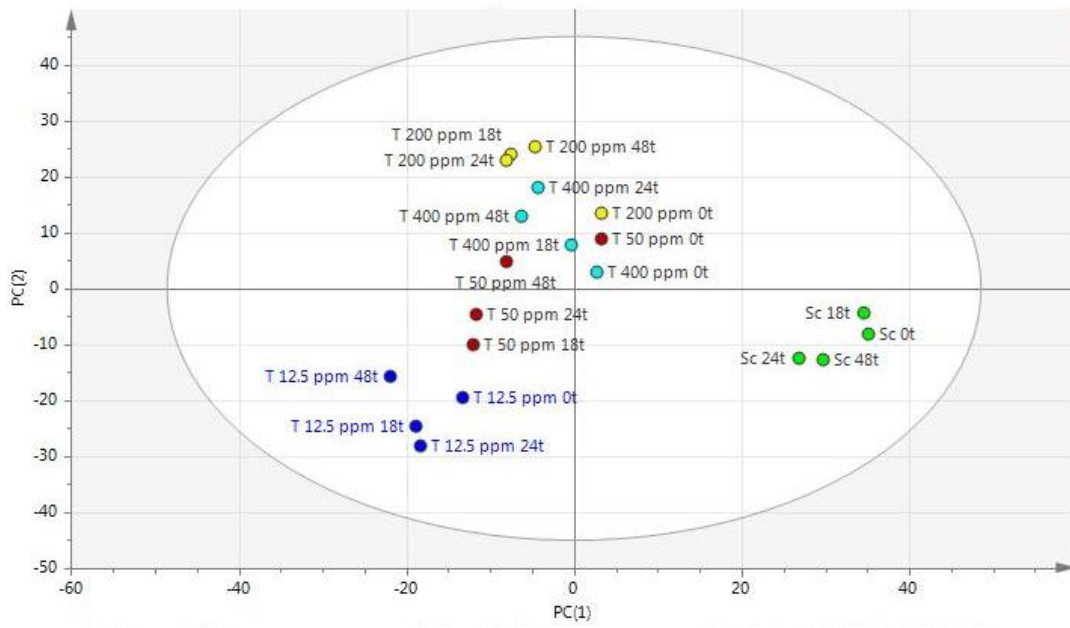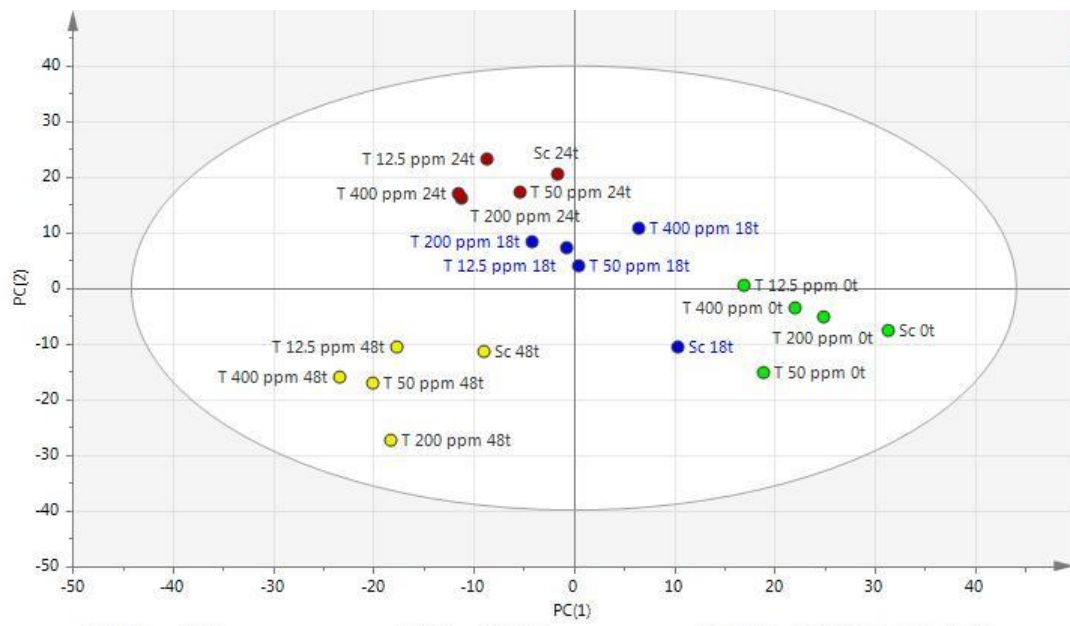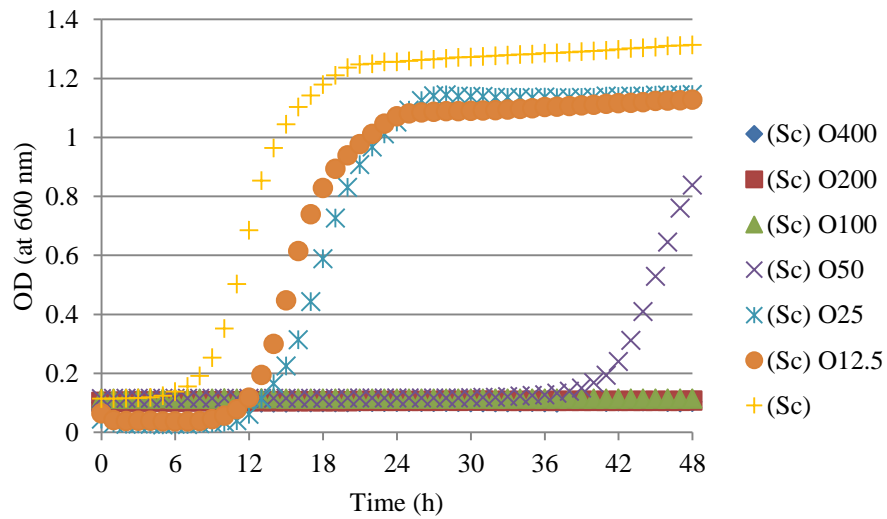
(a)
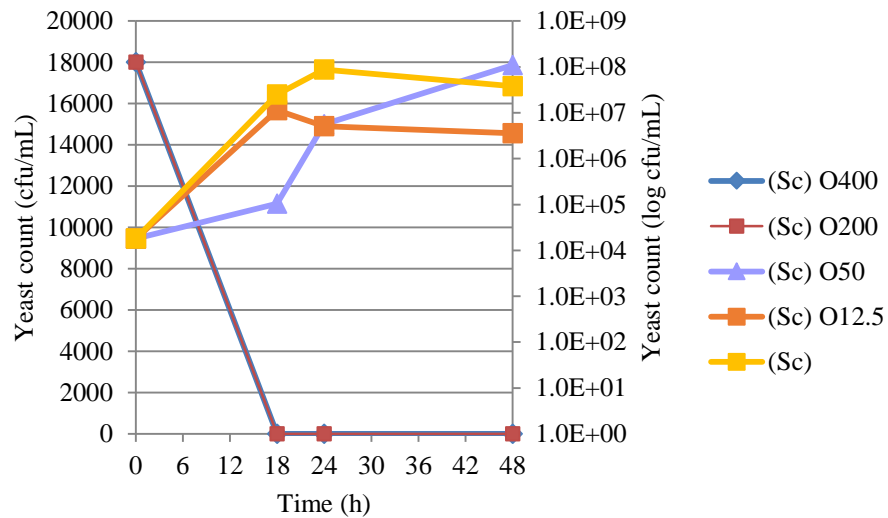
(b)

Figure 5.6. Antimicrobial effects of oleuropein (O) as (a) spectroscopic measurements, (b) yeast colony count (cfu/mL), (c, d) mid-IR measurements shown by score plots of PLS-DA with 2nd derivative and (e) FTIR spectral data at different concentrations (400, 200, 100, 50, 25, 12.5 ppm) on the growth of *S. cerevisiae* (Sc). (a): Readings were carried on with 1 h intervals, at 30°C for 48 h without shaking. (b): Sampling was done at critical points (0, 18, 24, 48 h). (c): Classification according to concentration. (d): Classification according to sampling time. (e): Data at 18 h and the colors black, blue, purple, grey and red indicates Sc, 400 ppm O, 200 ppm O, 50 ppm O and 12.5 ppm O, respectively

Figure 5.6 (Cont.)

(c)

(d)
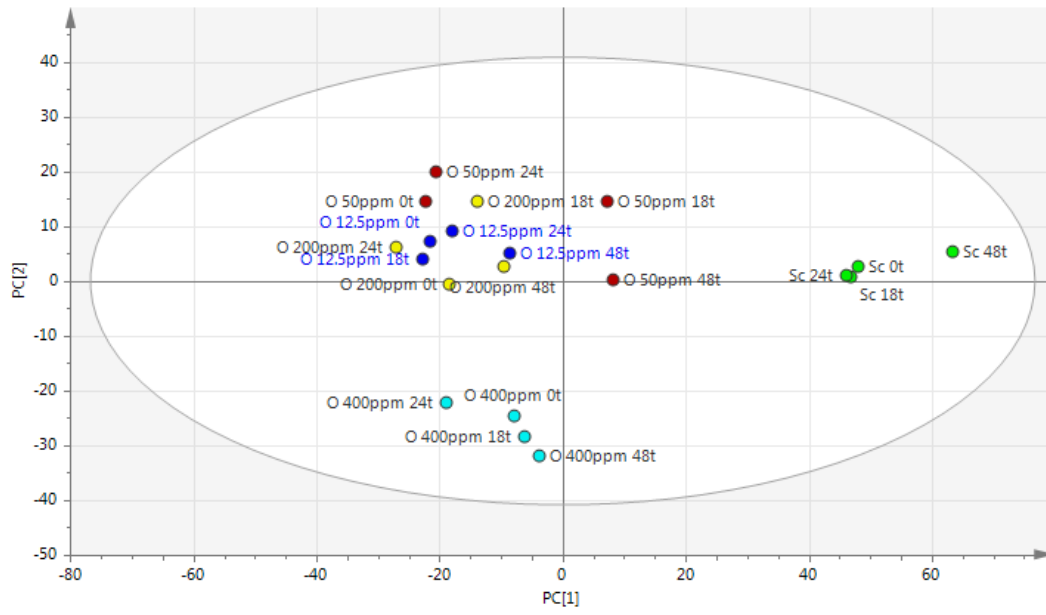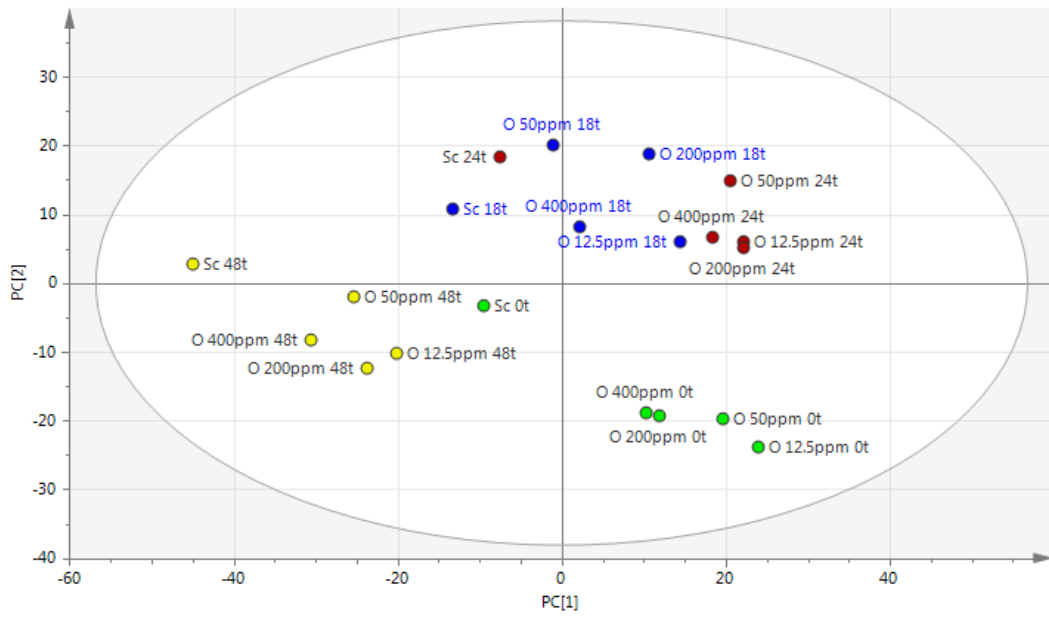
Figure 5.6 (Cont.)

(e)
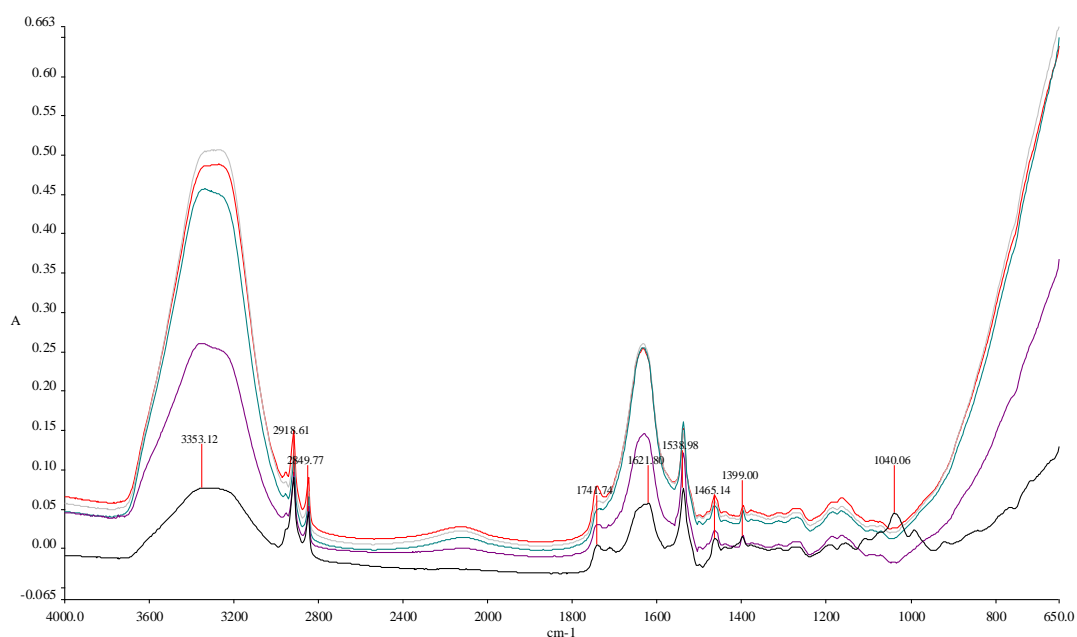
The growth of *A. pullulans* with various concentrations of oleuropein showed a decreasing pattern with increased concentrations of oleuropein (Figure 5.7, a). As seen in this figure, even 100 ppm of oleuropein still had significant antimicrobial effect against *A. pullulans* as higher concentrations. Figure 5.7 (b) shows that this phenolic compound is effective on *A. pullulans* at both 18 h and 24 h with 4 log reduction on yeast count with 50 ppm concentration, and this result matched with OD measurements results. According to PLS-DA score plot (Figure 5.7 (c)), all oleuropein concentrations, even 12.5 ppm, clustered separately from the yeast itself and all sampling periods were differentiated from each other (d). As it could be observed from FTIR spectra (Figure 5.7, e), the biggest changes were in DNA fingerprint region [900-600 cm^{-1}], carbohydrate region [1200-900 cm^{-1}] and amide region [1750-1500 cm^{-1}] as with *S. cerevisiae*. VIP of the PLS-DA model of FTIR data of this yeast for oleuropein indicates that the important spectral regions are [900-1200 cm^{-1}], [1300-1800 cm^{-1}] and [2800-2900 cm^{-1}].
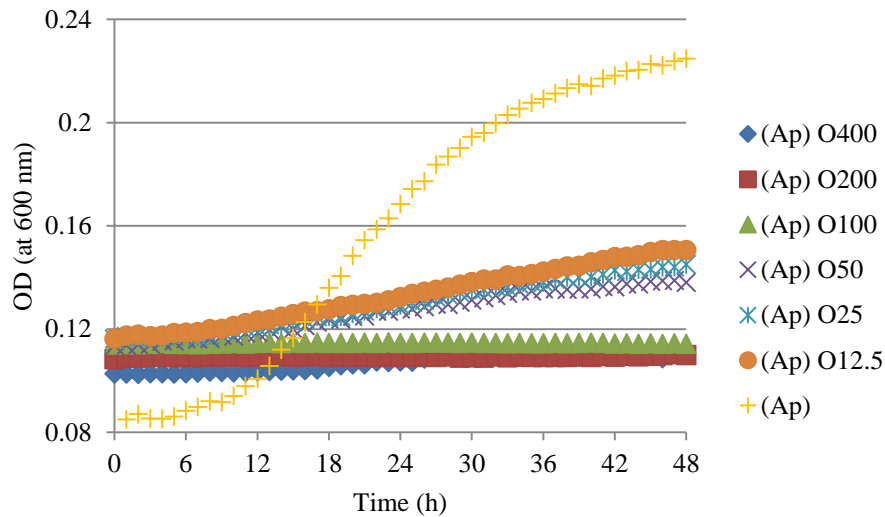
(a)
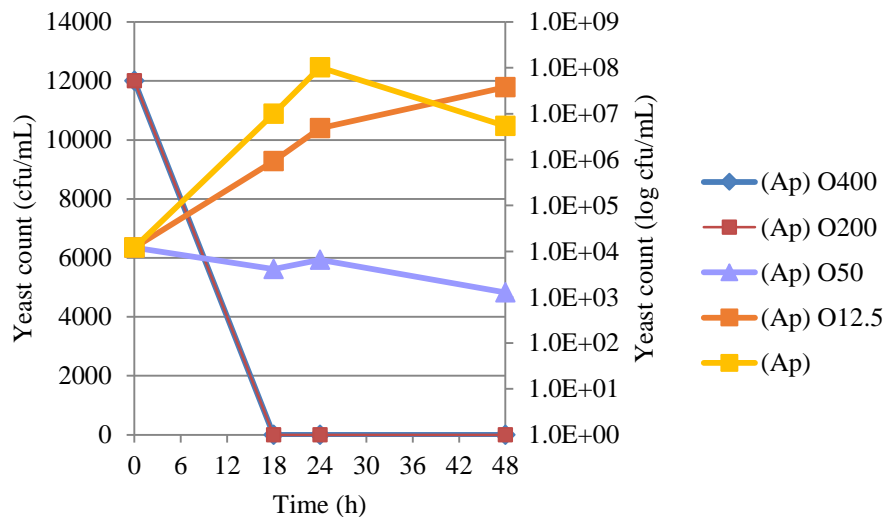
(b)

Figure 5.7. Antimicrobial effects of oleuropein (O) as (a) spectroscopic measurements, (b) yeast colony count (cfu/mL), (c, d) mid-IR measurements shown by score plots of PLS-DA with 2nd derivative and (e) FTIR spectral data at different concentrations (400, 200, 100, 50, 25, 12.5 ppm) on the growth of *A. pullulans* (Ap). (a): Readings were carried on with 1 h intervals, at 30°C for 48 h without shaking. (b): Sampling was done at critical points (0, 18, 24, 48 h). (c): Classification according to concentration. (d): Classification according to sampling time. (e): Data at 18 h and the colors black, red, pink, green and grey indicates Ap, 400 ppm O, 200 ppm O, 50 ppm O and 12.5 ppm O, respectively

Figure 5.7 (Cont.)

(c)

(d)
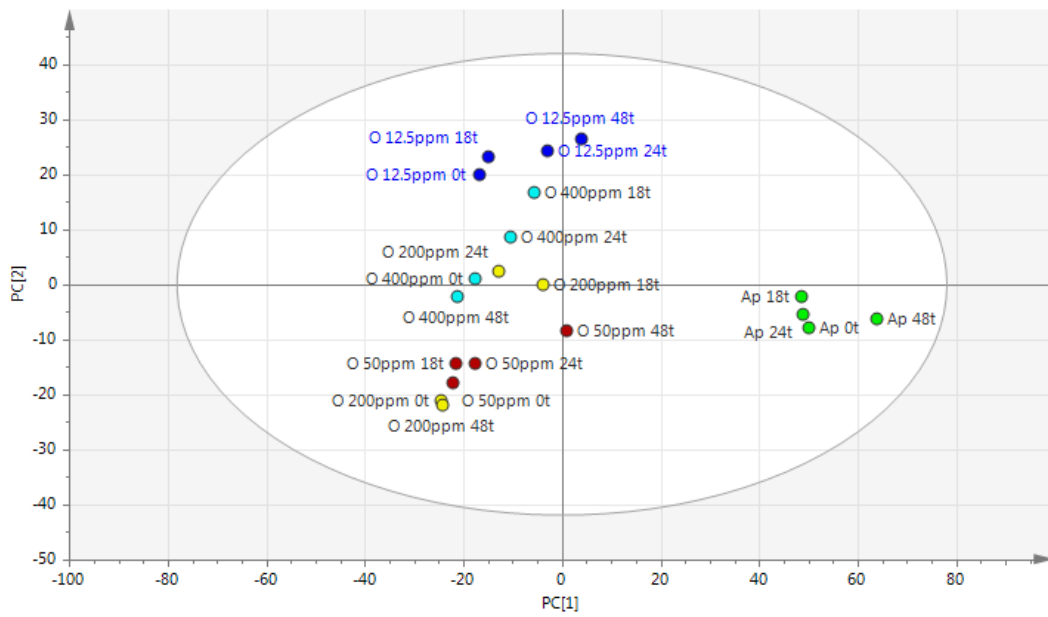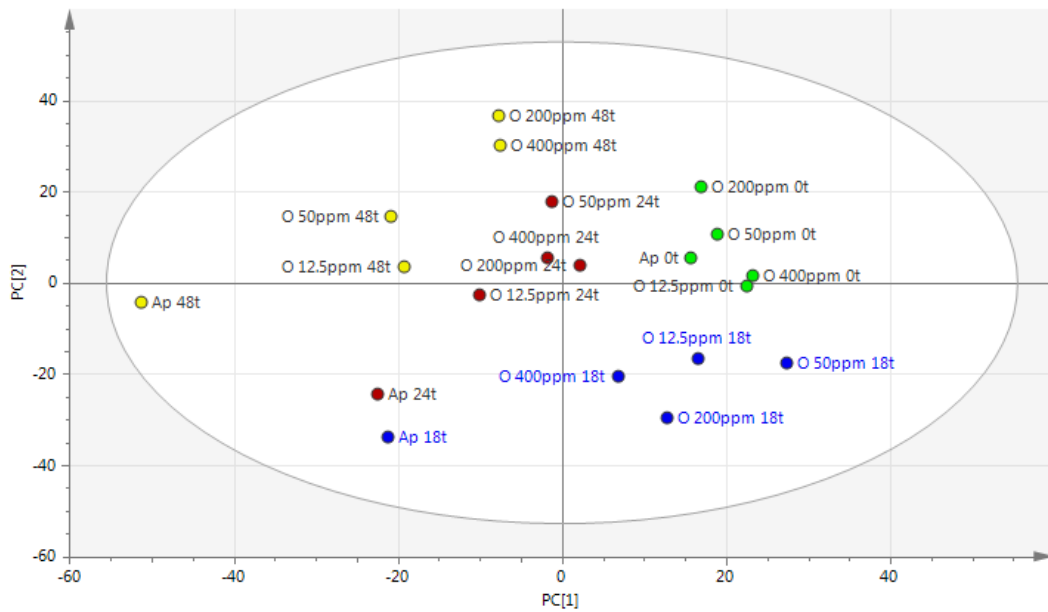
Figure 5.7 (Cont.)
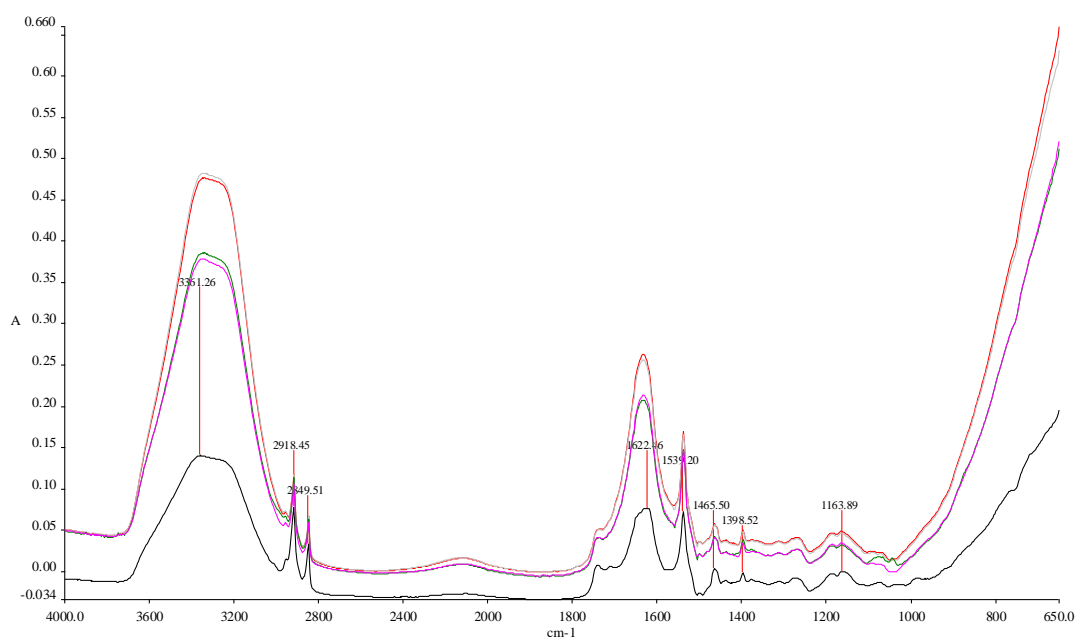
(e)

5.2.2.4 Antimicrobial Activity of *Luteolin*

The effects of various luteolin concentrations (12.5, 25, 50, 100, 200 and 400 ppm) on determined level of *S. cerevisiae* (~1.8x 10^4 cfu/mL) as spectroscopic measurements, yeast colony count (CFU/mL) and mid-IR spectroscopic measurements are shown in Figure 5.8; whereas the results of the same measurements performed for *A. pullulans* (1.2 x 10^4 cfu/mL) are presented in Figure 5.9.

As it could be observed from Figure 5.8 (a) luteolin has the highest antimicrobial activity on *S. cerevisiae* with the concentrations of 400, 200, 100 and 50 ppm. Even 12.5 ppm of luteolin extended the lag phase of *S. cerevisiae* (10^4 cfu/mL) to 16 h. Figure 5.8 (b) shows that both 400 and 200 ppm of luteolin had the highest activity that led to 4 log reduction of *S. cerevisiae* after 18 h. In addition, even 50 ppm luteolin concentration decreased the yeast count 2 log after 18 h and 24 h. In Figure 5.8 (c), it could be easily observed that except for the lowest luteolin concentration, all concentrations showed similar antimicrobial activity on *S. cerevisiae* which were clustered very far away from the yeast itself. There is also a big difference between the 0 h and 18 h, however 24 h and 48 h clustered together, except also for the lowest concentration Figure 5.8 (d). As it could seen fom FTIR spectra (Figure 5.8, e), the biggest changes were observed in DNA fingerprint region [900-600 cm^{-1}], carbohydrate region [1200-900 cm^{-1}] and –OH groups

126

[3600 cm^{-1}] of the yeast exposed to luteolin. VIP values of the PLS-DA model of FTIR data of this yeast for luteolin indicate that the important spectral regions are [900-1200 cm^{-1}], [1300-1900 cm^{-1}] and [2800-2900 cm^{-1}].

All of the luteolin concentrations seemed to have significant antimicrobial activity on *A. pullulans* according to spectrophotometric measurements (Figure 5.9, a). When it was compared with the yeast count graphics, it could be said that 400 and 200 ppm luteolin had the highest activity beginning from 18 h (Figure 5.9, b). The other two concentrations showed 3 log reduction on the count of *A. pullulans* at the same incubation time. In Figure 5.9 (c), the differentiation of especially 400 ppm and 200 ppm of luteolin could be observed which were far from *A. pullulans* itself. The main difference was seen at 18 h (Figure 5.9, d) like previous findings of spectrophotometric measurements and yeast count. FTIR spectra (Figure 5.9, e) also show that the biggest changes were in DNA fingerprint region [900-600 cm^{-1}], carbohydrate region [1200-900 cm^{-1}] and –OH groups [3600 cm^{-1}] of *A. pullulans*. VIP of the FTIR data of this yeast for luteolin indicates that the important spectral regions are [900-1200 cm^{-1}], [1300-1900 cm^{-1}] and [2800-2900 cm^{-1}].
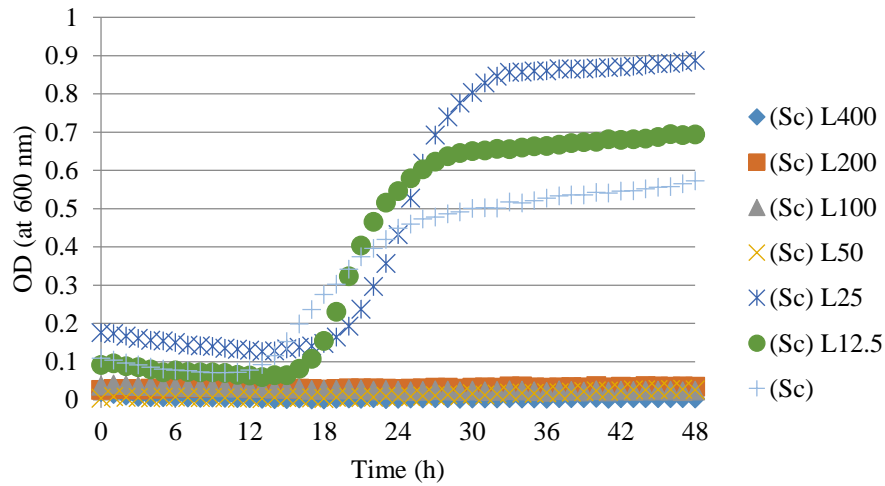
(a)
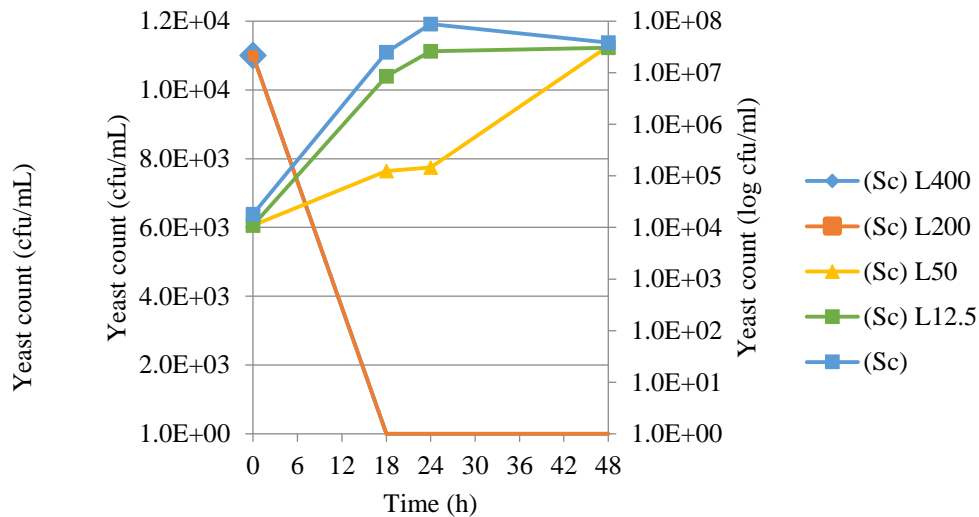
(b)

Figure 5.8. Antimicrobial effects of luteolin (L) as (a) spectroscopic measurements, (b) yeast colony count (cfu/mL), (c, d) mid-IR measurements shown by score plots of PLS-DA with 2nd derivative and (e) FTIR spectral data at different concentrations (400, 200, 100, 50, 25, 12.5 ppm) on the growth of *S. cerevisiae* (Sc). (a): Readings were carried on with 1 h intervals, at 30°C for 48 h without shaking. (b): Sampling was done at critical points (0, 18, 24, 48 h). (c): Classification according to concentration. (d): Classification according to sampling time. (e): Data at 18 h and the colors pink, black, green, grey and red indicates Sc, 400 ppm L, 200 ppm L, 50 ppm L and 12.5 ppm L, respectively

Figure 5.8 (Cont.)

(c)

(d)
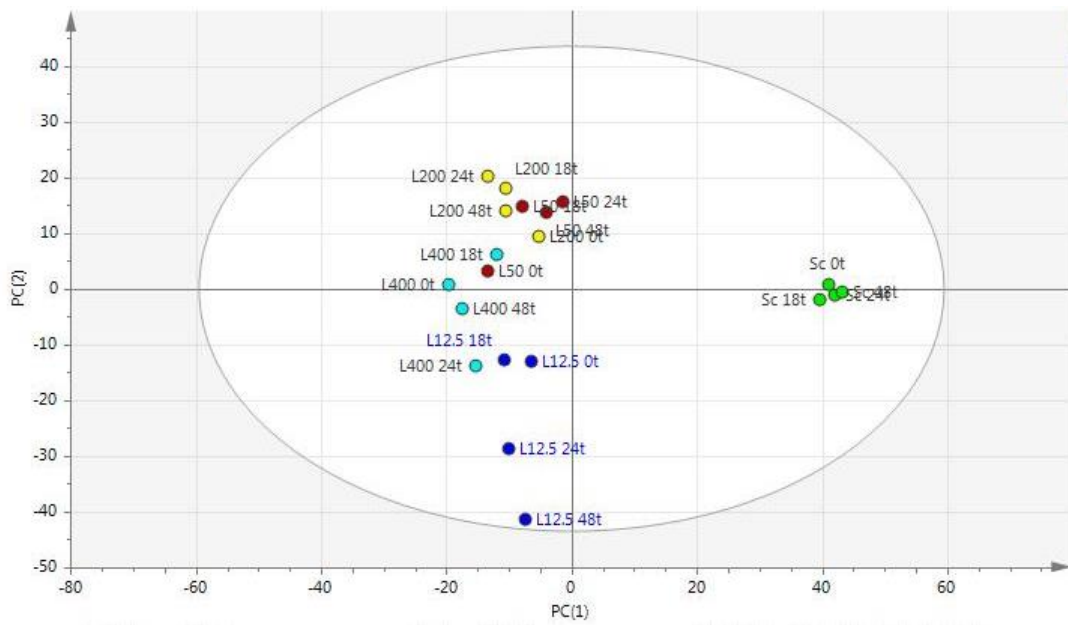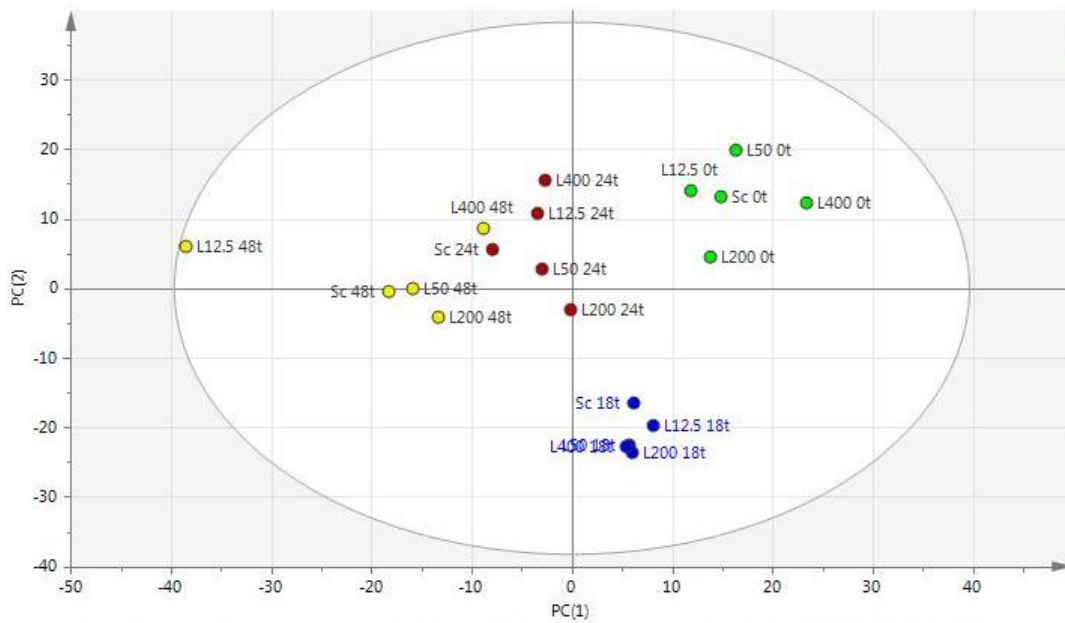
Figure 5.8 (Cont.)
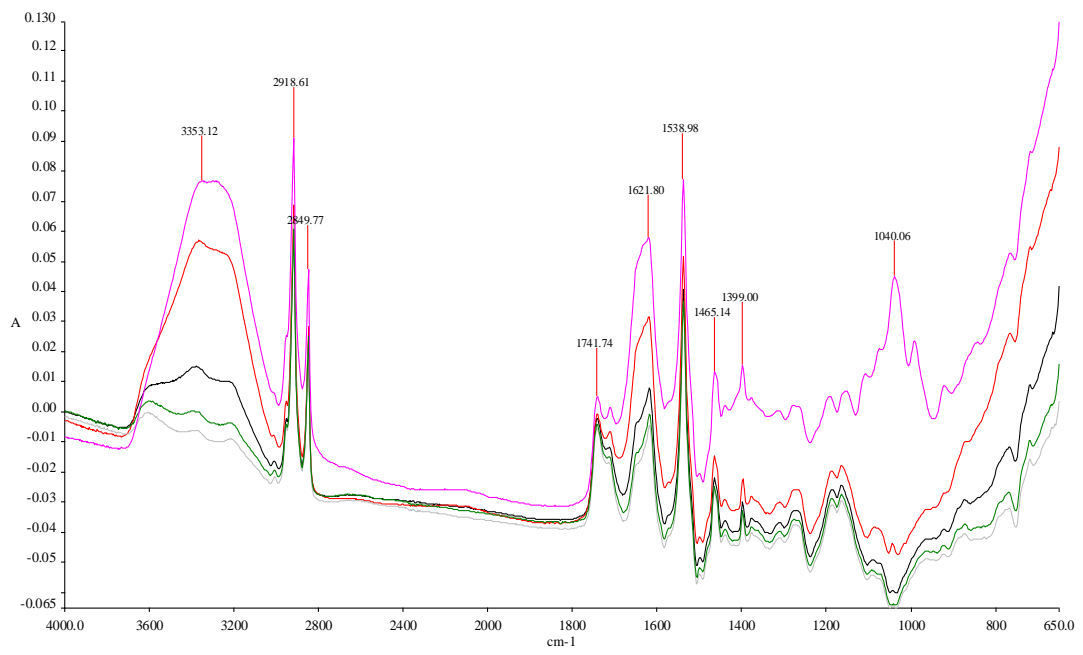
(e)
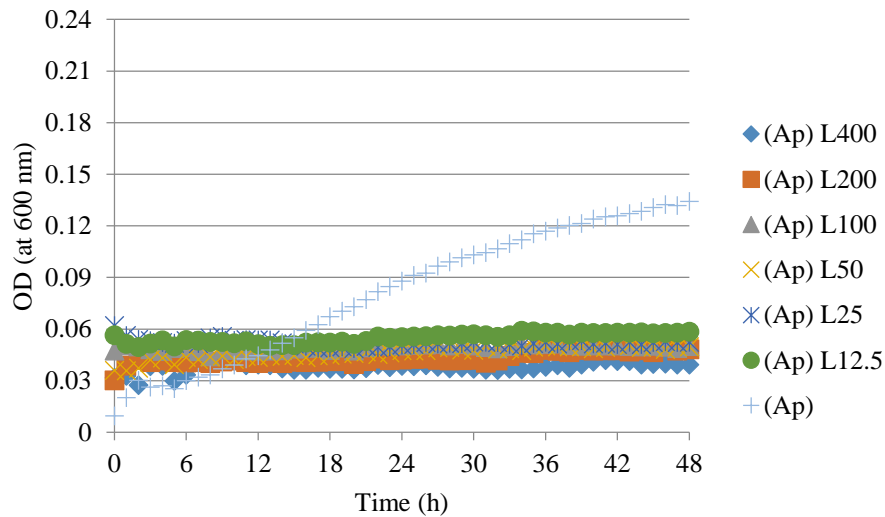
(a)
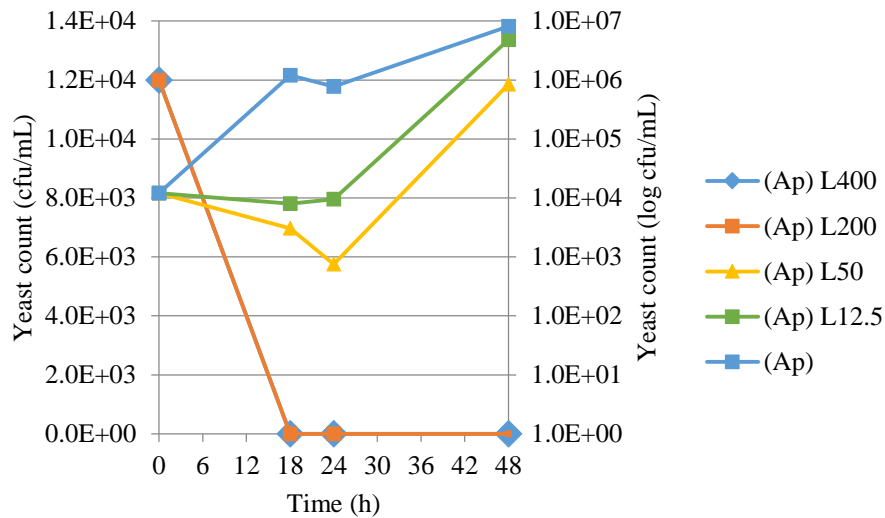
(b)

Figure 5.9. Antimicrobial effects of luteolin (L) as (a) spectroscopic measurements, (b) yeast colony count (cfu/mL), (c, d) mid-IR measurements shown by score plots of PLS-DA with 2nd derivative and (e) FTIR spectral data at different concentrations (400, 200, 100, 50, 25, 12.5 ppm) on the growth of *A. pullulans* (Ap). (a): Readings were carried on with 1 h intervals, at 30°C for 48 h without shaking. (b): Sampling was done at critical points (0, 18, 24, 48 h). (c): Classification according to concentration. (d): Classification according to sampling time. (e): Data at 18 h and the colors black, red, pink, green and grey indicates Ap, 400 ppm L, 200 ppm L, 50 ppm L and 12.5 ppm L, respectively

(Cont. on next page)

Figure 5.9 (Cont.)

(c)

(d)

Figure 5.9 (Cont.)
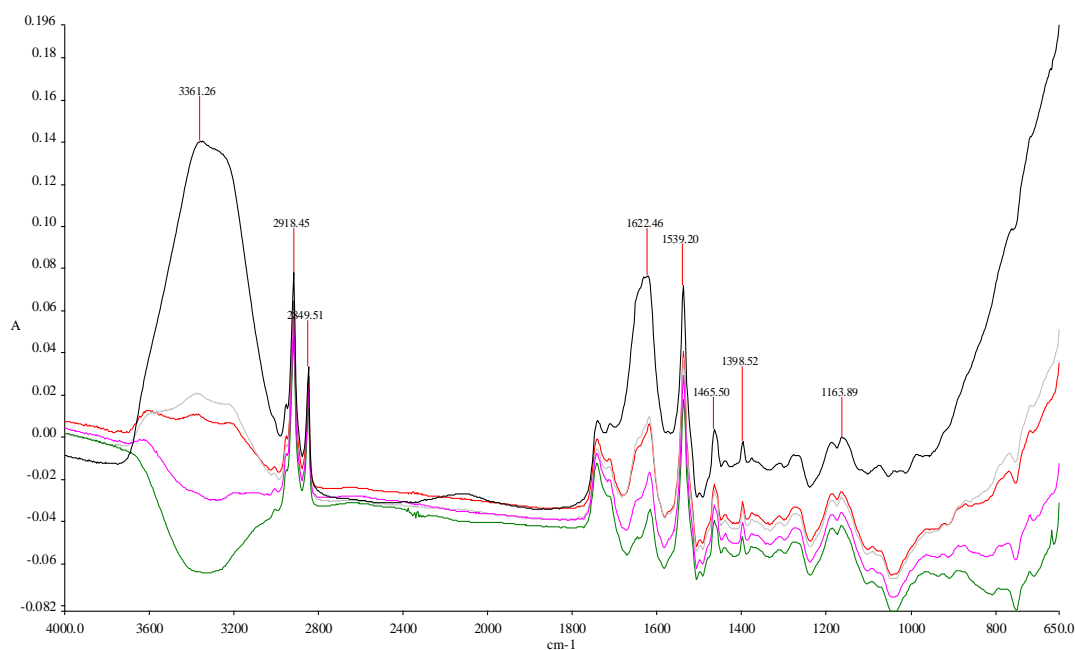
(e)

5.2.2.5 Antimicrobial Activity of *Apigenin*

The effects of various apigenin concentrations (12.5, 25, 50, 100, 200 and 400 ppm) on determined level of *S. cerevisiae* (~1.8x 10^4 cfu/mL) as spectroscopic measurements, yeast colony count (CFU/mL) and mid-IR spectroscopic measurements are shown in Figure 5.10; whereas the results of the same measurements performed for *A. pullulans* (1.2 x 10^4 cfu/mL) are shown in Figure 5.11.

Apigenin showed the highest antimicrobial activity on *S. cerevisiae* with the concentrations of 400, 200 and 100 ppm (Figure 5.10, a). As seen in Figure 5.10 (b), at 18 h which corresponds to exponential phase for *S. cerevisiae*, 400 and 200 ppm of apigenin had totally fatal effect. 50 ppm of apigenin caused 1 log reduction in number at 18 h. Figure 5.10 (c) shows the similar effects of 400 and 200 ppm of apigenin on *S. cerevisiae* and the different cluster of the lowest concentration of this phenol. According to PLS-DA score plot (Figure 5.10 (d)), the different clusters of the results of 18 h could be easily observed which was in parallel finding with the yeast count results. FTIR spectra (Figure 5.10, e) indicate that the biggest changes of FTIR spectra were in DNA fingerprint region [900-600 cm^{-1}], carbohydrate region [1200-900 cm^{-1}] and amide region [1750-

133

1500 cm^{-1}]. VIP of the PLS-DA model of FTIR data of this yeast for apigenin indicates that the important spectral regions are [900-1200 cm^{-1}], [1300-1900 cm^{-1}] and [2800-2900 cm^{-1}].
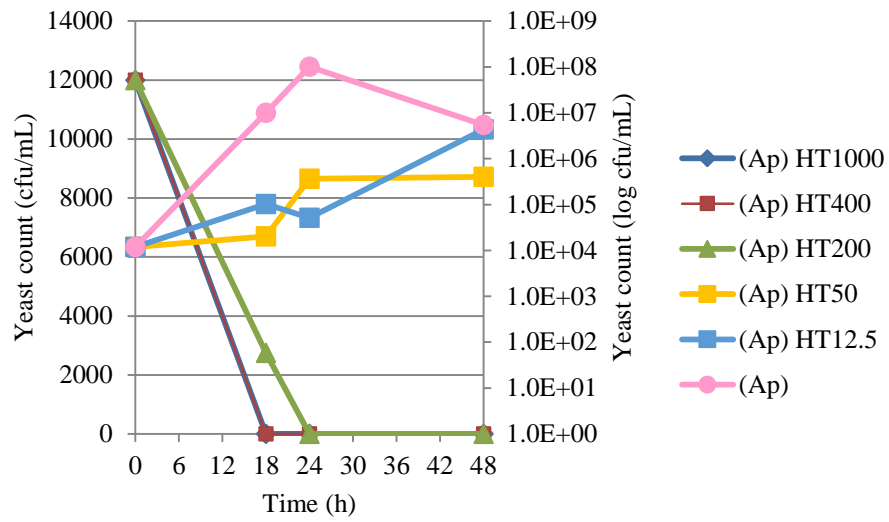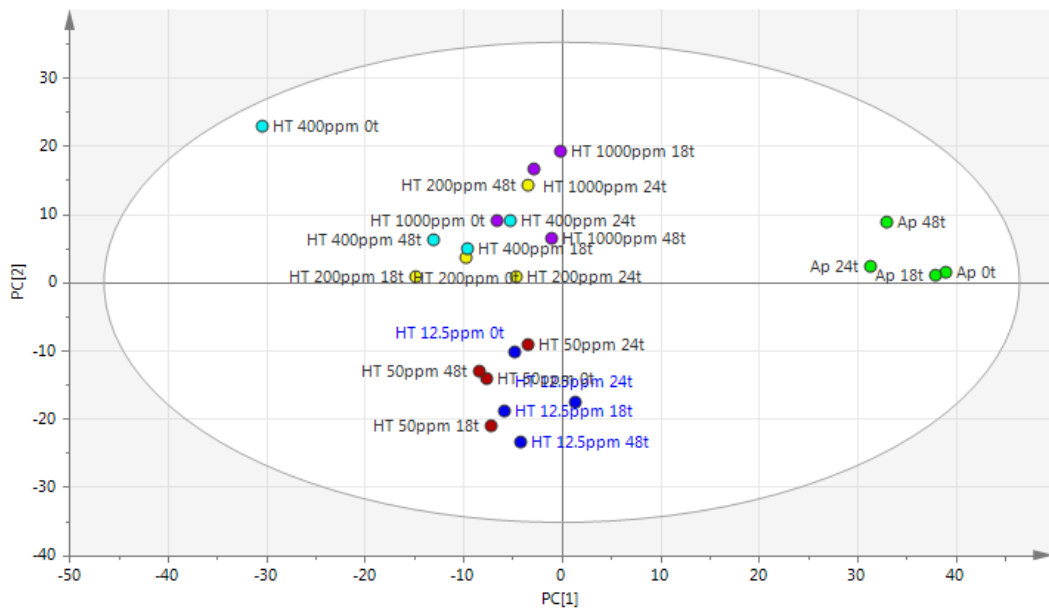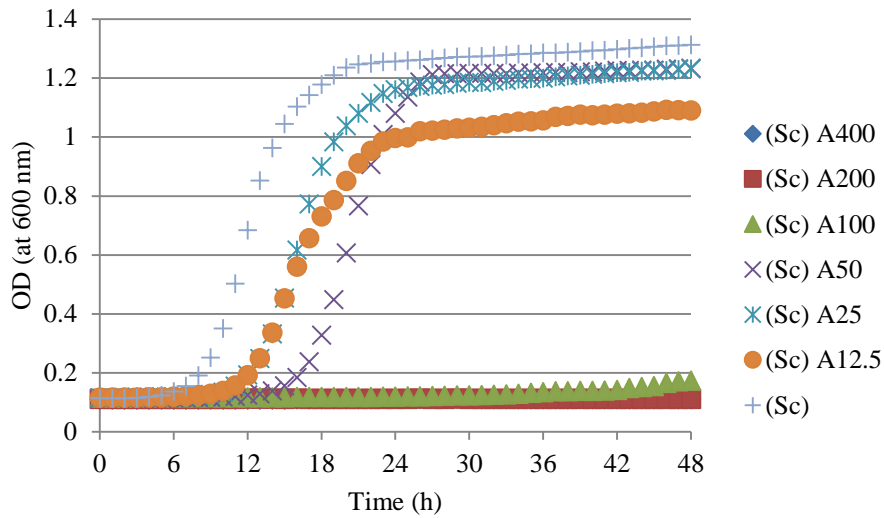

(a)
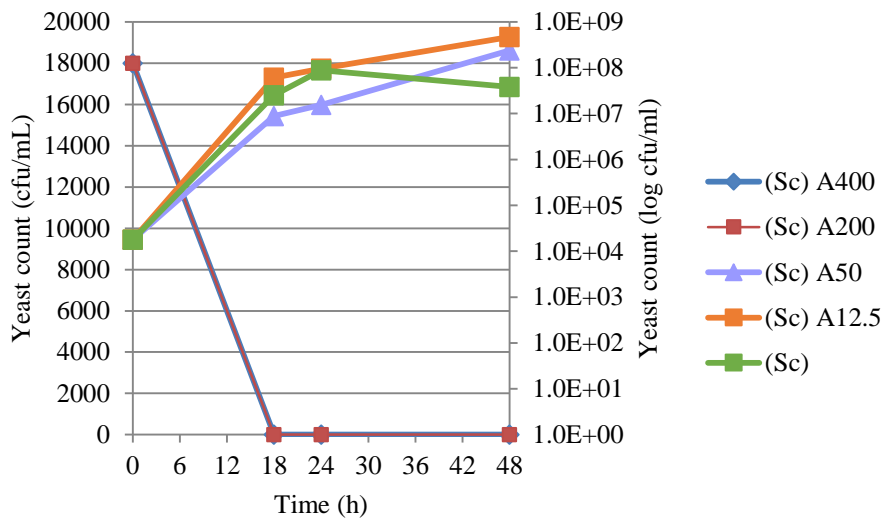
(b)

Figure 5.10. Antimicrobial effects of apigenin (A) as (a) spectroscopic measurements, (b) yeast colony count (cfu/mL), (c, d) mid-IR measurements shown by score plots of PLS-DA with 2nd derivative and (e) FTIR spectral data at different concentrations (400, 200, 100, 50, 25, 12.5 ppm) on the growth of *S. cerevisiae* (Sc). (a): Readings were carried on with 1 h intervals, at 30°C for 48 h without shaking. (b): Sampling was done at critical points (0, 18, 24, 48 h). (c): Classification according to concentration. (d): Classification according to sampling time. (e): Data at 18 h and the colors black, red, pink, green and grey indicates Sc, 400 ppm A, 200 ppm A, 50 ppm A and 12.5 ppm A, respectively

Figure 5.10 (Cont.)

(c)

(d)
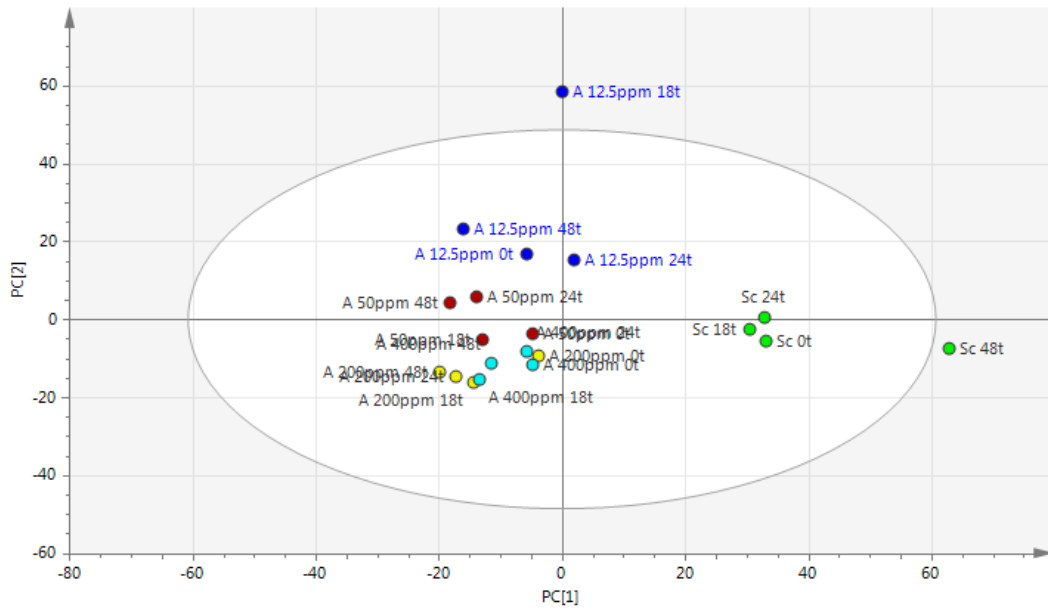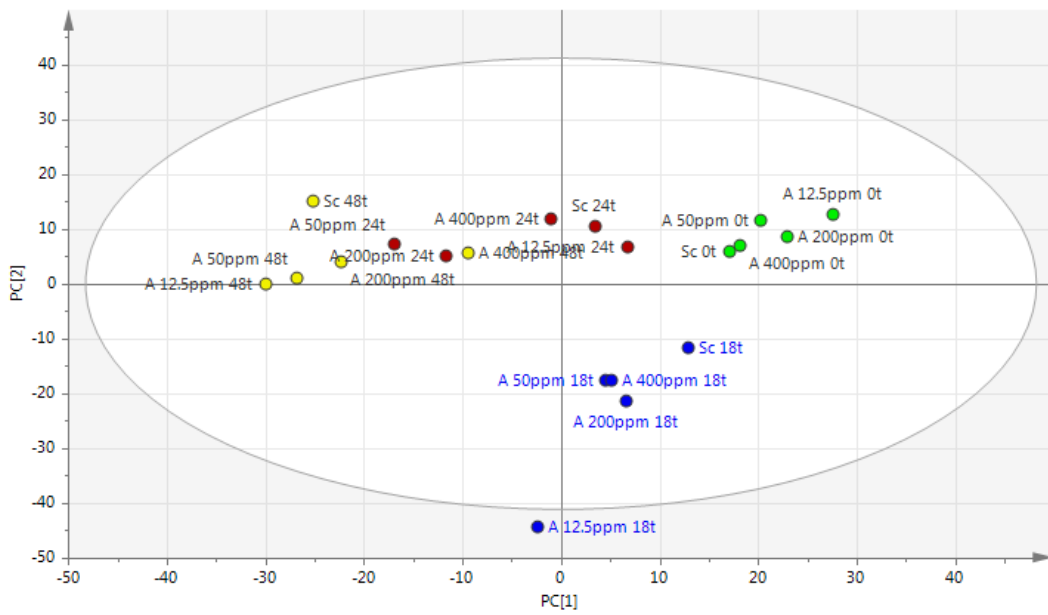
Figure 5.10 (Cont.)

(e)
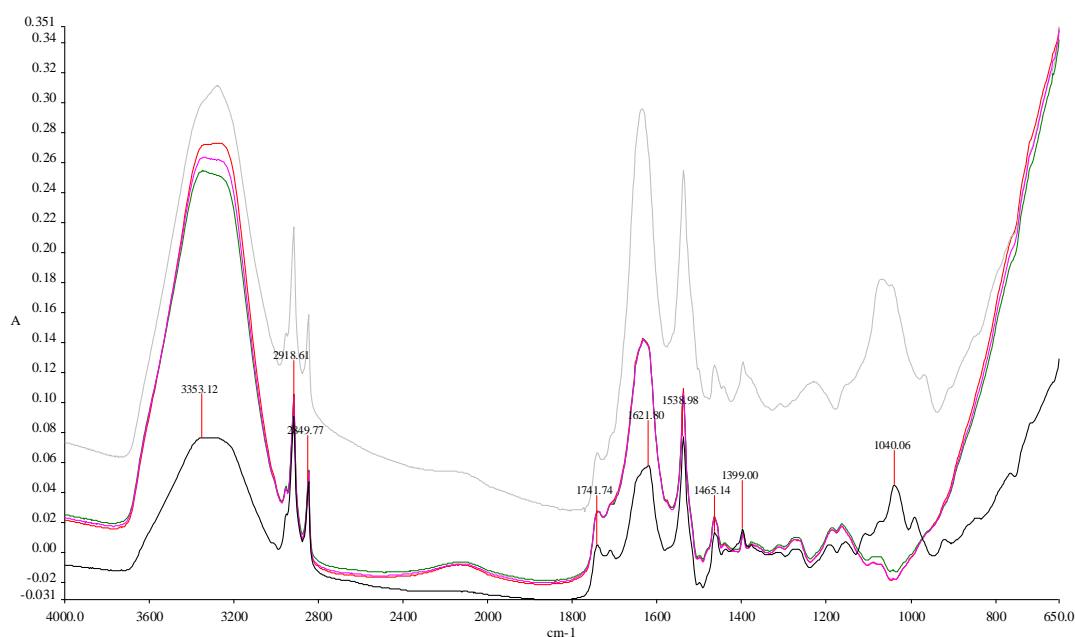
The growth of *A. pullulans* exposed to various concentrations of apigenin showed a decreasing pattern with increased concentration (Figure 5.11, a). In addition, 400 and 200 ppm of apigenin had significant antimicrobial effect against *A. pullulans*. According to Figure 5.11 (b), contact with 50 ppm apigenin resulted in 3 log reduction at 18 h; and further decrease in yeast count to 4 log was observed at 24 h. Figure 5.11 (c) indicates that the lowest apigenin concentration, especially at 18 h, was differentiated from all other concentrations. The main difference between concentrations was at 18 h which was similar with yeast count results (Figure 5.11, d). FTIR spectra of the yeast (Figure 5.11, e) show that the biggest changes due to exposure to apigenin were in DNA fingerprint region [900-600 cm^{-1}], carbohydrate region [1200-900 cm^{-1}] and amide region [1750-1500 cm^{-1}], as similar with *S. cerevisiae*. VIP of the FTIR data of this yeast for apigenin indicates that the important spectral regions are [900-1200 cm^{-1}], [1300-1800 cm^{-1}] and [2800-2900 cm^{-1}].
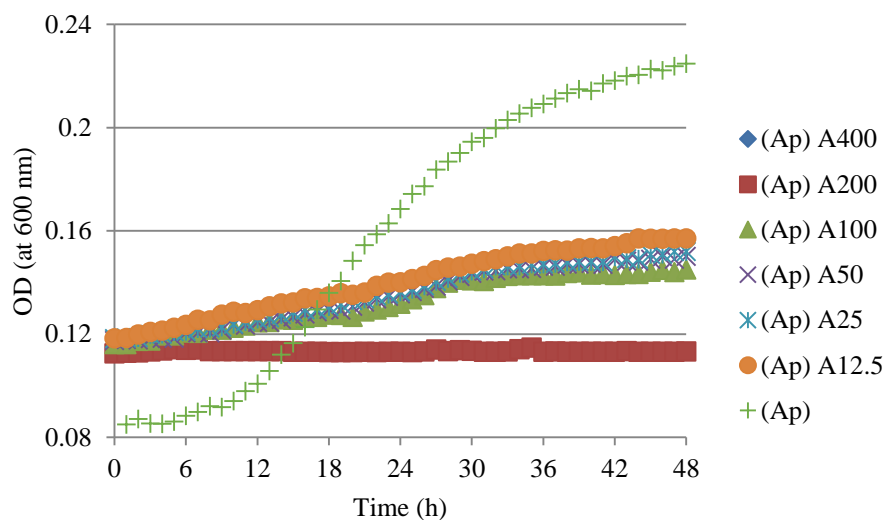
(a)
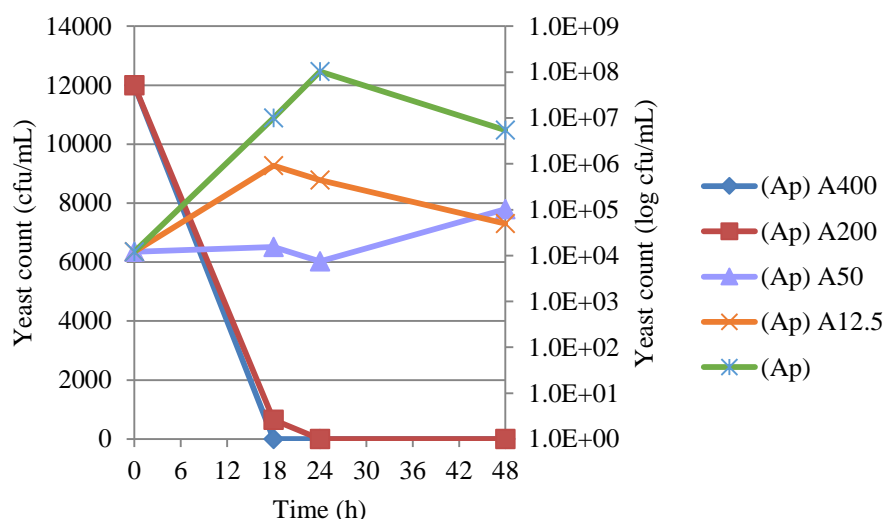
(b)

Figure 5.11. Antimicrobial effects of apigenin (A) as (a) spectroscopic measurements, (b) yeast colony count (cfu/mL), (c, d) mid-IR measurements shown by score plots of PLS-DA with 2nd derivative and (e) FTIR spectral data at different concentrations (400, 200, 100, 50, 25, 12.5 ppm) on the growth of *A. pullulans* (Ap). (a): Reading was carried on with 1 h intervals, at 30°C for 48 h without shaking. (b): Sampling was done at critical points (0, 18, 24, 48 h). (c): Classification according to concentration. (d): Classification according to sampling time. (e): Data at 18 h and the colors black, red, pink, green and grey indicates Ap, 400 ppm A, 200 ppm A, 50 ppm A and 12.5 ppm A, respectively

(Cont. on next page)

Figure 5.11 (Cont.)

(c)

(d)

Figure 5.11 (Cont.)
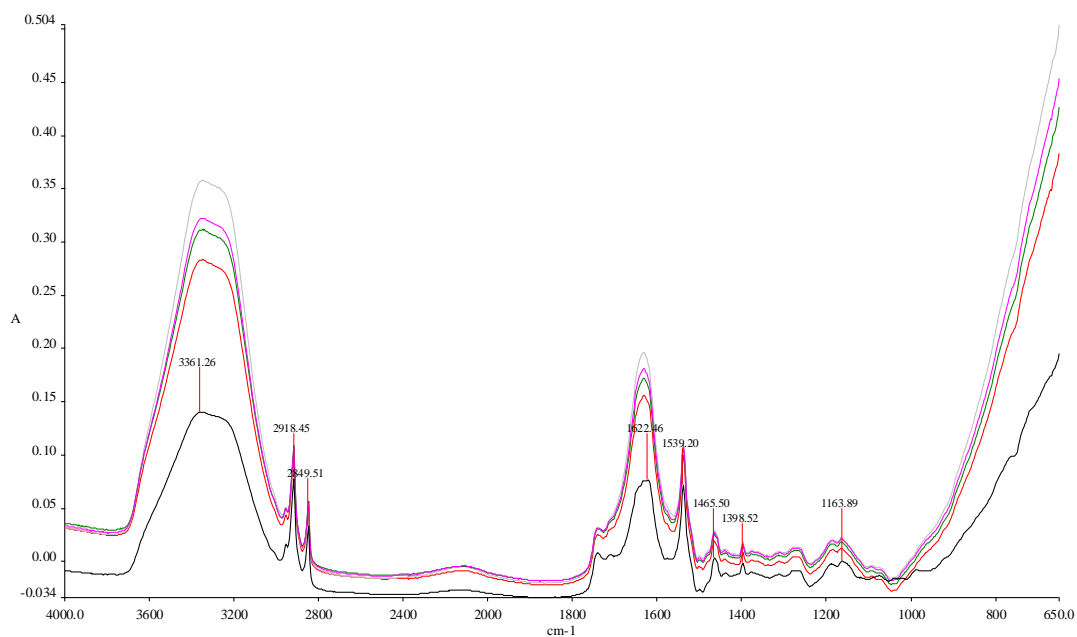
(e)

Figure 5.12 shows the FTIR spectral data of the all phenolic compounds with 400 ppm concentrations at 18 h using both (a) *S. cerevisiae* and (b) *A. pullulans.* The main differences between the spectra of yeast itself and yeast treated with phenol solutions could be easily observed for each yeast. In addition, differences between phenolic compounds with respect to the wavenumbers in which they have effect on could be seen from the spectra.
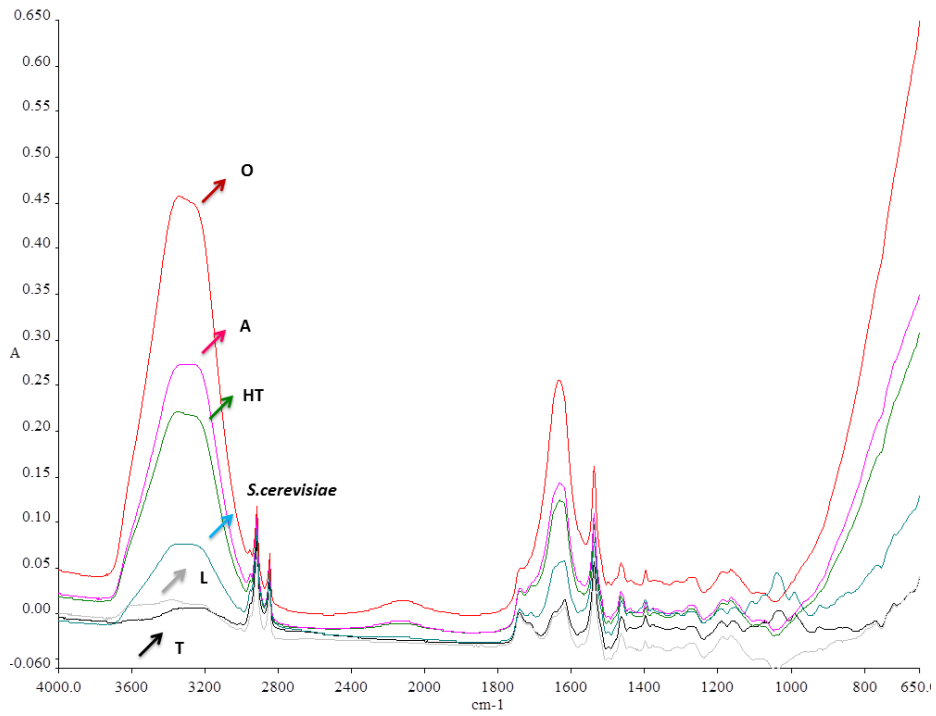
(a)
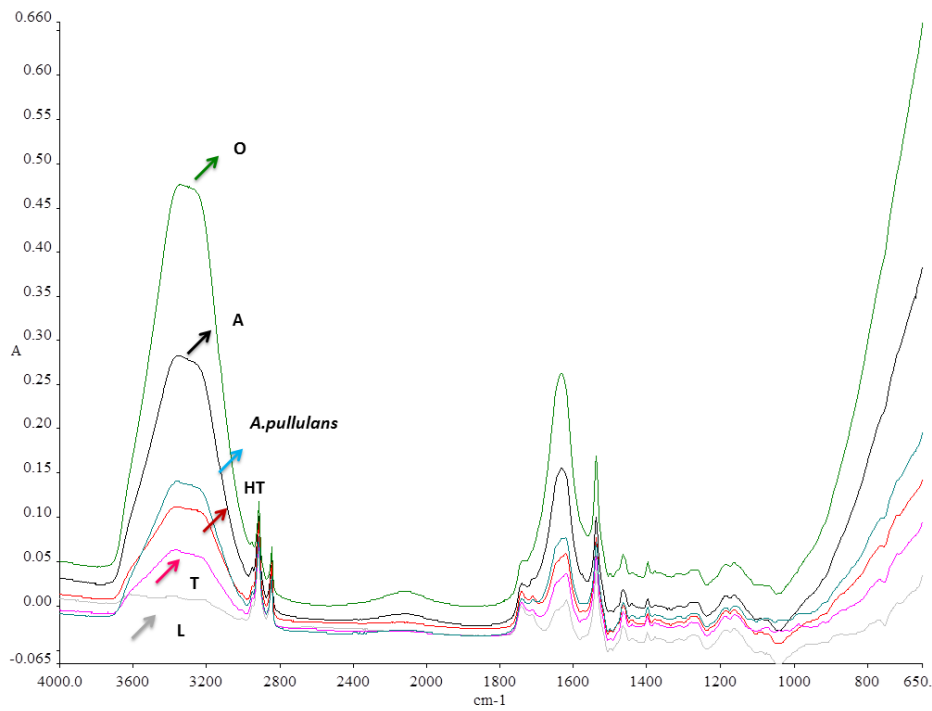
(b)

Figure 5.12. FTIR spectral data of phenolic compounds (oleuropein, apigenin, hydroxytyrosol, luteolin and tyrosol) at 400 ppm concentration at 18 h incubation with (a) *S. cerevisiae* and (b) *A. pullulans*

FTIR data of both yeasts treated with the phenolic compounds were also simultaneously evaluated using multivariate statistical analysis in order to show clusters in the same figure. Figure 5.13 shows antimicrobial effects of tyrosol (T) as 2nd derivative of mid-IR measurements shown by score plots of PLS-DA on the growth of both *S. cerevisiae* and *A. pullulans*. The different clusters of especially 200 ppm and 400 ppm tyrosol-treated yeasts can be easily observed in Figure 5.13 (a). However, lower tyrosol concentrations resulted more scattered scheme. In Figure 5.13 (b), low tyrosol concentration (12.5 ppm) and the time 0 were excluded from the whole data and it is shown that while the clusters of low tyrosol concentrations are distinct for each yeast, yeasts treated with high tyrosol concentrations are close to each other. The distant clusters of the results at 0 and 48 h and the closeness at 18 and 24 h could be easily observed in Figure 5.13 (c). Figure 5.13 (d) indicates that it is possible to differentiate two different yeasts treated with the same phenolic compound, tyrosol, within the same graphic. Since the best clustering was obtained with tyrosol among all phenolic compounds when the mid-IR measurements of both yeasts were evaluated together, the score plots of other phenolic compounds are not shown. Loading plots of these data were also examined however no pattern was obtained.
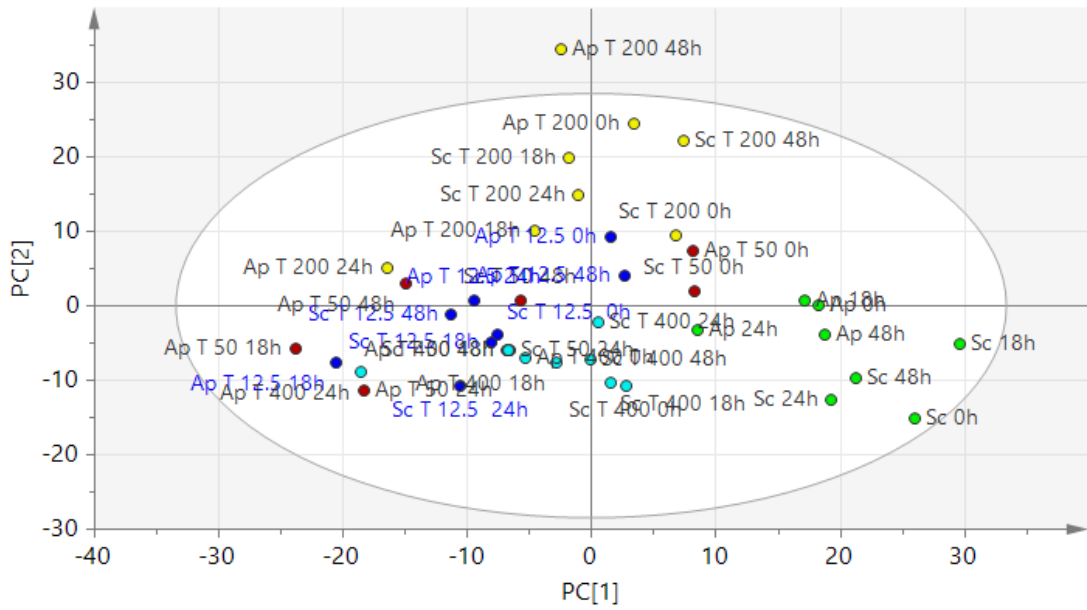
(a)
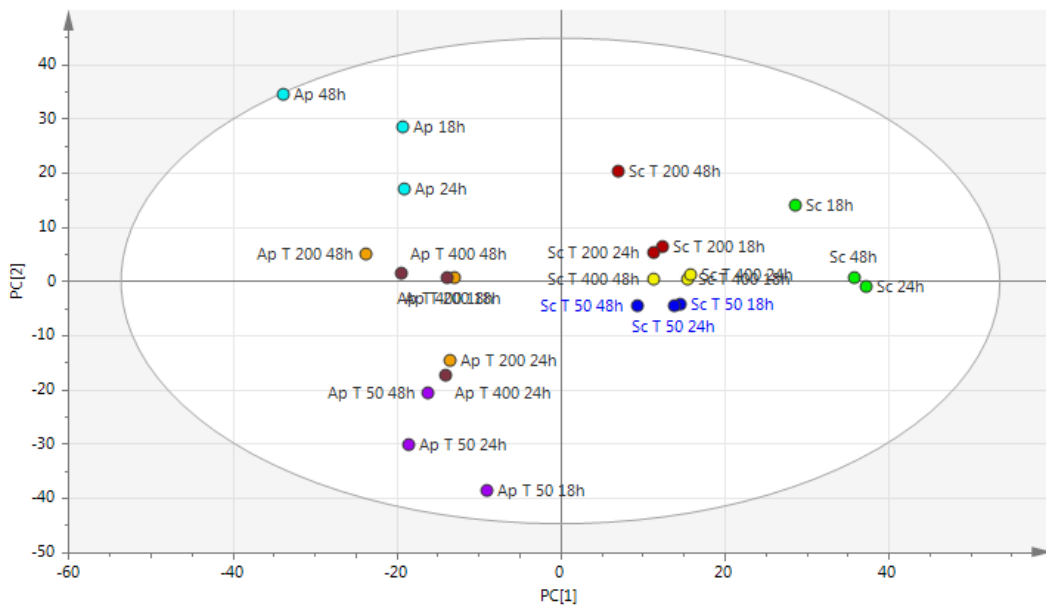
(b)

Figure 5.13. Antimicrobial effects of tyrosol (T) as mid-IR measurements shown by score plots of PLS-DA with 2nd derivative at different concentrations (400, 200, 50, 12.5 ppm) on the growth of *S. cerevisiae* (Sc) and *A. pullulans* (Ap). Classification according to (a): concentration, (b): concentration with exclusions of 0 h and 12.5 ppm, (c): sampling time, (d): yeast type

Figure 5.13 (Cont.)

(c)

(d)

The FTIR spectroscopy has been comprehensively used for understanding the main cellular composition since infrared spectra provide detailed information on cellular components like proteins, polysaccharides and lipids. In addition, it has been successfully used for identification and classification of specific microorganisms and cells infected with viruses, cancer cells and also infections caused by pathogens. Furthermore, an increasing number of studies are emerging in recent years involving FTIR spectroscopy

for assessment of the structural changes in food-related microorganisms in response to stress conditions (Skotti et al., 2014). Several authors have shown the use of FTIR spectroscopy as a tool to determine the cellular target of different antimicrobial compounds and food processing technologies. The most important differences were generally found in w4 spectral region (1200 to 900 cm^{-1}), indicating that some of the IR spectral changes were due to the damage or conformational/compositional alterations in the components of the cell wall and membrane. Some of the studies have been related with the assessment of the membrane properties of the food pathogens in changing environments. Various studies have focused on the use of FTIR spectroscopy for the detection of stress-injured microorganisms in food products subjected to preservation agents. In these studies, spectral variations observed between 1300 and 900 cm^{-1} were also linked to damage of cell walls and membranes. Some other studies have shown the use of FTIR spectroscopy for assessment of spore properties in different environments (Alvarez-Ordonez et al., 2011).

Although there are many studies monitoring the stress response of bacterial cells by FTIR spectroscopy, only a few researches have been published about yeasts. In the study of Corte et al. (2010), *S. cerevisiae* cells were exposed to four chemical compounds (sodium hypochlorite, sodium chloride, ethanol and sulfur dioxide) at five different concentrations in order to analyze the effect of the stress induced by these substances on the cells using FTIR analysis. The spectral areas in which the more intense variations took place were identified in the aforementioned study. Region corresponding to amides were found as the most affected part. In addition, the DNA fingerprint and the carbohydrate regions have significant differences. However, the DNA fingerprint area showed large variations even independently from the stress action. This area has always been accepted as characterizing microorganisms at species or strain level, but little is known about the cellular compounds producing the IR signal in this region. It was reported that the DNA fingerprint region could not be used to define a stress index and needs further investigation. The same research group (Corte et al., 2014) conducted a more recent study based on the measurement of metabolomic stress response induced by a surfactant (N-alkyltropinium) on the yeasts *S. cerevisiae* and *C. albicans*. In that study, FTIR spectroscopic analysis revealed that *S. cerevisiae* cells showed the maximum stress response in the regions of amides (w2) and fatty acids (w1); whereas *C. albicans* cells were most affected in amides (w2) and mixed (w3) regions. Saharan and Sharma (2011) performed a FTIR bioassay to examine ethanol stressed *Pachysolen tannophilus*. The

results of FTIR measurements were compared with those obtained by traditional biochemical methods. The data obtained from both FTIR and chemical methods showed that ethanol stress resulted in changes in carbohydrate, lipids and proteins. The technique was found as reliable and less labor intensive than the traditional chemical methods. As a result, spectrum of the 3000–2800 cm^{-1} regions showed that there is an increased absorption, mainly assigned to lipids. Changed absorption in this area was explained by the synthesis of large amounts of polyunsaturated fatty acids and this change in yeast membrane was indicated as one of the important markers for the ethanol stress. In addition to the fatty acid region, remarkable changes were also found in the amide I (1630–1700 cm^{-1}) and amide II (1500–1560 cm^{-1}) regions, probably due to change in protein conformation and also protein degradation, which mainly involve the cell membrane. Vibrational changes in the wavenumber of 1240 cm^{-1} mainly attributed to changes in DNA, RNA and phospholipids. The increased absorption of the polysaccharides region (1200–900 cm^{-1}) showed the excess synthesis of carbohydrates due to the increase of wall polysaccharides.

5.2.3. Monitoring of Antimicrobial Activity Using Phase Contrast and Scanning Electron Microscope

In order to show the antimicrobial activities of some of the phenolic compounds on the cell structure of yeasts; tyrosol, hydroxytyrosol and luteolin were chosen and their effects were investigated using phase contrast and scanning electron (SEM) microscopes. Each phenolic compound was assessed at low (200 ppm) and high (800 ppm) concentrations on the yeasts, *S. cerevisiae* and *A. pullulans*. Figure 5.14 and Figure 5.15 show some selected images of *S. cerevisiae* and *A. pullulans*, respectively, treated with these phenolics for various incubation periods.
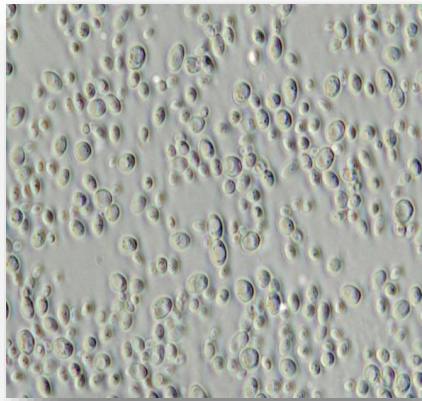
(a) Sc

(b) 18 h T800 ppm

(c) 48 h T800 ppm

(d) 18 h HT800 ppm
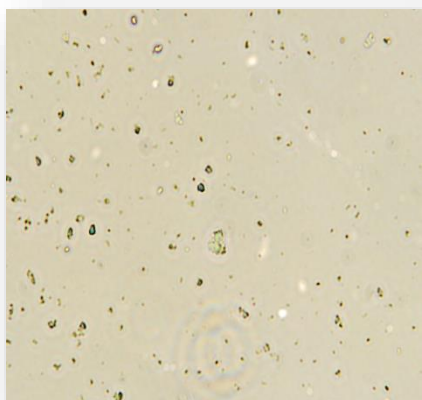
(e) 24 h HT800 ppm

(f) 18 h L800 ppm

Figure 5.14. The phase contrast microscope images of *S. cerevisiae* (Sc) cells under phase contrast microscope using 100X magnification after treatment with phenolic compounds (T: tyrosol, HT: hydroxytyrosol, L: luteolin) of 800 ppm concentration for various incubation periods (18, 24, 48 h)
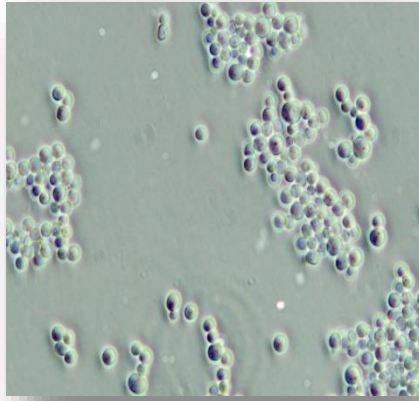
(a) Ap
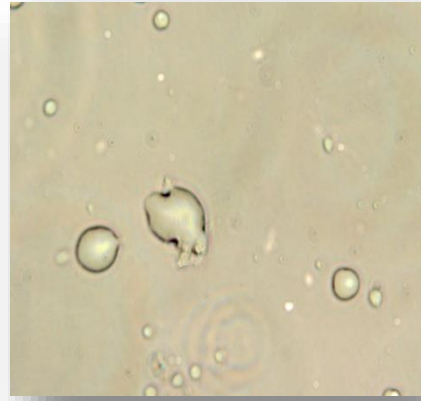
(b) 18 h T200 ppm
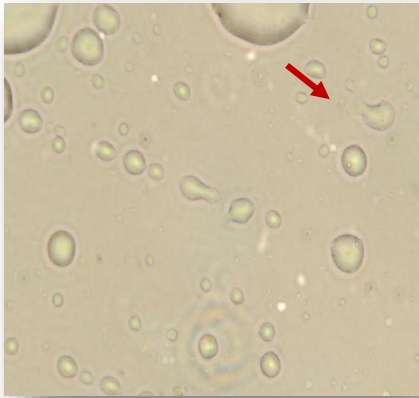
(c) 18 h T800 ppm

(d) 24 h HT800 ppm

(e) 24 h L800 ppm
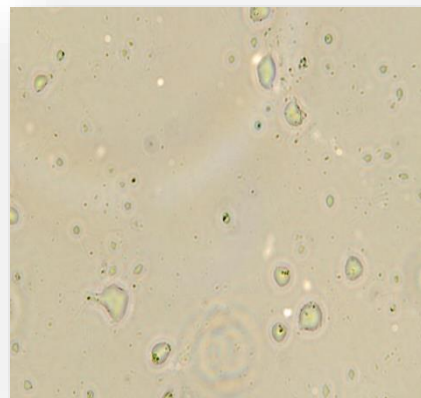
(f) 48 h L800 ppm

Figure 5.15. The phase contrast microscope images of *A. pullulans* (Ap) cells under phase contrast microscope using 100X magnification after treatment with phenolic compounds (T: tyrosol, HT: hydroxytyrosol, L: luteolin) of 200 ppm and 800 ppm concentrations for various incubation periods (18, 24, 48 h)

Among these phenolic compounds tyrosol was observed to have disruptive impact on the wall of both yeast cells, even at low concentration and early growth phase (Figure 5.14, b and c; Figure 5.15, b and c). Hydroxytyrosol caused both disruption and deformation of the cell wall on both yeasts (Figure 5.14, d and e; Figure 5.15, d). For luteolin treated yeasts, it was hard to observe intact cell wall of the yeast cells, especially for high concentration (Figure 5.14, f; Figure 5.15, e and f). The SEM images of these yeasts treated with the same phenolic compounds are shown in the Figure 5.16 and 5.17, in which the deformations on the yeast cell walls could be easily observed.

There are several studies in the literature dealing with the investigation of antimicrobial effects of phenolic compounds on microorganisms. Lee and Lee (2010) assessed the antioxidant and antimicrobial activities of both the individual and combined phenolics in olive leaf extract and found oleuropein as having a strong growth inhibition effect against *S. Enteritidis*. Bisignano et al. (1999) tested several bacterial species susceptibility to two olive secoiridoides, oleuropein and hydroxytyrosol and concluded that oleuropein inhibited the growth of several bacterial strains while it was ineffective against *Haemophilus influenzae* and *Moraxella catarrhalis*. Pereira et al. (2007) screened the phenolic compunds in olive leaf extracts including oleuropein, luteolin 7-O-glucoside and apigenin 7-O-glucoside for their antimicrobial activity against Gram + and Gram − bacteria and fungi. The values of microbial growth rate in the presence of different extract concentrations indicated that olive leaf had antimicrobial capacity on microorganisms, in the order of *B. cereus ~ C. albicans > E. coli > S. aureus > C. neoformans ~ K. pneumoniae ~ P. aeruginosa > B. subtilis*.
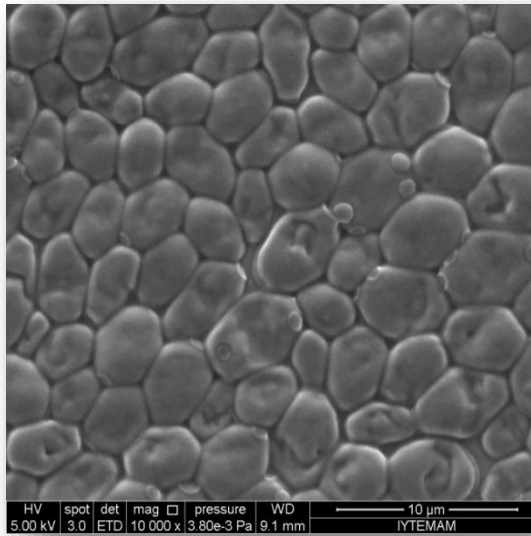
(a) Sc
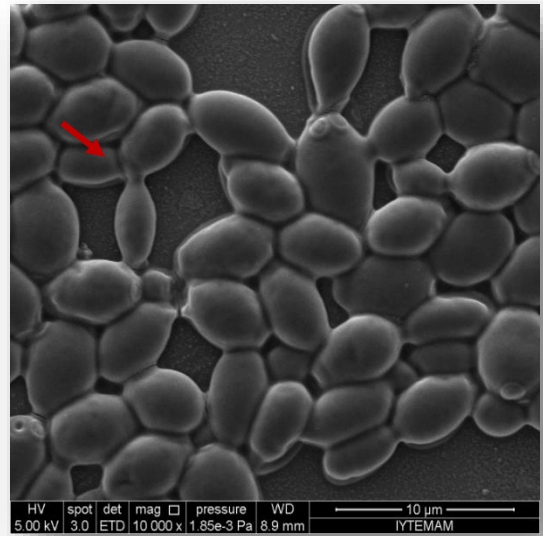
(b) Sc T200 ppm
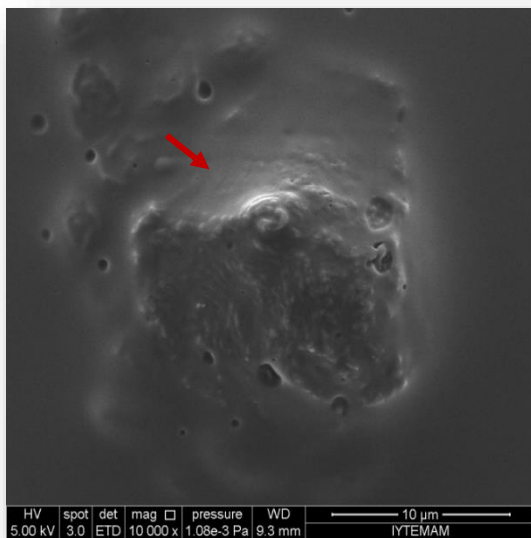
(c) Sc HT800 ppm
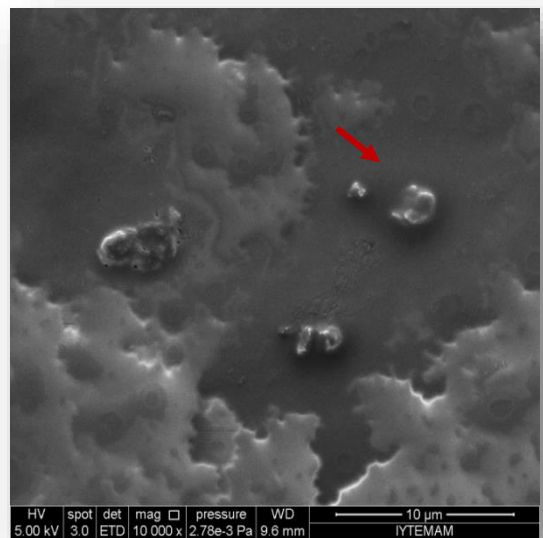
(d) Sc L200 ppm

Figure 5.16. The SEM images of *S. cerevisiae* (Sc) cells after treatment with phenolic compounds (T: tyrosol, HT: hydroxytyrosol, L: luteolin) in the concentrations of 200 ppm and 800 ppm (MAG= x10.000)
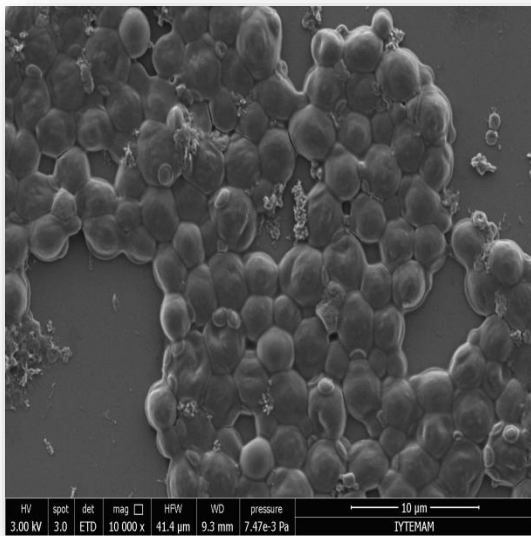
(a) Ap
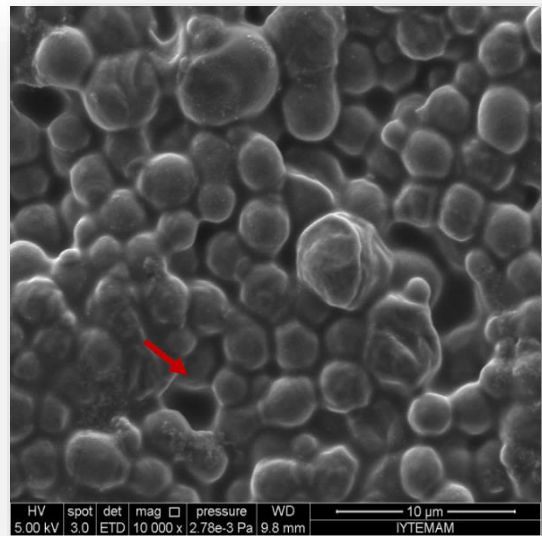
(b) Ap T200 ppm
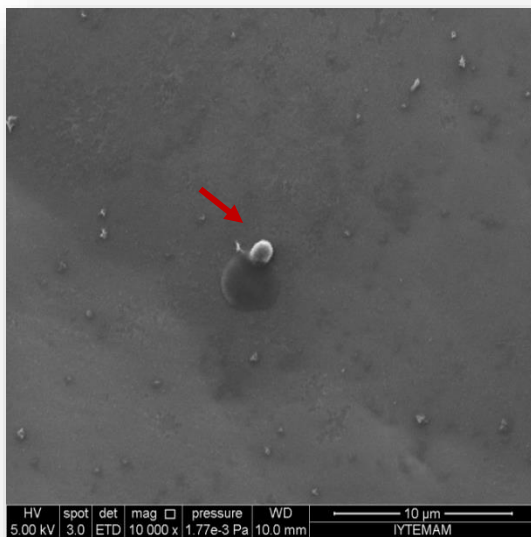
(c) Ap L200 ppm
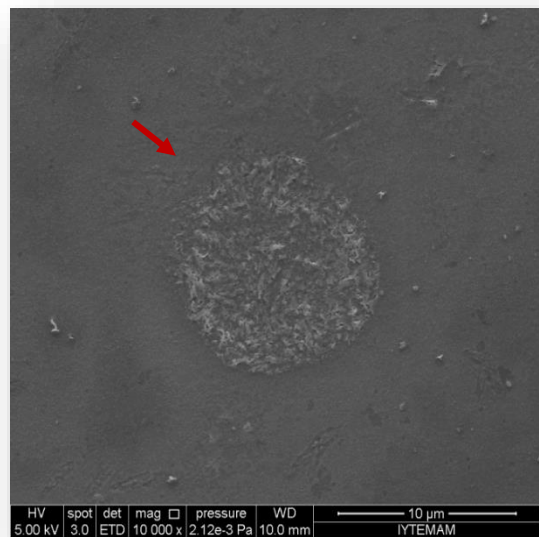
(d) Ap L200 ppm

Figure 5.17. The SEM images of *A.pullulans* (Ap) cells after treatment with phenolic compounds (T: tyrosol, HT: hydroxytyrosol, L: luteolin) in the concentration of 200 ppm (MAG= x10.000)

5.3. Conclusions

In the last part of this thesis study, two yeast species including *S. cerevisiae,* as a model and a "wine yeast" and *A. pullulans,* as the most common yeast identified from both harvest years of olive samples were selected to investigate the antimicrobial effects induced by olive phenolic compounds, including tyrosol, hydroxytyrosol, oleuropein, luteolin and apigenin using FTIR spectroscopy, besides absorbance measurements with microplate reader, yeast colony count and microscope images.

As a result, all phenolic compounds were found effective on both yeasts. While 200 ppm and higher concentrations were more effective; effects of lower levels depend on the types of phenolic compounds. In general, *A. pullulans* was found more sensitive to all phenolics than *S. cerevisiae.*

FTIR spectroscopy analysis have similar results with absorbance measurements and yeast colony count. According to FTIR spectral data, the biggest changes were observed in DNA fingerprint region for all phenolics. In addition, carbohydrate (associated with changes in cell wall or cell membrane) and amide (associated with protein degradation involving the cell wall) regions are the most affected parts. Changes in carbohydrate region generally includes the disappearance of carbohydrate peaks. It might be due to the complex formation between phenol and carbohydrate and it is more distinct for *S. cerevisiae.* The microscope results indicated that all phenolics caused significant morphological changes and damages on the cell wall included disruption and deformation of the cell wall. Therefore, it was concluded that FTIR spectroscopy could successfully be used to monitor and characterize antimicrobial activity of phenolic compounds on yeasts as complementary to microbiological methods.

CHAPTER 6

CONCLUSION

For *wine* analysis; it is possible to differentiate various grape/wine yeasts, even the same yeast originated from different sources, using FTIR spectroscopy with both sample preparation method, as newly-developed and well-known procedure. The main difference between two methods might arise from DNA fingerprint region. Since FTIR spectroscopy with multivariate statistical analysis gives parallel results with molecular analysis, it could be concluded that FTIR can be used with both sample preparation method for differentiation of wine yeasts during whole wine process, complementary with molecular and cultural methods. As a future study, wine fermentation process could be investigated for multiple years to increase the number of samples and so isolated yeasts from grape to wine and enlarge yeast database for FTIR.

For *olive* analysis; molecular tests revealed that Hurma olives of two harvest years have in common only for the yeast Aureobasidium sp. So, if there would be any link between natural debittering of Hurma olives and the yeast population of this olive type this could involve Aureobasidium sp. It is possible to see spectral differences between different yeasts originated from various olive samples including "Hurma" and isolated from different harvest years and differentiate them, using FTIR spectroscopy with both sample preparation method. However newly-developed procedure based on directly using of yeast cells for FTIR spectroscopy without any drying step provides <u>more scattered results</u> compared with well known procedure. Since chemometric analyses were in parallel with DNA-based methods it could be concluded that FTIR can be used as a complementary method for molecular analysis and need to be improved by adding more yeasts to its reference library. As a future study, enzymatic activity (β-glucosidase) of isolated yeasts from Hurma olives, especially *Aureobasidium sp.* could be investigated to understand their role in debittering process.

For *antimicrobial activity* studies; FTIR spectroscopy have similar results with absorbance measurements and yeast colony count. According to FTIR spectral data, the biggest changes were observed in DNA fingerprint region, carbohydrate region which is associated with changes in cell wall or cell membrane and amide region which is related

with protein degradation involving the cell wall. The microscope investigation results also confirmed the results of FTIR spectroscopy for both yeasts as *S. cerevisiae* and *A. pullulans*. Therefore, FTIR spectroscopy could successfully be used to monitor and characterize antimicrobial activity of phenolic compounds on yeasts as complementary to microbiological methods. As a future study, the mechanism of chemical changes in yeast cells by phenolics according to FTIR spectra could be studied in more detail.

REFERENCES

Aktaş, A. B. (2014a). Chemical characterization of 'hurma' olive grown in Karaburun Peninsula. Published master thesis, Izmir Institute of Technology, Izmir.

Aktas, A. B., Ozen, B., Tokatli, F., & Sen, I. (2014b). Phenolics profile of a naturally debittering olive in comparison to regular olive varieties. *Journal of the Science of Food and Agriculture*, 94(4), 691-698.

Al-Qadiri, H. M., Al-Alami, N. I., Al-Holy, M. A., & Rasco, B. A. (2008a). Using Fourier transform infrared (FT-IR) absorbance spectroscopy and multivariate analysis to study the effect of chlorine-induced bacterial injury in water. *Journal of agricultural and food Chemistry*, 56(19), 8992-8997.

Al-Qadiri, H. M., Lin, M., Al-Holy, M. A., Cavinato, A. G., & Rasco, B. A. (2008b). Detection of Sublethal Thermal Injury in Salmonella enterica Serotype Typhimurium and Listeria monocytogenes Using Fourier Transform Infrared (FT-IR) Spectroscopy (4000 to 600 cm− 1*). Journal of food science*, 73(2), M54-M61.

Alvarez-Ordonez, A., Halisch, J., & Prieto, M. (2010). Changes in Fourier transform infrared spectra of< i> Salmonella enterica</i> serovars Typhimurium and Enteritidis after adaptation to stressful growth conditions. *International journal of food microbiology*, 142(1), 97-105.

Alvarez-Ordonez, A., Mouwen, D. J. M., Lopez, M., & Prieto, M. (2011). Fourier transform infrared spectroscopy as a tool to characterize molecular composition and stress response in foodborne pathogenic bacteria. *Journal of microbiological methods*, 84(3), 369-378.

Alves, M., Gonçalves, T., & Quintas, C. (2012). Microbial quality and yeast population dynamics in cracked green table olives' fermentations. *Food Control*, *23*(2), 363-368.

Ami, D., Natalello, A., Schultz, T., Gatti-Lafranconi, P., Lotti, M., Doglia, S. M., & De Marco, A. (2009). Effects of recombinant protein misfolding and aggregation on bacterial membranes. *Biochimica et Biophysica Acta (BBA)-Proteins and Proteomics*, 1794(2), 263-269.

Aponte, M., Ventorino, V., Blaiotta, G., Volpe, G., Farina, V., Avellone, G., ... & Moschetti, G. (2010). Study of green Sicilian table olive fermentations through microbiological, chemical and sensory analyses. *Food microbiology*,*27*(1), 162-170.

Arias, C. R., Burns, J. K., Friedrich, L. M., Goodrich, R. M., & Parish, M. E. (2002). Yeast species associated with orange juice: evaluation of different identification methods. *Applied and Environmental Microbiology*, *68*(4), 1955-1961.

Arroyo-López, F. N., Duran-Quintana, M. C., Ruiz-Barba, J. L., Querol, A., & Garrido-Fernández, A. (2006). Use of molecular methods for the identification of yeast associated with table olives. *Food microbiology*, *23*(8), 791-796.

Arroyo-López, F. N., Querol, A., Bautista-Gallego, J., & Garrido-Fernandez, A. (2008). Role of yeasts in table olive production. *International Journal of Food Microbiology*, *128*(2), 189-196.

Arroyo-López, F. N., Bautista-Gallego, J., Domínguez-Manzano, J., Romero-Gil, V., Rodriguez-Gómez, F., García-García, P., & Jiménez-Díaz, R. (2012). Formation of lactic acid bacteria–yeasts communities on the olive surface during Spanish-style Manzanilla fermentations. *Food microbiology*,*32*(2), 295-301.

Barata, A., Malfeito-Ferreira, M., & Loureiro, V. (2012). The microbial ecology of wine grape berries. *International journal of food microbiology*, 153(3), 243-259.

Barnett, J. A., Payne, R. W., & Yarrow, D. Yeasts: characteristics and identification, 1990.

Baum, D. (2008). Reading a phylogenetic tree: The meaning of monophyletic groups. *Nature Education*, *1*(1), 190.

Bautista-Gallego, J., Rodríguez-Gómez, F., Barrio, E., Querol, A., Garrido-Fernández, A., & Arroyo-López, F. N. (2011). Exploring the yeast biodiversity of green table olive industrial fermentations for technological applications.*International journal of food microbiology*, *147*(2), 89-96.

Bendini, A., Cerretani, L., Carrasco-Pancorbo, A., Gómez-Caravaca, A. M., Segura-Carretero, A., Fernández-Gutiérrez, A., & Lercker, G. (2007). Phenolic molecules in virgin olive oils: a survey of their sensory properties, health effects, antioxidant activity and analytical methods. An overview of the last decade Alessandra. *Molecules*, *12*(8), 1679-1719.

Bisignano, G., Tomaino, A., Cascio, R. L., Crisafi, G., Uccella, N., & Saija, A. (1999). On the in-vitro antimicrobial activity of oleuropein and hydroxytyrosol. *Journal of pharmacy and pharmacology*, 51(8), 971-974.

Borcakli, M., Özay, G., Alperden, I., Özsan, E., & Erdek, Y. (1993). Changes in chemical and microbiological composition of two varieties of olive during fermentation. *Grasas y Aceites*, *44*(4-5), 253-258.

Boskou, G., Salta, F. N., Chrysostomou, S., Mylona, A., Chiou, A., & Andrikopoulos, N. K. (2006). Antioxidant capacity and phenolic profile of table olives from the Greek market. *Food Chemistry*, 94(4), 558-564.

Brereton, R. G. (2003). Chemometrics Data Analysis for the Laboratory and Chemical Plant. UK: John Wiley & Sons Ltd.

Breuer, U., & Harms, H. (2006). Debaryomyces hansenii—an extremophilic yeast with biotechnological potential. *Yeast*, 23(6), 415-437.

Buratti, S., Ballabio, D., Giovanelli, G., Dominguez, C. Z., Moles, A., Benedetti, S., & Sinelli, N. (2011). Monitoring of alcoholic fermentation using near infrared and mid infrared spectroscopies combined with electronic nose and electronic tongue. *Analytica chimica acta*, *697*(1), 67-74.

Büchl, N. R., Wenning, M., Seiler, H., Mietke-Hofmann, H., & Scherer, S. (2008). Reliable identification of closely related Issatchenkia and Pichia species using artificial neural network analysis of Fourier-transform infrared spectra. *Yeast*, *25*(11), 787-798.

Cai, J., Roberts, I. N., & Collins, M. D. (1996). Phylogenetic relationships among members of the ascomycetous yeast genera Brettanomyces, Debaryomyces, Dekkera, and Kluyveromyces deduced by small-subunit rRNA gene sequences. *International journal of systematic bacteriology*, *46*(2), 542-549.

Campaniello, D., Bevilacqua, A., D'Amato, D., Corbo, M. R., Altieri, C., & Sinigaglia, M. (2005). Microbial characterization of table olives processed according to Spanish and natural styles. *Food Technology and Biotechnology*,*43*(3), 289-294.

Canal, C., & Ozen, B. (2015). Monitoring of Wine Process and Prediction of Its Parameters with Mid-Infrared Spectroscopy. *Journal of Food Process Engineering*.

Chen, Y. C., Eisner, J. D., Kattar, M. M., Rassoulian-Barrett, S. L., Lafe, K., Bui, U., & Cookson, B. T. (2001). Polymorphic internal transcribed spacer region 1 DNA sequences identify medically important yeasts. *Journal of Clinical Microbiology*, 39(11), 4042-4051.

Ciafardini, G., & Zullo, B. A. (2000). β-Glucosidase activity in olive brine during the microbiological debittering process. *Advances in food sciences*, *22*(3-4), 69-76.

Cocolin, L., Bisson, L. F., & Mills, D. A. (2000). Direct profiling of the yeast dynamics in wine fermentations. *FEMS Microbiology Letters*, *189*(1), 81-87.

Cohen, Z. & Ratledge, C. (2005). Single Cell Oils. Champaign, IL: AOCS Press.

Corte, L., Rellini, P., Roscini, L., Fatichenti, F., & Cardinali, G. (2010). Development of a novel, FTIR (Fourier transform infrared spectroscopy) based, yeast bioassay for toxicity testing and stress response study. *Analytica chimica acta*, 659(1), 258-265.

Corte, L., Tiecco, M., Roscini, L., Germani, R., & Cardinali, G. (2014). FTIR analysis of the metabolomic stress response induced by N-alkyltropinium bromide surfactants in the yeasts Saccharomyces cerevisiae and Candida albicans. Colloids and Surfaces B: Biointerfaces, 116, 761-771.

Coton, E., Coton, M., Levert, D., Casaregola, S., & Sohier, D. (2006). Yeast ecology in French cider and black olive natural fermentations. *International journal of food microbiology*, *108*(1), 130-135.

Cozzolino, D., Cynkar, W. U., Shah, N., Dambergs, R. G., & Smith, P. A. (2009). A brief introduction to multivariate methods in grape and wine analysis. *International Journal of Wine Research*, 1, 123-130.

Desnos-Ollivier, M., Ragon, M., Robert, V., Raoux, D., Gantier, J. C., & Dromer, F. (2008). Debaryomyces hansenii (Candida famata), a rare human fungal pathogen often misidentified as Pichia guilliermondii (Candida guilliermondii). *Journal of clinical microbiology*, 46(10), 3237-3242.

Di Egidio, V., Sinelli, N., Giovanelli, G., Moles, A., & Casiraghi, E. (2010). NIR and MIR spectroscopy as rapid methods to monitor red wine fermentation.*European Food Research and Technology*, *230*(6), 947-955.

Dufour, M., Simmonds, R. S., & Bremer, P. J. (2003). Development of a method to quantify in vitro the synergistic activity of "natural" antimicrobials. *International journal of food microbiology*, 85(3), 249-258.

Embong, Z., Hitam, W. H. W., Yean, C. Y., Rashid, N. H., Kamarudin, B., Abidin, S. K., ... & Ravichandran, M. (2008). Specific detection of fungal pathogens by 18S rRNA gene PCR in microbial keratitis. BMC ophthalmology, 8(1), 7.

Essendoubi, M., Toubas, D., Bouzaggou, M., Pinon, J. M., Manfait, M., & Sockalingum, G. D. (2005). Rapid identification of Candida species by FT-IR microspectroscopy. *Biochimica et Biophysica Acta (BBA)-General Subjects*, 1724(3), 239-247.

Eriksson, L., Byrne, T., Johansson, E., Trygg, J., & Vikström, C. (2013). *Multi-and megavariate data analysis basic principles and applications*. Umetrics Academy.

Essendoubi, M., Toubas, D., Lepouse, C., Leon, A., Bourgeade, F., Pinon, J. M., ... & Sockalingum, G. D. (2007). Epidemiological investigation and typing of Candida

glabrata clinical isolates by FTIR spectroscopy. *Journal of microbiological methods*, 71(3), 325-331.

Esteve-Zarzoso, B., Belloch, C., Uruburu, F., & Querol, A. (1999). Identification of yeasts by RFLP analysis of the 5.8 S rRNA gene and the two ribosomal internal transcribed spacers. *International Journal of Systematic Bacteriology*,*49*(1), 329-337.

Fernández, A. G., Fernandez-Diez, M. J., & Adams, M. R. (1997). *Table olives: production and processing*. Springer Science & Business Media.

Garcia-Martos, P., Dominguez, I., Marin, P., Linares, M., Mira, J., & Calap, J. (1999). [Onychomycoses caused by non-dermatophytic filamentous fungi in Cadiz]. *Enfermedades infecciosas y microbiologia clinica*, *18*(7), 319-324.

Granchi, L., Bosco, M., Messini, A., & Vincenzini, M. (1999). Rapid detection and quantification of yeast species during spontaneous wine fermentation by PCR–RFLP analysis of the rDNA ITS region. *Journal of Applied Microbiology*,*87*(6), 949-956.

Gümüş, S. G., & Gümüş, A. H. (2009). The problems of the wine sector in Turkey during the EU accession process. *Ege Üniversitesi Ziraat Fakültesi Dergisi*, *46*(1), 43-51.

Helm, D., Labischinski, H., Schallehn, G., & Naumann, D. (1991). Classification and identification of bacteria by Fourier-transform infrared spectroscopy. *Journal of general microbiology*, *137*(1), 69-79.

Henderson, D. O., Mu, R., & Gunasekaran, M. (1995). A rapid method for the identification of Candida at the species level by Fourier transform infrared spectroscopy. *Biomedical Letters*, 223-228.

Hernandez, A., Martín, A., Aranda, E., Pérez-Nevado, F., & Córdoba, M. G. (2007). Identification and characterization of yeast isolated from the elaboration of seasoned green table olives. *Food microbiology*, *24*(4), 346-351.

Himmelreich, U., Somorjai, R. L., Dolenko, B., Lee, O. C., Daniel, H. M., Murray, R., & Sorrell, T. C. (2003). Rapid identification of Candida species by using nuclear magnetic resonance spectroscopy and a statistical classification strategy. *Applied and environmental microbiology*, 69(8), 4566-4574.

Hoffman, C. S., & Winston, F. (1987). A ten-minute DNA preparation from yeast efficiently releases autonomous plasmids for transformaion of Escherichia coli. Gene, 57(2), 267-272.

https://www.studyblue.com

http://www.ebi.ac.uk/Tools/msa/clustalo/

http://www.ncbi.nlm.nih.gov/BLAST/

Hui, Y. H., & Evranuz, E. Ö. (Eds.). (2012). *Handbook of Plant-based fermented food and beverage technology*. CRC Press.

Hurtado, A., Reguant, C., Esteve-Zarzoso, B., Bordons, A., & Rozès, N. (2008). Microbial population dynamics during the processing of Arbequina table olives. *Food Research International*, *41*(7), 738-744.

IOC, 2015. http://www.internationaloliveoil.org/news/view/666-year-2014-news/518-market-newsletter-june-2014. Retrived, Octorber, 2015.

Jemai, H., Bouaziz, M., & Sayadi, S. (2009). Phenolic composition, sugar contents and antioxidant activity of Tunisian sweet olive cultivar with regard to fruit ripening. *Journal of agricultural and food chemistry*, 57(7), 2961-2968.

Kailis, S., & Harris, D. J. (2007). *Producing table olives*. Landlinks press.

Kalogereas, S. A. (1932). Table olives.

Karaosmanoğlu, H. (2009). Antimicrobial and antioxidant activities of Turkish extra virgin olive oil from different varieties.

Kotzekidou, P. (1997). Heat resistance of Byssochlamys nivea, Byssochlamys fulva and Neosartorya fischeri isolated from canned tomato paste. *Journal of Food Science*, *62*(2), 410-412.

Kurtzman, C., & Fell, J. W. (Eds.). (1998). *The Yeasts-A Taxonomic Study*. Elsevier.

Kurtzman, C. P., & Fell, J. W. (2006). Yeast systematics and phylogeny—implications of molecular identification methods for studies in ecology. In *Biodiversity and Ecophysiology of Yeasts* (pp. 11-30). Springer Berlin Heidelberg.

Kurtzman, C., Fell, J. W., & Boekhout, T. (Eds.). (2011). *The yeasts: a taxonomic study* (Vol. 1). Elsevier.

Kurtzman, C. P., & Robnett, C. J. (1998). Identification of clinically important ascomycetous yeasts based on nucleotide divergence in the 5'end of the large-subunit (26S) ribosomal DNA gene. *Journal of Clinical Microbiology*, 35(5), 1216-1223.

Kümmerle, M., Scherer, S., & Seiler, H. (1998). Rapid and reliable identification of food-borne yeasts by Fourier-transform infrared spectroscopy. *Applied and environmental microbiology*, 64(6), 2207-2214.

Lanciotti, R., Gianotti, A., Baldi, D., Angrisani, R., Suzzi, G., Mastrocola, D., & Guerzoni, M. E. (2005). Use of Yarrowia lipolytica strains for the treatment of olive mill wastewater. *Bioresource Technology*, *96*(3), 317-322.

Lee, O. H., Lee, B. Y., Lee, J., Lee, H. B., Son, J. Y., Park, C. S., & Kim, Y. C. (2009). Assessment of phenolics-enriched extract and fractions of olive leaves and their antioxidant activities. *Bioresource technology*, *100*(23), 6107-6113.

Lee, O. H., & Lee, B. Y. (2010). Antioxidant and antimicrobial activities of individual and combined phenolics in Olea europaea leaf extract. Bioresource technology, 101(10), 3751-3754.

Lerma-García, M. J., Ramis-Ramos, G., Herrero-Martínez, J. M., & Simó-Alfonso, E. F. (2010). Authentication of extra virgin olive oils by Fourier-transform infrared spectroscopy. *Food Chemistry*, *118*(1), 78-83.

Libkind, D., Gadanho, M., van Broock, M., & Sampaio, J. P. (2005). Sporidiobolus longiusculus sp. nov. and Sporobolomyces patagonicus sp. nov., novel yeasts of the Sporidiobolales isolated from aquatic environments in Patagonia, Argentina. *International journal of systematic and evolutionary microbiology*, 55(1), 503-509.

Looder J., (1970). Criteria and Methods Used in Classification in the Yeast. A Taxonomic Study, North-Holland, Amsterdam.

Malacrino, P., Tosi, E., Caramia, G., Prisco, R., & Zapparoli, G. (2005). The vinification of partially dried grapes: a comparative fermentation study of Saccharomyces cerevisiae strains under high sugar stress. *Letters in applied microbiology*, 40(6), 466-472.

Maquelin, K., Kirschner, C., Choo-Smith, L. P., Ngo-Thi, N. A., Van Vreeswijk, T., Stämmler, M.,& Puppels, G. J. (2003). Prospective study of the performance of vibrational spectroscopies for rapid identification of bacterial and fungal pathogens recovered from blood cultures. *Journal of clinical microbiology*, 41(1), 324-329.

Maresova, L., & Sychrova, H. (2007). Applications of a microplate reader in yeast physiology research. *Biotechniques*, 43(5), 667-672.

Marquina, D., Peres, C., Caldas, F. V., Marques, J. F., Peinado, J. M., & Spencer-Martins, I. (1992). Characterization of the yeast population in olive brines. *Letters in Applied Microbiology*, *14*(6), 279-283.

Materassi, R., Miclaus, N., & Pelagatti, O. (1975). Research into the ability of yeast to hydrolize oleuropein. *Annali dell'Istituto Sperimentale per l'Elaiotecnica, Pescara (Italy).*

Mills, D. A., Johannsen, E. A., & Cocolin, L. (2002). Yeast diversity and persistence in botrytis-affected wine fermentations. *Applied and environmental microbiology*, 68(10), 4884-4893.

Moreira, J. L., & Santos, L. (2004). Spectroscopic interferences in Fourier transform infrared wine analysis. *Analytica chimica acta*, *513*(1), 263-268.

Naumann, D., Helm, D., & Labischinski, H. (1991). Microbiological characterizations by FT-IR spectroscopy. *Nature*, *351*(6321), 81-82.

Lasch, P., & Naumann, D. (2000). Infrared spectroscopy in microbiology. *Encyclopedia of analytical chemistry.*

Ngo-Thi, N. A., Kirschner, C., & Naumann, D. (2003). Characterization and identification of microorganisms by FT-IR microspectrometry. *Journal of Molecular Structure*, 661, 371-380.

Nisiotou, A. A., Chorianopoulos, N., Nychas, G. J., & Panagou, E. Z. (2010). Yeast heterogeneity during spontaneous fermentation of black Conservolea olives in different brine solutions. *Journal of applied microbiology*, *108*(2), 396-405.

Oberreuter, H., Mertens, F., Seiler, H., & Scherer, S. (2000). Quantification of micro-organisms in binary mixed populations by Fourier transform infrared (FT-IR) spectroscopy. *Letters in applied microbiology*, 30(1), 85-89.

Oelofse, A., Malherbe, S., Pretorius, I. S., & Du Toit, M. (2010). Preliminary evaluation of infrared spectroscopy for the differentiation of Brettanomyces bruxellensis strains isolated from red wines. *International journal of food microbiology*, 143(3), 136-142.

OIV. (2009). International Methods of Analysis of Wines and Musts.

Oliveira, M., Brito, D., Catulo, L., Leitão, F., Gomes, L., Silva, S., ... & Peres, C. (2004). Biotechnology of olive fermentation of 'Galega'Portuguese variety.*Grasas y aceites*, *55*(3), 219-226.

Pereira, A. P., Ferreira, I. C., Marcelino, F., Valentão, P., Andrade, P. B., Seabra, R., & Pereira, J. A. (2007). Phenolic compounds and antimicrobial activity of olive (Olea europaea L. Cv. Cobrançosa) leaves. *Molecules*, 12(5), 1153-1162.

Pincus, D. H., Salkin, I. F., Hurd, N. J., Levy, I. L., & Kemna, M. A. (1988). Modification of potassium nitrate assimilation test for identification of clinically important yeasts. *Journal of clinical microbiology*, 26(2), 366-368.

Puxeu, M., Andorra, I., & De Lamo-Castellví, S. (2015). Monitoring Saccharomyces cerevisiae Grape Must Fermentation Process by Attenuated Total Reflectance Spectroscopy. *Food and Bioprocess Technology*, 8(3), 637-646.

Querol, A., Barrio, E., Huerta, T., & Ramón, D. (1992). Molecular monitoring of wine fermentations conducted by active dry yeast strains. *Applied and Environmental Microbiology*, 58(9), 2948-2953.

Sabate, J., Cano, J., Esteve-Zarzoso, B., & Guillamón, J. M. (2002). Isolation and identification of yeasts associated with vineyard and winery by RFLP analysis of ribosomal genes and mitochondrial DNA. *Microbiological research*, 157(4), 267-274.

Saharan, R. K., & Sharma, S. C. (2011). FTIR spectroscopy and biochemical investigation of ethanol stressed yeast Pachysolen tannophilus. *Vibrational Spectroscopy*, 55(1), 85-89.

Saiki, R. K., Gelfand, D. H., Stoffel, S., Scharf, S. J., Higuchi, R., Horn, G. T., ... & Erlich, H. A. (1988). Primer-directed enzymatic amplification of DNA with a thermostable DNA polymerase. *Science*, 239(4839), 487-491.

Santos, C., Fraga, M. E., Kozakiewicz, Z., & Lima, N. (2010). Fourier transform infrared as a powerful technique for the identification and characterization of filamentous fungi and yeasts. *Research in microbiology*, 161(2), 168-175.

Schleicher, E., Heßling, B., Illarionova, V., Bacher, A., Weber, S., Richter, G., & Gerwert, K. (2005). Light-induced reactions of Escherichia coli DNA photolyase monitored by Fourier transform infrared spectroscopy. *FEBS Journal*, 272(8), 1855-1866.

Schütz, M., & Gafner, J. (1993). Analysis of yeast diversity during spontaneous and induced alcoholic fermentations. *Journal of Applied Bacteriology*, 75(6), 551-558.

Sen, I., & Tokatli, F. (2014). Authenticity of wines made with economically important grape varieties grown in Anatolia by their phenolic profiles. *Food Control*, 46, 446-454.

Serban, S., Danet, A. F., & El Murr, N. (2004). Rapid and sensitive automated method for glucose monitoring in wine processing. *Journal of agricultural and food chemistry*, *52*(18), 5588-5592.

Sibbett, G. S., & Ferguson, L. (2005). *Olive production manual* (Vol. 3353). UCANR Publications.

Simopoulos, A. P. (2001). The Mediterranean diets: What is so special about the diet of Greece? The scientific evidence. *The Journal of nutrition*, 131(11), 3065S-3073S.

Sipiczki, M. (2003). Candida zemplinina sp. nov., an osmotolerant and psychrotolerant yeast that ferments sweet botrytized wines. *International journal of systematic and evolutionary microbiology*, 53(6), 2079-2083.

Skotti, E., Kountouri, S., Bouchagier, P., Tsitsigiannis, D. I., Polissiou, M., & Tarantilis, P. A. (2014). FTIR spectroscopic evaluation of changes in the cellular biochemical composition of the phytopathogenic fungus Alternaria alternata induced by extracts of some Greek medicinal and aromatic plants. *Spectrochimica Acta Part A: Molecular and Biomolecular Spectroscopy*, 127, 463-472.

Sockalingum, G. D., Bouhedja, W., Pina, P., Allouch, P., Mandray, C., Labia, R., ... & Manfait, M. (1997). ATR–FTIR Spectroscopic Investigation of Imipenem-Susceptible and-ResistantPseudomonas aeruginosaIsogenic Strains. *Biochemical and biophysical research communications*, 232(1), 240-246.

Subramanian, A., Ahn, J., Balasubramaniam, V. M., & Rodriguez-Saona, L. (2007). Monitoring biochemical changes in bacterial spore during thermal and pressure-assisted thermal processing using FT-IR spectroscopy. *Journal of agricultural and food chemistry*, 55(22), 9311-9317.

Thi, N. N., & Naumann, D. (2007). Investigating the heterogeneity of cell growth in microbial colonies by FTIR microspectroscopy. *Analytical and bioanalytical chemistry*, *387*(5), 1769-1777.

Timmins, E. M., Quain, D. E., & Goodacre, R. (1998). Differentiation of brewing yeast strains by pyrolysis mass spectrometry and Fourier transform infrared spectroscopy. *Yeast*, 14(10), 885-893.

Tofalo, R., Chaves-López, C., Di Fabio, F., Schirone, M., Felis, G. E., Torriani, S., ... & Suzzi, G. (2009). Molecular identification and osmotolerant profile of wine yeasts that ferment a high sugar grape must. *International journal of food microbiology*, 130(3), 179-187.

Turkish Food Codex. (2008a). Communication of Wine (Vol. 2008/67)

Udelhoven, T., Naumann, D., & Schmitt, J. (2000). Development of a hierarchical classification system with artificial neural networks and FT-IR spectra for the identification of bacteria. *Applied Spectroscopy*, 54(10), 1471-1479.

Urtubia, A., Pérez-Correa, J. R., Meurens, M., & Agosin, E. (2004). Monitoring large scale wine fermentations with infrared spectroscopy. *Talanta*, *64*(3), 778-784.

Wenning, M., Seiler, H., & Scherer, S. (2002). Fourier-transform infrared microspectroscopy, a novel and rapid tool for identification of yeasts. *Applied and environmental microbiology*, 68(10), 4717-4721.

Wenning, M., & Scherer, S. (2013). Identification of microorganisms by FTIR spectroscopy: perspectives and limitations of the method. *Applied microbiology and biotechnology*, 97(16), 7111-7120.

Vaughn, R. H., Stevenson, K. E., Davé, B. A., & Park, H. C. (1972). Fermenting yeasts associated with softening and gas-pocket formation in olives. *Applied microbiology*, *23*(2), 316-320.

Vierstraete, A. (1999). Principle of the PCR. *University of Ghent, Belgium.*

Zalar, P., Gostinčar, C., De Hoog, G. S., Uršič, V., Sudhadham, M., & Gunde-Cimerman, N. (2008). Redefinition of Aureobasidium pullulans and its varieties. *Studies in Mycology*, 61, 21-38.

Zoidou, E., Melliou, E., Gikas, E., Tsarbopoulos, A., Magiatis, P., & Skaltsounis, A. L. (2009). Identification of Throuba Thassos, a traditional Greek table olive variety, as a nutritional rich source of oleuropein. *Journal of agricultural and food chemistry*, *58*(1), 46-50.

Zoumpopoulou, G., Papadimitriou, K., Polissiou, M. G., Tarantilis, P. A., & Tsakalidou, E. (2010). Detection of changes in the cellular composition of Salmonella enterica serovar Typhimurium in the presence of antimicrobial compound (s) of Lactobacillus strains using Fourier transform infrared spectroscopy. *International journal of food microbiology*, *144*(1), 202-207.

APPENDIX A

MORPHOLOGICAL AND CULTURAL TEST RESULTS OF WINE YEASTS

Table A.1.The results of *macroscopic* morphological analysis of wine yeasts

Yeast code	Wine source-Sampling time*	Growth in Liquid Culture				Growth in Solid Media				
		Film formation	*Haze*	*Sediment (fine/coarse)*	*Suspended particle*	*Colony texture (dull/shiny)*	*Colony shape (convex/concave)*	*Colony border (smooth/rough)*	*Colony color*	*Colony size (mm)*
1	Syrah-I	-	+	fine	-	shiny	convex	smooth	white	1
2	Sangiovese-I	-	+	fine	-	shiny	convex	smooth	light pink	3
3	Muscat-I	+	+	coarse	+	dull	-	smooth	white	3
4	Chardonnay-II	-	-	coarse	+	shiny	convex	smooth	white	2
5	Sangiovese-II	-	+	coarse	+	shiny	convex	smooth	white	2
6	Muscat-III	-	+	coarse	+	shiny	convex	smooth	white	2
7	Merlot-III	-	+	coarse	-	shiny	convex	smooth	white	2
8	Cabernet-II	-	-	fine	-	shiny	convex	smooth	white	2
9	Sangiovese-IV	-	-	fine	-	shiny	convex	smooth	white	2
10	Merlot-I	-	-	fine	-	shiny	-	smooth	white	2
11	Boğazkere-II	-	+	fine	-	shiny	convex	smooth	white	2
12	Chardonnay-III	-	+	fine	-	shiny	convex	smooth	white	1
13	Syrah-III	-	+	coarse	+	shiny	convex	smooth	white	2
14	Merlot-I	+	+	coarse	+	dull	-	rough	white	2
15	Merlot-IV	-	+	coarse	+	shiny	convex	smooth	white	2
16	Cabernet-III	-	+	coarse	+	shiny	convex	smooth	white	1
17	Boğazkere-II	-	+	coarse	+	shiny	convex	smooth	white	1
18	Syrah-I	+	+	coarse	+	dull	-	rough	white	2
19	Cabernet-I	-	+	fine	-	shiny	convex	smooth	white	2

Table A.2.The results of *microscopic* morphological analysis of wine yeasts

Yeast code	Wine source-Sampling time	Cell Shape	Cell Size (μm)	Form of asexual reproduction	Sporulation on McClary acetate agar	Sporulation on Gorodkowa agar
1	Syrah-I	ovoid	4,86	polar budding	-	-
2	Sangiovese-I	ovoid	3,67	polar budding	-	-
3	Muscat-I	ovoid	5,41	fussion	+	-
4	Chardonnay-II	ovoid	6,04	polar budding	-	-
5	Sangiovese-II	ovoid	6,37	polar budding	-	-
6	Muscat-III	ovoid	6,25	polar budding	+	-
7	Merlot-III	ovoid	7,02	polar budding	-	-
8	Cabernet-II	spherical	6,65	polar budding	-	-
9	Sangiovese-IV	spherical	5,93	polar budding	-	-
10	Merlot-I	lemon shaped	6,13	bipolar budding	-	-
11	Boğazkere-II	ovoid	6,77	fussion	-	-
12	Chardonnay-III	ovoid	5,4	polar budding	-	-
13	Syrah-III	ovoid	4,83	polar budding	-	-
14	Merlot-I	ovoid	4,27	polar budding	-	-
15	Merlot-IV	ovoid	7,66	polar budding	+	+
16	Cabernet-III	ovoid	6,21	polar budding	-	-
17	Boğazkere-II	ovoid	7,93	polar budding	-	-
18	Syrah-I	ovoid	5,37	fussion	-	-
19	Cabernet-I	ovoid	5,74	fussion	-	-

Table A.3.Cultural test results of wine yeasts

Yeast code	Wine source-Sampling time	API 20 C AUX: Carbohydrate Assimilation Test																			Nitrogen Assimilation	Durham
		D-GLUcose	GLYcerol	calcium 2-Keto-Gluconate	L-ARAbinose	D-XYLose	ADOnitol	XyLiTol	D-GALactose	INOsitol	D-SORbitol	Methyl-αD-Glucopyranoside	N-Acetyl-Glucosamine	D-CELlobiose	D-LACtose	D-MALtose	D-SACcharose (sucrose)	D-TREhalose	D-MeLeZitose	D-RAFfinose		
1	Syrah-I	+	+	+	-	-	+	+	+	-	+	+	+	+	-	+	+	+	+	-	-	+
2	Sangiovese-I	+	+	+	-	-	+	+	+	-	+	+	+	+	-	+	+	-	+	-	-	+
3	Muscat-I	+	-	-	-	-	-	-	-	-	-	-	-	-	-	-	-	-	-	-	-	+
4	Chardonnay-II	+	-	-	-	-	-	-	+	-	+	+	-	-	-	+	+	-	+	+	-	+
5	Sangiovese-II	+	-	-	-	-	-	-	+	-	-	-	-	-	-	+	+	+	+	+	-	-
6	Muscat-III	+	+	-	-	-	-	-	+	-	-	-	-	-	-	+	+	-	-	+	-	-
7	Merlot-III	+	-	-	-	-	-	-	+	-	-	-	-	-	-	+	+	-	-	+	-	+
8	Cabernet-II	+	-	-	-	-	-	-	-	-	-	-	-	-	-	+	+	-	-	+	+	+
9	Sangiovese-IV	+	-	-	-	-	-	-	-	-	-	-	-	-	-	+	+	+	+	+	-	+
10	Merlot-I	+	-	+	-	-	-	-	-	-	-	-	-	+	-	-	-	-	-	-	-	+
11	Boğazkere-II	+	+	-	-	-	-	-	-	-	-	-	-	-	-	+	+	+	+	+	-	+
12	Chardonnay-III	+	+	-	-	-	-	-	+	-	+	+	-	-	-	+	+	+	+	+	-	+
13	Syrah-III	+	-	-	-	-	-	-	+	-	-	-	-	-	-	+	+	-	-	+	+	+
14	Merlot-I	+	-	-	-	-	-	-	-	-	-	-	-	-	-	-	-	-	-	-	+	+
15	Merlot-IV	+	-	-	-	-	-	-	+	-	-	+	-	-	-	+	+	-	-	+	-	+
16	Cabernet-III	+	-	-	-	-	-	-	+	-	-	+	-	-	-	+	+	-	-	+	-	+
17	Boğazkere-II	+	-	-	-	-	-	-	+	-	-	-	-	-	-	+	+	-	-	+	-	+
18	Syrah-I	+	-	-	-	-	-	-	-	-	-	-	-	-	-	-	-	-	-	+	-	+
19	Cabernet-I	+	-	-	-	-	-	-	-	-	-	-	-	-	-	+	+	-	-	+	-	+

APPENDIX B

YEAST IDENTIFICATION KEY

1) Growth on Sabouraud's, malt agars or yeast nitrogen base with glucose agar […2]

2) a. Germ tubes produced [*Candida albicans* or *Candida dubliniensis*]
    b. No germ tubes produced […3]

3) a. Hyphae or pseudohyphae absent or scarce […4]
    b. Hyphae or pseudohyphae well developed […16]

4) a. Inositol assimilated (rarely negative), starch synthesized […5]
    b. Inositol not assimilated, starch not synthesized […9]

5) a. Nitrate assimilated […6]
    b. Nitrate not assimilated […7]

6) a. Sucrose assimilated [*Cryptococcus albidus*]
    b. Sucrose not assimilated [*Cryptococcus terreus*]

7) a. Lactose assimilated [*Cryptococcus laurentii*]
    b. Lactose not assimilated [….8]

8) a. Galacticol assimilated; melanin synthesized [*Cryptococcus neoformans*]
    b. Galacticol not assimilated; melanin not synthesized [*Cryptococcus unigunulatus*]

9) a. Cultures red or orange; nitrate not assimilated [*Rhodotorula mucilaginosa*]
    b. Cultures not red or orange; nitrate assimilated or not assimilated […10]

10) a. Nitrate assimilated […11]
    b. Nitrate not assimilated […12]

11) a. Methanol assimilated [*Pichia angusta*]
    b. Methanol not assimilated [*Pichia jadinii*]

12) a. Lactose assimilated [*Candida famata*]
    b. Lactose not assimilated […13]

13) a. D-Xylose and cellobiose assimilated (see also *C. famata* and *C. norvegensis*) [*Candida guilliermondii*)
    b. D-Xylose assimilated; cellobiose not assimilated […14]

14) a. Galacticol assimilated [*Candida haemulonii*]
    b. Galacticol not assimilated […15]

15) a. Raffinose assimilated and fermented [*Saccharomyces cerevisiae*]
    b. Raffinose neither assimilated nor fermented [*Candida glabrata* or *Candida norvegensis* (*Pichia norvegensis*)]

16) a. Arthroconidia produced […17]
    b. Arthroconidia not produced […22]

17) a. Diazonium Blue B (DBB) reaction positive […18]
    b. DBB reaction negative […19]

18) a. Nitrate assimilated [*Trichosporon pullulans*]
    b. Nitrate assimilated [*Trichosporon avoides* complex]

19) a. D-Xylose assimilated […20]
    b. D-Xylose not assimilated [*Geothricum capitatum*]

20) a. Cellobiose assimilated [*Geotrichu m fermentas*]
    b. Cellobiose not assimilated […21]

21) a. Arthroconidia in chains within primary filaments [*Galactomyces geotrichum*]
    b. Arthroconidia in branched chains arising on branches from primary filaments [*Geothrichum klebahnii*]

22) a. Lactose fermented [*Candida kefyr* (*Kluyveromyces marxianus*)]
    b. Lactose not fermented […23]

23) a. Raffinose and melibiose assimilated [*Candida guilliermondii*]
    b. Raffinose and melibiose not assimilated […24]

24) a. Trehalose assimilated […25]
    b. Trehalose not assimilated [*Candida krusei*]

25) a. Cellobiose assimilated […26]
    b. Cellobiose not assimilated […28]

26) a. L-rhamnose assimilated (rarely negative) [*Clavispora (Candida) lusitaniae*]
    b. L-rhamnose not assimilated [27]

27) a. Triphenyl Tetrazolium Chloride (TTC) reaction positive [*Candida tropicalis*]
    b. TTC) reaction negative to weak [*Candida viswanathii*]

28) a. Maltose fermented, TTC reaction positive or negative […29]
    b. Maltose not fermented, TTC reaction positive (rose to red color) [*Candida parapsilosis*]

29) a. Sucrose fermented, TTC reaction positive (deep maroon color) [*Candida tropicalis*]
    b. Sucrose not fermented, TTC reaction negative […30]

30) a. Maltose assimilated (repeat germ tube test) [*Candida albicans*]
    b. Maltose not assimilated [*Candida zeylanoides*]

APPENDIX C

MORPHOLOGICAL AND CULTURAL TEST RESULTS OF OLIVE YEASTS

Table C.1. The results of *macroscopic* morphological analysis of olive yeasts from 2011 harvest year

Yeast code*	Olive source**- Sampling week	Growth in Liquid Culture				Growth in Solid Media				
		Film formation	Haze	Sediment (fine/coarse)	Suspended particle	Colony texture (dull/shiny)	Colony shape (convex/concave)	Colony border (smooth/rough)	Colony color	Colony size (mm)
Cd1	HO-2	-	+	fine	-	shiny	convex	smooth	white	3
Cd2	HO-2	-	+	fine	-	shiny	convex	smooth	white	3
Dh1	HO-2	-	+	fine	-	shiny	convex	smooth	white	3
Dh2	HO-2	-	+	fine	-	shiny	convex	smooth	white	2
Dh3	HO-2	-	+	fine	-	shiny	convex	smooth	white	1
Dh4	HO-2	-	-	fine	-	shiny	convex	smooth	white	1
Cz1	HO-2	-	+	fine	+	shiny	convex	smooth	white	2
Dh5	HO-2	-	-	fine	-	shiny	convex	smooth	white	2
Mv1	HO-3	-	+	fine	-	shiny	convex	smooth	white	2
Mv2	HL-4	-	+	fine	-	shiny	convex	smooth	white	2
Cz2	HL-4	-	+	fine	-	shiny	convex	smooth	white	1
Dh6	HO-4	-	-	fine	-	shiny	convex	smooth	light pink	1
Mv3	HO-4	-	+	fine	-	shiny	convex	smooth	light pink	2
Mv4	HO-4	-	+	fine	+	shiny	convex	smooth	light pink	2
Mv5	HO-4	-	+	fine	-	shiny	convex	smooth	light pink	2
Mv6	HO-4	-	+	fine	-	shiny	convex	smooth	light pink	2
Mv7	HO-4	-	+	fine	-	shiny	convex	smooth	light pink	2
Mv8	HO-4	-	+	fine	-	shiny	convex	smooth	light pink	2
Mv9	HO-4	-	+	fine	-	shiny	convex	smooth	light pink	2

Table C.1 (Cont.)

Yeast code*	Olive source**-Sampling week	Growth in Liquid Culture				Growth in Solid Media				
		Film formation	*Haze*	*Sediment (fine/coarse)*	*Suspended particle*	*Colony texture (dull/shiny)*	*Colony shape (convex/concave)*	*Colony border (smooth/rough)*	*Colony color*	*Colony size (mm)*
Mv10	HO-4	-	+	fine	+	shiny	convex	smooth	light pink	2
Mv11	HO-4	-	+	fine	-	shiny	convex	smooth	white	1
Ap1	HO-4	-	+	fine	-	shiny	flat	rough	white	4
Ap2	HO-4	-	+	fine	-	shiny	flat	rough	white	1
Mp1	HO-4	-	+	fine	-	shiny	convex	smooth	white	1
Mv12	HO-4	-	+	fine	-	shiny	convex	smooth	white	1
Me1	HO-4	-	+	fine	+	shiny	convex	smooth	yellow	3
Mv13	HO-4	-	-	fine	-	shiny	convex	smooth	light pink	1
Mv14	HO-4	-	-	fine	-	shiny	convex	smooth	light pink	1
Mv15	HO-4	-	-	fine	-	shiny	convex	smooth	light pink	1
Mv16	HO-4	-	-	fine	-	shiny	convex	smooth	light pink	1
Ap3	GL-4	+	+	fine	-	shiny	flat	rough	white	1
Ap4	GL-4	+	+	fine	-	shiny	flat	rough	white	3
Rm2	GO-4	+	+	fine	-	shiny	convex	smooth	pink	3
Rm3	GO-4	-	+	fine	-	shiny	convex	smooth	pink	2
Rm4	HL-5	-	+	fine	+	shiny	convex	smooth	yellow	2
Rm5	GO-5	-	+	fine	-	shiny	convex	smooth	yellow	2
Rm6	HL-5	-	+	fine	-	shiny	convex	smooth	yellow	2
Rm7	HO-5	-	+	fine	-	shiny	convex	smooth	yellow	2
Ap5	GL-7	-	-	fine	+	shiny	flat	rough	white	1
Rm8	GL-7	-	+	fine	-	shiny	convex	smooth	pink	2
Rm9	GL-7	-	+	fine	-	shiny	convex	smooth	yellow	1
Rm10	HL-7	-	+	fine	-	shiny	convex	smooth	pink	2
Rm11	HL-7	-	+	fine	-	shiny	convex	smooth	pink	2
Rm12	HL-7	-	-	fine	+	shiny	convex	smooth	pink	2
Rm13	HL-6	-	+	fine	-	shiny	convex	smooth	pink	2

* Yeast codes that were reformed after sequence analysis

**HO: Hurma olive, GO: Gemlik olive, HL: Hurma leaves, GL: Gemlik leaves, A: air samples

Table C.2. The results of *microscopic* morphological analysis of olive samples from 2011 harvest year

Yeast code*	Olive source**- Sampling week	Cell Shape	Cell Size (µm)	Form of asexual reproduction	Sporulation on McClary acetate agar	Sporulation on Gorodkowa agar
Cd1	HO-2	ovoid	2.6	polar budding	-	-
Cd2	HO-2	ovoid	3.04	polar budding	-	-
Dh1	HO-2	ovoid	2.7	polar budding	-	-
Dh2	HO-2	spherical	3.89	polar budding	-	-
Dh3	HO-2	ovoid	2.48	polar budding	-	-
Dh4	HO-2	ovoid	2.55	polar budding	-	-
Cz1	HO-2	spherical	3.91	polar budding	-	-
Dh5	HO-2	ovoid	4.43	polar budding	-	-
Mv1	HO-3	ellipsoidal	4.31	polar budding	-	-
Mv2	HL-4	ellipsoidal	3.63	polar budding	-	-
Cz2	HL-4	spherical	5.13	polar budding	-	-
Dh6	HO-4	ellipsoidal	3.41	polar budding	-	-
Mv3	HO-4	ellipsoidal	4.25	polar budding	-	-
Mv4	HO-4	ellipsoidal	4.97	polar budding	-	-
Mv5	HO-4	ellipsoidal	4.86	polar budding	-	-
Mv6	HO-4	ovoid	4.93	polar budding	-	-
Mv7	HO-4	ellipsoidal	5.02	polar budding	-	-
Mv8	HO-4	ovoid	4.56	polar budding	-	-
Mv9	HO-4	ellipsoidal	4.75	polar budding	-	-
Mv10	HO-4	ovoid	5.9	polar budding	-	-
Mv11	HO-4	ellipsoidal	3.53	polar budding	-	-
Ap1	HO-4	ovoid	5.43	polar budding	-	-
Ap2	HO-4	ovoid	7.19	polar budding	-	-
Mp1	HO-4	ellipsoidal	4.9	polar budding	-	-
Mv12	HO-4	ellipsoidal	4.86	polar budding	-	-
Me1	HO-4	ellipsoidal	5.47	polar budding	-	-
Mv13	HO-4	ellipsoidal	5.19	polar budding	-	-
Mv14	HO-4	ellipsoidal	4.56	polar budding	-	-
Mv15	HO-4	ellipsoidal	4.03	polar budding	-	-
Mv16	HO-4	ellipsoidal	4.82	polar budding	-	-
Ap3	GL-4	ovoid	3.37	polar budding	-	-
Rm1	GL-4	ellipsoidal	5.6	polar budding	-	-
Ap4	GL-4	ellipsoidal	7.03	polar budding	-	-

(Cont. on next page)

Table C.2 (Cont.)

Yeast code*	Olive source**- Sampling week	Cell Shape	Cell Size (µm)	Form of asexual reproduction	Sporulation on McClary acetate agar	Sporulation on Gorodkowa agar
Rm2	GO-4	ovoid	4.86	polar budding	-	-
Rm3	GO-4	ovoid	4.58	polar budding	-	-
Rm4	HL-5	spherical	5.17	fussion	-	-
Rm5	GO-5	spherical	5.18	polar budding	-	-
Rm6	HL-5	ellipsoidal	4.47	fussion	-	-
Rm7	HO-5	spherical	3.99	polar budding	-	-
Ap5	GL-7	spherical	7.4	fussion	-	-
Rm8	GL-7	ovoid	4.44	polar budding	-	-
Rm9	GL-7	spherical	3.34	polar budding	-	-
Rm10	HL-7	ovoid	5.37	polar budding	-	-
Rm11	HL-7	ovoid	5.13	polar budding	-	-
Rm12	HL-7	ovoid	4.68	polar budding	-	-
Rm13	HL-6	spherical	3.35	polar budding	-	-

Table C.3. The results of *macroscopic* morphological analysis of olive samples from 2012 harvest year

Yeast code*	Olive source**- Sampling week	Growth in Liquid Culture				Growth in Solid Media				
		Film Formation	*Haze*	*Sediment (fine/coarse)*	*Suspended particle*	*Colony texture (dull/shiny)*	*Colony shape (convex/concave)*	*Colony border (smooth/rough)*	*Colony color*	*Colony size (mm)*
Ap6	A-5	+	+	coarse	+	shiny	convex	smooth	beige	2
Ap7	HL-5	+	+	coarse	+	shiny	convex	smooth	beige	2
Ap8	HO-5	+	+	coarse	+	shiny	convex	smooth	beige	2
Ap9	HO-5	+	+	coarse	+	shiny	convex	smooth	beige	2
Ap10	HL-6	+	+	coarse	+	shiny	convex	smooth	beige	2
Ap11	HO-6	-	+	fine	-	shiny	convex	smooth	beige	2
Ap12	HO-6	+	+	coarse	+	shiny	convex	smooth	beige	2
Ap13	GO-6	+	+	coarse	-	shiny	convex	smooth	beige	2
Ap14	HO-6	+	+	coarse	-	shiny	convex	smooth	beige	2
Ap15	HO-5	+	+	coarse	+	shiny	convex	smooth	beige	2
Ap16	HL-6	+	+	coarse	+	shiny	convex	smooth	beige	1
Ap17	HL-5	+	+	coarse	+	shiny	convex	smooth	beige	1
Ap18	GL-5	+	+	fine	+	shiny	convex	smooth	beige	2
Ap19	HL-2	+	+	fine	-	shiny	convex	smooth	beige	2
Ap20	GO-6	+	+	fine	+	shiny	convex	smooth	beige	2
Ap21	HO-6	+	+	fine	+	shiny	convex	smooth	beige	3
Au1	HO-6	+	+	coarse	+	shiny	convex	smooth	yellow	2
Au2	HL-7	+	+	fine	-	shiny	convex	smooth	beige	2
Au3	GL-6	-	+	fine	-	shiny	convex	smooth	beige	2
Au4	HL-4	+	+	coarse	+	shiny	convex	smooth	beige	2
Au5	HL-6	+	+	coarse	+	shiny	convex	smooth	yellow	1
Au6	GL-6	+	+	coarse	+	shiny	convex	smooth	yellow	1
Au7	HL-6	-	+	coarse	+	shiny	convex	smooth	yellow	1
Cu1	HL-5	-	-	fine	-	shiny	convex	smooth	white	2
Au8	HL-4	-	+	coarse	+	shiny	convex	smooth	beige	2
Ss1	HL-2	+	+	fine	+	shiny	convex	smooth	beige	2
Ss2	GL-6	+	+	fine	+	shiny	convex	smooth	beige	1
Au9	GL-6	+	+	coarse	+	shiny	convex	smooth	beige	2
Au10	HL-4	+	+	coarse	+	shiny	convex	smooth	beige	1
Au11	GL-4	+	+	coarse	+	shiny	convex	smooth	beige	2
Ss3	HL-2	+	+	fine	+	shiny	convex	smooth	pink	3

(Cont. on next page)

Table C.3 (Cont.)

Yeast code*	Olive source**- Sampling week	Growth in Liquid Culture				Growth in Solid Media				
		Film Formation	*Haze*	*Sediment (fine/coarse)*	*Suspended particle*	*Colony texture (dull/shiny)*	*Colony shape (convex/concave)*	*Colony border (smooth/rough)*	*Colony color*	*Colony size (mm)*
Ap22	HO-7	+	+	coarse	+	shiny	convex	smooth	beige	2
Ap23	HL-7	-	+	coarse	-	shiny	convex	smooth	beige	2
Ap24	GL-7	-	+	coarse	+	shiny	convex	rough	white	1
Rm14	A-2	-	+	fine	+	shiny	convex	smooth	pink	3
Rm15	A-1	-	+	fine	+	shiny	convex	smooth	pink	3
Ap25	HL-6	-	+	coarse	+	shiny	convex	smooth	beige	2
Ap26	HL-4	+	+	coarse	+	shiny	convex	smooth	beige	3
Ap27	GL-6	-	+	coarse	-	shiny	convex	smooth	beige	2
Ap28	HL-6	+	+	coarse	+	shiny	convex	smooth	beige	2
Ca1	HL-4	-	+	fine	-	shiny	convex	smooth	beige	1
Ca2	HL-2	-	+	coarse	-	shiny	convex	smooth	beige	1
Ap29	HL-2	+	+	fine	+	shiny	convex	smooth	beige	2
Ap30	GL-2	-	+	coarse	+	shiny	convex	smooth	beige	3
Ap31	GL-2	-	+	fine	-	shiny	convex	smooth	beige	3
Ap32	HL-2	-	+	coarse	-	shiny	convex	smooth	beige	2
Ap33	HL-4	+	+	coarse	-	shiny	convex	smooth	beige	2
Ap34	GL-6	+	+	coarse	+	shiny	convex	smooth	beige	2
Ap35	HL-6	+	+	coarse	+	shiny	convex	smooth	beige	2
Ap36	GL-3	-	+	fine	-	shiny	convex	smooth	beige	2
Ca3	HL-2	-	+	coarse	-	shiny	convex	smooth	white	1
Ap37	GL-6	-	+	fine	-	shiny	convex	smooth	beige	2
Ap38	GL-6	+	+	coarse	+	shiny	convex	smooth	beige	2
Sp1	HL-2	+	+	fine	-	shiny	convex	smooth	pink	2
Rm16	HL-2	+	+	fine	+	shiny	convex	smooth	pink	2
Au12	HL-1	-	+	fine	+	shiny	convex	smooth	beige	2
Au13	HL-4	-	+	coarse	+	shiny	convex	smooth	beige	2
Au14	HL-1	-	+	coarse	+	shiny	convex	smooth	beige	3
Au15	HL-4	+	+	coarse	+	shiny	convex	smooth	beige	3
Ap39	GL-3	-	+	fine	-	shiny	convex	smooth	beige	2
Au16	HL-2	-	+	coarse	+	shiny	convex	smooth	beige	3

Table C.3 (Cont.)

Yeast code*	Olive source**- Sampling week	Growth in Liquid Culture				Growth in Solid Media				
		Film Formation	*Haze*	*Sediment (fine/coarse)*	*Suspended particle*	*Colony texture (dull/shiny)*	*Colony shape (convex/concave)*	*Colony border (smooth/rough)*	*Colony color*	*Colony size (mm)*
Au17	GL-4	-	+	coarse	+	shiny	convex	smooth	beige	3
Au18	HL-1	+	+	fine	+	shiny	convex	smooth	beige	2
Au19	HO-6	+	+	fine	+	shiny	convex	smooth	beige	2
Ap40	GL-6	+	+	coarse	+	shiny	convex	smooth	beige	2
Au20	GL-6	+	+	coarse	+	shiny	convex	smooth	beige	2
Cp1	GO-5	-	+	fine	-	shiny	convex	smooth	white	1
Cg1	GO-5	-	-	fine	-	shiny	convex	smooth	white	2
Au21	GO-8	-	+	fine	-	shiny	convex	smooth	beige	2
Cu2	HO-5	-	-	fine	-	shiny	convex	smooth	white	2
Au22	HL-8	+	+	coarse	+	shiny	convex	smooth	beige	2
Au23	GL-6	-	+	coarse	+	shiny	convex	smooth	beige	2
Au24	HL-6	+	+	coarse	+	shiny	convex	smooth	beige	2
Au25	HL-6	+	+	coarse	+	shiny	convex	smooth	beige	2
Ss4	HO-8	+	+	coarse	-	shiny	flat	rough	yellow	3
Ap41	HO-5	+	+	fine	+	shiny	convex	smooth	white	2
Ap42	GL-5	+	+	coarse	+	shiny	convex	smooth	beige	2
Au26	HO-7	+	+	coarse	+	shiny	convex	smooth	beige	2
Cm1	GL-4	-	+	coarse	-	shiny	convex	smooth	white	2
Me2	GO-6	+	+	coarse	+	shiny	convex	smooth	beige	2
Ph1	HO-6	-	+	fine	-	shiny	flat	rough	white	3
Ap43	GO-5	-	+	coarse	+	shiny	convex	smooth	beige	2
Mp2	GO-5	-	+	fine	+	shiny	convex	smooth	white	2
Ap44	GO-5	-	+	coarse	+	shiny	convex	smooth	beige	2
Ap45	GO-5	+	+	coarse	+	shiny	convex	smooth	beige	3
Ap46	GL-5	-	+	coarse	+	shiny	convex	smooth	beige	2
Ap47	GO-5	-	+	coarse	+	shiny	convex	smooth	beige	3
Ap48	GO-5	-	-	fine	+	shiny	convex	smooth	light pink	2
Ap49	HL-5	-	+	fine	+	shiny	convex	smooth	beige	2
Ap50	HL-5	-	+	coarse	+	shiny	convex	smooth	beige	2
Me3	GO-5	-	+	coarse	-	shiny	convex	smooth	beige	2

Table C.3 (Cont.)

Yeast code*	Olive source**-Sampling week	Growth in Liquid Culture				Growth in Solid Media				
		Film Formation	*Haze*	*Sediment (fine/coarse)*	*Suspended particle*	*Colony texture (dull/shiny)*	*Colony shape (convex/concave)*	*Colony border (smooth/rough)*	*Colony color*	*Colony size (mm)*
Ap51	GO-5	+	+	coarse	+	shiny	convex	smooth	yellow	2
Ap52	HL-5	+	+	coarse	+	shiny	convex	smooth	beige	2
Ap53	HL-8	-	+	coarse	+	shiny	convex	smooth	beige	2
Ap54	GL-8	-	+	coarse	+	shiny	convex	smooth	beige	2
Ap55	GL-5	+	+	coarse	+	shiny	convex	smooth	yellow	2
Ap56	HL-5	+	+	coarse	+	shiny	convex	smooth	beige	2
Wi1	HL-5	-	+	fine	-	shiny	flat	rough	yellow	3
Ap57	GO-8	-	+	fine	-	shiny	convex	smooth	beige	3
Mf1	HL-8	+	+	coarse	+	shiny	flat	rough	yellow	3
Ap58	GL-7	-	+	fine	-	shiny	convex	smooth	beige	2
Ap59	HL-7	-	+	coarse	+	shiny	convex	smooth	beige	2
Ss5	GL-7	+	+	coarse	+	shiny	convex	smooth	beige	2
Pp1	HO-6	+	-	-	-	dull	convex	smooth	beige	2
Ap60	HL-7	-	+	fine	+	shiny	convex	smooth	beige	2
Ap61	HL-7	+	+	fine	+	shiny	convex	smooth	beige	2
Ap62	GL-7	-	+	fine	+	shiny	convex	smooth	beige	1
Ap63	HL-7	-	+	fine	+	shiny	convex	smooth	beige	2
Ap64	GL-7	-	+	fine	-	shiny	convex	smooth	white	2
Ap65	HO-6	-	+	fine	-	shiny	convex	smooth	beige	2
Ap66	HO-5	+	+	fine	+	shiny	convex	smooth	beige	3
Ap67	GL-7	-	+	coarse	+	shiny	convex	smooth	beige	3
Ap68	GL-7	+	+	fine	-	shiny	convex	smooth	beige	1
Ap69	HO-7	-	+	fine	-	shiny	convex	smooth	beige	2
Ap70	GL-5	+	+	coarse	+	shiny	convex	smooth	beige	2
Ap71	HO-7	-	+	coarse	+	shiny	convex	smooth	beige	2
Wi2	GL-5	-	-	-	-	shiny	convex	smooth	white	2
Ap72	GO-7	+	+	fine	-	shiny	convex	smooth	white	2
Cp2	HL-7	-	+	coarse	-	shiny	convex	smooth	white	2
Ap73	HL-5	-	+	coarse	+	shiny	convex	smooth	beige	2
Ap74	GL-7	-	+	coarse	+	shiny	convex	smooth	beige	2

Table C.3 (Cont.)

Yeast code*	Oive source**- Sampling week	Growth in Liquid Culture				Growth in Solid Media				
		Film Formation	*Haze*	*Sediment (fine/coarse)*	*Suspended particle*	*Colony texture (dull/shiny)*	*Colony shape (convex/concave)*	*Colony border (smooth/rough)*	*Colony color*	*Colony size (mm)*
Ap75	HO-6	+	+	coarse	+	shiny	convex	smooth	yellow	2
Wi3	HO-3	-	+	fine	-	shiny	flat	rough	yellow	3
Ap76	HL-7	+	+	coarse	+	shiny	convex	smooth	beige	2
Ap77	HL-7	-	+	coarse	+	shiny	convex	smooth	beige	2
Ap78	GO-7	-	+	fine	+	shiny	convex	smooth	beige	3
Ap79	GL-6	+	+	coarse	+	shiny	convex	smooth	beige	2
Ap80	HO-6	-	+	coarse	+	shiny	convex	smooth	beige	2
Ph2	A-6	+	+	coarse	+	dull	concave	smooth	white	2
Ap81	A-7	+	+	coarse	+	shiny	convex	smooth	beige	2
Ap82	HL-5	+	+	coarse	+	shiny	convex	smooth	beige	2
Wi4	HO-1	-	+	fine	-	shiny	flat	rough	yellow	3
Ap83	GO-5	-	-	fine	+	shiny	convex	smooth	beige	2
Cp3	GL-7	-	+	coarse	-	shiny	convex	smooth	white	2
Ap84	HL-7	-	+	coarse	+	shiny	convex	smooth	white	3
Ap85	HO-7	+	+	coarse	+	shiny	convex	smooth	beige	2

* Yeast codes that were reformed after sequence analysis

**HO: Hurma olive, GO: Gemlik olive, HL: Hurma leaves, GL: Gemlik leaves, A: air samples

Table C.4. The results of *microscopic* morphological analysis of olive samples from 2012 harvest year

Yeast code*	Oive source**-Sampling week	Cell Shape	Cell Size (µm)	Form of asexual reproduction	Sporulation on McClary acetate agar	Sporulation on Gorodkowa agar
Ap6	A-5	lemon	7.32	polar, bipolar budding	-	-
Ap7	HL-5	ellipsoidal	7.78	fussion	-	+
Ap8	HO-5	ellipsoidal	6.72	fussion	-	-
Ap9	HO-5	ellipsoidal	8.78	polar budding	-	-
Ap10	HL-6	ellipsoidal	8.1	polar budding	-	-
Ap11	HO-6	lemon	8.49	polar budding	-	-
Ap12	HO-6	ellipsoidal	8.76	fussion	+	+
Ap13	GO-6	lemon	7.88	polar, bipolar budding	-	-
Ap14	HO-6	ellipsoidal	7.45	polar budding	+	+
Ap15	HO-5	ellipsoidal	7.59	polar budding, fussion	+	+
Ap16	HL-6	lemon	6.9	polar, bipolar budding	-	+
Ap17	HL-5	lemon	6.82	polar, bipolar budding	-	+
Ap18	GL-5	lemon	7.1	polar, bipolar budding	-	-
Ap19	HL-2	lemon	7.73	polar, bipolar budding	+	-
Ap20	GO-6	lemon	7.58	polar budding	-	-
Ap21	HO-6	lemon	7.6	polar, bipolar budding	-	-
Au1	HO-6	elongated	8.5	fussion	-	-
Au2	HL-7	ellipsoidal	8.29	fussion	+	+
Au3	GL-6	ellipsoidal	8.61	polar, bipolar budding	-	-
Au4	HL-4	ellipsoidal	8.3	polar budding	-	-
Au5	HL-6	lemon	7.86	polar budding	-	+
Au6	GL-6	lemon	7.47	polar, bipolar budding	-	+
Au7	HL-6	lemon	6.43	polar budding	-	-
Cu1	HL-5	spherical	5.54	polar budding	-	-
Au8	HL-4	ellipsoidal	7.64	polar budding	-	-
Ss1	HL-2	ovoid	6.94	polar budding	-	-
Ss2	GL-6	ellipsoidal	5.13	polar budding	+	-
Au9	GL-6	ellipsoidal	7	fussion	-	-
Au10	HL-4	ellipsoidal	7.44	polar budding, fussion	-	-
Au11	GL-4	lemon	7.56	polar budding	-	-
Ss3	HL-2	ellipsoidal	4.56	polar budding	-	+
Ap22	HO-7	lemon	7.87	polar budding	-	-
Ap23	HL-7	lemon	8.31	polar budding	-	-

(Cont. on next page)

Table C.4 (Cont.)

Yeast code*	Oive source**-Sampling week	Cell Shape	Cell Size (μm)	Form of asexual reproduction	Sporulation on McClary acetate agar	Sporulation on Gorodkowa agar
Ap24	GL-7	lemon	7.53	polar budding	-	-
Rm14	A-2	spherical	4.55	polar budding	-	-
Rm15	A-1	ovoid	4.43	polar budding	-	-
Ap25	HL-6	ovoid	8.04	fussion	+	+
Ap26	HL-4	ovoid	7.34	polar budding	-	-
Ap27	GL-6	lemon	7.11	polar budding	-	-
Ap28	HL-6	lemon	8.26	polar, bipolar	-	-
Ca1	HL-4	spherical	5.88	polar budding	-	+
Ca2	HL-2	lemon	5.7	polar budding	-	-
Ap29	HL-2	lemon	5.99	polar budding	-	-
Ap30	GL-2	lemon	8.71	polar budding	-	-
Ap31	GL-2	lemon	6.38	polar, bipolar budding	-	-
Ap32	HL-2	lemon	6.31	polar budding	-	-
Ap33	HL-4	lemon	9.3	polar budding, fussion	-	-
Ap34	GL-6	lemon	7.41	polar, bipolar budding	-	-
Ap35	HL-6	ovoid	7.76	polar budding, fussion	-	-
Ap36	GL-3	lemon	4.9	polar, bipolar budding	-	-
Ca3	HL-2	spherical	4.86	polar budding	+	+
Ap37	GL-6	ovoid	6.5	polar budding	-	-
Ap38	GL-6	lemon	7.53	polar,bipolar budding	-	+
Sp1	HL-2	ovoid	6.7	polar budding	-	+
Rm16	HL-2	ellipsoidal	3.3	polar budding	+	+
Au12	HL-1	ellipsoidal	7.69	polar budding	-	+
Au13	HL-4	lemon	7.37	polar budding	-	-
Au14	HL-1	lemon	7.21	polar,bipolar budding	-	+
Au15	HL-4	lemon	7.32	polar budding	+	-
Ap39	GL-3	ellipsoidal	6.69	polar budding	-	-
Au16	HL-2	lemon	6.96	polar budding	-	-
Au17	GL-4	lemon	6.95	polar budding	-	-
Au18	HL-1	lemon	7.92	polar budding	-	-
Au19	HO-6	ellipsoidal	7.94	polar budding	+	+
Ap40	GL-6	lemon	6.71	polar budding	-	+

(Cont. on next page)

Table C.4 (Cont.)

Yeast code*	Oive source**-Sampling week	Cell Shape	Cell Size (µm)	Form of asexual reproduction	Sporulation on McClary acetate agar	Sporulation on Gorodkowa agar
Au20	GL-6	lemon	8.86	polar budding	+	-
Cp1	GO-5	ellipsoidal	4.5	polar budding, fussion	+	-
Cg1	GO-5	ellipsoidal	4.82	polar budding, fussion	+	+
Au21	GO-8	lemon	7.65	polar budding	-	-
Cu2	HO-5	ellipsoidal	5.4	polar budding	-	-
Au22	HL-8	lemon	7.12	polar,bipolar budding	-	-
Au23	GL-6	lemon	7.39	polar budding	-	-
Au24	HL-6	lemon	6.58	polar budding	+	+
Au25	HL-6	lemon	6.46	polar,bipolar budding	-	-
Ss4	HO-8	ellipsoidal	5.46	polar budding	+	-
Ap41	HO-5	ellipsoidal	6.86	polar budding, fussion	+	+
Ap42	GL-5	ellipsoidal	7.32	polar budding	-	+
Au26	HO-7	lemon	7.91	polar budding	-	-
Cm1	GL-4	lemon	7.17	polar budding	-	-
Me2	GO-6	ellipsoidal	7.4	polar budding, fussion	-	-
Ph1	HO-6	ellipsoidal	6.19	polar budding	-	-
Ap43	GO-5	lemon	7.24	polar budding	-	-
Mp2	GO-5	ellipsoidal	4.54	polar budding	+	+
Ap44	GO-5	ellipsoidal	6.37	polar budding	+	+
Ap45	GO-5	lemon	7.8	polar budding	+	+
Ap46	GL-5	lemon	6.27	polar budding	-	+
Ap47	GO-5	lemon	6.59	polar budding	+	+
Ap48	GO-5	spherical	4.4	polar budding	-	-
Ap49	HL-5	lemon	8.27	polar budding	-	-
Ap50	HL-5	lemon	7.14	polar budding	+	+
Me3	GO-5	lemon	7.78	polar budding	-	+
Ap51	GO-5	ellipsoidal	8.97	polar budding	+	+
Ap52	HL-5	lemon	7.65	polar budding	-	+
Ap53	HL-8	lemon	6.65	polar budding	-	+
Ap54	GL-8	ellipsoidal	7.93	polar budding	-	+
Ap55	GL-5	ellipsoidal	9.39	polar budding	+	+
Ap56	HL-5	lemon	8.35	polar budding	-	-
Wi1	HL-5	ellipsoidal	4.66	polar budding	+	+
Ap57	GO-8	lemon	9.12	polar budding	-	-
Mf1	HL-8	lemon	6.89	polar budding	-	+

Table C.4 (Cont.)

Yeast code*	Oive source**- Sampling week	Cell Shape	Cell Size (μm)	Form of asexual reproduction	Sporulation on McClary acetate agar	Sporulation on Gorodkowa agar
Ap58	GL-7	lemon	7.92	polar budding	-	-
Ap59	HL-7	ellipsoidal	6.56	polar budding	+	+
Ss5	GL-7	ellipsoidal	7.5	polar budding	+	+
Pp1	HO-6	elongated	10.05	polar budding, fussion	+	+
Ap60	HL-7	lemon	5.41	polar budding	+	+
Ap61	HL-7	ovoid	7.19	polar budding	-	+
Ap62	GL-7	lemon	7.76	polar budding	-	+
Ap63	HL-7	lemon	5.34	polar budding	-	-
Ap64	GL-7	ellipsoidal	5.91	polar budding	+	+
Ap65	HO-6	ellipsoidal	7.93	polar budding	+	+
Ap66	HO-5	lemon	8.32	polar budding	-	+
Ap67	GL-7	lemon	6.34	polar budding	+	-
Ap68	GL-7	ellipsoidal	5.39	polar budding	-	-
Ap69	HO-7	ellipsoidal	8.44	polar budding	+	+
Ap70	GL-5	lemon	8.03	polar budding	+	-
Ap71	HO-7	lemon	7.32	polar budding	-	+
Wi2	GL-5	ellipsoidal	4.01	polar budding	-	+
Ap72	GO-7	ellipsoidal	5.45	polar budding, fussion	+	+
Cp2	HL-7	ovoid	6.83	polar budding	-	+
Ap73	HL-5	lemon	7.1	polar budding	-	-
Ap74	GL-7	ovoid	8.17	polar budding	-	+
Ap75	HO-6	lemon	6.9	polar budding	-	-
Wi3	HO-3	lemon	7.5	polar budding	-	+
Ap76	HL-7	lemon	10.16	polar, bipolar budding	-	-
Ap77	HL-7	lemon	7.45	polar budding	-	-
Ap78	GO-7	lemon	7.22	polar budding	-	-
Ap79	GL-6	ellipsoidal	7.33	polar budding	-	-
Ap80	HO-6	lemon	7.36	polar budding, fussion	-	+
Ph2	A-6	elongated	9.47	fussion	+	+
Ap81	A-7	ellipsoidal	7.39	polar budding	-	-
Ap82	HL-5	lemon	8.11	polar budding, fussion	-	-
Wi4	HO-1	lemon	7.45	polar budding	-	+
Ap83	GO-5	ellipsoidal	7.22	polar budding	-	-
Cp3	GL-7	spherical	6.98	polar budding	-	-
Ap84	HL-7	ellipsoidal	7.34	polar budding, fussion	+	+
Ap85	HO-7	lemon	7.53	polar budding	-	+

Table C.5. Cultural test results of olive samples from 2011 harvest year

Yeast code*	Oive source**- Sampling week	API 20 C AUX: Carbohydrate Assimilation Test																			Nitrogen Assimilation	Durham
		D-GLUcose	GLYcerol	calcium 2-Keto-Gluconate	L-ARAbinose	D-XYLose	ADOnitol	XyLiTol	D-GALactose	INOsitol	D-SORbitol	Methyl-aD-Glucopyranoside	N-Acetyl-Glucosamine	D-CELlobiose	D-LACtose	D-MALtose	D-SACcharose (sucrose)	D-TREhalose	D-MeLeZitose	D-RAFfinose		
Cd1	HO-2	+	+	-	+	-	-	-	+	-	+	-	+	+	-	+	+	+	+	+	-	+
Cd2	HO-2	-	+	-	+	+	+	+	+	-	+	-	+	+	-	+	+	+	+	-	-	+
Dh1	HO-2	+	+	-	+	+	+	+	+	-	+	-	+	+	-	+	+	+	+	-	-	+
Dh2	HO-2	-	-	-	-	-	-	-	-	-	-	-	-	-	-	-	-	-	-	-	-	+
Dh3	HO-2	+	+	-	+	+	+	+	+	-	+	-	+	+	-	+	+	+	+	-	-	+
Dh4	HO-2	-	-	-	-	-	-	-	-	-	-	-	-	-	-	-	-	-	-	-	-	-
Cz1	HO-2	+	+	+	-	-	+	-	+	-	+	+	+	+	-	+	+	+	+	-	-	+
Dh5	HO-2	-	-	-	-	-	-	-	-	-	-	-	-	-	-	-	-	-	-	-	+	+
Mv1	HO-3	+	+	+	-	-	+	-	+	-	+	+	+	-	-	+	+	+	+	-	-	+
Mv2	HL-4	+	+	+	+	+	-	-	+	-	-	+	+	+	+	+	+	+	-	-	-	+
Cz2	HL-4	+	+	+	+	+	+	-	+	+	+	+	+	+	+	+	+	+	+	+	-	+
Dh6	HO-4	+	+	+	-	-	+	+	+	-	+	+	+	+	-	+	+	+	+	-	-	+
Mv3	HO-4	+	+	+	-	-	+	+	+	-	+	+	+	+	-	+	+	+	+	-	-	-
Mv4	HO-4	+	+	+	-	-	+	+	+	-	+	+	+	+	-	+	+	+	+	-	-	+
Mv5	HO-4	+	+	+	-	-	+	+	+	-	+	+	+	+	-	+	+	+	+	-	-	+
Mv6	HO-4	+	+	+	-	-	+	+	+	-	+	+	+	+	-	+	+	+	+	-	-	+
Mv7	HO-4	+	+	+	-	-	+	+	+	-	+	+	+	+	-	+	+	+	+	-	-	+
Mv8	HO-4	+	+	+	-	-	+	+	+	-	+	+	+	+	-	+	+	+	+	-	-	+
Mv9	HO-4	+	+	+	-	-	+	+	+	-	+	+	+	+	-	+	+	+	+	-	-	+
Mv10	HO-4	+	+	+	-	-	+	+	+	-	+	+	+	+	-	+	+	+	+	-	-	+
Mv11	HO-4	+	+	+	+	-	+	+	+	-	+	+	+	+	-	+	+	+	+	-	-	+
Ap1	HO-4	+	-	-	+	+	-	+	-	+	+	-	+	-	-	+	+	+	+	+	-	+
Ap2	HO-4	+	-	-	+	+	-	+	-	+	+	-	+	-	-	+	+	+	+	+	-	+
Mp1	HO-4	+	+	+	-	-	+	+	+	-	+	+	+	+	-	+	+	+	+	-	-	+
Mv12	HO-4	+	+	+	-	-	+	+	+	-	+	+	+	+	-	+	+	+	+	-	-	+
Me1	HO-4	-	-	-	-	-	-	-	-	-	-	-	-	-	-	-	-	-	-	-	-	+
Mv13	HO-4	+	+	+	-	-	+	+	+	-	+	+	+	+	-	+	+	+	+	-	-	+
Mv14	HO-4	+	+	+	-	-	+	+	+	-	+	+	+	+	-	+	+	+	+	-	-	+

Table C.5 (Cont.)

Yeast code*	Oive source**- Sampling week	API 20 C AUX: Carbohydrate Assimilation Test																			Nitrogen Assimilation	Durham
		D-GLUcose	*GLYcerol*	*calcium 2-Keto-Gluconate*	*L-ARAbinose*	*D-XYLose*	*ADOnitol*	*XyLiTol*	*D-GALactose*	*INOsitol*	*D-SORbitol*	*Methyl-αD-Glucopyranoside*	*N-Acetyl-Glucosamine*	*D-CELlobiose*	*D-LACtose*	*D-MALtose*	*D-SACcharose (sucrose)*	*D-TREhalose*	*D-MeLeZitose*	*D-RAFfinose*		
Mv15	HO-4	+	+	+	-	-	+	+	+	-	+	+	+	+	-	+	+	+	+	-	-	+
Mv16	HO-4	+	+	+	-	-	+	+	+	-	+	+	+	+	-	+	+	+	+	-	-	+
Ap3	GL-4	+	-	-	+	+	-	-	-	+	+	-	+	-	-	+	+	+	+	+	-	-
Rm1	GL-4	-	-	-	-	-	-	-	-	-	-	-	+	-	-	-	-	-	-	-	-	-
Ap4	GL-4	+	-	-	+	+	+	+	+	+	+	-	+	-	-	+	+	+	+	+	-	-
Rm2	GO-4	+	+	-	+	-	-	-	+	-	-	-	-	-	-	-	-	-	-	-	-	-
Rm3	GO-4	-	-	-	-	-	-	-	-	-	-	-	-	-	-	-	-	-	-	-	-	-
Rm4	HL-5	+	+	+	+	+	-	-	+	+	-	-	+	+	+	+	+	+	-	-	+	+
Rm5	GO-5	+	+	+	+	+	-	-	+	+	-	-	+	+	+	+	+	+	-	-	-	+
Rm6	HL-5	+	+	-	+	+	-	-	+	-	-	+	+	+	-	+	+	+	-	-	-	-
Rm7	HO-5	+	+	+	+	+	-	-	+	+	-	-	+	+	+	+	+	+	-	-	-	+
Ap5	GL-7	+	+	+	+	+	+	+	+	+	-	-	+	+	-	+	+	+	+	+	-	-
Rm8	GL-7	+	-	-	+	-	+	+	+	+	+	-	+	+	-	+	+	+	+	+	-	-
Rm9	GL-7	+	-	+	+	+	+	+	+	-	-	-	+	-	+	+	+	+	+	+	-	+
Rm10	HL-7	+	+	-	+	+	-	-	+	-	-	-	-	+	-	+	+	+	+	+	-	-
Rm11	HL-7	+	-	-	+	+	-	-	+	-	-	-	-	-	-	+	+	+	+	+	-	-
Rm12	HL-7	+	+	-	+	+	-	-	+	-	+	+	+	-	+	+	+	+	-	-	-	-
Rm13	HL-6	+	+	-	+	+	+	+	+	-	+	-	-	-	-	+	+	+	+	+	-	-

* Yeast codes that were reformed after sequence analysis.

**HO: Hurma olive, GO: Gemlik olive, HL: Hurma leaves, GL: Gemlik leaves, A: air samples

Table C.6. Cultural test results of olive samples from 2012 harvest year

Yeast code*	Oive source**-Sampling week	N.A. ***	Durham	Yeast code*	Oive source**-Sampling week	N.A. ***	Durham	Yeast code*	Oive source**-Sampling week	N.A. ***	Durham
Ap6	A-5	-	+	Ap22	HO-7	-	+	Au18	HL-1	-	+
Ap7	HL-5	-	-	Ap23	HL-7	-	-	Au19	HO-6	-	-
Ap8	HO-5	-	-	Ap24	GL-7	-	+	Ap40	GL-6	-	+
Ap9	HO-5	-	+	Rm14	A-2	+	+	Au20	GL-6	-	-
Ap10	HL-6	-	+	Rm15	A-1	+	+	Cp1	GO-5	-	+
Ap11	HO-6	-	+	Ap25	HL-6	-	+	Cg1	GO-5	-	+
Ap12	HO-6	-	+	Ap26	HL-4	-	-	Au21	GO-8	-	-
Ap13	GO-6	-	+	Ap27	GL-6	-	+	Cu2	HO-5	+	+
Ap14	HO-6	-	-	Ap28	HL-6	-	-	Au22	HL-8	-	-
Ap15	HO-5	-	-	Ca1	HL-4	+	+	Au23	GL-6	-	+
Ap16	HL-6	-	+	Ca2	HL-2	+	+	Au24	HL-6	-	+
Ap17	HL-5	-	-	Ap29	HL-2	-	+	Au25	HL-6	-	+
Ap18	GL-5	-	-	Ap30	GL-2	-	-	Ss4	HO-8	-	+
Ap19	HL-2	-	-	Ap31	GL-2	-	+	Ap41	HO-5	-	-
Ap20	GO-6	-	+	Ap32	HL-2	-	+	Ap42	GL-5	+	-
Ap21	HO-6	-	-	Ap33	HL-4	-	+	Au26	HO-7	+	-
Au1	HO-6	-	-	Ap34	GL-6	-	-	Cm1	GL-4	-	+
Au2	HL-7	-	+	Ap35	HL-6	-	+	Me2	GO-6	-	+
Au3	GL-6	-	+	Ap36	GL-3	+	-	Ph1	HO-6	-	+
Au4	HL-4	-	-	Ca3	HL-2	+	-	Ap43	GO-5	-	+
Au5	HL-6	-	+	Ap37	GL-6	-	+	Mp2	GO-5	-	+
Au6	GL-6	-	-	Ap38	GL-6	-	+	Ap44	GO-5	-	-
Au7	HL-6	-	+	Sp1	HL-2	-	+	Ap45	GO-5	-	+
Cu1	HL-5	+	-	Rm16	HL-2	+	+	Ap46	GL-5	-	-
Au8	HL-4	-	-	Au12	HL-1	-	+	Ap47	GO-5	-	+
Ss1	HL-2	-	+	Au13	HL-4	-	+	Ap48	GO-5	-	-
Ss2	GL-6	+	-	Au14	HL-1	-	-	Ap49	HL-5	+	-
Au9	GL-6	-	+	Au15	HL-4	-	+	Ap50	HL-5	-	+
Au10	HL-4	-	-	Ap39	GL-3	-	-	Me3	GO-5	-	+
Au11	GL-4	-	+	Au16	HL-2	-	+	Ap51	GO-5	-	+
Ss3	HL-2	+	+	Au17	GL-4	-	+	Ap52	HL-5	-	+

(Cont. on next page)

Table C.6 (Cont.)

Yeast code*	Oive source**-Sampling week	N.A. ***	Durham	Yeast code*	Oive source**-Sampling week	N.A. ***	Durham
Ap53	HL-8	-	-	Ap71	HO-7	-	-
Ap54	GL-8	-	-	Wi2	GL-5	-	+
Ap55	GL-5	-	+	Ap72	GO-7	-	+
Ap56	HL-5	-	+	Cp2	HL-7	-	-
Wi1	HL-5	+	+	Ap73	HL-5	-	-
Ap57	GO-8	-	-	Ap74	GL-7	+	-
Mf1	HL-8	+	-	Ap75	HO-6	-	+
Ap58	GL-7	-	+	Wi3	HO-3	-	+
Ap59	HL-7	-	+	Ap76	HL-7	-	-
Ss5	GL-7	-	+	Ap77	HL-7	-	+
Pp1	HO-6	-	+	Ap78	GO-7	-	+
Ap60	HL-7	-	+	Ap79	GL-6	-	+
Ap61	HL-7	+	+	Ap80	HO-6	-	+
Ap62	GL-7	-	-	Ph2	A-6	-	+
Ap63	HL-7	-	-	Ap81	A-7	-	+
Ap64	GL-7	-	+	Ap82	HL-5	-	+
Ap65	HO-6	-	-	Wi4	HO-1	-	-
Ap66	HO-5	-	+	Ap83	GO-5	-	-
Ap67	GL-7	-	-	Cp3	GL-7	-	+
Ap68	GL-7	-	+	Ap84	HL-7	-	-
Ap69	HO-7	-	+	Ap85	HO-7	-	-
Ap70	GL-5	-	-				

* Yeast codes that were reformed after sequence analysis.

**HO: Hurma olive, GO: Gemlik olive, HL: Hurma leaves, GL: Gemlik leaves, A: air samples

***N.A.: Nitrogen assimilation

VITA

CANAN CANAL
06.04.1984, Kayseri, Turkey
cengiz.canan@gmail.com

RESEARCH INTERESTS
Microbiology, Molecular Biology, Food Chemistry, Yeasts, Pathogens, Characterization of microorganisms, FTIR spectroscopy, PCR

EDUCATION
Ph.D., 2009-2015, Izmir Institute of Technology, Department of Food Engineering (Thesis: Applications of mid-IR spectroscopy for identification of wine and olive yeasts and characterization of antimicrobial activities of phenolics on yeasts)
M.Sc., 2006-2008, Hacettepe University, Department of Food Engineering (Thesis: Determination of the contamination level of Listeria monocytogenes using by molecular techniques on vegetables with green leaves around Ankara)
B.Sc., 2002-2006, Ankara University, Department of Food Engineering

PUBLICATIONS
Aytac, S. A., Ben, U., **Cengiz, C**., & Taban, B. M. (2010). Evaluation of Salmonella and Listeria monocytogenes contamination on leafy green vegetables. J Food Agric Environ, 8, 275-279.
Canal, C., & Ozen, B. (2015). Monitoring of Wine Process and Prediction of Its Parameters with Mid-Infrared Spectroscopy. *Journal of Food Process Engineering.*

DEGREES AND HONORS
06/2005-09/2005: Research scholan rship given by Wageningen University

2006: B.Sc. graduation at the 3rd place of department and faculty.

2006-2008: MSc. Scholarship given by The Scientific and Technical Research Council of Turkey (TUBITAK)

02/2005-05/2008: ERASMUS student in Universität für Bodenkultur Wien

2009-2015: PhD. Scholarship given by The Scientific and Technical Research Council of Turkey (TUBITAK)

PROJECTS
1. Regulation of lipase expression in *Aspergillus niger* (Wageningen University/2005)
2. Ankara ve Çevresinde Yetiştirilen Çiğ Tüketilen Yeşil Yapraklı Sebzelerin *Salmonella* spp. ve *Listeria monocytogenes* İçeriklerinin Moleküler Teknikler Kullanılarak Belirlenmesi (TÜBİTAK/2006-2008)
3. Enzymatic Synthesis of Keto-Sugars: Production of Health-Promoting Prebiotic Sugars Using Fungal Pyranose Dehydrogenase (Influence of O-glycosylation on yield and proteolysis in heterologous protein production in *Pichia pastoris*) (Austrian Development Agency/2008)
4. *Camplyobacter jejuni* varlığının Kitli Nükleik Asit (LNA) molekülleri kullanılarak saptanması (BAP/2010-2010)
5. Karaburun Yarımadasında Yetişen 'Hurma' Zeytininin Bazı Kimyasal ve Mikrobiyolojik Özelliklerinin Karakterizasyonu (TÜBİTAK/2011-2013)
6. Şarap prosesinin orta bölge infrared spektroskopi ile izlenmesi (BAP/2012-2013)